DOCKING-DEPENDENT REGULATION OF CHECKPOINT KINASE CHK1 BY THE GROWTH REGULATOR $p21^{WAF1}$

Yew Kwang Toh B.Sc. (Hons)

Thesis submitted to The University of Edinburgh for the degree of

Doctor of Philosophy

December 2008

List of contents

CHAPTER 2: MATERIALS AND METHODS

CHAPTER 4: CHARACTERISATION OF ALLOSTERIC REGULATION OF CHK1

Figures and Tables

Acknowledgement

First of all, I'm grateful to Kathryn for the opportunity to work on this project and for her constant patience and support during the course of the work. Ted has been helpful in offering positive advice. I owe a big thank you to both Jenny and Sarah for their technical assistance and advice and also for their constructive critique of my thesis. David and Mary have also been very kind in sharing their data. I would also like to thank past and present members of both Ball and Hupp lab for their help. CRUK has been kind to fund my studentship and this work. Last but most importantly, thanks to the support from my family, especially Libai and Edison who has been a bundle of joy (most of the time).

Declaration

I hereby declare that I am the author of this thesis and that I performed all the work described herein, except where specifically stated. All sources of information have been acknowledged by means of reference. The work described in this thesis has not been accepted in any previous application for a degree.

Yew Kwang Toh Date

Abbreviation

5-FU	5-Fluorouracil
6-TG	6-Thioguanine
9-1-1	Rad9-Rad1-Hus1
53BP1	p53-binding protein 1
A-T	Ataxia telangiectesia
AGC	Containing PKA, PKG, PKC families
AIF	Apoptosis-inducing factor
APC	Anaphase Promoting Complex
Aph	Aphidicolin
Arg (R)	Arginine
Asp (D)	Aspartic acid
ATM	Ataxia telangiectesia mutated protein
ATR	ATM-Rad3-related protein
ATRIP	ATR-interacting protein
BAX	BCL2-associated X protein
BRCA1	Breast cancer type 1 susceptibility protein
BubR1	Mitotic checkpoint serine/threonine protein kinase Bub1-related protein kinase
$CaCl_2$	calcium chloride
CAK	Cdk-activating kinase
CAMK	Calcium/calmodulin-dependent protein kinase
CaM kinase II	calcium/calmodulin-dependent protein kinase II
CD	circular dichroism
Cdc20	Cell division cycle 20
Cdc25	A family of cell division cycle 25
Cdc45	Cell division control protein 45
Cdh1	Cdc20 homology 1
Cdk	Cyclin-dependent kinase
Chk1	Checkpoint kinase 1
Chk2	Checkpoint kinase 2
Cip/Kip	Cdk-interacting protein/ Kinase inhibitory protein

CK1	Casein kinase 1
CKI	Inhibitor of cyclin-dependent kinase
CMGC	Containing CDK, MAPK, GSK3, CLK families
CPT	Camptothecin
Crm1	A nuclear export factor
C-terminal	Carboxy-terminal
Cul1	E3 ligases cullin family
Cul4a	E3 ligases cullin family
Cys (C)	Cysteine
DBH	debromohymenialdisine
DDR	DNA damage response
dH_2O	distilled H_2O
DISC	Death-induced signalling complex
DMEM	Dulbecco's modified eagle's medium
DMSO	dimethyl sulfoxide
DNA	Deoxyribonucleic acid
Dnmt	DNA methyltransferase
dNTP	deoxynucleotide triphosphate
Dox	Doxorubicin
DP	E2F dimerisation partner
DSB	double-stranded break
DT40	Chicken lymphoblast
DTT	dithiothreitol
E2	Ubiquitin-conjugating enzyme
E2F	A family of activating transcription factors
E3	A ligase which transfers ubiquitin from E2 to substrate
EDTA	ethylenediaminetetraacetic acid
EGF	epidermal growth factor
ERK	extracellular signal-regulated kinase
FADD	Fas-associated death domain
FBS	Fetal Bovine Serum
FEN 1	Flap endonuclease 1
FHA	Forkhead-associated domain
Fus3	cell fusion-3

GCN5	Histone acetyltranferase
Gln (Q)	Glutamine
Glu (E)	Glutamic acid
Gly (G)	Glycine
GSK3	glycogen synthase kinase 3
H2Ax	Histone 2Ax
H3	Histone 3
HCl	hydrochloric acid
HDACs	Histone deacetylases
HIV-1	human immunodeficiency virus type 1
HPLC	High performance liquid chromatoography
HPV	human papillomavirus
HR	Homologous recombination
HRP	Horseradish peroxidase
Hsp90	Heat shock protein 90
HU	Hydroxyurea
IAP	Inhibitor of apoptosis
IC_{50}	Concentration of drug that is required for 50% inhibition *in vitro*
Ink4	Inhibitor of Cdk4
IPTG	isopropyl-β-D-1-thiogalactopyranoside
IR	ionising radiation
JNK	c-Jun N-terminal kinase
kDa	kilo-Dalton
KOH	potassium hydroxide
LB	Luria-Bertani
Leu (L)	Leucine
LOH	loss of heterozygosity
Lys (K)	Lysine
MAD2	Mitotic spindle assembly checkpoint protein
MAPK	Mitogen-activated protein kinase
MCM 2-7	Minichromosome maintenance protein 2-7
MEK	MAPK/ERK kinase
MDC	mediator of DNA damage checkpoint protein 1

Mdm2	Murine double minute 2 protein (E3 ubiquitin ligase)
MIC1	Macrophage inhibitory cytokine 1
MK2	Mitogen-activated protein kinase-activated protein kinase 2
MMS	methyl methanesulfonate
$MnCl_2$	maganese chloride
MOI	multiplicity of infection
MOPS	3-(N-morpholino)propanesulfonic acid
MPF	M-phase promoting factor
MRN	Mre11-Rad50-Nbs1
N-terminal	amino-terminal
NaCl	sodium chloride
NaOH	sodium hydroxide
Nbs1	Nijmegen breakage syndrome protein 1
$Ndc80^{Hec1}$	Kinetochore protein Hec1
HDX	hydrogen/deuterium exchange
NHEJ	Non-homologous end joining
Nnf1R	Kinetochore-associated protein
NMR	nuclear magnetic resonance
Ni-NTA	nickel-nitrilotriacetic acid
Nuf2R	Kinetochore protein
$p21^{waf1}$	Cyclin-dependent kinase inhibitor
p53	Tumour suppressor p53
PALA	*N*-(phosphonacetyl)-$_L$-aspartate
PARP1	poly (ADP-ribose) polymerase family, member 1
PBS	phosphate buffered saline
PCNA	Proliferating Cell Nuclear Antigen
PCR	polymerase chain reaction
PDK1	3-phosphoinositide-dependent kinase 1
Phe (F)	Phenylalanine
PIF	PDK1-interacting fragment
PIKK	Phospho-inositide 3-kinase-like-kinase
PIP	PCNA-interacting protein
PKB/Akt	Protein kinase B/RAC-serine/threonine protein kinase
PKC	Protein kinase C

Plk1	Polo-like kinase 1
PPM1D	Protein phosphatase magnesium-dependent 1 delta
pRb	Retinoblastoma protein
PTEN	Phosphatase and tensin homologue
PUMA	p53-upregulated modulator of apoptosis
Rad17	RF-C/activator 1 homolog (Cell cycle checkpoint protein)
RbCl	rubidium chloride
R.L.U	relative light units
RNA	ribonucleic acid
ROS	reactive oxygen species
RPA	Replication protein A
rpm	revolutions per minute
RUNX	Runt-related transcription factor
SCD	SQ/TQ cluster domain
$SCF^{\beta TrCP}$	Skp, Cullin, F-box containing complex
SDFs	Senescence-associated DNA damage foci
SDS	sodium dodecyl sulfate
SDS-PAGE	sodium dodecyl sulfate polyacrylamide gel electrophoresis
Ser (S)	Serine
siRNA	small interference RNA
SSB	Single-stranded break
ssDNA	single-stranded DNA
STE	Homologs of yeast Sterile 7, Sterile 11, Sterile 20 kinases
TBE	Tris-Borate-EDTA
Tbx2	T-box protein 2
Thr (T)	Threonine
TK	Tyrosine kinase
TKL	Tyrosine kinase-like
Tlk1	Tousled-like kinase 1
TopBP1	Topoisomerase (DNA) II binding protein 1
Tyr (Y)	Tyrosine
U2OS	Human epithelial cell line
UCN-01	7-hydroxystaurosporine
UV	Ultraviolet

Vpr	HIV-1 Viral protein R
WD40	40 amino acids motifs, often terminating in Trp-Asp (W-D)
WS-1	Human fibroblast
X	any amino acid
ZBTB4	zinc finger and BTB domain-containing protein 4
ZNF76	Zinc-finger protein 76

ABSTRACT

Checkpoint kinase 1 (Chk1) is a key player in the DNA damage response signalling pathway and the mode of Chk1 activation whereby it undergoes ATR-dependent phosphorylation at Ser^{317} and Ser^{345} is well characterised. It has been suggested that phosphorylation at the ATR sites relieves the auto-inhibitory action conferred by the C-terminal negative regulatory domain on the catalytic core of Chk1. In this study, we show that Chk1 activity can also be stimulated by docking to an N-terminal region of the growth regulator $p21^{waf1}$ and this docking domain is necessary for efficient Chk1-dependent phosphorylation of p21 at Ser^{146}. In addition, Chk1 and p21 are shown to form a transient interaction by immunoprecipitation. Interestingly, although the isolated p21 docking domain can activate Chk1 *in trans*, a mutant where the C-terminal 70 amino acids are truncated is refractory to stimulation whereas mutation of the ATR phospho-acceptor sites does not affect docking dependent activation. Furthermore, when the amino acid sequence of the p21 docking domain was aligned with the sequence of Chk1, homology to the αF region on the kinase domain was identified. Mutation of two conserved tryptophan residues within the homology region appears to release the C-terminus from intramolecular interactions rendering it susceptible to cleavage and refractory to allosteric stimulation. Furthermore, small peptides based on this region of Chk1, like the p21 docking domain, are able to activate Chk1 *in trans* and disrupt interaction between the N-terminal and C-terminal domains. Interestingly, peptide microarray showed that Chk1 stimulated by activating peptide is able to phosphorylate novel peptide substrates which are not observed with unstimulated Chk1. The data suggest that the last C-terminal 70 amino acids of Chk1 play an important role in auto-inhibition through interaction with the αF region of the core catalytic domain. Binding to p21 is able to activate Chk1 by inhibiting the auto-inhibitory interaction independent of phosphorylation at the Ser^{317} and Ser^{345} sites. Furthermore, activating peptide is able to modulate Chk1 specificity towards other substrates.

CHAPTER 1: INTRODUCTION

1.1 Introduction

The survival of a human being is dependent on the homeostatic control between cellular proliferation, differentiation and death; this is tightly regulated in normal tissue yet is aberrant in disease processes such as cancer. Central to this homeostatic control is the coupled regulation of cell division and maintenance of genomic integrity. DNA damage, due to exogenous and endogenous elements such as ultraviolet irradiation and reactive oxygen species, is ubiquitous throughout the cell cycle and can create potentially lethal genetic lesions that will disrupt this homeostasis (Sancar et al., 2004). To guard against propagation of deleterious genetic material, damaged cells activate a global response known as the DNA damage response that includes DNA repair mechanisms, cell cycle checkpoints and apoptosis (Norbury and Hickson, 2001). Cell cycle or DNA damage checkpoints function to arrest the cell cycle to facilitate DNA repair and might be involved in the induction of transcriptional programs that determine damaged cell fate (Lowndes and Murguia, 2000). Checkpoint kinases Chk1 and Chk2 play an important role in transducing checkpoint signals emanating from ATR and ATM to the downstream cell cycle effector molecules (Bartek and Lukas, 2003). The introduction chapter will cover an overview of cell cycle mechanisms and the DNA damage response before focusing on the checkpoint kinase Chk1. The results chapters will discuss findings on the mechanistic regulation of Chk1 through a chemical genetics approach using small peptide-mimetic ligands based on the growth regulator $p21^{waf1}$ before concluding with a discussion on future work.

1.2 Overview of Cell Cycle

The eukaryotic cell cycle is an ordered set of events and is divided into four phases: S-phase is the period when chromosomes are replicated and it is preceded by a gap-phase termed G_1 and followed by another gap-phase called G_2. Collectively, G_1, S and G_2 are known as interphase where the cell grows by synthesizing new cellular proteins and starts deoxyribonucleic acid (DNA) replication. M-phase refers to mitosis when the cell undergoes division into two daughter cells. However not all cells in the human body are dividing. Indeed the majority of cells exist in a terminally differentiated state. Furthermore, stem cells or cells deprived of external growth stimuli reside in G_0-phase known as the quiescent state. Quiescent cells can re-enter the cell cycle at G_1-phase upon appropriate growth stimuli. This is in contrast to senescent cells which are arrested permanently and cannot be stimulated to re-enter the cell cycle by known growth stimuli. The normal progression of the cell cycle is critical for faithful segregation of parental genetic material to its progeny as misregulation often causes diseases such as cancer (Murray and Hunt, 1993).

A close understanding of cell cycle mechanisms is needed to devise strategies to combat the uncontrolled divisions of cells that can lead to cancer. Much of our knowledge comes from studies on *Saccharomyces cerevisiae* and *Saccharomyces pombe, Caenorhabditis elegans* and *Xenopus lavis*. Interestingly, many of their cell cycle mechanisms are conserved across species and indeed are observed in the mammalian cell cycle (Murray and Hunt, 1993). A brief overview of cell cycle regulation is introduced in the following section.

1.2.1 G_1/S-phase

G_1 refers to the gap period before S-phase and after M-phase. This is when cells start to synthesize new proteins required in S-phase for DNA replication. Tight regulation is necessary to maintain the cell in G_1 before it is ready to engage in DNA replication and central to this are the cyclin-dependent kinases (CDKs) and the retinoblastoma protein (pRb) (Alberts et al., 2002).

Hypophosphorylated pRb interacts with a family of activating transcription factors, termed E2F, which prevents their transcriptional activation of cell cycle genes necessary for G_1/S progression and DNA synthesis. In addition, pRb also functions as a transcriptional repressor module with histone deacetylases (HDACs) at the promoter of S-phase genes. Phosphorylation and inactivation of pRb is mediated by CDKs (Stevaux and Dyson, 2002).

CDKs have been described as engines that drive the events of the eukaryotic cell cycle. They are serine/threonine kinases that phosphorylate a number of substrates such as pRb, p53 and other CDKs. Activation of CDKs depends on the presence of a positive regulatory subunit (cyclin), the concentration of which oscillates during the cell cycle; its appropriate phosphorylation status; and sequestering of their inhibitors, cyclin-dependent kinase inhibitors (CKIs) (Morgan, 1997, Ekholm and Reed, 2000).

Levels of cyclin D peak at late G_1-phase and this is dependent on growth factor stimulation. Cyclin D then forms a complex with CDK4/6. As aforementioned,

CDKs also need to be appropriately phosphorylated to form active complexes. Phosphorylation on threonine residue 161 (Thr^{161}), by CDK-activating kinase (CAK) coupled with removal of inhibitory phosphate groups on Thr^{14} and tyrosine residue 15 (Tyr^{15}), by the Cdc25A phosphatase, activates CDK4/6 activity. CDK4/6-cyclin D complexes then phosphorylate pRb, which block pRb's transcriptional repression function and releases E2F transcriptional activating factors. This initiates the cell cycle to progress through the restriction point in G_1-phase, which signifies an irreversible commitment to undergo cell division even in the absence of mitogenic signals (Donjerkovic and Scott, 2000). Levels of cyclin A and cyclin E are up-regulated by the activation of E2F and they form complexes with CDK2 to maintain the inactivation of pRb, which is necessary for entry into S-phase. Once the cell progresses to S-phase, cyclin E becomes degraded while the levels of cyclin A persist into mitosis (Donjerkovic and Scott, 2000, Ho and Dowdy, 2002).

The activity of CDKs is also dependent on regulation by cyclin-dependent kinase inhibitors (CKIs) which are largely grouped into two families: namely, inhibitor of CDK4 (Ink4) and CDK-interacting protein/ Kinase inhibitory protein (Cip/Kip). Due to their anti-proliferative function, they are also known as tumour suppressors (Vidal and Koff, 2000).

INK4 is comprised of four members, namely $p16^{INK4a}$, $p15^{INK4b}$, $p18^{INK4c}$ and $p19^{INK4d}$ which inhibit the D-type cyclin-dependent kinases (CDK4/6) by binding in competition with cyclin D. All four members are characterised by the presence

of four ankyrin repeats of which the third repeat is essential for CDK4/6 interaction (Roussel, 1999). The Cip/Kip family including $p21^{cip1/waf1}$, $p27^{kip1}$ and $p57^{kip2}$ share a conserved N-terminal domain and inhibit Cdk4- and Cdk2-binding complexes stoichiometrically by interacting with both CDKs and cyclins to prevent a functional CDK-cyclin complex. In addition, $p21^{cip1/waf1}$ inhibits DNA synthesis by binding with proliferating cell nuclear antigen (PCNA), a processivity factor of DNA polymerase delta (pol δ) (Vidal and Koff, 2000). More functions of $p21^{waf1}$ will be described in the introduction to Chapter 3.

1.2.2 S-phase

The control of S-phase is a very complex process that is independent of external growth factors as compared to the G_1 phase. It is intrinsically controlled by the E2F transcription factor family which up-regulates the genes required for deoxynucleotide triphosphate (dNTP) and DNA synthesis, including thymidylate synthase (TS) and DNA polymerase pol α. The level of E2F is negatively regulated via feedback from the increased dNTPs. As DNA synthesis is completed at the end of S-phase, dNTPs would accumulate and thereby mediate E2F inactivation (Pardee et al., 2004).

CDK2-cyclin A/E complexes also regulate S-phase progression. As aforementioned, they phosphorylate pRb and facilitate the release of E2F which then forms active transcriptional dimers with the DP proteins. In addition, CDK2-cyclin E also phosphorylates the components of a pre-replication complex which

then associates with Cdc45 to activate the replication origin and initiate DNA replication. CDK2-cyclin A has also been implicated in the control of DNA replication by activating existing pre-replication complexes and elongation and also preventing re-replication (Woo and Poon, 2003). In the late S-phase, E2F is phosphorylated by CDK2-cyclin A and targeted for degradation to ensure the unidirectional progression of S-phase and prevent the initiation of a new S-phase prior to mitosis (Pardee et al., 2004).

1.2.3 G_2/M-phase

After DNA replication is completed, the cell enters G_2 phase which is a gap period before mitosis. In this phase, synthesis of proteins required for mitosis occurs. Transition through G_2/M-phase was first found to be mediated by a protein called M-phase promoting factor (MPF). Later it was elucidated that MPF is made up of a catalytic subunit, CDK1 and a regulatory subunit, cyclin B (Murray and Hunt, 1993). CDK1 is activated by phosphorylation on Thr^{161} mediated by a Cdk-activating kinase (CAK) and dephosphorylation on Thr^{14} and Tyr^{15} mediated by protein phosphatase Cdc25C (Nigg, 2001). Active CDK1 then phosphorylates numerous substrates such as nuclear lamins, condensins and other microtubule-binding proteins necessary for the onset of mitosis.

In addition, once the cell progresses into late G_2-phase, cyclin A begins to associate with CDK1, where it could potentially be involved in the reorganization of the cytoskeleton for mitosis (Hutchison and Glover, 1995). Furthermore,

increasing evidence has shown that CDK2-cyclin A has a critical role in the timing of mitosis through regulation of CDK1-cyclin B activation (Mitra and Enders, 2004, Gong et al., 2007, De Boer et al., 2008).

1.2.4 M-phase

The mitotic phase can be broken down into different stages: namely prophase, prometaphase, metaphase, anaphase, telophase and cytokinesis.

Prophase is characterised by chromatid condensation and the self-assembly of the mitotic spindle, a structure required for the separation of chromosomes into two daughter cells. During this period, the nuclear envelope also begins to breakdown. It disappears completely in prometaphase and the kinetochores on the chromosomes are attached to the mitotic spindle via the microtubules extending from the centrosomes. In metaphase, the chromosomes are aligned along the metaphase plate in the middle of the cell. They are kept in this position by the balance of microtubule forces emanating from the opposite spindle poles, until the separation of sister chromatids in anaphase (Nigg, 2001, Alberts et al., 2002).

The transition from metaphase to anaphase is triggered by the activation of the Anaphase Promoting Complex (APC). APC functions to mediate the degradation of CDK1-cyclin B and an inhibitory protein called securin. Following the inactivation of securin, separase then mediates the cleavage of cohesin, a subunit responsible for the binding of the sister chromatids and therefore facilitating the

separation of chromatids (Alberts et al., 2002). APC, also known as the cyclosome, is a multi-subunit 20S E3-ubiquitin ligase that couples ubiquitin molecules onto its substrates in a concerted effort with E2 ubiquitin-conjugating enzymes. Activation of APC is dependent on Polo-like kinase 1 (Plk1)-mediated phosphorylation. This modification primes APC for binding to its regulatory factors, namely cell division cycle 20 (Cdc20) and Cdc20 homology 1 (Cdh1) which are characterised by seven WD40 motif repeats (Fang et al., 1999, Baker et al., 2007). It has been suggested that APC exhibits differential substrate selectivity depending on the activator it binds to, Cdc20 or Cdh1 (Peters, 2006). Mitotic exit is also regulated by APC where it mediates the destruction of Plk1 and Aurora B (Baker et al., 2007).

Anaphase is characterised by the movement of each set of chromosomes towards opposite poles. The nuclear envelope then begins to reform around the daughter chromosomes as they start to decondense in telophase. Cytokinesis is marked by the formation of an actomyosin-based contractile ring that splits the cell into two daughter cells. Following cytokinesis completion, the cell cycle progresses into G_1 phase (Nigg, 2001).

1.3 DNA damage response

DNA is the blueprint of life as it contains the genetic code which is central to the development and function of living organisms. DNA is constantly damaged by omnipresent endogenous cellular metabolites such as reactive oxygen species that arise during respiration or environmental genotoxic agents such as ultraviolet (UV)

radiation and other chemical agents. These DNA-damaging agents cause chemical modifications to the DNA bases, DNA backbone breakages, including single- and double-stranded breaks, and DNA-DNA or DNA-protein cross-linkages that encumber transcription and/or replication (Sancar et al., 2004). For example, UV radiation generates 6-4 photoproduct and cyclobutane-pyrimidine dimers which distort the DNA helix and cause DNA replication arrest (Ward et al., 2004). Damaged genetic material can form transcripts for the synthesis of aberrant protein molecules that may function in the development and progression of diseases.

To ensure genomic stability and maintain the fidelity of DNA replication so as to minimize the occurrence of heritable mutations, nature has built in a set of evolved surveillance and response mechanisms to monitor cell cycle progression and cope with DNA damage. When a cell encounters damage, the appropriate DNA repair mechanism is promptly activated to repair the lesions. At the same time, cell cycle progression is arrested by checkpoint activation to facilitate DNA repair. If the damage is too extensive to be repaired, these potentially deleterious mutations are removed from the proliferating pool by either inducing a permanent proliferative arrest, known as senescence, or programmed cellular death, termed apoptosis. This convoluted cellular response is known as the DNA damage response (DDR) (Sancar et al., 2004, Bartek et al., 2007). The following section will briefly outline the various elements involved.

1.3.1 DNA damage checkpoint

DNA damage checkpoints or cell cycle checkpoints are activated to halt cell cycle progression in response to DNA damage. Perhaps it is not well-appreciated that key elements of the checkpoint pathways also operate in the unperturbed cell cycle to ensure the fidelity of normal cell cycle progression (Sancar et al., 2004). As aforementioned, cell division is an ordered set of events. These checkpoints ensure that certain events are completed before progression onto the next phase; for example, if the chromosomes are not aligned properly along the metaphase plate, transition into anaphase is blocked to prevent aneuploidy (Hutchison and Glover, 1995). Similarly, these checkpoints function to sequester damaged cells in the affected cell cycle phase until DNA damage is repaired to avert improper segregation of damaged chromosomes and ensure genomic stability. However, checkpoint function is not limited to cell cycle arrest and its action also percolates throughout the entire DDR network, resulting in coordinated spatial and temporal activation of DNA repair and induction of transcriptional programmes (Zhou and Elledge, 2000). Due to their pivotal role in DDR and cell cycle progression, it is not surprising to note that checkpoint pathways are well conserved across species ranging from *Saccharomyces cerevisiae* to *Xenopus lavis* and mammals, though its specificities may differ.

Checkpoint signalling pathways are generally made up of three important groups of proteins (Figure 1.1) (Sancar et al., 2004):

1. Sensor proteins – these recognise aberrant DNA structure and initiate the biochemical pathway,

2. Transducer proteins – these serve to amplify the signals from the sensors by phosphorylating other target proteins,

3. Effector proteins – these aim to arrest cell cycle progression.

1.3.1.1 Sensor proteins

Sensor proteins are found at the top of the checkpoint signalling pathway where they scan the DNA structure for strand breakage, incomplete DNA replication, undesirable DNA adducts or other abnormalities and then initiate biochemical signals that modulate the function of their downstream target proteins. Two major players in DNA damage checkpoints are the phospho-inositide 3-kinase-like-kinase (PIKK)-related proteins: Ataxia telangiectesia mutated protein (ATM) and ATM-Rad3-related protein (ATR). They are serine/threonine kinases with conserved kinase domains at the C-termini (Abraham, 2001) and serve overlapping yet distinct branches of the checkpoint network depending on the type of DNA damage. Primarily, ATM responds to double-stranded DNA breaks (DSBs) induced by ionising radiation (IR), while ATR is activated upon single-stranded DNA breaks (SSBs) generated by UV irradiation or stalled DNA replication (Sancar et al., 2004).

ATR has been found to be an essential protein in embryonic development where ATR-null mouse embryos fail to develop beyond the blastocyst stage (Brown and Baltimore, 2000). In *Xenopus*, ATR is found to associate with chromatin that is dependent on RNA primer synthesis by DNA polymerase pol α in the absence and

presence of stalled replication forks (Hekmat-Nejad et al., 2000). Following activation of the ATR-dependent checkpoint, nucleotide and base excision repair is stabilised by binding to a heterotrimeric protein complex called replication protein A (RPA) (Michael et al., 2000). This facilitates the loading of ATR onto the RPA-coated ssDNA which is dependent on ATR-interacting protein (ATRIP) (Zou and Elledge, 2003). Rad17, part of the replication factor C homolog also binds to the RPA coated-ssDNA and loads the Rad9-Rad1-Hus1 (9-1-1) complex onto the chromatin (Zou et al., 2003). The 9-1-1 complex is structurally related to PCNA, a protein that functions as a clamp to hold the chromatin together during replication (Shiomi et al., 2002). Rad17 association with the chromatin is ATR-independent but it is phosphorylated by ATR after stress and this phosphorylation is dependent on the 9-1-1 complex. Ablation of the Rad9 subunit of the 9-1-1 complex diminished ATR function, leading to gross chromosomal aberration. Hence, it has been postulated that sensor proteins localise onto the chromatin independently but interact to initiate the checkpoint signalling pathway (Zou et al., 2002, Dang et al., 2005). It should also be noted that ATR can also be activated by RPA-independent mechanism (Dodson et al., 2004) as it was found that TopBP1 can increase the activity of ATR even in the absence of RPA. This suggests that two different initiating signals may exist for activating ATR-dependent checkpoint responses (Kumagai et al., 2006). Activated ATR phosphorylates numerous checkpoint substrates including Chk1, RPA and BRCA1 which contain a consensus motif – serine (Ser)/Thr followed by a glutamine (Gln) residue (SQ/TQ) (Kim et al., 1999).

ATM is a 370 kDa protein kinase primarily activated in response to ionising radiation where double stranded breaks are induced. Its function is defective in ataxia-telangiectasia (A-T) patients who display radiation hypersensitivity, aberrant checkpoint function and increased chromosomal breakage (Kastan and Lim, 2000). Upon initiation of DNA lesions, ATM undergoes intermolecular autophosphorylation at Ser^{1981} which causes the inactive ATM dimers to dissociate and form active monomers that initiate an ATM-dependent checkpoint signalling cascade. ATM activation appears to be independent of DNA DSB binding, but may be triggered from changes in chromatin structure (Bakkenist and Kastan, 2003). However, ATM activation does seem to depend on a functional Mre11-Rad50-Nbs1 (MRN) complex. MRN may help to tether ATM to the double-stranded breaks through ATM-dependent phosphorylation of histone H2AX (Uziel et al., 2003) which also serves to localise the assembly of the DNA repair complex (Bartek and Lukas, 2007). Further evidence for MRN-dependent activation of ATM has shown that purified inactive dimeric ATM displays an 80-200 fold increase in activity in the presence of the MRN complex and linear DNA (Lee and Paull, 2005). Furthermore, it was also suggested that ATM-dependent phosphorylation of Nbs1, part of the MRN complex, may contribute to the recruitment of ATM substrates (Lee and Paull, 2007). Based on studies hitherto, it was proposed that damaged DNA is bound directly and processed by the MRN complex, which facilitates the recruitment and activation of ATM. Active monomeric ATM then serves to phosphorylate substrates localised or recruited to the lesions. In addition, ATM also phosphorylates histone H2AX surrounding the site of DSB which facilitates the recruitment of yet more substrates, thereby

reinforcing the signal (Kurz and Lees-Miller, 2004). Like ATR, activated ATM preferentially phosphorylates substrates on a general consensus motif – a Ser/Thr residue which is followed by a Gln (SQ/TQ). Among its putative substrates are Chk2 which is phosphorylated on Thr^{68} and p53 which is phosphorylated on Ser^{15} (Kim et al., 1999, Matsuoka et al., 2000).

The above summary of the ATM/ATR-signalling machinery depicts it as a multi-protein complex, however it is important to note that this is also a dynamic collection of protein complexes whose members change with the type of DNA damage, location relative to the site of damage and time after damage initiation (Abraham, 2001).

1.3.1.2 Transducers

Checkpoint kinase 1 and 2 (Chk1 and Chk2) are the downstream targets of the checkpoint pathway that relay and amplify the ATR and ATM initiating signals. Until recently, it was thought that Chk1 is primarily activated by ATR in response to replication blocks and UV treatment, while Chk2 is modified by ATM upon IR-induced double stranded breaks (Abraham, 2001). In fact, studies have shown that ATR-Chk1 and ATM-Chk2 are not exclusive branches of the DNA damage response pathway, but demonstrate a high degree of cross-talk where ATM is capable of activating Chk1 in response to IR (Gatei et al., 2003). This has been demonstrated in a study where ATM and Chk1 cooperate in response to IR to down-regulate the activity of mammalian Tousled-like kinase 1 (Tlk1), a kinase

that is potentially involved in the regulation of chromatin assembly and DNA replication in S-phase (Groth et al., 2003). Similarly, ATR has also been demonstrated to phosphorylate Chk2 *in vitro* (Matsuoka et al., 2000).

Chk2 is a nuclear Ser/Thr protein kinase which can be activated in response to DNA damage throughout the cell cycle, even in quiescent cells (Lukas et al., 2001). Chk2 contains three functional domains – an N-terminal SQ/TQ cluster domain (SCD), a forkhead-associated domain (FHA) and a C-terminal kinase domain. The SCD contains 7 SQ/TQ motifs of which Thr^{68} is the principal phosphorylation site, whereas the FHA domain is involved in protein-protein and intramolecular interactions (Figure 1.2) (Ahn et al., 2004). Phosphorylation of Thr^{68} induces Chk2 dimerisation where the FHA domain of the first molecule interacts with the phospho-Thr^{68} region of the second molecule (Ahn et al., 2002). This dimerisation is likely to initiate autophosphorylation of Thr^{383} and Thr^{387} within the activation loop of the kinase domain, resulting in active Chk2 molecules (Lee and Chung, 2001). Aside from a role in dimerisation, phospho-Thr^{68} may also facilitate association with other FHA domain-containing proteins such as the mediator of DNA damage checkpoint protein 1 (MDC1) FHA domain which binds selectively to phospho-Thr^{68} of Chk2 (Lou et al., 2003). An important scaffold molecule in Chk2 activation is BRCA1, which is required for Thr^{68} phosphorylation by ATM (Foray et al., 2003). Following ATM-dependent activation, Chk2 is released from the damaged DNA-associated complex to target its downstream substrates, thus amplifying the checkpoint signal (Lukas et al.,

2003) and this may involve Chk2-dependent phosphorylation of BRCA1 (Ahn et al., 2004).

A detailed overview of Chk1 protein kinase will be discussed in the later sections.

1.3.1.3 Effectors

Chk1 and Chk2 transduce checkpoint activation signals to numerous effectors of which the best characterised are the dual-specificity phosphatases Cdc25A and Cdc25C. Phosphorylation on Ser^{124} by both checkpoint kinases mediates the degradation of Cdc25A. This prevents the removal of inhibitory phosphate groups on Thr^{14} and Tyr^{15} of Cdk2, thus halting G_1/S-phase progression (Falck et al., 2001, Sorensen et al., 2003). Similarly, Chk1 and Chk2 phosphorylation of Cdc25C on Ser^{216} promotes 14-3-3 binding and initiates Cdc25C cytoplasmic relocalisation (Peng et al., 1997, Matsuoka et al., 1998, Lopez-Girona et al., 1999). As a result, Cdk1-cyclin B remains inactivated and G_2/M transition is prevented.

In addition, Chk2 phosphorylates E2F1 at Ser^{364} which results in increased protein stabilisation and transcriptional activation leading to apoptosis (Stevens et al., 2003). Chk1 and Chk2 phosphorylation of p53 at Ser^{15}, Thr^{18}, Ser^{20} and Ser^{37} has been reported *in vitro* (Shieh et al., 2000, Hirao et al., 2000, Craig et al., 2003). Modification of these residue is thought to disrupt interaction with its inhibitory protein, murine double minute 2 protein (MDM2), leading to increased transcriptional activation of its target genes including $p21^{waf1}$ (Chehab et al., 1999,

Bean and Stark, 2001). This illustrates how Chk1 and Chk2 integrate the checkpoint activation signal from ATR/ATM to phosphorylate numerous substrates and effect a cell cycle arrest.

1.3.2 DNA repair

Multiple DNA repair mechanisms have evolved to cope with the myriad of DNA damage which occurs within the cell. This includes base excision repair which deals with damaged DNA bases, nucleotide excision repair, which removes UV-induced DNA lesions such as thymine dimers and mismatch repair, which corrects replication errors (Houtgraaf et al., 2006).

Double-stranded DNA break induced by ionising radiation and reactive oxygen species are lethal forms of DNA damage and if left unchecked, can initiate carcinogenesis and apoptosis. Two distinct repair mechanisms have developed to manage DSBs, namely homologous recombination (HR) and non-homologous end joining (NHEJ). HR utilises the extensive DNA homology region on the undamaged sister chromatid to generate a relatively error-free repair, whereas NHEJ facilitates the ligation of free ends without the presence of a homologous template in a more error-prone manner. Due to its requirement for a sister chromatid, HR is only activated in S or G_2-phase whereas G_1 and G_0 or terminally differentiated cells rely on NHEJ (Wyman and Kanaar, 2006). It has been recognised that DNA damage is often associated with phosphorylation of histone H2AX which is believed to facilitate recruitment of DNA damage response

proteins (Fernandez-Capetillo et al., 2004). Indeed, it has been shown that in response to DSBs, ATM/ATR-mediated H2AX phosphorylation is necessary for the recruitment of cohesin during the HR reaction (Unal et al., 2004, Strom et al., 2004). In addition, the fact that the MRN complex may process the DSB ends in HR demonstrates how the checkpoint signals and DNA repair pathway are integrated (Khanna and Jackson, 2001).

1.3.3 Apoptosis

Programmed cell death or apoptosis is activated in response to irreparable DNA damage as it is deleterious for the excessively damaged chromosomes to be replicated. Furthermore, some cells such as lymphocytes and epithelial cells in gut are highly sensitive to low level of DNA damage and will activate the apoptotic program instead. However it is not clear what causes the cell to trigger its apoptotic program after it is overwhelmed by excessive DNA damage. One of the key players could be the p53 protein. After genotoxic stress, p53 is phosphorylated by ATM and the checkpoint kinases which promotes dissociation from its inhibitor, MDM2 (Colman et al., 2000). This results in increased p53-dependent transcriptional activation of genes which include DNA repair proteins and cell cycle inhibitors. It is believed that post-translational modifications and increased levels of p53 protein in response to high levels of DSBs can lead to up-regulation of pro-apoptotic genes such as BCL2-associated X protein (Bax), p53-upregulated modulator of apoptosis (PUMA), FAS (apoptosis stimulating factor) receptor and Noxa (Yu and Zhang, 2003, Roos and Kaina, 2006). Puma and Noxa facilitate

cytochrome C release from the mitochondria by activating Bax or Bak mitochondrial translocation and also by inhibiting anti-apoptotic Bcl2-family proteins. Cytochrome C activates Apaf-1 which leads to apoptosome assembly and caspase activation (Borges et al., 2008). Similarly, in the presence of DNA damage, c-Jun NH(2)-terminal kinase (JNK) promotes Bax translocation into the mitochondria through phosphorylation of 14-3-3 complex, a cytoplasmic anchor of Bax (Tsuruta et al., 2004). In addition to cytochrome C, Smac/Diablo (second mitochondria-derived activator of caspases) is also released into the cytoplasm to induce apoptosis via the apoptosome-dependent pathway and cleavage of inhibitors of apoptosis (IAPs) (Kim, 2005). Activated p53 is also known to trigger the death-receptor pathway that involves the Fas receptor and its ligand, both of which are upregulated in response to UV irradiation (Roos and Kaina, 2006, Timares et al., 2008). Activated Fas ligand-receptor mediates the formation of a death-inducing signalling complex (DISC), which contains the Fas-associated death domain (FADD) and caspase 8. In type I cell death, processed caspase 8 directly activates the executioner molecule, caspase 3 whilst in type II cell death, caspase 8 functions to release pro-apoptotic proteins such as cytochrome C from the mitochondria which then amplifies the apoptotic signal (Kim, 2005).

Given the fact that over 50 % of tumour cells are defective in p53, a p53-independent apoptotic mechanism appears necessary (Roos and Kaina, 2006). One such pathway involves E2F1 and the p53 homolog, p73 protein. Upon DNA damage, Chk1 and Chk2 mediate E2F1 stabilisation through phosphorylation. This results in the transactivation of the p73 gene and increased DNA-damage induced

cell death in a p53-independent manner (Urist et al., 2004). p73 has been shown to mediate the transactivation of PUMA which leads to Bax mitochondria translocation and cytochrome C release (Melino et al., 2004). A caspase-independent pathway also exists via the apoptosis-inducing factor (AIF). Upon pro-apoptotic signals, flavoprotein AIF translocates from the permeable mitochondria to the nucleus, where it binds to DNA and induces chromatin condensation and DNA fragmentation through unknown mechanism (Cande et al., 2002).

1.3.4 Senescence or Adaptation

Damaged cells do not always undergo apoptosis; they can also initiate another response by undertaking an irreversible growth arrest, termed cellular senescence, so that deleterious effects are not propagated to its progeny (Bartek and Lukas, 2007). DNA damage-initiated senescent cells are often characterised by senescence-associated DNA damage foci (SDFs) which contain DDR proteins such as ATM, 53BP1 (p53-binding protein 1) and phosphorylated histone (γ-H2AX) (Campisi and d'Adda di Fagagna, 2007). However, it is not clear if SDFs play a key role in the induction of senescence or whether it is just an artefact created as a result of an earlier response to facilitate DNA repair. Increasing evidence points to p53 as an important link in senescence. Tumour cells with wild-type p53 are more likely to senesce in response to chemotherapy as compared to cells with mutant p53 (Ling et al., 2000, Roberson et al., 2005). This is often accompanied by increased expression of $p21^{waf1}$ which is involved in G_1 arrest (Di

Leonardo et al., 1994, Herbig et al., 2004). Senescence growth arrest can also be mediated through the p16 pathway. Telomere damage induces the delayed expression of p16 which mediates G_1/S arrest through pRb pathway, especially in a defective p53 setting (Jacobs and de Lange, 2005). However, the mechanism by which the p53 or p16 pathway in controlling senescence is not clear. It is also not clear what governs the cell in its choice between apoptosis or senescence. It was speculated that the nature and intensity of damage may be important as well as the cell type as damaged fibroblasts and epithelial cells are likely to senesce while damaged lymphocytes tend to undergo apoptosis (Campisi and d'Adda di Fagagna, 2007).

Adaptation, a process whereby the cells resume cell cycle progression in the presence of persistent DNA damage, was first described in yeast *S.cerevisiae* (Toczyski et al., 1997). It was later reported that checkpoint adaptation also exists in *Xenopus* in response to DNA replication blocks and in human cells after IR (Yoo et al., 2004, Syljuasen et al., 2006). The molecular mechanisms of checkpoint adaptation are relatively unknown, however evidence points to polo-like kinase 1 (Plk1) as the dominant player in this network. Plk1 deletion or depletion in *S.cerevisiae* and human cells respectively prevent mitotic entry in later stages after DNA damage (Toczyski et al., 1997, Syljuasen et al., 2006). One possible mechanism might involve the link between Plk1 and Chk1. Plk1 has been shown to phosphorylate Claspin at Ser^{934} resulting in its dissociation from chromatin in *Xenopus* and this prevents Claspin-mediated activation of Chk1 (Yoo et al., 2004). In human cells, Claspin undergoes β-TrCP-SCF ubiquitin ligase-

dependent degradation after phosphorylation by Plk1 in checkpoint recovery (Mailand et al., 2006, Peschiaroli et al., 2006). Checkpoint recovery allows the cells to re-enter the cell cycle after DNA damage is repaired through attenuation of checkpoint signals. Checkpoint recovery and adaptation pathways often involve the same components (Bartek and Lukas, 2007) however, Claspin might be dispensable for checkpoint adaptation as depletion of Claspin in human cells did not accelerate mitotic entry after IR (Syljuasen, 2007). It is possible that Plk1 may activate phosphatases such as PPM1D (Protein phosphatase magnesium-dependent 1 delta) that dephosphorylates Chk1 (Lu et al., 2005). It is also suggested that CDK1-cyclin B may be targeted by Plk1 during G_2 checkpoint adaptation as the level of inhibitory phosphorylations on CDK1-cyclin B is decreased by Plk1-mediated degradation of Wee1 kinase (van Vugt et al., 2004). At the same time, cyclin B levels increase during prolonged G_2 arrest and this triggers the termination of IR-induced checkpoint in HeLa cells (Syljuasen, 2007). It is not clear what the physiological significance of checkpoint adaptation is. One possible reason could be to allow the damaged cells to move into a phase where apoptosis is initiated. Another interesting theory is that adaptation may exist to allow natural evolution at the expense of genomic instability (Syljuasen, 2007).

1.4 Checkpoint kinase 1

Checkpoint kinase 1 or Chk1 was first discovered in fission yeast and operates in DNA damage checkpoints (Walworth et al., 1993, al-Khodairy et al., 1994). Its checkpoint function is largely conserved among *S.cerevisiae*, *S.pombe*, *Drosophila*,

X.laevis and mammals, though the checkpoint signal specificity that regulates Chk1 has diverged. Sequence analysis also revealed a high degree of similarity among Chk1 homologs (Fogarty et al., 1997, Sanchez et al., 1997, Nakajo et al., 1999, Chen and Sanchez, 2004). Although both fission and budding yeast Chk1 are dispensable for viability, Chk1 has been shown to be an essential kinase in the development of mammalian embryonic stem cells and Chk1-null murine embryos fail to develop beyond the blastocyst stage and exhibit grossly abnormal morphology (Takai et al., 2000, Liu et al., 2000). Similarly, abrogation of Chk1 in *Xenopus* embryos triggers apoptosis after the midblastula transition (Carter and Sible, 2003). Chk1-deficient somatic cells also display aberrant checkpoint function, indicating that Chk1 is required for the normal proliferation of adult somatic cells (Zachos et al., 2003, Lam et al., 2004). Cytogenetic analysis discovered that the *CHK1* gene is localised to chromosome 11q24, which is adjacent to the *ATM* gene at 11q23 (Sanchez et al., 1997). Northern blot analysis showed that the *CHK1* gene is detected in all human tissues examined and in large amounts in human thymus, testis, small intestine and colon (Sanchez et al., 1997). Chk1 mutations are rare in human tumours, however loss of heterozygosity (LOH) at chromosome 11q21-24, a region containing several tumour suppressors including Chk1 is observed in a variety of human malignancies (Kramer et al., 2004a).

1.4.1 Chk1 Structure

Chk1 is made up of 476 amino acids which comprise an N-terminal catalytic domain (residues 1-265), for which the crystal structure has been elucidated, a flexible linker region and a less well-conserved C-terminal regulatory domain that is thought to contain a pseudosubstrate sequence which can auto-inhibit the catalytic domain (Figure 1.3) (Chen et al., 2000). A detailed outline of Chk1 structure is given in the introduction to Chapter 4.

1.4.2 Regulation of Chk1

1.4.2.1 Post-translational modification

The Chk1 protein kinase contains several conserved SQ/TQ phosphorylation motifs in the regulatory domain which are recognised by ATR/ATM. Of these SQ/TQ sites, Ser^{345} was the first residue found to be phosphorylated by ATR in response to UV, IR and hydroxyurea (HU) treatment (Liu et al., 2000). Subsequent studies have shown that Ser^{317} is also phosphorylated by ATR and site-directed mutagenesis indicates that phosphorylation on Ser^{317} and Ser^{345} contributes to the activation of Chk1 and its increased kinase activity (Zhao and Piwnica-Worms, 2001). As aforementioned, ATM is also capable of phosphorylating Chk1 on Ser^{317} and Ser^{345}, further demonstrating a high degree of crosstalk and connectivity between the ATM and ATR pathways (Gatei et al., 2003, Kurz et al., 2004). It has been suggested that Ser^{317} and Ser^{345} phosphorylation induce a conformational change within Chk1 leading to the release of the regulatory domain autoinhibition which activates the kinase (Zhao and Piwnica-Worms, 2001).

In addition, phosphorylation of $Ser^{317/345}$ has been shown to promote dissociation of Chk1 from chromatin, leading to phosphorylation of Chk1's soluble substrates (Smits et al., 2006). Indeed, the spatial effect of phosphorylated Chk1 is observed after laser microirradiation where it spreads rapidly throughout the nucleus (Bekker-Jensen et al., 2006). The localisation effect of $Ser^{317/345}$ phosphorylation was further elucidated in an elegant study where phosphorylation at Ser^{317} was found to be important for Chk1 release from the chromatin and for subsequent effective modification on Ser^{345} which promotes its cytoplasmic localisation and association with the centrosomes (Niida et al., 2007). It was observed that centrosomal localisation of Chk1 is important for checkpoint function as forced immobilisation of $Ser^{317/345}$ mutants at the centrosome prevents mitotic catastrophe, indicating that two-step phosphorylation of Ser^{317} and Ser^{345} regulates centrosomal association (Niida et al., 2007). However, in another study, Ser^{345} phosphorylation was seen to produce different results. It was determined that sequences around Ser^{345} form a putative 14-3-3 binding motif and that phosphorylation at this site mediates 14-3-3 association which blocks Crm1-dependent nuclear export of Chk1 (Jiang et al., 2003).

Other studies have shown that ATR-dependent phosphorylation on Ser^{345} not only leads to Chk1 activation but also mediates delayed degradation by the cullin family E3-ligase members, Cul1 and Cul4A (Zhang et al., 2005). It was speculated that coupling of the activation and subsequent degradation of Chk1 prevents its constitutive activation and allows cellular recovery from checkpoint activation, thus permitting DNA replication to resume (Zhang et al., 2005). Oncogenic

PPM1D has been identified as the serine/threonine phosphatase which binds Chk1 and dephosphorylates ATR-mediated phospho-Ser^{345} but not phospho-Ser^{317}, leading to decreased Chk1 kinase activity and checkpoint recovery (Lu et al., 2005).

Further inhibitory mechanisms for Chk1 have been identified, for example, protein kinase B/Akt (PKB/Akt) phosphorylates a conserved site at Ser^{280} (Shtivelman et al., 2002). Analysis has pointed out that Ser^{280} modification prevents complex formation, presumably with Claspin, as well as ATR-activating phosphorylation at Ser^{345}, leading to defective checkpoint function (King et al., 2004). Phosphatase and tensin homologue (PTEN) is an inhibitor of PKB/Akt. Chk1 kinase activity is significantly lower in $PTEN^{-/-}$ cells as compared to wild-type cells and this is due to activated PKB/Akt-dependent phosphorylation of Chk1 on Ser^{280} (Puc et al., 2005). In addition, it was shown that Ser^{280} phosphorylation triggers monoubiquitination of Chk1 on Lys^{274} and mediates enhanced cytoplasmic localisation, leading to defective checkpoint function (Puc and Parsons, 2005).

Phosphorylation of Chk1 at novel sites, Ser^{286} and Ser^{301}, were also reported (Shiromizu et al., 2006). These modifications were mediated by CDK1 during early mitosis. The physiological significance of this phosphorylation is not clear as it does not affect Chk1 subcellular localisation and kinase activity. However phosphorylation at Ser^{286} and Ser^{301} appeared to block $Ser^{317/345}$ phosphorylation in nocodazole-arrested mitotic cells, suggesting that CDK1-targeted mitotic phosphorylation of Chk1 might prevent Chk1 activation during early mitosis

(Shiromizu et al., 2006). This mode of mechanism was seen in Cdc25C where phosphorylation at Ser^{214} by CDK1 prevents Chk1-inactivating phosphorylation on Ser^{216} during mitosis (Bulavin et al., 2003).

A large-scale proteomic analysis of ATM/ATR phosphorylated substrates in response to DNA damage has identified Chk1 Ser^{308} as a novel phosphorylation site, though its biological significance is unknown (Matsuoka et al., 2007). It is however possible that Ser^{308} is an autophosphorylation site, just as Ser^{296} is suggested to be (Clarke and Clarke, 2005). Autophosphorylation of Chk1 was first observed in *S.pombe* studies but has been suggested to have minimal effect on Chk1 kinase activity (Walworth and Bernards, 1996, Chen et al., 2000). Chk1 autophosphorylation sites have not been mapped out but deletion analysis suggested that they are found in the C-terminal domain and possibly the linker region (Chen et al., 2000, Ng et al., 2004).

1.4.2.2 Adaptor proteins

In addition to post-translational modifications, adaptor proteins are also involved in the regulation of Chk1. A well-characterized example is Claspin. It was first identified as a novel essential upstream regulator of *Xenopus* Chk1 (xChk1), where immunodepletion of *Xenopus* Claspin (xClaspin) resulted in the abrogation of xChk1 activation and therefore DNA replication checkpoint (Kumagai and Dunphy, 2000). In addition, xATR/ATRIP phosphorylated xChk1 only weakly in the absence of xClaspin (Kumagai et al., 2004). Claspin has also been found to

associate with ATR and Rad9, a subunit of the 9-1-1 complex (Chini and Chen, 2003) and it is thought that a transient interaction between xClaspin and chromatin is sufficient for the activation of xChk1 (Lee et al., 2005).

Phosphorylation of Claspin is required for its interaction with Chk1 since dephosphorylation of xClaspin abolishes binding with xChk1 (Kumagai and Dunphy, 2000) and in the mammalian system, this is dependent on ATR and phosphorylated Rad17 (Wang et al., 2006). Using deletion analysis, it was found that binding involves a 57 amino acid region in the C-terminal domain of xClaspin which contains two highly conserved repeated phospho-peptide motifs (ExxxLC(S/T)GxF). Phosphorylation of Ser^{864} and Ser^{895} in each repeat is essential for xChk1 interaction with Claspin as mutation at either serine residue reduced xChk1 binding by more than 50 % and the double-mutant was unable to associate with xChk1 (Kumagai and Dunphy, 2003). On the other hand, human Claspin has three Chk1-binding motifs of which phosphorylation at Thr^{916} and Ser^{945} but not Ser^{982} are necessary for Chk1 recognition and its subsequent activation (Clarke and Clarke, 2005). It also seems that differential phosphorylation requirements exist in response to distinct types of DNA damage. xClaspin is phosphorylated at Thr^{817} and Ser^{819} in the SQ/TQ motifs recognized by xATR upon double-stranded breaks whilst Ser^{864} and Ser^{895} are phosphorylated in response to stalled replication forks. This may suggest that the specificity of Claspin in response to different DNA damage could be determined by site-specific phosphorylation, which would potentially expand the functional diversity of the protein (Yoo et al., 2006).

It was originally thought that ATR was the kinase that phosphorylates xClaspin on Ser^{864} and Ser^{895}, as xATR depletion abrogated xClaspin phosphorylation and thus binding to xChk1 (Kumagai and Dunphy, 2003). However, the serine residues phosphorylated do not resemble the preferred ATR substrate consensus motif (SQ/TQ) and furthermore, direct phosphorylation of Claspin by ATR has not been observed. Thus it seems that an intermediate kinase might be responsible for the modification (Kumagai and Dunphy, 2003). Interestingly, in mammalian systems, Chk1 was found to phosphorylate Claspin at Thr^{916} and it was therefore suggested that Claspin and Chk1 could interact in a phosphorylation-independent manner to initiate ATR-mediated activation of Chk1 and that this association is maintained through Chk1 phosphorylation of Claspin (Chini and Chen, 2006). Indeed, Claspin stabilization has been shown to require active Chk1 kinase. This highlighted the existence of a positive autoregulatory feedback loop, in which Chk1 stabilizes Claspin, while Claspin facilitates the activation of Chk1 (Chini et al., 2006).

The Claspin docking site has also been mapped to a region surrounded by positively charged residues that contains Lys^{54}, Arg^{129}, Thr^{153} and Arg^{162} within the kinase domain of xChk1 (Jeong et al., 2003). Interestingly, these four residues form a putative phosphate-binding site that is involved in Chk1 catalytic activity (Chen et al., 2000). This could explain the phosphorylation requirement of Claspin to associate with Chk1. Furthermore, it was also suggested that given the spacing between the two Chk1-binding motifs in xClaspin, two Chk1 monomers could interact with a single molecule of Claspin to facilitate Chk1 intermolecular

autophosphorylation. However this remains to be seen (Jeong et al., 2003). Although no stable interaction between Claspin and the C-terminal domain of Chk1 has been observed, it appears that this regulatory domain also has a role in mediating Claspin-Chk1 interaction as deletion of all or part of the xChk1 regulatory domain significantly diminished binding of xChk1 to xClaspin (Jeong et al., 2003).

The significance of Claspin in the checkpoint pathway has been highlighted by the observation that it is targeted for inactivation during the adaptation process in *Xenopus* studies. This involves the docking of xPolo-like kinase (xPlk) onto xClaspin primed by phosphorylation at Thr^{906} which then allowes xPlk-dependent phosphorylation of xClaspin at Ser^{934}. This leads to the dissociation of xClaspin from chromatin, xClaspin inactivation and therefore attenuation of the checkpoint response (Yoo et al., 2004). Interestingly, the temporal regulation of Claspin and Chk1 are similar; both protein levels peak at unperturbed late S-phase and their levels declined in mitosis (Chini and Chen, 2003). Increasing evidence has shown that Claspin can function in the cell cycle progression of unperturbed cells when its localization to the replication fork is dependent on replication initiation proteins, MCM 2-7 and Cdc45, but independent of ATR, RPA and Rad17 in *Xenopus* (Lee et al., 2003). Electron microscopy studies have also revealed that Claspin is a ring-shaped molecule that can encircle the DNA, specifically at the single-stranded branch points, with high affinity, and this suggests that Claspin may monitor unperturbed DNA replication and function as a direct sensor protein at the stalled replication fork (Sar et al., 2004). In unperturbed cycling cells, Claspin is also

targeted for degradation at the onset of mitosis. This is dependent on Plk1-mediated phosphorylation of a phosphodegron motif (^{29}DSGxxS^{40}) located in the N-terminal domain of Claspin, which is then recognized by SCF$^{\beta TrCP}$ ubiquitin ligase. Mutant Claspin which cannot be degraded stabilizes Chk1 activation, thus abrogating cell cycle progression into mitosis (Mailand et al., 2006, Peschiaroli et al., 2006, Mamely et al., 2006). Claspin is also targeted for cleavage by caspase-7 at Asp^{1072} during apoptosis, illustrating a key regulation in the balance between cell cycle arrest and apoptosis in response to DNA damage. This cleavage separates the two functional domains of Claspin, a Chk1-binding N-terminal domain and a DNA-binding C-terminal domain (Clarke et al., 2005).

In mammalian cells, other proteins have also been implicated in the activation of Chk1 as siRNA-mediated depletion of Claspin did not fully block Chk1 activation following DNA damage (Chini and Chen, 2003). Claspin has been shown to associate with BRCA1 where it mediates BRCA1 phosphorylation on Ser^{1524}. This modification is significantly reduced upon Claspin-depletion. Claspin could also cooperate with BRCA1 to regulate Chk1 activation after UV or IR as siRNA-mediated ablation of either Claspin or BRCA1 greatly diminished Chk1 phosphorylation on Ser^{345}. However, combination of both siRNAs did not result in greater inhibition of Chk1 activation (Lin et al., 2004). In *Xenopus*, xClaspin and xBRCA1 have been shown to act synergistically to potentiate the activation of xChk1 as addition of both exogenous xClaspin and xBRCA1 to cells depleted of endogenous xClaspin and xBRCA1 resulted in stronger phosphorylation of xChk1 than addition of either protein alone (Yoo et al., 2006). TopBP1 has also been

implicated in the activation of Chk1 as it is required for ATR-mediated phosphorylation of Chk1 and its various substrates; phosphorylation of Chk1 is greatly diminished in TopBP1-deficient cells as compared to Claspin-deficient cells (Liu et al., 2006). Diminshed Chk1 phosphorylation may however be explained by the xTopBP1-dependent activation of xATR which places TopBP1 upstream of Claspin in the signalling cascade (Kumagai et al., 2006). In another study, Mediator of DNA Damage Checkpoint Protein 1 (MDC1) was implicated in ATR-dependent Chk1 activation as its depletion resulted in defective phosphorylation of Chk1 (Stewart et al., 2003). It also appears that ATM phosphorylation of Chk1 is dependent on a functional Nijmegen breakage syndrome protein 1 (Nbs1) which may facilitate Chk1 access to ATM (Gatei et al., 2003).

1.4.3 Functions of Chk1

Even though the role of Chk1 in the checkpoint response has been conserved among organisms ranging from yeasts to mammals, it has evolved to take on a broader responsibility in the mammalian DNA damage response. Indeed, while *S.cerevisiae* Chk1 is only activated in the late S and G2 phase, mammalian Chk1 also functions in the intra-S phase and the mitotic/spindle checkpoint. Although, Chk1 is largely expressed in the S and G_2-phase (Lukas et al., 2001), it has been implicated in the G_1/S phase checkpoint where UV-induced degradation of Cdc25A is dependent on Chk1 but not p53 (Mailand et al., 2000). The following sections summarise the role of Chk1 in the mammalian checkpoints.

1.4.3.1 G_2/M Checkpoint

The G_2/M checkpoint serves as a control for cell cycle transition from G_2-phase to mitotic-phase of which the centrosome acts as a 'command centre' (Doxsey, 2001). Increasing evidence has highlighted the importance of its role and a rapidly growing list of cell cycle regulatory proteins such as Chk1, Chk2, p53, Aurora A, Plk1, Cdc25, CDK1 and cyclin B are found to associate with the centrosome (Kramer et al., 2004a).

It recently became clear that CDK1-cyclin B is first activated at the centrosome in prophase for mitotic initiation (Jackman et al., 2003). As aforementioned, Cdc25C is a positive regulator of CDK1-cyclin B but in the event of unreplicated or damaged DNA, it becomes phosphorylated by Chk1 on Ser^{216} which creates a 14-3-3 binding site (Sanchez et al., 1997). This forces the cytoplasmic sequestration of Cdc25C and/or masks the residues required for interaction with CDK1-cyclin B (Dalal et al., 1999, Morris et al., 2000, Sancar et al., 2004). However it has been reported that ionising radiation treatment did not lead to increased Cdc25C Ser^{216} phosphorylation and inactivation of Cdc25C did not correlate with increased 14-3-3 association. It has been suggested that inactivation of Cdc25C results from novel Chk1-mediated phosphorylation sites, though this has yet to be demonstrated (Blasina et al., 1999). It was shown that Chk1-targeted phosphorylation of Cdc25A on Ser^{178} and Thr^{507} inhibits Cdk1 association via 14-3-3 binding (Chen et al., 2003a). On the other hand, Chk1 further enforces the inactivation of CDK1-cyclin B through its phosphorylation of Wee1 kinase on Ser^{549} which creates a 14-3-3 binding site and enhances its kinase activity (O'Connell et al., 1997, Lee et al.,

2001, Rothblum-Oviatt et al., 2001). Similarly, the tyrosine kinase Mik1 is stabilised by Chk1 upon DNA damage checkpoint activation in fission yeast (Baber-Furnari et al., 2000). Wee1 and Mik1 catalyse the inactivation of CDK1 through inhibitory phosphorylation on Tyr^{15}.

Chk1's role in mediating the inactivation of CDK1-cyclin B at the centrosome is emphasised by reports that Cdk1 activation is correlated with Chk1 disappearance from the centrosome (Kramer et al., 2004b), and depletion of Chk1 resulted in activation of CDK1-cyclin B (Hu et al., 2001). Furthermore, forced immobilisation of kinase-dead Chk1 at the centrosome prompted premature activation of CDK1 while wild-type Chk1 prevented the timely activation of CDK1 (Kramer et al., 2004b).

Chk1 also negatively controls the level of CDK1-cyclin B by regulating transcriptional repression. In unperturbed cells, Chk1 actively phosphorylates histone H3 at Thr^{11} and this is dependent on Chk1's association with chromatin. This modification allows the histone acetyltransferase, GCN5, to bind and mediate the recruitment of transcription factors and elevate the transcriptional level of CDK1 and cyclin B. In the event of DNA damage, phosphorylated Chk1 undergoes chromatin dissociation, resulting in hypophosphorylated histone H3-Thr^{11}, reduced GCN5 binding and thus transcriptional repression of CDK1 and cyclin B (Shimada et al., 2008).

It is also interesting to note that viral infection can activate the Chk1 response as demonstrated by human immunodeficiency virus type 1 (HIV-1) viral protein R (Vpr). This protein induced a G_2 arrest that was dependent on ATR and Chk1-mediated inactivation of Cdk1-Cyclin B, although it was not clear whether Vpr actually inflicts DNA damage or it elicits a signal that mimics DNA damage (Roshal et al., 2003). Similarly, accumulation of reactive oxygen species (ROS) induced G_2/M arrest that is also dependent on Chk1 (Zhang et al., 2001).

1.4.3.2 Intra-S Checkpoint

During DNA replication in S-phase, genotoxic stress can cause stalled replication forks, preventing cell cycle progression. If left unchecked, stalled replication forks will become unstable and are prone to collapse, resulting in genomic instability and chromosomal aberrations. Therefore checkpoints are activated to arrest the cell cycle, block late origin firing, stabilise stalled replication forks and then re-initiate DNA replication (Paulsen and Cimprich, 2007). Increasing evidence has also shown that Chk1 is an essential kinase involved in the regulation of S-phase progression in unperturbed cells (Syljuasen et al., 2005, Petermann et al., 2006).

Replication blocks can cause the uncoupling of DNA polymerase and helicase activities and lead to excessively long stretches of ssDNA that are coated with RPA (replication protein A) as evident in Xenopus studies (Walter and Newport, 2000). This provides an initiating signal for ATR activation in cells following UV irradiation (Ward et al., 2004). Activated Chk1 then phosphorylates Cdc25A

phosphatase at Ser^{124} which prompts proteolytic degradation. Hyper-phosphorylated Cdc25A fails to remove phosphate groups at CDK2-Cyclin E, thus mediating S-phase arrest (Xiao et al., 2003, Zhao et al., 2002). In addition, Chk1 also functions to inhibit late replicon initiation via the same Cdc25A pathway where loss of Chk1 stimulates the initiation of DNA replication, even in the absence of DNA damage (Feijoo et al., 2001, Heffernan et al., 2002, Miao et al., 2003).

It has been suggested that Chk1 functions to stabilise stalled replication forks and/or restart replication blocks. This follows the discovery that Chk1-deficient DT40 cells failed to maintain viable replication structures and were unable to restart DNA replication after release from replication block (Zachos et al., 2003, Zachos et al., 2005). Using a DNA fibre-labelling technique, it was further reported that ablating Chk1 resulted in reduced global rates of replication fork progression. This suggested that Chk1 is involved in maintaining the stability of replication forks (Petermann et al., 2006).

Proliferating cell nuclear antigen (PCNA) is a homotrimeric ring protein that acts as a processivity factor for DNA polymerase Pol δ in both DNA replication and DNA repair (Moldovan et al., 2007). A link between PCNA and Chk1 was first described in *S.pombe* where PCNA together with $p21^{waf1}$ functions to inhibit cell cycle progression through Chk1 protein kinase upon DNA damage (Tournier et al., 1996). Since then, Chk1 and Claspin have been shown to interact with PCNA and this interaction is reduced in the event of DNA damage (Brondello et al., 2007,

Yang et al., 2008, Scorah et al., 2008). Chk1 association with PCNA is dependent on a highly conserved PCNA-interacting protein (PIP) box motif (^{378}TRFF^{381}) identified in the Chk1 C-terminal domain. Furthermore, mutation of the PIP box leads to defective G_2/M and S-phase checkpoint due to reduced ATR-dependent phosphorylation of Chk1 and hence defective dissociation of Chk1 from chromatin (Scorah et al., 2008). It was also demonstrated that Chk1, together with Claspin and Timeless, regulates DNA damage-induced PCNA ubiquitination in an ATR-independent manner (Yang et al., 2008). However, in another study, ATR was implicated in ubiquitination of PCNA. It was shown that monoubiquitination of PCNA is ATR/Chk1-dependent and is required for interaction with the translesion synthesis DNA polymerase Pol κ. This allows replication forks to continuously advance along damaged DNA, thereby attenuating the S-phase checkpoint (Bi et al., 2006).

These observations supported the concept that the ATR-Chk1 pathway operates in S-phase to regulate DNA replication and that this checkpoint signal is amplified in the presence of genotoxic stress, though the mechanism of amplification remains unclear.

1.4.3.3 Mitotic Spindle Checkpoint

The mitotic spindle checkpoint is activated to prevent unattached or poorly attached kinetochore-microtubules and chromosome mis-segregation. Defects in

the spindle checkpoint are associated with chromosomal instability and aneuploidy (Kops et al., 2005).

Chk1 has been implicated in the mitotic spindle checkpoint. Studies in budding yeast revealed that in the presence of DNA damage, Securin, an anaphase inhibitor, is stabilised by Chk1-mediated phosphorylation which blocks its ubiquitination mediated by the Anaphase Promoting Complex (APC). Hence the cell cycle is blocked before anaphase, presumably to allow DNA repair before sister chromosome segregation (Sanchez et al., 1999) (Wang et al., 2001). In mammalian cells, Chk1 positively regulates the spindle checkpoint through the activation of Aurora B. Optimal Aurora B activity is required for the phosphorylation and localisation of the spindle checkpoint protein BubR1 to the kinetochores which sustains mitotic arrest (Zachos et al., 2007). These data suggest that Chk1 is a positive regulator of the mitotic spindle checkpoint.

Alternatively, Chk1 has been proposed to negatively regulate the spindle checkpoint. Chk1-depleted cells displayed metaphase arrest which was dependent on hyper-activated polo-like kinase 1 (Plk1) (Tang et al., 2006a). Plk1 has been shown to be a positive regulator of the spindle checkpoint (Tang et al., 2006b). Co-depletion of spindle checkpoint proteins BubR1 or Mad2 with Chk1 is able to reverse the effects of Chk1 depletion-induced metaphase block, suggesting that Chk1 could function to inactivate the spindle checkpoint via negative regulation of Plk1 (Tang et al., 2006a). It has been suggested that the differences in these observations may be due to different degrees of Chk1 depletion (Zachos et al.,

2007), as seen in the case of kinetochore proteins (Nuf2R, Ndc80^{Hec1} and Nnf1R), where 80 % depletion of the proteins activates the spindle checkpoint while 99 % depletion inactivates it (Meraldi et al., 2004, McAinsh et al., 2006).

1.4.4 Cellular Responses of Chk1 to anticancer treatment

Most of the therapeutic agents applied in clinical cancer therapy cause DNA damage and thus induce cell cycle checkpoint activation. Given that over half of tumour cells have defects in the p53 and pRb pathway, they rely heavily on the checkpoint kinases to maintain cell cycle arrest. Cancerous cells are able to exploit this double-edged checkpoint mechanism to keep DNA-damaged cells in check and repair the damage necessary to maintain cancer cell propagation, giving rise to chemotherapeutic resistance. Indeed, gene expression profiling has shown that Chk1 is often over-expressed in tumour tissues as compared to normal adjacent cells, demonstrating the over-reliance on this checkpoint kinase for cell cycle progression in tumour tissues (Cho et al., 2005). Furthermore, a genetic alteration analysis of 25 human tumour cell lines revealed no mutation for *CHK1* gene, indicating that integrity of this protein is important to the viability of the tumour cells (Ejima and Yang, 1999). However, in another study, a shorter isoform of CHK1 gene is preferentially expressed in small cell lung cancer as compared to non-small cell lung cancer and normal lung tissues. It was revealed that this shorter *CHK1* isoform lacked 32 amino acids within the carboxyl portion of the kinase domain that could affect substrate recognition (Haruki et al., 2000). It has nevertheless been postulated that targeting Chk1 could be an attractive approach to

circumvent chemotherapeutic resistance. Normal healthy cells with an active p53 pathway are less sensitive to the loss of Chk1 due to the presence of intact and redundant checkpoint pathways. This was clearly shown with WS-1 fibroblasts which exhibited significantly less, and tolerable, cellular apoptosis as compared to U2OS tumour cells in response to antimetabolites (Cho et al., 2005). Moreover normal cells are arrested in G_1 phase in a p53-dependent manner, whereas over half of tumour tissues which are p53-deficient depend more on the S and G_2/M checkpoints. Thus Chk1 represents an Achilles heel in cancer cells that can be targeted to augment conventional therapies. The therapeutic potential of Chk1 inhibitor as a component of cancer therapy is briefly reviewed here.

As aforementioned, inhibiting Chk1 function does not significantly affect normal cells due to compensation from other checkpoint pathway mechanisms. Another point to note is that Chk1 inhibition has very little effect on apoptosis in the absence of DNA-damaging drugs, thus underpinning it as a valid drug target without manifesting cytotoxicity on its own (Chen et al., 2003b).

Many studies have been published investigating the potential of Chk1 abrogation as a chemo-sensitizer in cancer cells treated with anti-cancer agents eliciting various phases of cell cycle arrest. Antimetabolites, such as 5-Fluorouracil (5-FU) and HU which are used widely in cancer treatment, activate Chk1 and elicit S-phase cell cycle arrest through Chk1-mediated Cdc25A degradation and subsequent inhibition of Cdk2. Downregulation of Chk1 potentiates the toxicity of antimetabolites through abrogation of S-phase checkpoint which results in mitotic

catastrophe and eventual apoptosis (Xiao et al., 2005b, Cho et al., 2005). It has also been shown that ablation of Chk1 function also results in increased cellular apoptosis in the presence of DNA-damaging agents such as 6-thioguanine (6-TG), doxorubicin (Dox) and camptothecin (CPT), mediating G_2/M cell cycle arrest (Jackson et al., 2000, Yan et al., 2004, Chen et al., 2006). Similarly, Chk1 inhibition also sensitises cells to anti-mitotic agents such as Taxol and augments mitotic catastrophe and apoptosis (Xiao et al., 2005a). Conversely, it has been shown that Chk1 is required for optimal spindle poison-induced cell death (Zachos et al., 2007).

The importance of Chk1 downregulation in chemotherapy was highlighted in an elegant test which studied the relevancy of three checkpoint kinases, namely Chk1, Chk2 and mitogen-activated protein kinase-activated protein kinase 2 (MK2) in cancer therapy. It showed that only downregulation of Chk1, but not Chk2 or MK2, abrogated chemotherapeutics-induced cell cycle arrest, leading to cell death. Thus this places Chk1 inhibition as the only viable checkpoint target of these three kinases for anticancer treatment (Xiao et al., 2006).

There are conflicting reports on whether targeted Chk1-mediated sensitisation of tumour cells to the cytotoxicity of anti-cancer agents is p53-dependent (Cho et al., 2005, Chen et al., 2006, Vitale et al., 2007). It is noted that topoisomerase inhibitors which impinge upon G_2/M arrest exhibit selective p53 status and DNA replication inhibitors affecting S-phase progression showed no dependence on p53. It was suggested that Chk1 and p53 cooperate to maintain G2 arrest, whereas p53

is not required for S-phase checkpoint, though the mechanisms remain elusive (Tse and Schwartz, 2004). In a recent study, human fibroblast cells starved for pyrimidine nucleotides by treatment with *N*-(phosphonacetyl)-$_L$-aspartate (PALA) exhibited G_1, G_2 and S-phase checkpoint arrest by activating the ATR-Chk1-p53 pathway. This was dependent on functional p53 and its target proteins, p21 and macrophage inhibitory cytokine 1 (MIC1) (Hastak et al., 2008). In cells lacking p53 or with a defective p53 pathway, failure to arrest DNA synthesis during depletion of pyrimidine nucleotides caused irreversible DNA damage that led to apoptosis (Agarwal et al., 1998, Agarwal et al., 2006). It is therefore important to determine which class of therapeutic drugs should be given in conjunction with Chk1 inhibitors, depending on p53 status of the cancer patient, in order to enhance the efficacy of the chemotherapeutic agents.

On a separate note, although methyl methanesulfonate (MMS), HU and aphidicolin (Aph) lead to stalled replication forks, the mechanisms by which replication forks are blocked in response to these agents may vary. Indeed, lesions induced by MMS may be repaired or even bypassed, however this is not observed with HU- or APH-induced replication blocks (Paulsen and Cimprich, 2007). Therefore, it is important to exercise caution when interpreting results even though they affect the same checkpoint.

On an interesting note, activation of cellular senescence programs lead to the suppression of Chk1, as evidenced by the loss of phosphorylation on Ser^{345} and S-phase arrest in response to UV irradiation and CPT treatment. This was

accompanied by chromosomal instability. Thus it was hypothesized that the stimulation of senescence signalling could provide a novel and promising approach for sensitising cells towards cytotoxic drugs (Gabai et al., 2008).

Although it has been shown that Chk1 is a highly promising and viable drug target, caution needs to be exercised as to how it will perform in clinical trials; conflicting /various conclusions may be drawn from the same cell line depending on the drug type, dosage, incubation time, variant cell line, analytical method and different conclusions may be obtained with distinct cell lines due to various defects in the pathway. A prime example of this is the p53-dependence at different phases of cell cycle arrest. Hence, dissecting the interaction of cell cycle checkpoints is an important step to developing effective therapeutic strategies.

1.4.5 Chk1 inhibitors

7-hydroxystaurosporine (UCN-01), initially developed as a novel protein kinase C (PKC) inhibitor, was identified as a viable drug targeting Chk1 that sensitises tumour cells to a wide variety of genotoxic agents (Tse et al., 2007). This inhibitor is 100,000 times more potent than caffeine at abrogating checkpoint arrest (Bunch and Eastman, 1996). Unfortunately, its Phase I/II clinical development has been limited by unfavourable pharmacokinetics and toxicity. UCN-01 exhibited cytotoxicity when administered on its own and importantly it binds avidly to plasma proteins, leading to excess UCN-01 concentration in blood plasma and thus compromising patient safety (Sausville et al., 2001). Furthermore, UCN-01

inhibits a plethora of kinases including Chk2 and Cdk1. Thus identification of alternative highly selective Chk1 inhibitors represents a high priority.

An indolocarbazole named isogranulatimide is structurally related to UCN-01 and was recently shown to inhibit Chk1 selectively (40-fold over Chk2) with an IC_{50} of 100 nM. Its mechanism of action was elucidated where it served as an ATP-competitive Chk1 inhibitor with an additional hydrogen bonding to the ATP-binding pocket compared to UCN-01. This caused a conformational change in the kinase's glycine-rich loop which may contribute to Chk1 inhibition (Jiang et al., 2004). A bis-imide granulatimide analogue was also discovered to inhibit Chk1 with an IC_{50} of 2 nM (Henon et al., 2007).

In addition to developing small-molecule inhibitors to Chk1, alternative ways to down-regulate Chk1 function have been examined. It was shown that using 17AAG, an Hsp90 inhibitor, resulted in the depletion of Chk1 protein and sensitization to gemcitabine (Arlander et al., 2003). In a later study, Chk1 was found to be a chaperone Heat Shock Protein 90 (Hsp90) client and poorly chaperoned Chk1 displayed a very low level of catalytic activity (Arlander et al., 2006). Similarly, using Hsp90 inhibitor, geldanamycin abrogates G_2-phase arrest in p53-negative leukaemia cells through the depletion of Chk1 (Sugimoto et al., 2008). Geldanamycin is known to induce proteosomal degradation of Chk1 (Nomura et al., 2005).

It is likely that more Chk1 inhibitors with increasing potency and selectivity will be discovered in the future. However, an inhibitor exhibiting high enzyme selectivity in a biochemical assay may not be replicated once the compounds enter the cells (Collins and Garrett, 2005). Thus it is important to develop a reliable cell-based assay for measuring inhibitor potency *in vivo*.

1.5 Project Objectives

Chk1 plays an integral role in mediating cell cycle checkpoint pathways and is a promising target for anticancer therapy. The mode of Chk1 activation whereby it undergoes ATR-dependent phosphorylation at Ser^{317} and Ser^{345} has been well characterised and this affects Chk1 association with chromatin. Intrinsic kinase activity is kept at basal level through Chk1 C-terminal domain inhibitory action on the N-terminal catalytic domain. Deletion or truncation of this C-terminal domain relieves autoinhibition (Katsuragi and Sagata, 2004), resulting in increased kinase activity. However it was not clear what mechanisms counteract the autoinhibition. The aims of the project were firstly to validate and characterise Chk1 as a potential regulator of the tumour modifier $p21^{waf1}$ and to dissect the intermolecular interaction between these two proteins in order to better understand the basis of Chk1 substrate recognition. Having discovered that p21 could function as an allosteric activator Chk1 catalytic activator, I then went on to delineate the mechanism by which substrate docking modulate Chk1 function using peptidomimetic ligands.

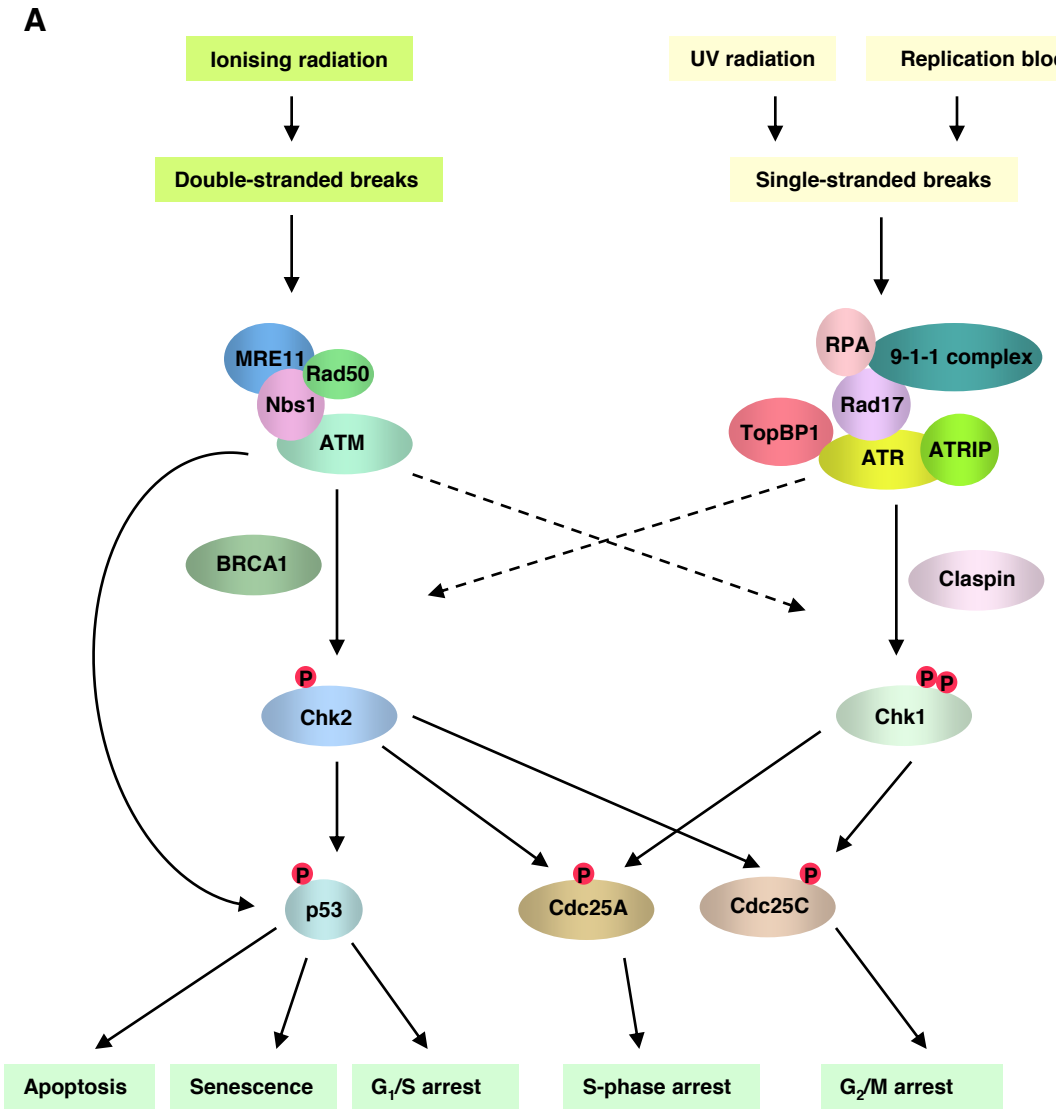

Figure 1.1 A simplified illustration of the ATM and ATR signalling pathway.

(A) Ionising radiation induces double-stranded breaks that leads to activation of ATM in conjunction with the MRN complex. Activated ATM then catalyses the phosphorylation of Chk2 on Thr^{68} that is dependent on BRCA1. On the other hand, UV radiation and/or replication blocks elicit single-stranded break which is coated with RPA. This initiates the ATR signalling cascade that leads to the activation of Chk1 in the presence of adaptor protein Claspin. Both transducer molecules Chk1 and Chk2 go on to phosphorylate effector molecules such as Cdc25A and Cdc25C to regulate S-phase and G_2/M arrest respectively. Furthermore, ATM and Chk2 is able to activate p53 to initiate G_1/S arrest, apoptosis or senescence depending on the condition of DNA damage.

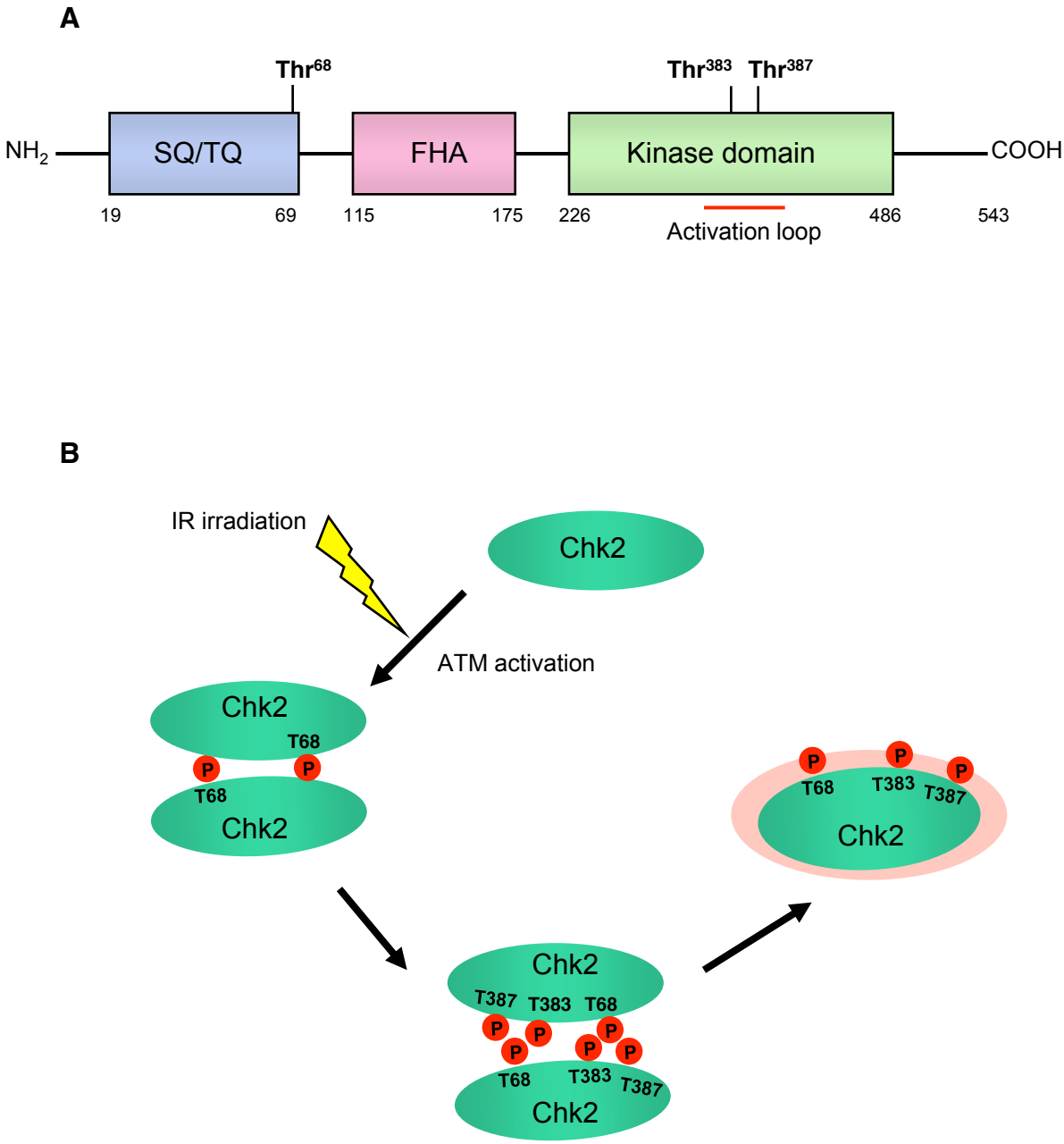

Figure 1.2 A schematic functional domain architecture of Chk2 and its mode of activation.

(A) Chk2 contains three functional domains: a SQ/TQ cluster domain (amino acids 19-69) where Thr^{68} is the main ATM phosphorylation site; a forkhead-associated domain (FHA) (amino acids 115-175) involved in phosphoprotein interaction; kinase domain (amino acids 226-486). (B) In the event of IR irradiation, activated ATM phosphorylates Chk2 on Thr^{68} which induces its dimerisation of another Thr^{68}-phosphorylated Chk2 via the FHA domain. This event initiates inter-molecular autophosphorylation on Thr^{383} and Thr^{387} within the activation loop of the kinase domain, leading to active Chk1 molecules.

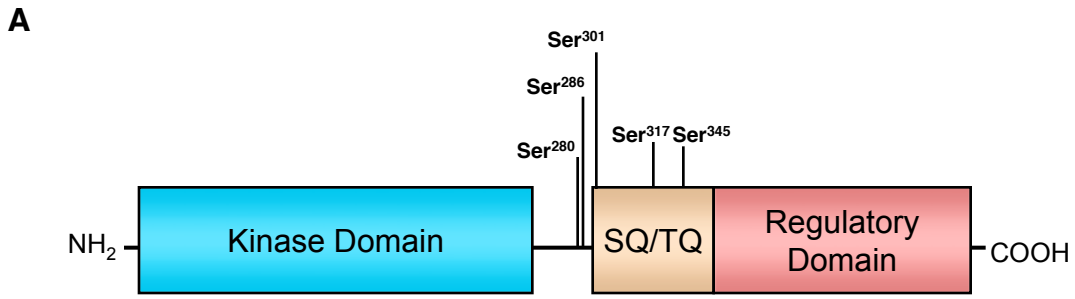

Figure 1.3 A schematic functional domain architecture of Chk1.

(A) Chk1 contains a N-terminal kinase domain, a flexible linker region and C-terminal regulatory domain thought to autoinhibit the catalytic activity of Chk1. Like Chk2, Chk1 also has a SQ/TQ cluster region of which Ser^{317} and Ser^{345} are phosphorylated by ATR. Ser^{280} phosphorylation by PKB/Akt is thought to inactivate Chk1. Cdk1 is thought to phosphorylate Chk1 on Ser^{286} and Ser^{301}.

CHAPTER 2: MATERIALS AND METHODS

2.1 General Reagents

Chemicals and reagents were supplied by Sigma unless otherwise stated. Tissue culture reagents including Dulbecco's modified eagle's medium (DMEM), McCoy's 5A medium, penicillin/streptomycin solution, trypsin-EDTA solution and Lipofectamine™2000 were supplied by Invitrogen unless otherwise stated, while fetal bovine serum (FBS) was supplied by Autogen Bioclear.

2.2 Cell Culture

2.2.1 Mammalian cell culture

2.2.1.1 Cell lines

All cells were kept in a humidified incubator at 37°C. Media were supplemented with 10 % (v/v) fetal bovine serum (FBS). D-MEM was further supplemented with 1 % (v/v) penicillin/streptomycin.

Cell Line	**Source**	**Medium**	**% CO_2**
HeLa	Adenocarcinoma	D-MEM	5
HCT116 WT	Colorectal carcinoma	McCoy's 5A	10
HCT116 p21-/-	Colorectal carcinoma	McCoy's 5A	10

Table 2.1 List of cell lines used in this study.

2.2.1.2 Culturing and cryopreservation of cells

Adherent cell culture were grown to confluency in 10 cm^2 culture dishes containing 10 ml tissue culture medium in optimal conditions before passaging with 1/10 dilution. Cell passaging was performed in a laminar flow hood using aseptic techniques: The medium was discarded before the cells were rinsed with sterile 1x phosphate buffered saline (PBS). Two ml of warmed 1x Trypsin-EDTA solution was added to cover the adhering cell layer and the culture dish was incubated at 37°C until the cells started to detach from the culture dish. Eight ml of appropriate warmed tissue culture medium was added to inhibit further trypsin activity before 1ml of cells culture were transferred to a 9 ml of fresh warmed tissue culture medium in new tissue culture dish.

To cryopreserve cell lines, cells were grown to 90 % confluency in 10 cm^2 tissue culture dish before trypsinised as above. The cells were transferred to a sterile 15 ml Vulcan tube and centrifuged at 1000 revolutions per minute (rpm) for 5 minutes at room temperature. Cell pellet were resuspended gently with 3 ml of freezing medium (50 % (v/v) FBS, 10 % (v/v) dimethyl sulfoxide (DMSO), 40 % (v/v) Tissue culture medium (according to cell line)) and transferred to cryovial (Nunc) at 1 ml /vial. The vials were placed in a Nalgene™ Cryo 1°C freezing storage box at -70°C overnight before transferred to a liquid nitrogen freezer for long-term storage.

To recover cells from liquid nitrogen storage, the cryovial was thawed quickly at 37°C by swirling. Thawed cells were transferred to a sterile 15 ml Vulcan tube.

Nine ml of warmed appropriate tissue culture medium was added drop by drop with swirling before the cells were centrifuged at 1000 rpm for 5 minutes at room temperature. The medium was discarded and the cells were resuspended with 2 ml of tissue culture medium before transferred to a new 10 cm^2 tissue culture dish containing 8 ml of fresh tissue culture medium.

2.2.1.3 Transient transfections

Cells were seeded onto new 10 cm^2 plate in growth medium without antibiotics and grown to 90 % confluency. The cells were transfected with plasmid DNA (in a pcDNA^{TM} 3.2/V5-DEST gateway vector) (Invitrogen) using Lipofectmine^{TM} 2000 (Invitrogen) according to manufacturer's handbook. Eight μg of plasmid DNA was transfected using 8 μl of Lipofectamine^{TM} 2000 in a 1:1 ratio. Cells were then incubated at 37^{o}C overnight before they were harvested or subjected to chemical treatment.

2.2.1.4 Aphidicolin treatment

Aphidicolin (Calbiochem) was dissolved in ethanol at a stock concentration of 2.95 mM and addeded directly to the cell culture to give a final concentration of 20 μM. Treated cells were incubated at 37^{o}C for 4 hours before cells were harvested.

2.2.1.5 Cycloheximide treatment

Cycloheximide was dissolved in DMSO at a stock concentration of 100 mg/ml and added directly to the cell culture to give a final concentration of 30 μg/ml. Cells were harvested at the appropriate time point after treatment.

2.2.2 Bacterial Cell Culture

2.2.2.1 Bacterial Media

Both Lucia-Bertani (LB) medium (1 % (w/v) Tryptone, 0.5 % (w/v) Yeast Extract, 1 % (w/v) NaCl) and LB agar (1 % (w/v) Tryptone, 0.5 % (w/v) Yeast Extract, 1 % (w/v) NaCl, 1.5 % (w/v) Agar, granulated) were sterilised by autoclaving at 121°C for 20 minutes. LB agar was liquefied by heating in a microwave oven. Warmed LB agar was added with selective antibiotic(s) before poured into 90 mm diameter Petri dishes (Sterilin) and left to cool. The culture dishes were stored at 4°C for no longer than one month. Prior to use, the plates were dried at 37°C for 1 hour.

2.2.2.2 Preparation of competent cells

A starter culture was prepared by inoculating 5 μl of DH5α in 2 ml of LB medium and incubated overnight at 37°C at 225 rpm. The starter culture was diluted 1:100 in 200 ml of LB medium and incubated at 37°C at 225 rpm until an OD_{600nm} of between 0.3 and 0.5 was reached. The cells were centrifuged at 4000 x g for 20 minutes at 4°C and resuspended in 80 ml of ice-cold transforming buffer I (30 mM

Potassium acetate, 100 mM RbCl, 10 mM $CaCl_2$, 50 mM $MnCl_2$, 15 % (v/v) glycerol; adjusted to pH 5.8 with acetic acid and sterilised by filtration),. After 10 minutes incubation at 4°C, the cells were centrifuged at 4000 x g for 5 minutes at 4°C and gently resuspended in 8 ml of transforming buffer II (10 mM MOPS, 75 mM $CaCl_2$, 10 mM RbCl, 15 % (v/v) glycerol; adjusted to pH 6.5 with postassium hydroxide and sterilised by filtration). After incubation at 4°C, the cells were aliquoted (100 µl) into sterile microcentrifuge tubes and snap-frozen in liquid nitrogen and stored at -70°C.

2.2.2.3 Transformation of *E.coli* competent cells

Competent *E.coli* cells were transformed with plasmid DNA. Fifty µl of DH5α competent cells were thawed on ice and mixed with 100 ng of plasmid DNA. The cells were incubated on ice for 30 minutes before heat-shocked at 42°C for 45 seconds. Following 2 minutes of incubation on ice, 500 µl of LB medium was added and the cell suspension was incubated at 37°C at 225 rpm for 1 hour. One hundred µl of the cell suspension was then plated onto the warmed LB agar plate containing the selective antibiotics required for the plasmid of interest and incubated overnight at 37°C.

2.2.3 *Sf9* insect cells

2.2.3.1 Culturing of *Sf9* insect cells

Sf9 insect cells were cultured with Sf-900 II serum-free medium supplemented with 1 % (v/v) penicillin/streptomycin in suspension in a spinner flask at 27°C. Cells were subcultured to 1 x 10^6 viable cells/ml when the viable cell density reached 3 x 10^6 viable cells/ml.

2.2.3.2 Transformation of DH10Bac™ *E.coli* with plasmid DNA

For the purpose of converting plasmid containing human *CHK1* gene into Bacmid for infection of *Sf9* insect cells, DH10Bac™ competent cells were used. Two hundred µl of DH10Bac™ competent cells were thawed on ice and mixed gently with 1 ng of Gateway pDEST™ 10 plasmid DNA containing gene of interest. The cells were incubated on ice for 30 minutes before they were heat-shocked for 45 seconds at 42°C. Following 2 minutes incubation on ice, 800 µl of Luria-Bertani (LB) medium was added and the cell culture was incubated at 37°C at 225 rpm for 4 hours. 10-fold serial dilutions (10^{-1}, 10^{-2}, 10^{-3}) of the cells with LB medium were prepared and 100 µl of each dilution was plated on LB agar plate containing 50 µg/ml kanamycin, 7 µg/ml gentamicin, 10 µg/ml tetracycline, 100 µg/ml Bluo-gal and 40 µg/ml isopropyl-β-D-1-thiogalactopyranoside (IPTG) and incubated for 48 hours at 37°C. White colonies were picked and restreaked on fresh LB agar containing the above-mentioned antibiotics, Bluo-gal and IPTG and incubated overnight at 37°C to confirm that successful recombination had occurred.

2.2.3.3 Isolating Recombinant Bacmid DNA

A single white colony of DH10 containing recombinant Bacmid was picked to inoculate 2 ml of LB medium containing 50 μg/ml kanamycin, 7 μg/ml gentamicin and 10 μg/ml tetracycline and incubated at overnight at 37°C. One and a half ml of bacterial culture was transferred to a 1.5 ml microcentrifuge tube and centrifuged at 14,000 x g for 1 minute. The supernatant was removed and the cell pellet was resuspended in 0.3 ml of Solution I (15 mM Tris-HCl, pH 8.0, 10 mM EDTA, 100 μg/ml RNase A) before mixed with 0.3 ml of Solution II (0.2 N NaOH, 1 % (w/v) SDS). The cell suspension was incubated at room temperature for 5 minutes or till the suspension turned from turbid to almost translucent. After incubation, 0.3 ml of 3 M potassium acetate, pH 5.5 was added and the solution was mixed gently. The suspension was then incubated on ice for 10 minutes before centrifuged at 14,000 x g for 10 minutes. The supernatant was transferred to a microcentrifuge tube containing 0.8 ml of isopropanol and inverted a few times before incubated on ice for 10 minutes. The sample was centrifuged for 15 minutes at 14,000 x g at room temperature and the supernatant was removed. Five hundred μl of 70 % ethanol was added to the DNA-pellet and the tube was inverted several times to wash the pellet before it was centrifuged for 5 minutes at 14,000 x g at room temperature. The supernatant was removed and the DNA-pellet was air-dry for 10 minutes at room temperature before plasmid DNA was dissolved in 40 μl of nuclease-free dH_2O.

2.2.3.4 Transfecting insect cells and isolating P1 viral stock

In order to generate recombinant baculovirus, insect cells were transfected with Bacmid DNA. Insect cells were seeded in 6-well dish at a density of 1 x 10^6 in 2 ml of growth medium containing antibiotics in each well and incubated for 1 hour at 27^{o}C to allow cell attachment. The bacmid DNA: Cellfectin® reagent (Invitrogen) complexes were prepared according to manufacturer's handbook and added to each wells containing cells. Cells were then incubated at 27^{o}C for 4 hours before the DNA:lipid complexes were removed. Two ml of growth medium containing antibiotics was then added to each wells and cells were incubated at 27^{o}C for 72 hours or till signs of viral infection were visible. After transfected cells displayed signs of late stage infection (e.g. cell detachment and granular appearance), the medium containing virus were collected from each well and centrifuged at 1000 rpm for 5 minutes. The clarified supernatant was recovered as P1 viral stock and stored at 4^{o}C and protected from light.

2.2.3.5 Amplification of Baculoviral stock

P1 viral stock was used to infect insect cells to generate a high titre P2 viral stock. Insect cells were seeded in 50 ml suspension culture at 2 x 10^6 cells/ml and infected at a multiplicity of infection (MOI) of 0.1 according to the manufacturer's handbook. Infected cells were incubated for 48 hours at 27^{o}C. After 48 hours, the culture was collected and centrifuged at 1000 rpm for 5 minutes. The clarified supernatant was recovered and stored at 4^{o}C and protected from light. P3 viral stock was also generated in the same way.

2.2.3.6 Recombinant protein expression from *Sf9* insect cells

Cells were grown at a density of 2 x 10^6 cells/ml before they were infected with P3 viral stock at a MOI of 10. Infected cells were incubated for 48 hours at 27°C before they were centrifuged at 4000 rpm at 4°C for 20 minutes.

2.3 Molecular Biology Methods

2.3.1 Amplification of plasmid DNA

A single colony of transformed bacteria was picked and used to inoculate 5 ml of LB medium containing selective antibiotics to generate a starter culture. The culture was incubated at 37°C at 225 rpm for 6-8 hours.

2.3.2 Purification of plasmid DNA

Plasmid DNA was isolated using Qiagen® plasmid DNA Mini or Maxi Kits. For Miniprep, the starter culture was used directly according to the manufacturer's instructions. For Maxiprep, The starter culture was diluted 1:500 in 250 ml of selective LB medium. The culture was incubated overnight at 37°C at 225 rpm. Cells were centrifuged at 6000 rpm for 20 minutes at 4°C and plasmid DNA was isolated according to the manufacturer's instruction. Plasmid DNA was resuspended in nuclease-free dH_2O and stored at -20°C.

2.3.3 Quantification of plasmid DNA

The concentration of plasmid DNA was determined by spectrophotometry at 260 nm using the PowerwaveXS™ Microplate Spectrophotometer (Bio-Tek). Plasmid DNA was diluted 1:100 in 100 µl of nuclease-free dH_2O and added to wells of a 96-well UV-Star™ Plate (Greiner). 100 µl of nuclease-free dH_2O was used as a blank control. DNA concentrations were calculated based on the basis that 50 µg/ml of DNA gives an OD_{260nm} of 1.0.

2.3.4 Agarose gel electrophoresis

One percent (w/v) Agarose gel was prepared by adding agarose to 1x Tris-Borate-EDTA (TBE) buffer (90 mM Tris-HCl, pH 8.0, 90 mM Boric acid, 2 mM EDTA, pH 8.0; adjusted to pH 8.0) and heated in a microwave oven until dissolved. The agarose solution was cooled till handwarmed before ethidium bromide was added to a final concentration of 0.5 µg/ml. The agarose solution was left to set in a horizontal agarose gel tray with a comb inserted. The agarose gel was placed in a horizontal electrophoresis gel tank (Jencons) filled with 1x TBE buffer. DNA samples were diluted 1:6 in 6x Agarose loading buffer (0.25 % (w/v) Bromophenol Blue, 0.25 % (w/v) Xylene cyanol FF, 15 % (w/v) Ficoll) and loaded onto the gel. The DNA samples were electrophoresed at 100 V for 50 minutes before bands were visualised under a UV transilluminator.

2.3.5 Site-directed mutagenesis

Primers containing the desired mutations were designed according to the quidelines in the QuikChange™ Site-Directed Mutagenesis Kit Manual (Stratagene). Oligonucleotides were purchased from Sigma-Aldrich in PAGE-purified form before reconstituted in nuclease-free dH_2O. Site-directed mutagenesis was carried using the QuikChange™ Site-Directed Mutagenesis Kit (Stratagene) according to manufacturer's instructions. After mutant strand synthesis reaction, 1 μl of *DpnI* restriction enzyme (10U/μl) was added to the amplification reaction and mixed. The reaction mixture was microcentrifuged for 1 minutes and incubated at 37°C for 1 hour to digest the parental (nonmutated) dsDNA. After incubation, 2 μl of *DpnI*-treated DNA was used to transform 25 μl of DH5α competent cells using heat-shock method (*Materials and Methods 2.2.2.3*).

2.3.6 Sequence analysis of plasmid DNA

All sequence analysis was performed by the Sequencing Unit at the MRC Human Genetics Unit, Edinburgh. Ten μl of sequencing reaction containing 2 μl of BigDye® Terminator 3.1 (Applied Biosystems), 3.2 pmol of primer, 1x BigDye Sequencing buffer (Applied Biosystems), 250 ng of DNA template and nuclease-free dH_2O was assembled. The sequencing reaction was thermal-cycled using cycling parameters according to the manufacturer's instructions.

The sequenced DNA was then precipitated by mixing the reaction with 2.5 µl of 125 mM EDTA and 30 µl of 100 % (v/v) ethanol. After vortexing, the reaction was incubated at room temperature for 15 minutes. After centrifuging at 13000 rpm for 20 minutes, the solution was removed and precipitated DNA was microcentrifuged for 20 seconds. Residual ethanol was removed before 30 µl of 70 % (v/v) ethanol was added to the precipitated DNA and centrifuged at 13000 rpm for 5 minutes. The ethanol was removed before the precipitated DNA was microcentrifuged for 20 seconds. Residual ethanol was removed and the precipitated DNA was left to air-dry before sequence-analysed.

2.4 Protein Detection

2.4.1 Cell lysis

2.4.1.1 Mammalian cells

Cells were washed with cold PBS and scraped into 200 µl of lysis buffer (50 mM Hepes, pH 7.4, 0.5 % (v/v) Triton X-100, 150 mM NaCl, 10 mM NaF, 1mM DTT, 1mM EDTA, 1mM EGTA, 10 mM sodium β-glycerophosphate, 5 mM sodium pyrophosphate, 1 mM sodium orthovanadate, 0.27 M sucrose, 1x Protease Inhibitors (1 µg/ml Leupeptin, 0.4 µg/ml Aprotinin, 0.2 µg/ml Pepstatin, 0.12 mM Benzamidine, 1 µg/ml Soya bean trypsin inhibitor, 40 µg/ml Pefabloc, 0.1 mM EDTA)). The cell lysate were transferred into a 1.5 ml microcentrifuge tube and resuspended by pipetting up and down. The cell lysates were then incubated on ice for 15 minutes before centrifuged at 13000 rpm for 15 minutes. The supernatant

was recovered as cleared cell lysate and snap-frozen in liquid nitrogen and stored at -70°C.

2.4.1.2 *Sf9* insect cells

Infected insect cells were centrifuged at 4000 rpm at 4°C for 20 minutes. Supernatant was removed and the pellet was resuspended with twice the cell pellet volume of lysis buffer (25 mM Hepes, pH 7.4, 20 mM NaF, 10 mM NaCl, 1x Protease Inhibitors (1 μg/ml Leupeptin, 0.4 μg/ml Aprotinin, 0.2 μg/ml Pepstatin, 0.12 mM Benzamidine, 1 μg/ml Soya bean trypsin inhibitor, 40 μg/ml Pefabloc, 0.1 mM EDTA)). After incubation on ice for 15 minutes, cell lysates were centrifuged at 13000 rpm for 15 minutes. The supernatant was recovered as cleared cell lysates and snap-frozen in liquid nitrogen and stored at -70°C.

2.4.2 Protein Quantification

Protein concentrations were determined using BCA™ Assay Kit (Pierce) in a 96-well plate. Bovine serum albumin (BSA) protein standards of known concentration were prepared in dH_2O. Cell lysate (1.25μl) was diluted in 23.75 μl of the appropriate lysis buffer. 25 μl of lysis buffer was used as a blank control. After 200 μl of working reagent was added to each sample and incubated at 37°C for 30 minutes, the protein concentration was determined at 562 nm using the PowerwaveXS™ Microplate Spectrophotometer (Bio-tek), Read-outs were

converted to concentrations using the standard curve generated from the known BSA standards and were adjusted by the dilution factor.

2.4.3 SDS polyacrylamide gel electrophoresis (SDS-PAGE)

Proteins were resolved on the basis of their molecular weight by discontinuous SDS-PAGE. SDS-PAGE at appropriate polyacrylamide concentrations was prepared using a Mini-PROTEAN3^{TM} (Bio-Rad) blot. Higher concentration of polyacrylamide was used to resolve lower molecular weight protein and vice versa. For example, Chk1 protein was usually resolved by 10 % resolving gel, p21 protein was resolved using 12 % gel and peptides were resolved by 15 % gel. The resolving gel (6 - 15 % Acrylamide, 390 mM Tris-HCl pH 8.8, 0.1 % SDS, 0.1 % Ammonium peroxidisulphate, polymerisation was initiated by adding 0.08 % TEMED) was overlaid with dH_2O to remove air bubbles and flatten the top surface before left to polymerise at room temperature. After the resolving gel was set, the dH_2O was removed and the stacking gel (5 % Acrylamide, 123 mM Tris-HCl pH 6.8, 0.1 % SDS, 0.1 % Ammonium peroxidisulphate, 0.1 % TEMED) was added with either a 10-well or 15-well comb and left to polymerise. After the stacking gel was set, the comb was removed and the gel cassette was assembled with the Mini-PROTEAN3^{TM} electrophoresis module and immersed in running buffer (192 mM Glycine, 25 mM Tris, 0.1 % (w/v) SDS).

SDS sample buffer (45 mM Tris-HCl, pH 6.8, 10 % glycerol, 1 % (w/v) SDS, 0.01 % (w/v) Bromophenol Blue, 50 mM DTT) was added to 50 μg of cell lysates

protein in a ratio of 1:4 (v/v) and the samples were heated at 95°C for 5 minutes prior to loading. Two µl of PageRuler™ Prestained Protein Ladder (Fermentas) was loaded as protein standards. Protein samples were separated by electrophoresis in running buffer at 80-150 V until the Bromophenol blue dye front reached the bottom of the gel.

2.4.4 Native PAGE

Proteins were resolved on the basis of their charge and molecular weight by native PAGE. The key parameters in native PAGE system are the pI of the protein of interest and the pH of the running buffer. If the pH of the running buffer is greater than the pI of the protein of interest, the protein will acquire a negative charge and migrate towards the positive electrode (anode). In contrast, if the pH of the running buffer is lower than the pI of the protein of interest, the protein will acquire a negative charge and migrate towards the negative electrode (cathode). Chk1 protein has a pI of 8.2. Polyacrylamide gel at 10 % or 15 % was prepared without SDS and using 390 mM Tris buffer, pH 8.8 and a Mini-PROTEAN3™ (Bio-Rad) blot. The resolving gel was overlaid with dH_2O to remove air bubbles and flatten the top surface before left to polymerise at room temperature. After the resolving gel was set, the dH_2O was removed and the stacking gel with a polyacrylamide concentration of 5 % (123 mM Tris buffer, pH 8.8 was used and SDS was not added) was added with either a 10-well or 15-well comb and left to polymerise. After the stacking gel was set, the comb was removed and the gel

cassette was assembled with the Mini-PROTEAN3^{TM} electrophoresis module and immersed in running buffer (without SDS).

Samples were prepared with 5 µl of the sample buffer (without SDS and DTT) abd resolved as in *Materials and Methods* 2.4.3.

2.4.5 Coomassie Brilliant Blue Staining

Resolving gels were submerged in Destain I (50 % (v/v) Methanol, 10 % (v/v) Acetic Acid) for more than 5 minutes in a tray with rocking. After that, Destain I was replaced with Coomassie Brilliant Blue stain (50 % (v/v) Methanol, 10 % (v/v) Acetic Acid, 0.2 % (w/v) Coomassie Blue R-250) and the gel was stained overnight with rocking. Stained gels were then destained with Destain II (7.5 % (v/v) Methanol, 10 % (v/v) Acetic Acid) to remove excess stain. Destaining was performed until the protein bands became visible and the gel background was clear. Gels were dried onto a 3 mm Whatman paper using a gel-dryer.

2.4.6 Immunoblotting

For the purpose of western blotting, resolved proteins were transferred electrophoretically to PROTRAN^{TM} nitrocellulose transfer membrane (Schleicher & Schuell Biosciences). Gel were equilibrated in tanks with transfer buffer (192 mM Glycine, 25 mM Tris, 20 % (v/v) Methanol) and assembled with an ice block. Electroblotting was performed at 100 V for 1 hour or at 20 mA overnight. After

transfer, the membrane was rinsed in PBS/T (0.1 % (v/v) Tween-20, 1x PBS (137 mM NaCl, 10 mM Na_2HPO_4, 2.7 mM KCl, 1.8 mM KH_2PO_4; adjusted to pH 7.4 with HCl) for 5 minutes before the protein were stained with black ink (Pelikan) diluted in PBS/T (1/250) for 10 minutes. The membrane was washed twice with PBS/T for 5 minutes to remove excess stain. Non-specific antibody binding was blocked with 5 % (w/v) dried skimmed milk diluted in PBS/T for 1 hour. The membrane was then incubated with the primary antibodies diluted in 5 % (w/v) milk-PBS/T for 1 hour at room temperature or overnight at 4°C. Any unbound antibody were removed with three 10 minutes washes in PBS/T at room temperature. The membrane was then incubated with the appropriate secondary antibody diluted 1/1000 in 5 % (w/v) milk-PBS/T for 1 hour at room temperature. Any unbound antibodies were removed with three 10 minutes washes in PBS/T. The membrane was then overlaid with enhanced chemiluminescence solution (ECL) (1 part of ECL solution I (100 mM Tris, pH 8.5, 2.5 mM Luminol stock, 0.4 mM p-Coumaric acid) mixed with 1 part of ECL solution II(100 mM Tris, pH 8.5, 0.02 % (v/v) H_2O_2)) for 1 minute. Excess ECL solution was drained before membranes were exposed to Hyperfilm™ ECL (Amersham Biosciences).

2.4.7 Stripping nitrocellulose membrane

Membranes were stripped to remove primary and secondary antibodies from the membrane before they were reprobed with additional antibodies. The membrane was incubated with two changes of stripping buffer (1.5 % (w/v) glycine, 0.1 % (w/v) SDS, 1 % (v/v) Tween-20; adjusted to pH 2.2 with HCl) for 10 minutes at

room temperature. The membrane was rinsed twice with PBS for 10 minutes and twice with PBS/T for 5 minutes before it was ready for the blocking stage as described in *Materials and Methods* 2.4.6.

2.4.8 Antibodies

2.4.8.1 Primary antibodies

Target	kDa	Type	Supplier	Dilution
Chk1 (G-4)	56	Mouse monoclonal	Santa Cruz	1:1000
Chk1	56	Sheep polyclonal	Millipore	1:1000
Chk1 phospho-Ser^{317}	56	Rabbit polyclonal	Cell Signalling Technology	1:1000
Chk1 phospho-Ser^{345}	56	Rabbit polyclonal	Cell Signalling Technology	1:1000
His tag	-	Mouse monoclonal	Novagen	1:1000
p21 (Ab-1)	21	Mouse monoclonal	Calbiochem	1:500
p21 phospho-Thr^{145}	21	Rabbit polyclonal	Santa Cruz	1:1000
p21 phospho-Ser^{146}	21	Goat polyclonal	Santa Cruz	1:1000
V5 tag	-	Mouse monoclonal	Abcam	1:1000

Table 2.2 List of primary antibodies used in this study.

2.4.8.2 Secondary antibodies

Secondary antibodies were sourced from Dako and HRP-conjugated forms of Rabbit α-Mouse IgG; Swine α-Rabbit IgG; Rabbit α-goat IgG; Rabbit α-sheep IgG were used.

2.5 *In vitro* Kinase assay

Kinase reactions containing 100 ng of protein kinase, 0.5-1 μg of substrate were assembled in kinase buffer (50 mM Hepes, pH 7.4, 0.1 mM EGTA, 0.1 % (v/v) β-mercaptoethanol, 20 mM Magnesium Acetate) in a final volume of 9 μl. The reactions were initiated by adding 1 μl of either 1 mM ATP or 1 mM ATP containing a 1/50 dilution of radiolabelled [γ^{32}P]-ATP (Perkin Elmer) (3000 Ci/mol) and incubated for 30 minutes at 30^{o}C. The reactions were stopped with 5 μl of 5x SDS sample buffer and reaction products were resolved by SDS-PAGE. Gels were dried onto 3 mm Whatman paper and exposed to a storage phosphor screen (Amersham Biosciences) overnight before [γ^{32}P] incorporation was visualised and quantified via a phosphorimager (Storm 840, Amersham Biosciences). Actual counts of [γ^{32}P] incorporation into reaction products was determined from a [γ^{32}P]-ATP standard curve.

2.6 Immunoprecipitation-kinase assay (IP-kinase)

To immunoprecipitate protein complexes from cell lysates, 2 mg of mammalian cell lysate was first pre-cleared with 40 μl of 50 % (w/v) Protein G Sepharose^{TM} 4 Fast Flow suspension (GE Life Sciences) (diluted in mammalian lysis buffer) for 1 hour at 4^{o}C with rotation. After incubation, the sample was microcentrifuged for 10 seconds and the cleared supernatant was recovered. The supernatant was then incubated with 2 μg of appropriate primary antibody and incubated for 2 hours at 4^{o}C. After incubation, 40 μl of 50 % (w/v) Protein G Sepharose^{TM} 4 Fast Flow suspension was added to the sample and incubated for a further hour at 4^{o}C. The

protein G/antibody complexes were collected by microcentrifuging for 30 seconds. The supernatant was removed and the beads were washed twice with 500 µl of lysis buffer. The beads was then split equally into two 0.6 ml microcentrifuge tubes. One of the samples was further washed with 200 µl of lysis buffer before 20 µl of 5x SDS sample buffer was added and it was subjected to SDS-PAGE. The other sample was washed twice with 200 µl of 2x kinase buffer before the beads were resuspended in 9 µl of kinase reaction buffer containing substrate and kinase buffer was added. The kinase reaction was initiated as described in *Materials and Methods* 2.5.

2.7 Enzyme-Linked ImmunoSorbent Assay (ELISA)

2.7.1 Indirect ELISA

Antigens were diluted to a final concentration of 1 µg/ml in 100 µl of 0.1 M $NaHCO_3$, pH 9.6 before added to each well of PVC 96-well microtitre plate. The microtitre plate was covered with parafilm and incubated overnight at 4°C. Excess antigens were removed by washing with four changes of 200 µl of PBS/T before non-specific antibody binding was blocked with 200 µl of 3 % (w/v) BSA in PBS/T for 1 hour at room temperature. Appropriate primary antibodies (diluted in 50 µl of 3 % (w/v) BSA-PBS/T) were added and incubated for 1 hour. Any unbound antibodies were washed off with six changes of 200 µl of PBS/T. Appropriate secondary antibodies (diluted in 50 µl of 3 % (w/v) BSA-PBS/T) were then added and incubated for 1 hour. Any unbound antibodies were washed off with six changes of 200 µl of PBS/T. Binding was detected by adding 50 µl of

ECL solution (1:1 ratio of ECL I and ECL II solution) and relative light units (R.L.U) were quantified using a luminometer (Fluoroskan Ascent FL).

2.7.2 Streptavidin capture of peptide antigens

Protein complexes were also captured in an ELISA format using streptavidin capture of biotinylated peptides. Biotinylated peptides were immobilised in PVC 96-well microtitre plate. First, each well was coated with 1 μg of streptavidin (diluted in 50 μl of dH_2O) and incubated overnight at 37°C. After incubation, the wells were washed with four changes of 200 μl of PBS/T. Appropriate amounts of peptides were diluted in 50 μl of dH_2O and added to each well and incubated at room temperature for 1 hour. Excess peptides were washed off with six changes of 200 μl of PBS/T before non-specific antibody binding was blocked with 3 % (w/v) BSA (diluted in 200 μl of PBS/T) for 1 hour. Appropriate primary antibodies (diluted in 50 μl of 3 % (w/v) BSA-PBS/T) were added and incubated for 1 hour. Any unbound antibodies were washed off with six changes of 200 μl of PBS/T. Appropriate secondary antibodies (diluted in 50 μl of 3 % (w/v) BSA-PBS/T) were then added and incubated for 1 hour. Any unbound antibodies were washed off with six changes of 200 μl of PBS/T. Binding was detected by adding 50 μl of ECL solution (1:1 ratio of ECL I and ECL II solutions) and R.L.U were quantified using a luminometer (Fluoroskan Ascent FL).

2.8 Isolation of p21 protein from inclusion bodies

Plasmids containing TrcHisA p21 wild-type or TrcHisA p21 ΔNT mutant were transformed into BL21 *E.coli* cells and streaked onto selective LB agar. Following overnight incubation at 37°C, a single colony was picked to inoculate a 10 ml of selective LB medium and incubated at 37°C at 225 rpm overnight. The overnight culture was then added to 500 ml of selective LB medium and incubated at 37°C at 225 rpm until an OD_{600nm} of 0.4 was reached. A final concentration of 1mM IPTG was then added and the culture was incubated for a further 2 hours at 37°C. Cells were collected by centrifuging at 8000 rpm at 4°C for 10 minutes. The cell pellet was resuspended in ice-cold 50 mM Tris-HCl, pH 8.0. The cell suspension was then centrifuged as before and the pellet was resuspended in 25 ml of ice-cold 50 mM Tris-HCl, pH 8.0. The cell suspension was centrifuged again as before and the final pellet was resuspended at 0.66 ml/g in 10 % (w/v) sucrose, 50 mM Tris-HCl, pH 8.0 lysis buffer. A final concentration of 150 μg/ml of lysozyme and 0.1 M of NaCl was added and the mixture was mixed gently and incubated at 0°C for 45 minutes. The cell lysate was then warmed to 37°C for 1 minute and returned to 0°C till the cell lysate turned viscous. The sample was then sonicated with three 10 seconds pulses before it was centrifuged at 10000 rpm at 4°C for 10 minutes. The inclusion bodies was resuspended in 25 ml of lysis buffer (50 mM Tris-HCl, pH 8.0, 2 mM EDTA, 100 mM NaCl, 1 mM PMSF, 0.5 % (v/v) Triton X-100, 1.2 mM Benzamidine, 10 μg/ml Leupeptin) and recentrifuged at 10000 rpm at 4°C for 10 minutes. This was repeated twice. The inclusion bodies was then resuspended in 5 ml of the solubilisation buffer (5 M guanidine hydrochloride, 50 mM Tris-HCl, pH 8.0, 0.005 % (v/v) Tween-80) and mixed gently for 5 hours at 4°C. The

suspension was then centrifuged at 10000 rpm at 4°C for 10 minutes. Five ml of the supernatant was then diluted into 20 ml of refolding buffer (50 mM Tris-HCl, pH 8.0, 0.005 % (v/v) Tween-80, 2 mM reduced glutathione, 0.02 mM oxidised glutathione) and mixed for 12-18 hours at 4°C. The diluted supernatant was then dialysed against dialysis buffer (50 mM Tris-HCl, pH 8.0, 300 mM NaCl, 0.005 % (v/v) Tween-80) for 1-2 hours at 4°C. The dialysis procedure was repeated 3 more times with decreased concentration of NaCl (250, 200, 150 mM). The dialysed supernatant was then centrifuged at 10000 rpm at 4°C for 10 minutes to remove any insoluble or precipitated proteins.

2.9 Purification of His-tagged proteins

Histidine tagged proteins were purified via nickel agarose affinity chromatography. *Sf9* insect cells were infected and Chk1 baculovirus for 48 hours at 27°C. After infection, the cells were collected by centrifuging at 4000 rpm for 20 minutes at 4°C. The cell pellet were then resuspended with twice the cell pellet volume of lysis buffer as described in *Materials and Methods* 2.4.1.2. Twenty ml of IMAC5 buffer (20 mM Tris-HCl, pH 8.0, 0.5 M NaCl, 5 mM imidazole) was then added to 25 ml of cell lysate before filtered through a 0.45 μm button filter. Two ml of Ni-NTA agarose slurry (Qiagen) was prepared with 3 ml of IMAC5 buffer and added to the filtered lysate. After incubation at 4°C for 1 hour, the lysate-Ni-NTA mixture was loaded onto a 10 ml polypropylene column and the flow-through was collected. The column was washed with 10 ml of IMAC5 buffer and then washed with 40 ml of IMAC25 buffer I (20 mM Tris-HCl, pH 8.0, 0.5 M NaCl, 25 mM

imidazole, 0.5 % (v/v) Triton X-100, 0.5 % (v/v) Tween-20) before a final wash of 10 ml of IMAC25 buffer II (20 mM Tris-HCl, pH 8.0, 0.5 M NaCl, 25 mM imidazole). All the wash fractions were collected for analysis. The protein was eluted with 20 ml of IMAC150 buffer (20 mM Tris-HCl, pH 8.0, 0.5 M NaCl, 5 mM imidazole). The eluted proteins/fraction was then concentrated with 35'000 PEG (Poly(ethylene glycol) (Fluka) using dialysis tubing of molecular weight cut-off of 6000-8000. PEG binds to H_2O. Concentrated proteins/fractions were then dialysed overnight with dialysis buffer (20 mM Hepes, pH 8.0, 10 % (v/v) glycerol, 1 mM DTT, 1 mM Benzamidine, 150 mM NaCl) at 4°C. The eluted protein was further dialysed with fresh dialysis buffer for 2 hours at 4°C. The flow-through, wash fractions and the dialysed eluted proteins were then analysed by SDS-PAGE and immunoblotting.

2.10 Gel Filtration/Size exclusion chromatography

Gel filtration chromatography is a method in which molecules are separated based on their sizes. Larger molecules are eluted first whilst smaller molecules require longer time to elute as they are retarded within the column. A gel filtration column Superdex 200 (Amersham Biosciences) was used with an AKTA FPLC (Amersham Biosciences). The column was equilibrated with two column volume (C.V) of buffer (20 mM Hepes, pH 8.0, 10 % (v/v) glycerol, 1 mM DTT, 1 mM Benzamidine, 150 mM NaCl) with a flow rate of 0.5 ml/minute. Purified recombinant insect cell-expressed Chk1 (Trp→$Ala^{192/208}$) was concentrated to about 500 µl using Centricon Centrifugal Filter Device, Ultracel YM-10

membrane (Millipore) according to manufacturer's instructions prior to loading onto the column. Sample was eluted with 1.5x C.V of buffer with a flow rate of 0.3 ml/minute and 0.5 ml fractions were collected. Elution fractions were then analysed by SDS-PAGE and immunoblotting.

2.11 PepChip Kinase assay

Trial/Evaluation PepChip kinase slides were purchased from Mimotopes. Each slide contains 2 duplicate sets of 192 peptides and each set contains 2 x 4 subarrays of 6 x 4 peptide spots. Fifty µl of kinase reaction containing 50 µg/ml of purified recombinant protein kinase in kinase buffer (50 mM Hepes, pH 7.4, 0.1 mM EGTA, 0.1 % (v/v) β-mercaptoethanol, 20 mM Magnesium Acetate), 0.01 % (v/v) Brij-35, 10 µM ATP and 300 µCi/ml [γ^{33}P]-ATP was assembled and overlaid onto the PepChip slide and incubated for 3 hours at 30^{o}C in a humidified chamber. After incubation, the slide was washed once with PBS/Tx (1x PBS, 1 % (v/v) Triton X-100), twice with NaCl/Tx (2 M NaCl, 1 % (v/v) Triton X-100) and twice with dH_2O and then air-dried. Slides were exposed to storage phosphorscreen and [γ^{33}P] incorporation into the peptide substrates on the PepChip slide were visualised by phosphorimager. The spot signals were correlated with the peptide sequences using the grid provided by the manufacturer and the coordinates were used to identify the peptide protein sequence from an excel spreadsheet also provided by the manufacturer.

CHAPTER 3: DOCKING-DEPENDENT REGULATION OF CHK1 BY $p21^{WAF1}$

3.1 Introduction

This chapter identifies $p21^{waf1}$ as potential novel substrate for checkpoint kinase Chk1. Furthermore, an N-terminal region of $p21^{waf1}$ has been characterised to function as a docking-dependent modulator of Chk1 catalytic activity. Therefore, I will start with a brief introduction into $p21^{waf1}$, a growth regulator.

3.1.1 Cyclin-dependent kinase inhibitor, $p21^{waf1/cip1}$

$p21^{waf1/cip1}$, or p21 as known hereinafter, is the first identified cyclin-dependent kinase (Cdk) inhibitor (CKI) which binds to Cdk2 and its associated cyclins, leading to the disruption of Cdk/cyclin-dependent phosphorylation of pRb (Harper et al., 1993). p21 belongs to the Cip/Kip family of cdk inhibitors which also includes $p27^{kip1}$ and $p57^{kip2}$ (Harper, 1997). In addition to cdk inhibition, p21 also regulates the cell cycle in multiple ways which will be briefly discussed here. Despite playing a major role in cell cycle regulation, p21 mutations are very rare (Shiohara et al., 1997). However, p21-deficient mice do develop spontaneous tumours by the age of 16 months, indicating the importance of p21 for tumour suppression (Martin-Caballero et al., 2001). Therefore a variety of mechanisms for p21 regulation exists at the transcriptional and post-translational level which will also be described here.

3.1.2 $p21^{waf1}$ structure

Proteolysis, circular dichroism (CD) and nuclear magnetic resonance (NMR) experiments have shown that p21 has a highly disordered structure (Kriwacki et al., 1996), which explains the lack of p21 crystal structure. However, p21 does adopt an ordered conformation upon association with Cdks (Kriwacki et al., 1996, Sung et al., 2001). It was discussed that this disorder-order transition for p21 could increase specificity for Cdk at the expense of binding affinity. Secondly, this highly disordered feature allows p21 to adopt multiple conformations in relation to different substrates and facilitate diverse binding events (Kriwacki et al., 1996). p21 shares a significant homology with p27 and p57 in the N-terminal region and targets a broad range of CDK-cyclin complexes, whereas the C-terminal region is less conserved (Figure 3.1) (Dotto, 2000).

The N-terminal region of p21 is necessary and sufficient to inhibit CDK-cyclin activity (Chen et al., 1995, Luo et al., 1995). It has been revealed that amino acids ^{17}ACRRLFGP^{24} (Cy1 motif) is important for the binding interface between p21 and cyclin E or cyclin A while a Cdk-binding region spanning amino acids ^{53}FVTETP^{58}, is required for Cdk2 association, suggesting that these two regions independently allow p21 association with Cdk2-cyclin A/E (Chen et al., 1996b). However, cyclin D1 only binds to p21 via the Cy1 motif when complexed with Cdk4 as either cyclin D1 or Cdk4 alone does not associate with p21 (Chen et al., 1996b). This cyclin-binding motif (RxL) is conserved among the p27, p57, regulators and substrates of Cdk-cyclin complexes (Dotto, 2000). It has been shown that both the N-terminal cyclin-binding motif and the Cdk-binding motif

are needed to inhibit Cdk2 kinase activity (Fotedar et al., 1996). Using data extrapolated from the crystal structure of the p21 relative, p27, with Cdk2, inhibition of Cdk kinase activity is mediated by p21 binding and subsequent Cdk2 structural changes. This results in a p21 N-terminal region buried inside the Cdk2 catalytic cleft, with Tyr^{77} sterically blocking the ATP-binding site of Cdk2 (Russo et al., 1996). It was also reported that amino acids 26-45 are potentially involved in p21 dimerisation (Chen et al., 1996a).

In contrast to the N-termini, the C-terminal regions of the CKI Cip/Kip family are poorly conserved. It was discovered that amino acids 139-164 of p21 are essential for binding to proliferating cell nuclear antigen (PCNA), a processivity factor for DNA polymerase δ, and inhibits DNA synthesis (Chen et al., 1995, Luo et al., 1995, Chen et al., 1996a). Association with PCNA is dependent on the removal of an inhibitory phosphate group at Ser^{146} of p21 (Scott et al., 2000). A second but lower affinity cyclin-binding motif – ^{152}HSKRRLIF^{159} (Cy2 motif) that resides within the PCNA-binding domain has also been identified, suggesting that PCNA may regulate p21 activity on Cdk-cyclins (Chen et al., 1996b). A peptidomimetic ligand containing the lower affinity cyclin-binding motif has been shown to be a potent inhibitor of Cdk4-cyclin D, but not Cdk2 (Ball et al., 1997). A basic nuclear localisation signal is also located within the C-terminal ^{140}RKR^{142} motif (Rodriguez-Vilarrupla et al., 2002).

3.1.3 Functions of $p21^{waf1}$

p21's role in mediating cell cycle arrest through the inhibition of Cdk-cyclin activity is well established. However it appears that cytoplasmic p21 also functions to facilitate the association of Cdk4/6 with cyclin D and promote their nuclear localisation, resulting in G_1 phase progression. It was also shown that low concentrations of p21 promote assembly of Cdk-cyclin complexes while high concentrations of p21 inhibit the activity of Cdk (LaBaer et al., 1997).

In addition, it has been shown that E2F-dependent transcription can also be repressed by a p21-dependent mechanism that is independent of Cdk activity (Delavaine and La Thangue, 1999). Similar to the reported direct association of p21 with E2F subunits (Delavaine and La Thangue, 1999), p21 was shown to bind to the N-terminus of c-Myc, disrupting the interaction between c-Myc and Max. This is thought to suppress c-Myc-dependent transcription and also activate DNA replication as c-Myc competes with PCNA for the same binding site on p21 (Kitaura et al., 2000).

On the other hand, p21 can function to inhibit DNA synthesis via negative regulation of PCNA. It has been suggested that p21 regulates PCNA function by preventing PCNA interaction with DNA-(cytosine-5) methyltransferase (MCMT), leading to unmethylated replicated DNA (Chuang et al., 1997). Similarly, p21 disrupts PCNA interaction with Fen 1 (a 5'-3' exonuclease involved in DNA replication) and concomitantly inhibits DNA synthesis (Warbrick et al., 1997). Apart from inhibiting DNA synthesis, numerous conflicting observations are

reported as to whether p21 can prevent PCNA-dependent DNA repair (Fotedar et al., 2004).

p21 also associates with poly (ADP-ribose) polymerase family, member 1 (PARP1) through the C-terminal PCNA-binding domain. Although the significance of the interaction is not clear, this is thought to cooperatively regulate PCNA functions during DNA synthesis/repair (Frouin et al., 2003). Similarly, human papillomavirus (HPV)-16 E7 oncoprotein can abrogate inhibition of CDK activity and PCNA-dependent DNA synthesis by competing for the same PCNA/cyclin-binding motif in the C-terminal domain of p21 (Funk et al., 1997).

The C-terminal domain of p21 has been shown to de-repress the transcriptional repression activity of a p300 sumoylation-dependent transcriptional repression domain, CRD1, independently of cyclin or PCNA binding (Garcia-Wilson and Perkins, 2005). Although direct interaction between CRD1 and p21 was not observed, it was believed that p21 could target other parts of the transcriptional repression machinery.

p21 is thought to protect against apoptosis as it was found to bind to procaspase-3 and block its cleavage into the active form. The binding module is located in the N-terminus of p21 but is independent of the Cdk- and cyclin-binding motifs. In contrast, interaction between p21 and the activated form of caspase-3 was not observed (Suzuki et al., 1998, Suzuki et al., 1999). Interestingly, activated caspase-3 is also able to cleave p21, resulting in a truncated form of p21 that failed

to localise in the nucleus and loss of p21 function (Gervais et al., 1998, Zhang et al., 1999b). Besides inhibition of caspase-3 activation, p21 also binds to the pro-apoptotic stress-activated protein kinase (SAPK) and inhibits its catalytic activity, possibly via blocking activating phosphorylation by its upstream MKK4 kinase (Shim et al., 1996). Interestingly, this anti-apoptotic function is mediated by cytoplasmic localisation of p21 which is dependent on phosphorylation by PKB/Akt (Blagosklonny, 2002). Futhermore, poor prognosis of many breast tumours is often associated with high expression of cytoplasmic p21, leading to the suggestion that p21 may be a cytoplasmic oncoprotein with anti-apoptotic activity (Winters et al., 2001, Blagosklonny, 2002). This showed that p21 may exhibit different functions depending on its subcellular localisation; regulation of cell cycle and transcription in the nucleus and modulation of apoptosis in the cytoplasm.

Besides modulating cell cycle control and apoptosis, p21 is also an important determinant in cell differentiation. Keratinocyte cell differentiation is induced by a proteosome-dependent decrease in p21 with overexpression of p21 inhibiting differentiation (Di Cunto et al., 1998). In contrast, p21 is reported to have a positive effect in retinoic acid-induced differentiation of acute promyelocytic leukaemia cells, as ablation of p21 prevents differentiation. This positive regulation is uncoupled from the cell cycle effects of p21 (Casini and Pelicci, 1999). Thus p21 is implicated as an important regulator of differentiation which can be either positive or negative depending on the cell type and specific stages of differentiation (Dotto, 2000).

3.1.4 Regulation of p21^{waf1}

Induction of the *p21* gene was first discovered to be transcriptionally regulated by the p53 protein (el-Deiry et al., 1993). Two conserved p53-binding sites were found in the p21 promoter sequence of which at least one is required for p53-dependent transcriptional activation of p21 (el-Deiry et al., 1995). Basal expression of p21 has been shown to be regulated by p53 in the absence of genotoxic stress (Tang et al., 1998). In response to DNA damage or ribonucleotide starvation, p21 transcript levels are upregulated by activated p53 (Di Leonardo et al., 1994, Linke et al., 1996). Apart from p53, breast cancer type 1 susceptibility protein (BRCA1) and the transcription factor Sp1 also mediate the induction of *p21* gene expression through the Sp1-binding sites (Biggs et al., 1996, Somasundaram et al., 1997). It was also demonstrated that p300/CBP could cooperate with Sp1 to positively regulate p21 expression (Billon et al., 1999). In addition, a number of proteins such as interferon regulatory factor 1 (IRF1) and transcription factor AP2 also function in p53-independent regulation of p21 expression as reviewed in (Gartel and Tyner, 1999).

Although p53-dependent transcriptional activation of p21 has been well-characterised, mechanisms of transcriptional repression of p21 are still under-appreciated. However it is clear that the c-Myc proto-oncogene functions to repress p21 transcription (Gartel and Radhakrishnan, 2005). c-Myc is a transcription factor that functions to activate or repress transcription of target genes through recruitment of distinct co-factors (Adhikary and Eilers, 2005, Cowling and Cole, 2006). In cell line studies, overexpression of c-Myc leads to

p21 repression and switches DNA damage-induced cell cycle arrest to an apoptotic response (Seoane et al., 2002, Arango et al., 2003). Conversely, down-regulation of c-Myc leads to an increased level of p21, implicating c-Myc as a bona fide transcriptional repressor of p21 (McConnell et al., 2003, Gui et al., 2004). Although it was shown that repression of p21 transcription by c-Myc occurred at a proximal promoter region, the mechanistic basis of the repression is not well-understood (Claassen and Hann, 2000). It was suggested that c-Myc-dependent inhibition of transcription factors Sp1/Sp3 or Miz-1 activity is needed for repression. In addition, active recruitment of the DNA methyltransferase 3a (Dnmt3a) co-repressor by c-Myc to the promoter region is also required for p21 repression (Brenner et al., 2005). Apart from c-Myc, other proteins such as polo-like kinase 1, histone deacetylase 1 and zinc-finger protein 76 (ZNF76) are able to functionally interfere with the transcriptional activators (p53 and Sp1/Sp3) and basal transcriptional machinery (TATA-binding protein) to repress p21 transcription (Lagger et al., 2003, Ando et al., 2004, Zheng and Yang, 2004). p21 repression through direct binding to the proximal promoter by transcription factors such as T-box protein 2 (Tbx2), Runt-related transcription factor 2 (RUNX2) and zinc finger and BTB domain-containing protein 4 (ZBTB4) has also been described (Westendorf et al., 2002, Prince et al., 2004, Weber et al., 2008). Increasing evidence also points towards epigenetic silencing as another system to regulate p21 transcription (Gartel and Radhakrishnan, 2005).

p21 has been reported to be phosphorylated at various sites catalysed by a diverse range of distinct kinases. The best characterised site is Thr^{145} which lies within the

PKB/Akt consensus phosphorylation site (Liang and Slingerland, 2003). Phosphorylation on Thr^{145} is thought to disrupt the hydrogen bonding pattern between Gln^{144}/Thr^{145} of p21 and PCNA, thereby destabilising the complex (Rossig et al., 2001, Child and Mann, 2006). In addition, PKB/Akt-catalysed Thr^{145} modification can induce relocalisation of p21 from the nucleus to the cytoplasm in endothelial cells (Zhou et al., 2001). However, it was also reported that increased PKB/Akt activity did not induce p21 cytoplasmic localisation in keratinocytes (Segrelles et al., 2006). Nevertheless, it is thought that cytoplasmic localisation limits p21 access to Cdk2 complexes, leading to defective cell cycle arrest (Asada et al., 1999).

PKCζ, a downstream target of 3-phosphoinositide dependent protein kinase 1 (PDK1), phosphorylates p21 on Ser^{146} which mediates degradation of p21 (Scott et al., 2002). Another study has also implicated PKC in the phosphorylation of p21 on Ser^{153}, and is thought to affect its subcellular localisation. Calmodulin is able to bind to the C-terminal domain of p21 at amino acids 145 to 164 and this binding blocks Ser^{153} modification and prevents nuclear export (Rodriguez-Vilarrupla et al., 2005). Besides Ser^{146} and Ser^{153}, PKC is also capable of phosphorylating p21 at Ser^{160}. This is thought to decrease p21 binding to PCNA as phosphorylation is likely to disrupt Ser^{146} hydrogen bonding with PCNA (Gulbis et al., 1996, Scott et al., 2000).

In addition, Thr^{57} has been described as a phosphorylation target of which GSK3β, p38α and JNK1 might be responsible. It is thought that Thr^{57} modification

stabilises p21, leading to elevated binding with cyclin B1 at the G_2/M transition (Rossig et al., 2002, Kim et al., 2002, Dash and El-Deiry, 2005). Furthermore, p38α and JNK are found to phosphorylate p21 on Ser^{130}, which is also thought to stabilise p21 (Kim et al., 2002). However a recent report showed that CDK2 targets p21 at Ser^{130} for proteosome-dependent degradation (Zhu et al., 2005). It is likely that a combination of post-translational modifications is needed to determine the type of regulation.

p21 stability is also reported to be regulated by WISp39 which contains a tetratricopeptide repeat (TPR) domain that allows recruitment of heat shock response protein Hsp90. p21, WISp39 and Hsp90 then form a heterotrimeric complex responsible for accurate p21 folding and stability (Jascur et al., 2005).

There is controversy regarding whether degradation of p21 is ubiquitin-dependent or –independent. A study has showed that p21 mutant, which cannot be ubiquitinated *in vivo*, still undergoes degradation and remains sensitive to proteasomal inhibition (Sheaff et al., 2000). This could be due to the direct interaction between the C-terminus of p21 and the C8α subunit of 20S proteosome in an ubiquitin-independent manner as deletion of the C8α binding region in p21 attenuates C8α binding and increases p21 stability (Touitou et al., 2001). However it has been suggested that there is no strong evidence of the existence of an active stand-alone 20S proteosome (Bloom and Pagano, 2004).

In contrast, p21 degradation has been shown to be mediated by a unique ubiquitination mechanism. In this system, degradation is dependent on an ubiquitin chain conjugated to the N-terminal methionine residue, instead of the conventional lysine residues. In addition, a functional NEDD8 conjugation system is required for p21 degradation *in vivo* (Bloom et al., 2003).

In response to low doses of UV irradiation, p21 is degraded via the Skp2-dependent proteosome pathway (Bendjennat et al., 2003). The initiating signal for UV-induced p21 degradation was shown to involve GSK3β-dependent phosphorylation of p21 at Ser^{114} (Lee et al., 2007).

3.1.5 Relationship between p21 and Chk1

The first link between p21 and Chk1 was uncovered in a fission yeast study where the association of p21 and PCNA is thought to lead to ATR-dependent activation of Chk1 (Tournier et al., 1996). Overexpression of PCNA led to G_2-phase arrest, while deletion of the *Chk1*$^+$ gene abolished this inhibition. The authors thought that the association of p21 and PCNA could be modulated by Chk1, though the mechanism is not clear.

In another study, Chk1 has been reported to be downregulated at the transcriptional level in a p53-dependent manner. This repression requires p21 and cells lacking p21 cannot downregulate Chk1. It was suggested that p53 and Chk1 are involved in a feedback loop mechanism where Chk1 stabilised p53 through

phosphorylation and p53 in turn downregulated Chk1. In the damaged cell context, Chk1 downregulation by p53 would prevent an excessively prolonged G_2-phase arrest that could trigger apoptosis (Gottifredi et al., 2001).

3.1.6 Objectives

In this chapter, I aim to validate and characterise Chk1 protein kinase as a potential regulator of p21 and dissect the intermolecular interaction between Chk1 and p21 to investigate the basis of Chk1 substrate recognition.

3.2 Results

3.2.1 Identification of Checkpoint kinase 1 (Chk1) as a p21^{waf1} kinase

p21 is an important component of the DNA damage response which functions to arrest the cell cycle by inhibiting cyclin-dependent kinase activity (Harper et al., 1993). Previous research from the Ball lab aiming to identify novel protein kinases for p21 has developed a screen for endogenous activity from whole cell lysates (Scott et al., 2002). Whole cell lysate from HeLa cells was subjected to three rounds of chromatographic fractionation using Q-Sepharose, SP-Sepharose and HS-Poros columns to obtain an active p21 kinase fraction. The active p21 kinase fraction was then analysed by gel filtration using a Superose 12 column. Each gel filtration column fraction was collected and the kinase activities were characterised. Four possible waves of kinase activities were noted. One of the kinases was found to be PKCζ (Scott et al., 2002) which correspond to the first activity from fraction 1 to 4 with the activity strongest in fraction 1 (PKCζ immunoblot not shown). A possible second wave of activity was observed in fraction 5 with the appearance of a slow mobility shift in the p21 blot (Figure 3.2; fraction 5; top and middle panel). The third possible activity was seen in fraction 6 to 7 where the slower mobilised p21 form is more dominant in the [γ^{32}P] blot (Figure 3.2; fraction 6 to 7; top panel). Lastly, the fourth activity was putatively identified as Chk1 (Figure 3.2; fraction 7 to 8; Scott and Ball, unpublished data). The experiments described herein were repeated twice and the results are consistent unless stated otherwise. Figures displayed herein are best representation of the results.

Using this data as a starting point, I decided to validate p21 as a potential substrate for Chk1. The Chk1 substrate consensus sequence was delineated to a Rxx(S/T) motif (O'Neill et al., 2002) and Chk1 has also been demonstrated to phosphorylate Cdc25C at Ser^{216} which contains the RxxS motif. In contrast, Chk1 was also reported to target substrate such as p53 at Ser^{15} and Ser^{20} which do not resemble the Cdc25C phosphorylation motif targeted by Chk1 (Shieh et al., 2000). Therefore it is possible that Chk1 could display flexible substrate specificity modulated by allosteric action. To identify a possible Chk1 substrate consensus sequence within p21, full-length p21 amino acid sequence was aligned with Cdc25C phosphorylation motif (amino acids 211 to 221) and p53 phosphorylation motif (amino acids 13 to 23). Analysis of the sequence revealed that a C-terminal p21 region which contains possible phospho-acceptor sites at Thr^{145} and Ser^{146}, shared a suggestive homology with the Cdc25C and p53 phosphorylation motifs (Figure 3.3). Furthermore, both Thr^{145} and Ser^{146} phospho-acceptor sites fit within the Chk1 substrate consensus motif, Rxx(S/T). Like p53 phosphorylation motif, p21 also contains a glutamine residue upstream of potential phospho-acceptor sites at Thr^{145} and Ser^{146}. In addition, p21 also shares negatively-charged aspartic acid residue and aromatic residue downstream of potential phospho-acceptor sites at Thr^{145} and Ser^{146}. This suggested that p21 could be a novel substrate for protein kinase Chk1.

Chk1, Chk2 and death-associated protein kinase (DAPK) belong to the same superfamily of calcium/calmodulin-dependent protein kinase and are also involved in stress response pathways (Figure 3.4). Both Chk2 and DAPK1 have been

demonstrated to phosphorylate p21 at Ser^{146} and Thr^{145} *in vitro* respectively (Craig et al., 2003, Fraser and Hupp, 2007). To test whether p21 is indeed a substrate of Chk1, a kinase assay was set up to compare the activity of Chk1, Chk2 and DAPK towards p21. Recombinant human p21 was expressed and purified from BL21 *E.coli*. Chk1 baculovirus was generated using methods outlined in Chapter 2 and titrated before studies were carried out to determine optimal expression conditions for parameters such as viral dilution (multiplicity of infection) and incubation time (data not shown). Using these optimal conditions, recombinant human N-terminally tagged His-Chk1 proteins were expressed in *Sf9* insect cell system by infecting with Chk1 baculovirus. The expressed proteins were purified using the Ni-NTA column. Recombinant human N-terminally tagged His-Chk2 and GST-DAPK1 core (kinase domain of DAPK1) were also expressed and purified from *Sf9* insect cells (both Chk2 and DAPK1 were kindly provided by Hupp lab). Protein concentrations of Chk1, Chk2 and DAPK1 were determined by BCA assay and normalised to 100 ng.

Kinase assay conditions such as kinase buffer, incubation time and temperature were also tested and optimised (data not shown). All kinase assays described hereinafter were incubated at 30°C for 30 minutes and then stopped by addition of SDS-sample buffer unless stated otherwise. In Figure 3.5A, [γ^{32}P] incorporation into p21 by Chk1 is comparable to that of DAPK1. Negative controls with either no kinase or substrate showed no [γ^{32}P] incorporation, indicating the absence of a contaminating kinase or substrate in the sample preparation. In addition, Chk1 was shown to phosphorylate p21 in a dose-dependent manner, demonstrating a linear

relationship (Figure 3.6B and C). In comparison to Chk1, Chk2 activity towards p21 was very weak (Figure 3.5A), suggesting that phosphorylation of p21 by calcium calmodulin family members is specific for some member and not others. Interestingly, previous studies have indicated that Chk1 and Chk2 have very similar substrate specificity (O'Neill et al., 2002). Thus the preferential phosphorylation of p21 by Chk1 suggested that there may be additional determinants outwith the phosphorylation motif. The above data suggested that Chk1 was an effective kinase towards p21 *in vitro*.

3.2.2 Chk1 phosphorylates p21 Ser^{146}

To further characterise Chk1 activity towards p21, a library of biotinylated overlapping 20-mer peptides based on the sequence of p21 were synthesized (Figure 3.6A). Peptides were dissolved in DMSO. Each p21 peptide was assembled with recombinant human Chk1 in a kinase reaction to identify the possible p21 phosphorylation region catalysed by protein kinase Chk1. DMSO was used as a negative control. In Figure 3.6B, there was a 16-fold increase of [γ^{32}P] incorporation into p21 peptide 10 and a 9-fold increase of [γ^{32}P] incorporation into p21 peptide 11 as compared to DMSO control. This indicated that the C-terminal domain of p21 contains phospho-acceptor sites targeted by Chk1. Peptide 10 and 11 contains possible phospho-acceptor sites at Ser^{137}, Thr^{145}, Ser^{146}, Thr^{148}, Ser^{153} and Ser^{160}. Interestingly, peptide 10 exhibited an approximately 2-fold increase of [γ^{32}P] incorporation as compared to peptide 11 suggesting that residues before Thr^{145} might be important for Chk1 substrate motif

recognition. Indeed, as revealed in Figure 3.3, a conserved arginine residue is located at P-3 position relative to the Thr^{145} and Ser^{146} phospho-acceptor site that fits Chk1 consensus substrate motif, Rxx(S/T). In addition, a conserved glutamine residue was found at P-1 position relative to Thr^{145} phospho-acceptor site. Perhaps this explained why peptide 11 which lacks the conserved arginine and glutamine residues showed lower [γ^{32}P]-ATP incorporation than peptide 10.

Phospho-specific antibodies toward Thr^{145} and Ser^{146} were used to determine whether these sites were phosphorylated by Chk1. The specificity of the p21 phospho-antibodies were first confirmed using an ELISA format (Figure 3.7A and B). Biotinylated p21 phospho-Thr^{145} ($KRRQ_PTSMTDFYHSKRRLIFS$) and phospho-Ser^{146} ($KRRQT_pSMTDFYHSKRRLIFS$) peptides together with a non-phosphorylated p21 peptide control (KRRQTSMTDFYHSKRRLIFS) were captured onto a 96-well plate coated with streptavidin before incubated with rabbit α-phospho-Thr^{145} or goat α-phospho-Ser^{146} antibodies. Any unbound primary antibodies were washed off before incubating with HRP-conjugated α-rabbit or α-goat secondary antibodies. Any unbound secondary antibodies were washed off before the bound antibodies were detected by enhanced chemiluminescence. The data showed that the phospho-Thr^{145} antibodies were only reactive towards phospho-Thr^{145} peptides and phospho-Ser^{146} antibodies were specific towards phospho-Ser^{146} peptides with little or no reactivity towards non-specific peptides. This indicated that the p21 α-phospho-Thr^{145} and α-phospho-Ser^{146} antibodies are specific.

Recombinant human p21 was then assembled with recombinant human Chk1, Chk2 or DAPK in kinase assay using unlabelled ATP before reaction products were resolved by SDS-PAGE. p21 phosphorylation was then analysed by immunoblotting with specific α-p21 phospho-Thr^{145} and phospho-Ser^{146} antibodies (Figure 3.7C). It showed that p21 Ser^{146} is predominately phosphorylated by Chk1 while Thr^{145} is mildly phosphorylated above background as compared to that by DAPK. It has been published that DAPK targeted p21 at Thr^{145} (Fraser and Hupp, 2007). Consistent with the [γ^{32}P]-ATP kinase assay, very weak phosphorylation of p21 Ser^{146} by Chk2 was detected, indicating that activation of Chk2 by allosteric mechanisms is required for efficient activity towards p21 as previously demonstrated (Craig et al., 2003). Total p21 protein level was detected to show equal loading of p21 in each reaction (Figure 3.7C). However as antibodies to phospho-Ser^{148} and phospho-Ser^{153} were not available, Chk1-dependent phosphorylated p21 was subjected to tryptic cleavage followed by high performance liquid chromatography (HPLC) separation by reverse phase. The phospho-peptides were then analysed by mass spectrometry and Edman degradation confirming Ser^{146} to be the major phospho-acceptor site for Chk1 on p21 (data not shown).

3.2.3 Activity of cellular Chk1 towards recombinant p21

Recombinant human Chk1 has been shown to phosphorylate p21 at Ser^{146}. To assess whether cellular Chk1 is active towards recombinant human p21, endogenous Chk1 was immunoprecipitated from HeLa and HCT116 p21$^{-/-}$ cells

and characterised in kinase assays. Before Chk1 immunoprecipitation-kinase (IP-kinase) assays were carried out, the conditions of the assay were first optimised. To determine whether DNA damage-induced activation of Chk1 is required for activity towards p21, HeLa and isogenic HCT116 $p21^{-/-}$ cells were treated with aphidicolin, a specific inhibitor of DNA polymerase α and δ and blocks cell cycle at early S-phase via the activation of Chk1 (Feijoo et al., 2001). The optimal concentration of aphidicolin required for Chk1 activation was determined by titration of the cell cycle inhibitor agent into the cell medium over 4 hours before cells were harvested and analysed by SDS-PAGE and immunoblotting. Ethanol (the aphidicolin carrier) was used as a negative control. As reported, treatment with aphidicolin leads to the activation of Chk1 which is accompanied by a mobility shift of the enzyme by SDS-PAGE and immunoblot analysis (Feijoo et al., 2001). Activation of Chk1 was visualised in three different cell lines (HeLa, HCT116 wild-type ($p21^{+/+}$) and HCT116 $p21^{-/-}$ cells) by immunoblotting using α-Chk1 antibodies. Following aphidicolin treatment, mobility shift of Chk1 was observed across all three cell lines (Figure 3.8A). Five μM of aphidicolin treatment was sufficient to see an activation of Chk1. Mobility shift of Chk1 was not observed in the presence of ethanol treatment alone.

To optimise the conditions for Chk1 activation, a time course of aphidicolin treatment was performed. Both HeLa and HCT116 wild-type cells were treated with 20 μM of aphidicolin for a period of 10 to 240 minutes. Twenty μM of aphidicolin treatment was chosen to ensure a robust activation of Chk1. Figure 3.8B showed that Chk1 mobility shift was visible from 30 minutes of aphidicolin

treatment onwards with the greatest effect observed for 120 minutes and 240 minutes of aphidicolin treatment. Therefore, 20 μM of aphidicolin treatment for 4 hours was set as the optimal condition to induce a DNA damage response in mammalian cells.

Immunoprecipitation assays would be used to isolate Chk1 from mammalian cells, however it is not known where the Chk1 antibodies binds to the protein with regard to the catalytic site or substrate binding site. Therefore to test that the substrate utilisation of immunoprecipitated Chk1 is not affected by the presence of antibodies used in the IP-kinase assay, sheep α-Chk1 antibodies were pre-incubated with recombinant human Chk1 protein kinase prior to assembly with recombinant human p21 in [γ^{32}P]-ATP kinase assay (Figure 3.9). This showed that in the presence of sheep α-Chk1 antibodies, [γ^{32}P] incorporation into p21 was slightly less than in the absence of sheep α-Chk1 antibodies. This indicated that catalytic activity of recombinant human Chk1 was only slightly affected in the presence of sheep α-Chk1 antibodies and thus it would be a suitable method/reagent to assay Chk1 catalytic activity *in vitro*.

Next, sheep α-Chk1 antibodies were used to immunoprecipitate Chk1 from cells and optimal buffer conditions were determined (data not shown). Cellular Chk1 was then immunoprecipitated from HeLa and isogenic HCT116 $p21^{-/-}$ cells and assayed for its activity towards recombinant human p21. As at this stage, it was not clear whether ATR-activation of Chk1 was required for its activity towards p21, therefore HeLa and HCT116 $p21^{-/-}$ were incubated in the presence or absence

of aphidicolin prior to cell lysis and immunoprecipitation of the endogenous enzyme. Immunoblotting of whole cell lysates using α-Chk1 antibodies showed that aphidicolin treatment led to activation of Chk1 as evidenced by the appearance of slower-migrated form of Chk1 (Figure 3.10; lower panel). Immunoblotting of Chk1 immunoprecipitates also suggested that similar amounts of Chk1 were immunoprecipitated from aphidicolin-treated and ethanol-treated cells (Figure 3.10; middle panel). Although it should be noted that the sheep α-Chk1 antibodies used does not immunoprecipitate the upper band (activating form). In fact, none of the commercial antibodies tested immunoprecipitated the upper band and the antibodies chosen for this assay was the best one for quantitative immunoprecipitation of total Chk1 protein. Analysis of the immunoprecipitated Chk1 showed that endogenous Chk1 from HeLa and HCT116 $p21^{-/-}$ cells were active towards recombinant human p21 (Figure 3.10; upper panel). [γ^{32}P] incorporation into p21 was greater in the presence of Chk1 immunoprecipitated from aphidicolin-treated HeLa as compared to Chk1 immunoprecipitated from untreated HeLa cells, suggesting that aphidicolin-treated HeLa Chk1 was catalytically more active than untreated HeLa Chk1 despite the absence of the activated upper band. However no difference in [γ^{32}P] incorporation into p21 was observed between Chk1 immunoprecipitated from untreated or aphidicolin-treated HCT116 $p21^{-/-}$ cells.

3.2.4 Co-immunoprecipitation of Chk1 and p21

We have shown that Chk1 co-eluted with a slower mobilised form of p21 in the gel filtration fraction and this form was suggestive of phosphorylation mediated by Chk1. I have also demonstrated that human recombinant and cellular Chk1 was active towards p21. Furthermore, the data suggests that p21 Ser^{146} is the major phospho-acceptor site catalysed by Chk1. To establish a physiological link, I attempted to look for evidence of physical interaction between Chk1 and p21 by co-immunoprecipitation. HCT116 wild-type cells were used as there is an abundant level of p21 and Chk1. Endogenous Chk1 was immunoprecipitated from HCT116 wild-type cells using sheep α-Chk1 antibodies, however there was no visible evidence of p21 co-immunoprecipitation (data not shown). To circumvent the possibility that the antibodies used to immunoprecipitate Chk1 could affect interaction of p21 and Chk1, endogenous p21 was immunoprecipitated from HCT116 wild-type cells using rabbit α-p21 antibodies. Again, there was no indication of Chk1 co-immunoprecipitation (data not shown), however non of the p21 antibodies available were able to quantitatively immunoprecipitated p21.

As pointed out, I was unable to identify a commercial Chk1 antibody that was able to quantitatively recover all form of Chk1 from the cells. Thus in collaboration with Prof. David Gillespie's group, we tried to look for physical interaction of chick Chk1 and human p21. Chick Chk1 was used due to the availability of a better antibody reagent that recognises the C-terminal domain of chick Chk1 and has been shown by the Gillespie group to quantitatively immunoprecipitate both endogenous and exogenous chick Chk1. They have also demonstrated that the

immunoprecipitated protein retains catalytic activity (M.T. Scott, personal communication). No equivalent reagent is available for the human protein. Chick Chk1 shares 84 % homology with human Chk1 (Figure 3.11). Full-length chick Chk1 or a kinase-dead version of chick Chk1 was transfected into Cos1 cells alone or together with human p21. Chick Chk1 was immunoprecipitated from Cos1 cells using the α-C-terminal Chk1 antibodies and immunoblotted for the presence of human p21. A low level of exogenous p21 was co-immunoprecipitated with full-length chick Chk1 (Figure 3.12). Interestingly, when a kinase-dead version of chick Chk1 was transfected into Cos1 cells, a greater level of exogenous p21 co-immunoprecipitated with it compared with wild-type Chk1 even though equal levels of wild-type and kinase-dead Chk1 was immunoprecipitated. The highly dynamic dissociation rates of enzyme-substrate complex may explain why a co-immunoprecipitation complex between endogenous Chk1 and p21 protein was not detected. The data suggested that Chk1 could form a transient interaction with p21 and this interaction was strengthened when a kinase-dead version of chick Chk1 was introduced. This also suggests of a physiological link between Chk1 and p21.

3.2.5 Chk1 catalytic activity can be allosterically regulated by a N-terminal region of p21

Protein kinases often achieve stringent substrate interaction through docking motif association (Remenyi et al., 2006, Goldsmith et al., 2007). Some members of the calcium-calmodulin dependent superfamily, for example DAPK1 and Chk2, have been shown to dock to their substrates enhancing specificity/activity (Craig et al.,

2003, Fraser and Hupp, 2007). As suggested earlier, the discrepancy between the ability of Chk1 and Chk2 to phosphorylate p21 may indicate additional determinants such as substrate docking. These substrate docking motif interactions aim to tether the substrate to its enzyme and/or induce allosteric activation of the protein kinases. If the substrate docking motif is involved in tethering the substrate to the enzyme, then a ligand based on the docking motif should be able to competitively inhibit the protein-protein interaction, leading to inefficient phosphorylation of the substrate (Figure 3.13A). This is observed in the docking-dependent regulation of pRb by CDK4 (Wallace and Ball, 2004). However if the substrate docking motif functions to activate the kinase allosterically, then the kinase activity will be stimulated by the ligand, leading to efficient phosphorylation of the substrate (Figure 3.13B). A prime example is the allosteric activation of Chk2 by two p53 DNA-binding domain peptides (Craig et al., 2003).

A library of p21 peptides (Figure 3.6A) was added to a Chk1 kinase assay containing p21 to test whether a tethering or allosteric docking mechanism is required for Chk1 activity towards p21 (Figure 3.14). Interestingly, [γ^{32}P] incorporation into p21 was significantly and consistently higher in the presence of peptide 4 as compared to the DMSO control or any other peptides. Peptide 2 also appeared to stimulate Chk1 catalytic activity towards p21 albeit to a lesser extent. In contrast, [γ^{32}P] incorporation into p21 appeared to be inhibited in the presence of peptide 10 and 11; this is most likely explained by the fact that both peptide 10 and 11 contain the Chk1 phospho-acceptor site at Ser^{146}, resulting in competition between full-length p21 and peptide substrate utilisation by Chk1. This data was

reproducible with different batches of p21 peptides synthesised from different companies. To further characterise peptide 4 stimulation of Chk1 catalytic activity, kinetic analyses were undertaken. Addition of peptide 4 into the Chk1 kinase assay showed increased [γ^{32}P] incorporation into Chk1 and p21 in a dose-dependent manner with increasing concentration of p21 peptide 4 (Figure 3.15A and B). This data suggested that p21 could function as a homotropic allosteric activator for Chk1, with peptide 4 functioning as a docking motif that allosterically stimulates Chk1 activity towards p21. It is possible that peptide 2 may also form the Chk1-p21 binding interface.

3.2.6 p21 peptide 4 forms a binding interface with Chk1

To further characterise p21 peptide 4 stimulation of Chk1 catalytic activity, I wanted to establish that p21 peptide 4 binds to Chk1. To investigate further, I examined peptide 4 binding to Chk1 using non-denaturing gel electrophoresis in the absence of SDS. In non-denaturing gel electrophoresis, proteins retain their folded conformation and biological activity, thus any binding events should be preserved. Biotinylated p21 peptide 4 and recombinant human Chk1 were assembled in a kinase assay with or without unlabelled ATP. The kinase reactions were stopped using sample buffer without SDS/DTT and immediately resolved by non-denaturing gel electrophoresis. p21 peptide 4 was detected by HRP-conjugated streptavidin. Interestingly, a band with a molecular weight of around 50-54 kDa was detected in the reaction without ATP (Figure 3.16). Chk1 has a molecular weight of around 54 kDa and therefore the detected band was indicative

of peptide 4 binding to Chk1. However this band was not detected in the presence of ATP, suggesting that peptide 4 binding to Chk1 may be ATP-dependent and that presence of ATP may dissociate Chk1 and peptide 4 interaction. Immunoblotting for Chk1 protein showed that Chk1 migrated slower in the presence of ATP due to autophosphorylation and this was not seen in the absence of ATP. Unbound peptide was detected and migrated below the 20 kDa mark. The above data suggested that the stimulatory peptide 4 could form a docking interface with Chk1 protein kinase and that this may be sensitive to the presence of ATP. This was later supported by data (in chapter 4) showing that p21 peptide 4 can disrupt the intramolecular interaction between the C-terminal and N-terminal domain of chick Chk1 (Figure 4.20).

3.2.7 p21 peptide 4 can allosterically regulate Chk1 catalytic activity towards other substrates

p21 peptide 4 has been demonstrated to form a docking motif that is able to allosterically activate Chk1. DAPK1 activity towards weaker substrates such as $p53^{N1-66}$ (an N-terminal domain of p53) has been shown to be allosterically enhanced in a docking-dependent manner, using potential docking motifs from high-affinity substrates such as p21 (Fraser and Hupp, 2007). However it is not clear if Chk1 activity towards other substrates can be modulated by p21-derived stimulatory peptide 4. To test this, peptide 4 was added to a Chk1 kinase assay containing either $p53^{N1-66}$ or Cdc25C as the substrate. [γ^{32}P] incorporation into $p53^{N1-66}$ was increased in the presence of peptide 4 (Figure 3.17). In addition, [γ^{32}P]

incorporation into Cdc25C was also enhanced in the presence of peptide 4. This showed that p21-derived peptide 4 can modulate Chk1 activity towards other substrates, perhaps suggesting that p21 might function as a regulatory molecule that modulates the activity of Chk1 *in vivo* towards distinct substrates.

To test whether the stimulatory effect of peptide 4 on Chk1 towards p21 is specific towards Chk1, peptide 4 was analysed for its ability to modulate Chk2 and DAPK1 activity towards p21. As DAPK1 and Chk2 are close relatives of Chk1, there is a possibility that they might be regulated by the same allosteric mechanism. Interestingly, Figure 3.18 showed that while p21 peptide 4 could stimulate Chk1 activity, [γ^{32}P] incorporation into p21 catalysed by DAPK1 core domain was slightly inhibited in the presence of peptide 4. Very little or no [γ^{32}P] incorporation into p21 catalysed by Chk2 was detected with or without peptide 4. The data suggested that p21 peptide 4 allosteric activation was specific to Chk1, but not DAPK1 and Chk2.

Allosteric regulation of Chk2 has been proposed to influence protein kinase substrate specificity (Craig et al., 2003). To address the concern that allosteric modulation of Chk1 activity might change its specificity in p21 phosphorylation and cause phosphorylation at additional/distinct sites on p21, we analysed Chk1 phosphorylation of the p21 peptide library in the presence of the stimulatory peptide 4. However similar to the earlier experiment (Figure 3.6B), only peptide 10 and 11 showed [γ^{32}P] incorporation above background levels, indicating that Ser^{146} in the C-terminal domain could remained as the major phospho-acceptor site

(Figure 3.19A). To confirm this I used phospho-specific antibodies to p21 Thr^{145} and Ser^{146}. Kinase reactions were assembled with or without peptide 4 and were resolved by SDS-PAGE and transferred to nitrocellulose membrane before immunoblotted with p21 Thr^{145} and Ser^{146} phospho-specific antibodies (Figure 3.19B). The level of phospho-Ser^{146} detected was not affected by the presence of peptide 4 stimulation, suggesting that Ser^{146} remained as the major phospho-acceptor site targeted by Chk1 but is not stimulated further. Interestingly, there was an increase of phosphate incorporation on phospho-acceptor site Thr^{145} in the presence of peptide 4. This could indicate that although Ser^{146} remained the predominant phospho-acceptor site, stimulation of Chk1 catalytic activity by peptide 4 could result in enhanced phosphate incorporation onto p21 Thr^{145}. The double phosphorylation at Thr^{145} and Ser^{146} is likely to explain the mobility shift observed on the phospho-Thr^{145} IgG immunoblot when the kinase reaction was incubated with p21 peptide 4 (Figure 3.19B; lane 1; upper panel), although it remains a possibility that the allosterically activated Chk1 could target other phosphorylatable serine and threonine residues in peptide 10 and 11.

3.2.8 Threonine^{55}, Proline^{58} and Tryptophan^{65} are critical amino acid residues for peptide 4 allosteric activation of p21

It has now been accepted that protein-protein interactions often involve linear interaction or docking motifs. These linear motifs are normally between three to ten amino acids of which a few may be critical to form a docking interaction (Remenyi et al., 2006). In order to identify the amino acids critical for the docking

interface between Chk1 and p21 peptide 4, single alanine mutations were introduced across peptide 4 (Figure 3.20A). The mutated peptides were assembled with Chk1 and p21 in kinase assays and analysed for their effect on [γ^{32}P] incorporation into p21 compared to unmutated peptide 4 (Figure 3.20B). Mutation of many residues showed little effect on peptide 4 stimulation of Chk1 towards p21, however alanine mutations at Thr^{55}, Pro^{58} and Trp^{65} strikingly attenuated the stimulatory effect of peptide 4 on Chk1 activity towards p21. This suggested that Thr^{55}, Pro^{58} and Trp^{65} are the critical residues required for the allosteric docking interaction between p21 peptide 4 and Chk1 and are required for activation of Chk1 towards substrates such as p21.

3.2.9 p21 peptide 4 functions as an allosteric docking motif required for efficient Chk1 phosphorylation of p21

The data shown hitherto suggested that p21 peptide 4 could allosterically modulate Chk1 catalytic activity. However it was not clear whether the loss of the peptide 4 region affects substrate utilisation. To test this, Chk1 kinetics of full-length p21 and p21 peptide 10 utilisation was analysed. A titration of full-length p21 or peptide 10 was assembled with Chk1 in [γ^{32}P]-ATP kinase assay. [γ^{32}P] incorporation into full-length p21 or peptide 10 was quantified using a phosphorimager. The Michaelis-Menten kinetic constants were calculated via Hanes plot using hyperbolic regression software. Hanes plot is a common linear representation that determines the important kinetic parameters K_m, V_{max} and V_{max}/K_m rapidly, where [S]/v is plotted against [S]. The Michaelis-Menten kinetic

model states that V_{max} is the enzyme's maximum reaction rate and K_m is the concentration of substrate at which the enzyme's reaction rate is half V_{max}. Although Figure 3.21 showed that the K_m for p21 peptide 10 was higher than that of full-length p21. It should be noted that the outlying K_m value in experiment set 2 for p21 peptide 10 could spuriously increase the average K_m. Hencefore a test of statistical significance is needed to determine whether there is a significant difference between the K_m value of full-length p21 and p21 peptide 10.

It was shown earlier that p21 peptide 4 was able to allosterically stimulate Chk1 activity and bound Chk1 in an ATP-dependent manner. Thus it is possible that the N-terminal domain of p21 is involved in a docking interaction with Chk1 that enhanced substrate specificity and enzymatic activity. To further assess the requirement of docking motif for substrate recognition, I generated an N-terminal (amino acids 1-65) truncated p21 mutant (p21 ΔNT) that was expressed in *E.coli* and purified using a two-step purification method (Figure 3.22A). N-terminally His-tagged p21 was first extracted from *E.coli* inclusion bodies and then further purified using Ni-NTA agarose before being analysed by coomassie blue stain and immunoblot (Figure 3.22B). The immunoblot showed that the His-tagged p21ΔNT mutant migrated at around 13-14 kDa which is consistent with the calculated molecular mass. To ensure that there were equal amounts of p21 in the kinase assays, the concentration of p21 ΔNT mutant was normalised to that of full-length p21 using an ELISA assay (Figure 3.23). A titration of full-length p21 and the ΔNT mutant was captured on a 96-well plate and overlaid with α-p21 C-terminal antibody. Any unbound α-p21 antibody was washed off before incubated with

HRP-conjugated secondary antibodies. Bound antibody was detected by enhanced chemiluminescence. The relative light unit values and concentration obtained for full-length p21 were computed to construct a XY-scatter plot from which a linear equation was derived. The concentration of p21 ΔNT mutant was then calculated from the equation. After the concentration of the p21 proteins were normalised, a titrated amount of full-length p21 and ΔNT mutant protein were assembled with Chk1 in [γ^{32}P]-ATP kinase assays. Figure 3.24A showed that [γ^{32}P] incorporation into p21 ΔNT mutant was marginally lower than that of full-length p21 and this change is reproducible in duplicate sets of experiment. This suggested that the deleted N-terminal domain of p21 is required to ensure maximal Chk1 activity towards p21, augmenting the idea that the p21 N-terminal domain contains a Chk1 docking site. To assess the possibility that p21 peptide 4 could function as docking motif in Chk1 substrate recognition, I tested if the addition of p21 peptide 4 could restore Chk1 optimal activity towards p21 ΔNT mutant (Figure 3.24B). Interestingly, [γ^{32}P] incorporation into p21 ΔNT mutant in the presence of peptide 4 was about 3-fold higher than in the absence of peptide 4. On the other hand, [γ^{32}P] incorporation into full-length p21 was only about 2-fold higher in the presence of peptide 4. This indicated that peptide 4 could function as a docking peptide in place of a deleted p21 N-terminal region and reconstitute all the regions of p21 required for optimal targeting by Chk1.

3.3 Discussion

3.3.1 Identification of Chk1 as a $p21^{waf1}$ kinase

p21 plays an important role in mediating cell cycle arrest. Upon appropriate signals, p21 functions to inhibit cyclin-dependent kinase (CDK) activity and DNA synthesis through negative regulation of PCNA (Harper et al., 1993, Chen et al., 1995). p21 has already been reported to be phosphorylated by a diverse range of protein kinases such as GSK3β, PKB/Akt and p38α (Rossig et al., 2001, Kim et al., 2002, Lee et al., 2007) and identification of novel protein kinase for p21 may contribute to a detailed understanding of the signalling pathways, in which p21 is involved. Gel filtration analysis showed that checkpoint kinase, Chk1 co-eluted with a kinase activity that generated a slower-migrated form of p21, suggesting that p21 could be a novel substrate of Chk1.

The substrate specificity of Chk1 has been elucidated to contain the consensus motif Rxx(S/T) (Hutchins et al., 2000, O'Neill et al., 2002). Modelling of the Chk1 kinase domain interaction with a peptide based on the phosphorylation site from Cdc25C revealed that the hydrophobic side chains at P-5 and P+1 positions of the substrate peptide, together with an arginine residue at P-3 position and small side chain at P+2 position are important for Chk1 substrate specificity (Chen et al., 2000). Protein sequence analysis showed that p21 (amino acid 141 – 151) seems to fit in well with the Chk1 consensus substrate motif, displaying an arginine residue at P-3 position, a hydrophobic side chain at P+1 and a small side chain at P+2 position relative to the Ser^{146} phospho-acceptor site (Figure 3.3). Furthermore, p21 also shares upstream glutamine residue and downstream negatively-charged

aspartic residue and aromatic residue relative to p21 Ser^{146} phospho-acceptor site with p53 Ser^{20} phospho-acceptor site. I have showed that recombinant human and cellular Chk1 phosphorylate recombinant p21 readily *in vitro* at the C-terminal end with Ser^{146} as the major phospho-acceptor site. Mass spectrometry and Edman degradation have further confirmed that Ser^{146} is the major phospho-acceptor site targeted by Chk1. As shown by immunoblotting, p21 Thr^{145} phospho-acceptor site could also be targeted by Chk1. However other potential phospho-acceptor sites such as Thr^{148}, Ser^{153} and Ser^{160} must also not be ruled out, Even though Thr^{148}, Ser^{153} and Ser^{160} do not contain an arginine residue at the P-3 position, allosteric regulation has been known to activate enzymes towards weak substrates (Craig et al., 2003, Fraser and Hupp, 2007).

Ionising radiation-induced phosphorylation of Chk1 at Ser^{345} is found to co-immunoprecipitate with p21, p53 and 14-3-3σ (Tian et al., 2002). In addition, p21 association with Chk1 is dependent on the presence of p53 (Tian et al., 2002). However, in this thesis, co-immunoprecipitation of endogenous Chk1 and p21 from mammalian cells proved to be difficult, possibly due to epitopes masked by the Chk1-p21 or other interacting protein binding interface. It is also possible that Chk1 is activated differently in aphidicolin-induced S-phase arrest as opposed to irradiation-induced G_2 arrest that could result in distinct protein partners. To circumvent this, collaboration was set up with Prof. David Gillespie's group to look at the physical interaction between chick Chk1 and human p21. Chick Chk1 shares a 84 % homology with human Chk1. Using α-C terminal Chk1 antibodies, transient co-immunoprecipitation of Chk1 and p21 was established and this

interaction was found to be more pronounced when a kinase-dead version of chick Chk1 was used. This is suggestive of a physiological link between Chk1 and p21.

However given the promiscuity of the protein kinase can display for substrates *in vitro*, more studies will be needed to confirm that p21 is a novel substrate for Chk1:-

1. Is p21 phosphorylated at the same site (Ser^{146}) in mammalian cells in response to activated Chk1 under DNA damaging conditions?
2. Do constitutively active mutants of Chk1 or kinases upstream of Chk1 lead to phosphorylation of p21 in cells?
3. Does inhibition of the Chk1 protein kinase, through Chk1 inhibitors or siRNA attenuate phosphorylation of p21?

3.3.2 Allosteric regulation of Chk1 by the N-terminal region of p21

It has been reported for many protein kinases that a consensus substrate phosphorylation motif is not sufficient to confer stringent selective substrate recognition (Remenyi et al., 2006, Goldsmith et al., 2007). Indeed, Chk1 has been shown to phosphorylate p53 on Ser^{15}, Ser^{20} and Ser^{37} *in vitro*, however these p53 sites do not share any similarity with the Chk1 substrate consensus motif (Shieh et al., 2000). Thus it has been postulated that Chk1 may be extremely flexible in its sequence requirements and substrate specificity. In the same study, Chk1 was shown to preferentially phosphorylate a tetrameric form of p53 as compared to monomeric p53 (Shieh et al., 2000). This could suggest that the tetramerisation

domain of p53 provides a docking platform for Chk1. Indeed, protein kinases often recognise their substrates through interactions in regions distinct to the active site (Figure 3.25). This involves modular protein-protein recognition domains such as SH2 and SH3 domains that are distinct to the catalytic domain. An example of this is the non-receptor tyrosine kinases (Miller, 2003). Another mode involves docking interactions – in this case, a docking domain on the protein kinase binds to a linear interaction motif or docking motif present in its substrate. A well-characterised example is MAPK with its docking requirement for D-site or DEF-motif (Tanoue et al., 2000, Sheridan et al., 2008). Similarly, Chk2 activity towards p53 transactivation domain is allosterically regulated by high-affinity p53 Box II and Box V peptides (Craig et al., 2003).

Using p21 substrate as a model substrate to investigate a docking-dependent regulation of Chk1 activity, it was shown that p21 peptide 4 was able to stimulate Chk1 activity towards p21 (Figure 3.14). Interestingly, peptide 4 binding to Chk1 appeared to be ATP-dependent (Figure 3.16). In the absence of ATP, binding of peptide 4 to Chk1 was observed and there was no binding of peptide 4 to Chk1 in the presence of ATP. It is possible that transient allosteric activation of Chk1 by p21 peptide 4 leads to an ATP-dependent event and in turn induces a conformational change within Chk1 that blocks or disrupts the peptide 4 docking site. The ATP-dependent event could be autophosphorylation of Chk1. Autophosphorylation has been observed in the C-terminal domain of Chk1 (Ng et al., 2004) and mass spectrometry data has suggested that Chk1 Ser^{407} is the major phospho-acceptor site.

p21 peptide 4 modulation of Chk1 activity did not appear to be limited to p21 and p21 peptide 4 could also stimulate Chk1 catalytic activity towards $p53^{N1-66}$ and Cdc25C. This suggests that Chk1 utilises a universal docking motif with characteristics of the p21 N-terminal domain for its allosteric activation. To test this possibility, I aligned the sequence of p21 peptide 4 with adaptor proteins Claspin and BRCA1, both of which have been reported to be involved in the activation of Chk1 (Figure 3.26A and B). Interestingly, sequence alignment identified homology between p21 peptide 4 and the C-terminal domain of Claspin and N-terminal of BRCA1. Although Chk1 has been reported to interact with the N-terminal domain of Claspin (Clarke and Clarke, 2005) whereas the C-terminal domain of Claspin is involved in DNA-binding (Clarke et al., 2005), it still remains to be seen whether the C-terminal region of Claspin can allosterically regulate Chk1 catalytic activity. Transfection of BRCA1 has been reported to induce an activation of Chk1 catalytic activity (Yarden et al., 2002). Therefore it raises the possibility that adaptor molecules such as BRCA1 and Claspin may share a similar docking motif that serve to activate Chk1 towards weak substrates that lack the docking motif. Indeed, it has been found that the cyclin subunit provides the docking groove for cyclin-dependent kinase which is necessary for substrate with RxL motif to dock to the cyclin/CDK complex (Loog and Morgan, 2005). Adaptor or scaffold proteins could also function as allosteric modulators beyond bridging the kinase and substrate together. The yeast Ste5 scaffold protein is reported to allosterically activate autophosphorylation in the activation loop of the MAPK Fus3 (cell fusion-3) (Bhattacharyya et al., 2006). Such non-substrate regulatory molecules are called heterotropic allosteric modulators. However, more

biochemical experiments are needed to determine the possibility that BRCA1 and Claspin may share a similar docking motif (p21 peptide 4) that could stimulate Chk1 catalytic activity. In addition, it is not known if allosteric docking regulate the specificity of Chk1 interacting partners and if so, whether docking interactions may enhance pathway specificity under certain conditions? A novel double peptide synthesis technique developed by Espanel *et al* (2003) to identify more low-binding affinity allosteric docking motifs will perhaps help to answer the above question (Espanel et al., 2003).

I have also shown that p21 peptide 4-dependent allosteric stimulation was specific to Chk1 but not DAPK1 and Chk2, two related calcium/calmodulin-dependent protein kinase superfamily members. In fact, DAPK1 catalytic activity was slightly inhibited in the presence of peptide 4. This suggested that although Chk1, Chk2 and DAPK are grouped under the same protein kinase superfamily, they do not share similar docking specificities.

Although allosteric regulation is often thought to influence protein kinase specificity, it was shown that p21 peptide 4-dependent activation of Chk1 is still catalytically active towards the C-terminal domain of p21 which includes Thr^{145} and Ser^{146}. Interestingly, phosphate incorporation onto Thr^{145} appeared to increase as a result of Chk1 activity enhanced by peptide 4 (Figure 3.19). Although, phosphorylation of either p21 Thr^{145} or Ser^{146} negatively regulates p21 function/stability, the physiological significance of p21 Thr^{145} and Ser^{146} phosphorylation at the same time is not clear.

3.3.3 Threonine^{55}, Proline^{58} and Tryptophan^{65} amino residues are critical for the function of allosteric docking motif

p21 peptide 4 is a twenty amino acid long peptide. Linear docking motifs often contains a few amino acids that are important for docking interactions. Alanine mutation analysis of p21 peptide 4 revealed Thr^{55}, Pro^{58} and Trp^{65} are the critical amino acids for stimulation of Chk1 activity by p21 peptide 4. Mutations on these sites strikingly abolish the stimulatory effect of peptide 4 on Chk1 catalytic activity. It was discussed that weak interactions involving intrinsically unstructured proteins such as p21 only require a small binding interface with a small number of energy-bearing residues while tight interactions often involved large binding interfaces (Galea et al., 2008). Interestingly, Pro^{58} and Trp^{65} are conserved among the Cip/Kip family of p21$^{cip1/waf1}$, p27^{kip1} and p57^{kip2} (Figure 3.27) (Lacy et al., 2004), suggesting that they might be important for allosteric binding interface. It would be interesting to see whether p21 mutated at these three residues would synergistically abolish Chk1 catalytic activity towards p21 completely and also whether p27 and p57 can activate Chk1 in a similar mechanism too.

3.3.4 A docking motif is required for efficient Chk1 activity towards p21

Kinetics and deletion analysis suggested that a protein-protein interaction which is distinct from the active site is important for Chk1 substrate recognition. Chk1 activity towards the C-terminal p21 peptide 10 required a very high substrate

concentration (Figure 3.21). Furthermore, Chk1 activity towards an N-terminal truncated p21 mutant protein is lower than the full-length p21 protein, suggesting that the first 66 amino acids of p21 may harbour a docking motif which is important for efficient Chk1 catalysis of substrates such as p21. By adding p21 peptide 4 into the assay, Chk1 activity towards p21 ΔNT recovered and interestingly is higher than that of stimulated Chk1 activity towards full-length p21 (Figure 3.24). This suggested that p21 peptide 4 could function as docking motif that allosterically activates Chk1 for efficient utilisation of substrate.

3.3.5 Possible Chk1-p21 signalling pathway

p21 was shown to contain an allosteric signal in the N-terminal region required for stimulating Chk1 function. However it is not clear whether p21 play a role in regulating Chk1 function *in vivo*. I have showed in the next chapter (Figure 4.5) that p21 did not affect the stability of Chk1 protein or the steady state levels of the protein or aphidicolin activation of Chk1 protein in isogenic HCT116 wild-type ($p21^{+/+}$) or HCT116 $p21^{-/-}$ cells.

Although we have yet to confirm Chk1-dependent phosphorylation of p21 Ser^{146} *in vivo*, an initial hypothesis was conceived from the available literature. PKCζ has been shown to mediate p21 degradation through phosphorylation on Ser^{146} (Scott et al., 2002), suggesting that Ser^{146} phosphorylation encodes for a degradation signal. Preliminary data from the Ball lab also showed that overexpression of exogenous Chk1 in HeLa cells led to decreased level of endogenous p21 (Figure

3.28) and that depletion of Chk1 using siRNA increased the half-life of p21. This could suggest that a Chk1-dependent pathway may regulate the stability of p21. It was reported that ubiquitin-dependent p21 degradation occurred in response to low (<40 J/m^2) but not high doses of UV and this was independent of p53 and pRb (Bendjennat et al., 2003). Furthermore, UV-induced degradation of p21 required an ATR-dependent pathway and was necessary for effective DNA repair (Bendjennat et al., 2003). This UV-induced degradation signal was thought to be mediated by glycogen synthase kinase 3β (GSK3β)-dependent phosphorylation on p21 Ser^{114} (Lee et al., 2007), although it has also been shown that p21 downregulation did not required GSK3 (Bendjennat et al., 2003). How the Lee et al, 2007 study relied heavily on overexpression of p21 mutants and previous studies have shown that overexpression of p21 dramatically alters the rate at which it is degraded (Cayrol and Ducommun, 1998). Therefore, it is possible that another checkpoint kinase might be responsible for the UV-induced degradation of p21. A likely candidate could be Chk1, as it is activated in response to UV in an ATR-dependent manner.

It was highlighted that p21 downregulation is required for monoubiquitination of DNA repair factor, PCNA, after replication stress as transient expression of stable p21 negatively regulated PCNA modification (Soria et al., 2006). Monoubiquitination of PCNA promotes DNA repair as monoubiquitin-modified PCNA preferentially interacts with DNA polymerase η (Pol η), which is capable of carrying out specialised translesion synthesis (TLS) past various DNA lesions (Kannouche et al., 2004). Although the signal for PCNA monoubiquitination is not

clear, it has been demonstrated that PCNA monoubiquitination required a stable Chk1-Claspin complex and a Claspin-associated protein, Timeless (Yang et al., 2008). So it could be possible that Chk1 signals in parallel for p21 degradation via p21 Ser^{146} phosphorylation to ensure PCNA monoubiquitination and facilitate DNA repair after replication stress (Figure 3.29).

Although this has not been experimentally determined, the biological functions of Chk1 might also be determined by its binding activity, rather than its catalytic activity. It was shown that docking of the enzyme to pRb was sufficient to inhibit caspase cleavage in the absence of CDK4 catalytic activity (Wallace and Ball, 2004). Similarly, inhibition of MyoD-regulated transcription by CDK4 is dependent on CDK4 docking but does not require CDK4 catalytic activity (Zhang et al., 1999a). Therefore it is also possible that Chk1 regulate p21 function in a docking-dependent manner that does not require Chk1 catalytic activity.

I have showed in the next chapter that [γ^{32}P] incorporation into an unknown protein was observed in the immunoprecipitates from HCT116 wild-type ($p21^{+/+}$) cells, but not HCT116 $p21^{-/-}$ cells (Figure 4.8). It is possible that p21 could function as a regulatory molecule for Chk1 instead, where it regulates Chk1 localisation or Chk1 interaction with other molecules.

3.3.6 Conclusions

In this study, I have shown that Chk1 is an efficient kinase towards p21, phosphorylating the major phospho-acceptor site at Ser^{146}. Using p21 as a model substrate, it was demonstrated that a p21 N-terminal region (amino acids 46 to 65) could function as an allosteric activator of Chk1. A peptidomimetic ligand (peptide 4) based on the p21 N-terminal region could also stimulate Chk1 activity towards substrate such as Cdc25 and $p53^{N1-66}$, suggesting the existence of a general allosteric regulator of Chk1. This mechanism of allosteric activation is specific to Chk1 but not DAPK1 and Chk2. In addition, it was discovered that $threonine^{55}$, $proline^{58}$ and $tryptophan^{65}$ formed the critical binding interface required for allosteric stimulation of Chk1. Furthermore, this p21 N-terminal region could contain a docking motif that is required for efficient catalysis of p21 by Chk1.

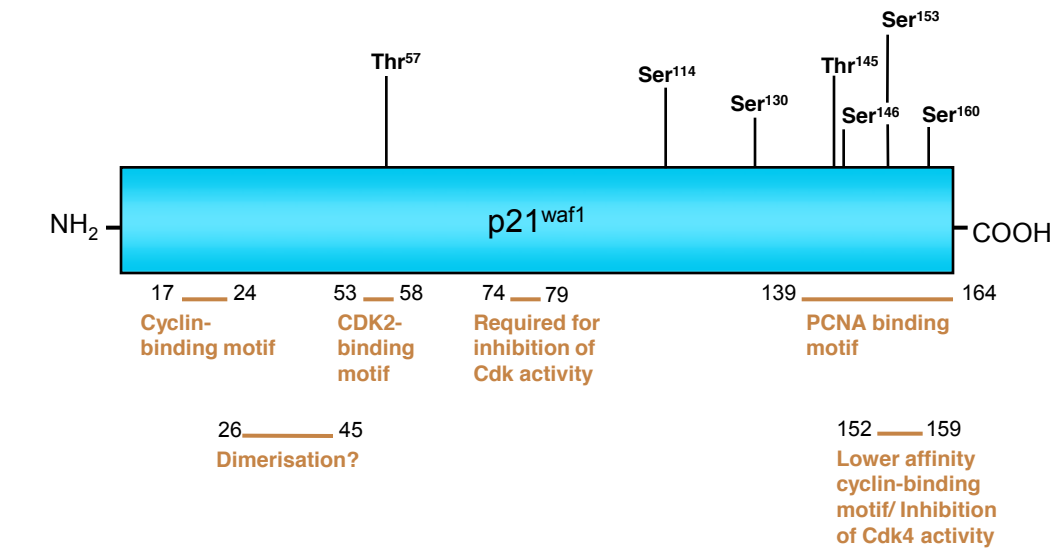

Figure 3.1 A schematic functional domain architecture of p21^{waf1}.

(A) p21^{waf1} is a 164 amino acid protein which has a highly disordered structure. The functional regions of p21 involved in protein-protein interactions have been determined and phosphorylation sites of p21 have been mapped.

A

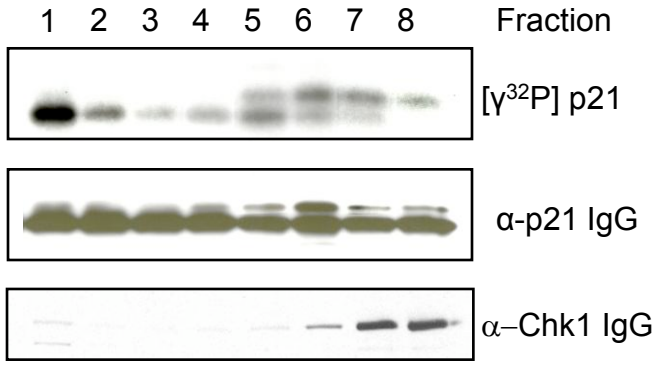

Figure 3.2 Identification of Chk1 as a p21 kinase.

(A) HeLa cell extracts were subjected to chromatographic fractionation using Q-Sepharose and SP-Sepharose columns. The active p21 kinase pool was then applied to a HS-Poros column and fractionated. The active HS-pool was then subjected to gel filtration on a Superose-12 column and the fractions were analysed. (Top panel) Total p21 kinase activity was determined as [γ^{32}P] incorporation into p21 protein by autoradiography. (Middle panel) Total p21 protein was detected in the immunoblot using α-p21 IgG. (Lower panel) Presence of Chk1 protein was detected in the immunoblot using α-Chk1 IgG. (Data provided by Mary Scott)

A

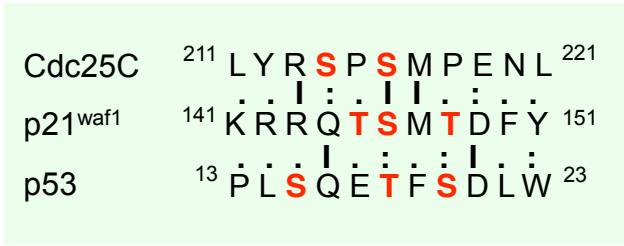

Figure 3.3 Sequence alignment between Cdc25C, p21 and p53.

(A) Sequence alignment between Cdc25C, p21 and p53 known phosphorylation sites revealed a suggestive homology with a line (|) representing conserved residues and colon (:) depicting semi-conserved residues. Potential known phospho-acceptor residues are coloured red.

A

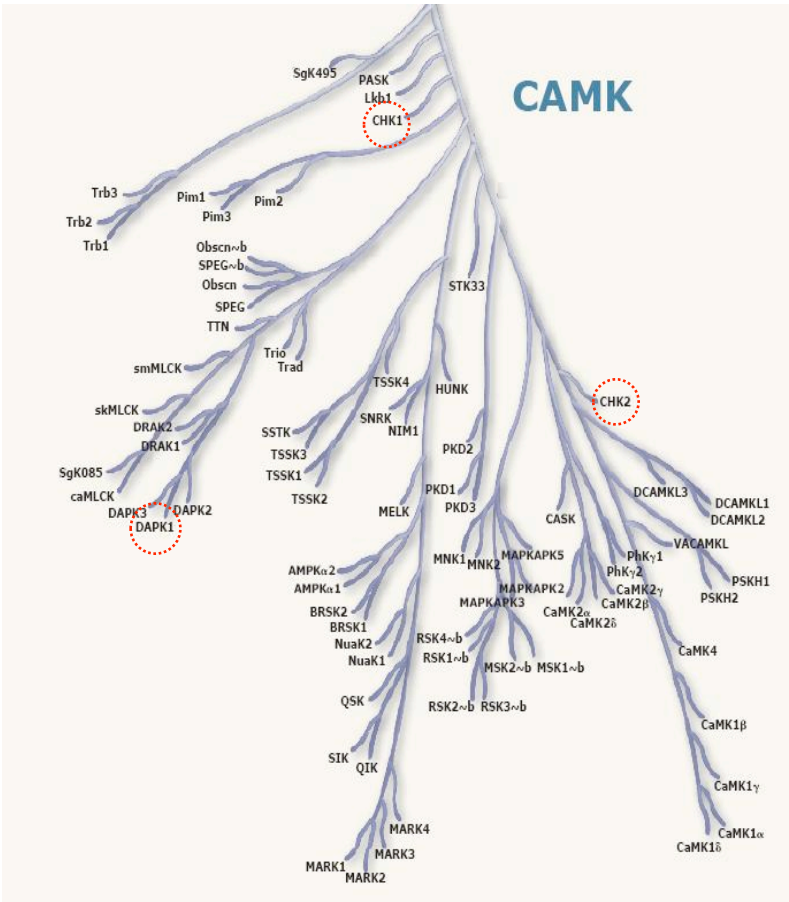

Figure 3.4 A dendrogram of the calcium/calmodulin-dependent protein kinase superfamily.

(A) DAPK1, Chk1 and Chk2 (circled red) belong to the superfamily of calcium/cadmodulin-dependent protein kinase. This dendrogram is adapted from the Human Kinome (http://kinase.com/mammalian/).

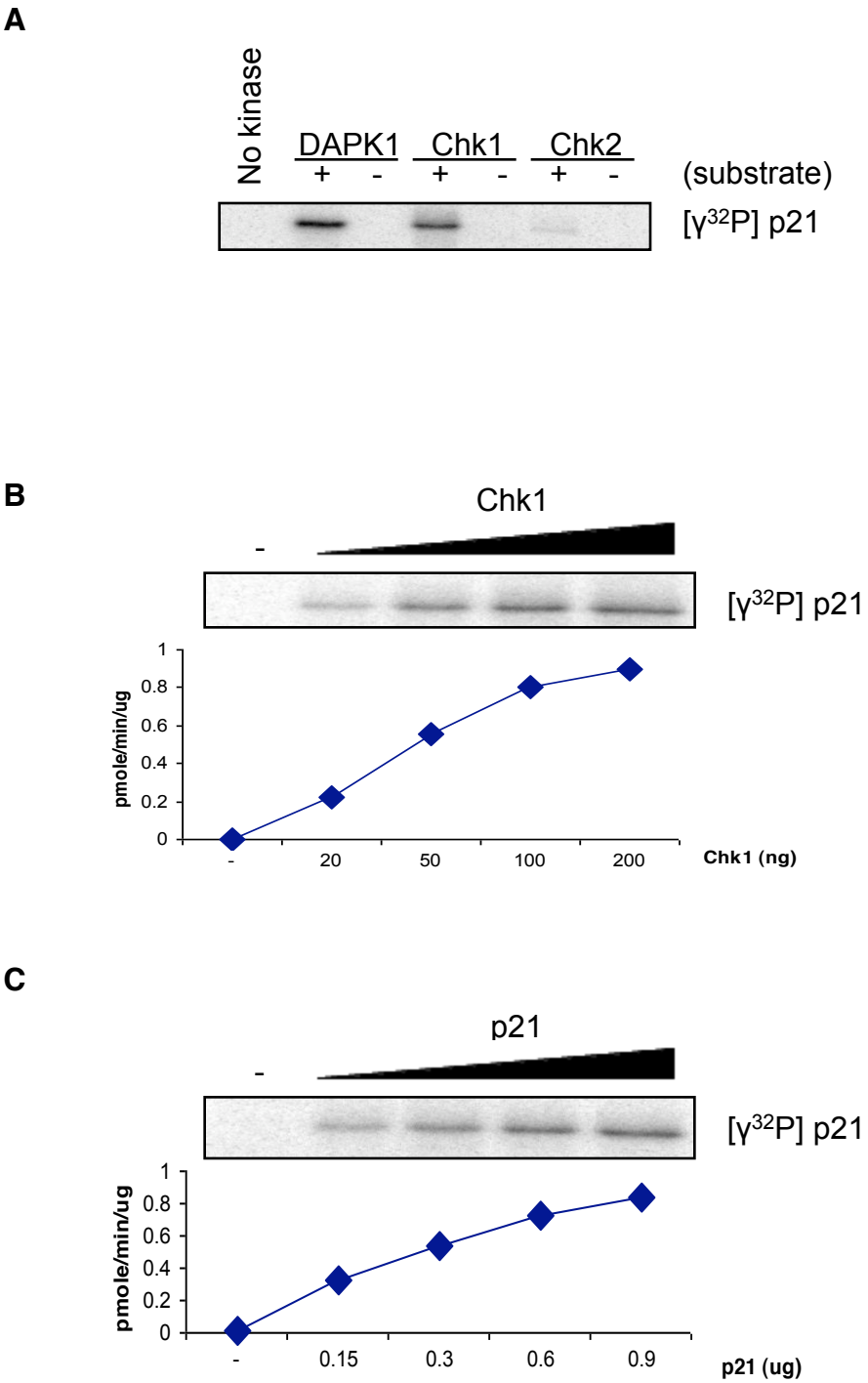

Figure 3.5 Purified recombinant human Chk1 phosphorylates recombinant human p21 *in vitro*.

(A) Kinase reactions containing 100 ng of either DAPK1 core/Chk1/Chk2 with or without p21 (0.6 µg) were assembled in the presence of [γ^{32}P]ATP. The reaction products were resolved by SDS-PAGE and [γ^{32}P] incorporation into p21 was visualised by autoradiography. (B) Kinase reactions containing 0.6 µg of p21 and titration of Chk1 (0 to 200 ng) were assembled in the presence of [γ^{32}P]ATP. (C) Kinase reactions containing 100 ng of Chk1 and titration of p21 (0 to 0.9 µg) were assembled in the presence of [γ^{32}P]ATP. The reaction products were resolved by 12% SDS-PAGE and [γ^{32}P] incorporation into p21 was visualised by autoradiography and quantified by phosphorimager.

A

p21 peptides sequences

1	[1] MSEPAGDVRQNPCGSKACRR [20]
2	[16] KACRRLFGPVDSEQLSRDCD [35]
3	[31] SRDCDALMAGCIQEARERWN [50]
4	[46] RERWNFDFVTETPLEGDFAW [65]
5	[61] GDFAWERVRGLGLPKLYLPT [80]
6	[76] LYLPTGPRRGRDELGGGRRP [95]
7	[81] GGRRPGTSPALLQGTAEEDH [110]
8	[106] AEEDHVDLSLSCTLVPRSGE [125]
9	[121] PRSGEQAEGSPGGPGDSQGR [140]
10	[136] DSQGRKRRQTSMTDFYHSKR [155]
11	[145] TSMTDFYHSKRRLIFSKRKP [164]

B

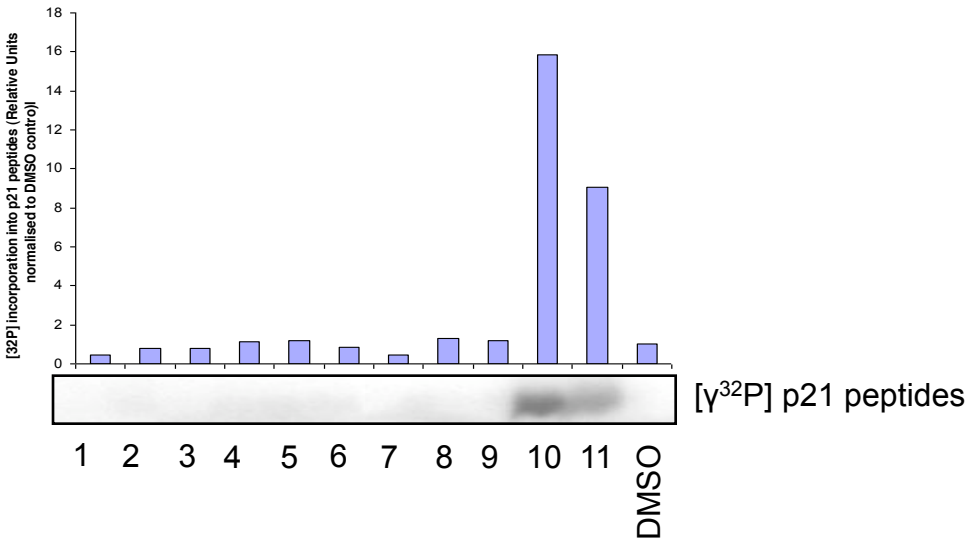

Figure 3.6 Recombinant human Chk1 phosphorylates recombinant human p21 C-terminal domain.

(A) List of biotinylated overlapping p21 20-mer peptides with SGSG spacing. (B) Kinase reaction containing 60 ng of Chk1, 1 µg of indicated p21 peptide (final peptide concentration ~ 50 nM) and [γ^{32}P]ATP were assembled. DMSO was used as negative control. The reaction products were resolved by 15% SDS-PAGE and [γ^{32}P] incorporation into p21 peptides were visualised by autoradiography, quantified by phosphorimager and normalised to DMSO control.

A

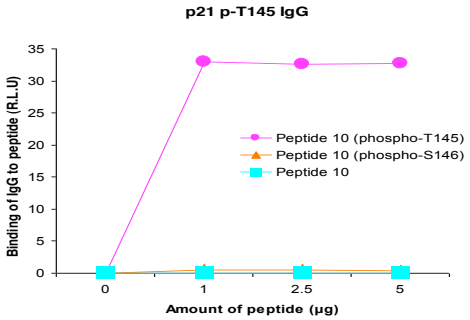

B

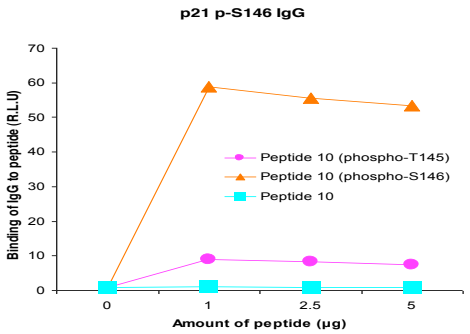

C

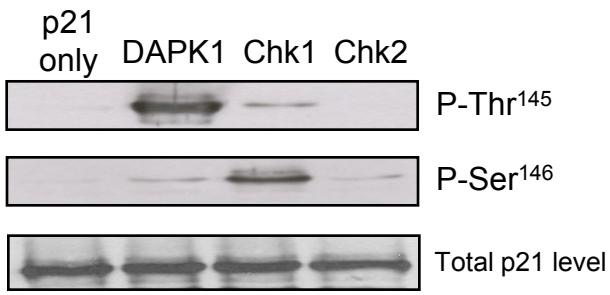

Figure 3.7 Recombinant human Chk1 phosphorylates recombinant human $p21^{waf1}$ at Ser^{146} *in vitro*.

(A and B) Specificity of α-p21 phospho-Thr^{145} IgG (A) or α-p21 phospho-Ser^{146} IgG (B) were tested via ELISA using streptavidin capture of biotinylated p21 phospho-Thr^{145} peptide, p21 phospho-Ser^{146} peptide and p21 peptide 10 (titrated from 0-5 µg). (C) Kinase reactions containing 100 ng of DAPK1 core/Chk1/Chk2 and 1 µg of p21 in the presence of unlabelled ATP were assembled. The reaction products were resolved by 12% SDS-PAGE and transferred to nitrocellulose membrane. Phosphorylation was detected using α-p21 phospho-Thr^{145} IgG or α-p21 phospho-Ser^{146} IgG. Total p21 level was detected with mouse α-p21 IgG.

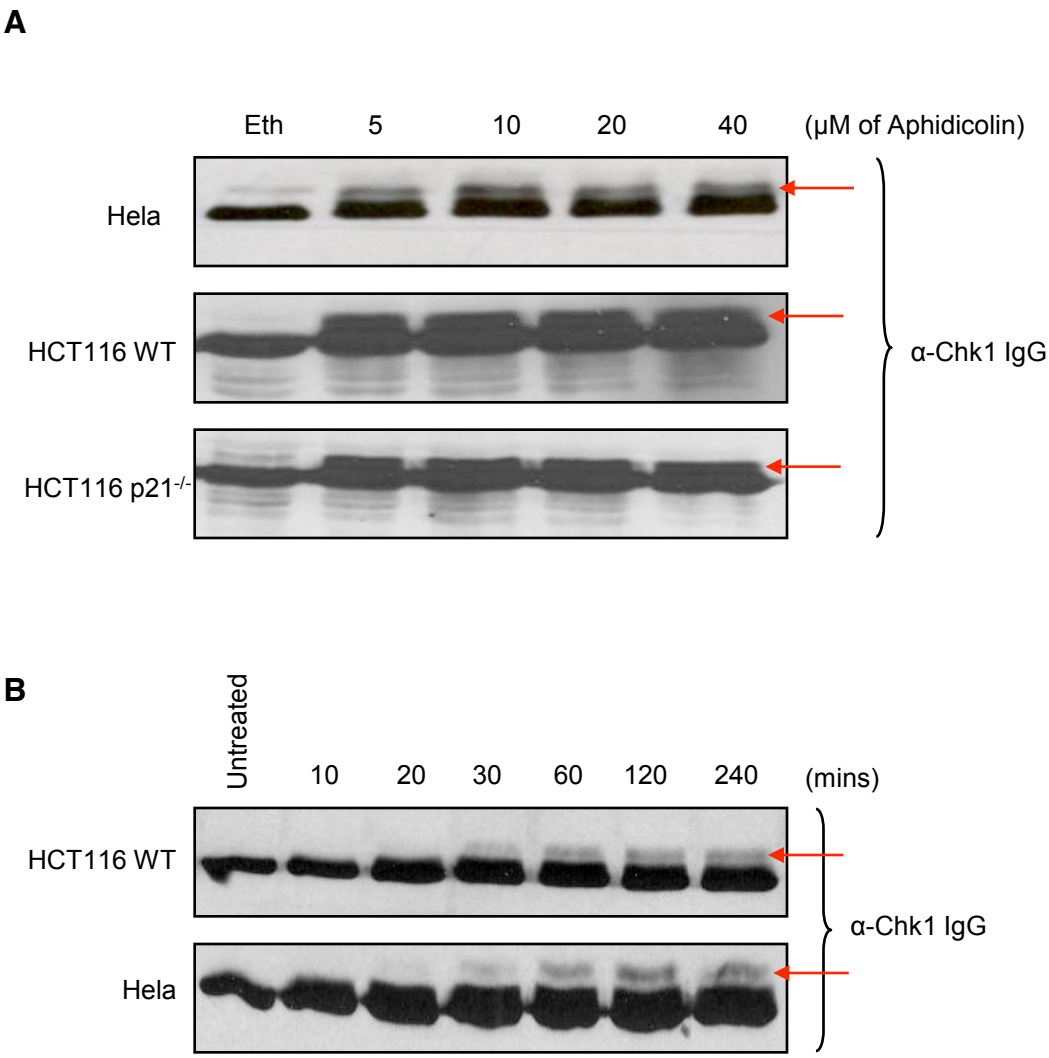

Figure 3.8 Activation of cellular Chk1 in response to aphidicolin treatment.

(A) Indicated cell lines were grown to >90% confluency before treated with a titration of aphidicolin (5 μM to 20 μM) or ethanol as control. After 4 hours, the cells were harvested and lysed. 50 μg of the whole cell lysates were resolved by 10% SDS-PAGE before transferred to nitrocellulose membrane. Chk1 protein was detected using mouse α-Chk1 IgG. Red arrows are indicative of activated forms of Chk1. (B) Indicated cell lines were grown to >90% confluency before treated with 20 μM of aphidicolin for the indicated times. The cells were harvested and lysed. 50 μg of the whole cell lysates were resolved by 10% SDS-PAGE before transferred to nitrocellulose membrane. Chk1 protein was detected using mouse α-Chk1 IgG. Red arrows are indicative of phosphorylated forms of Chk1.

A

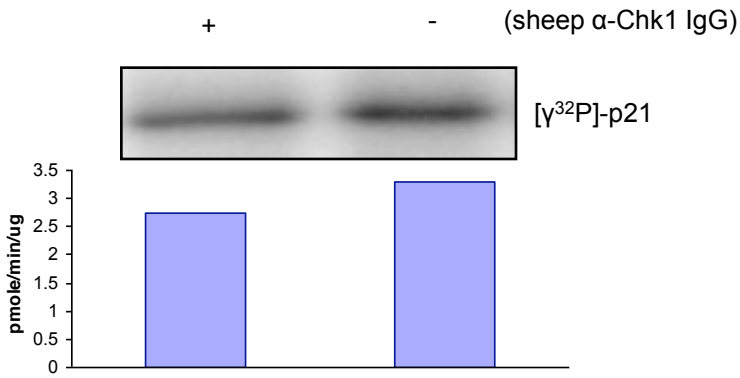

Figure 3.9 Recombinant human Chk1 kinase activity is not affected by immunoprecipitation antibodies.

(A) 100 ng of Chk1 was pre-incubated with 0.5 μg of sheep α-Chk1 IgG at 4°C for 1 hour before 0.6 μg of p21 and [γ^{32}P-ATP] were added for kinase reaction. The reaction products were resolved by 12% SDS-PAGE before [γ^{32}P] incorporation into p21 was visualised by autoradiography and quantified by phosphoimager

A

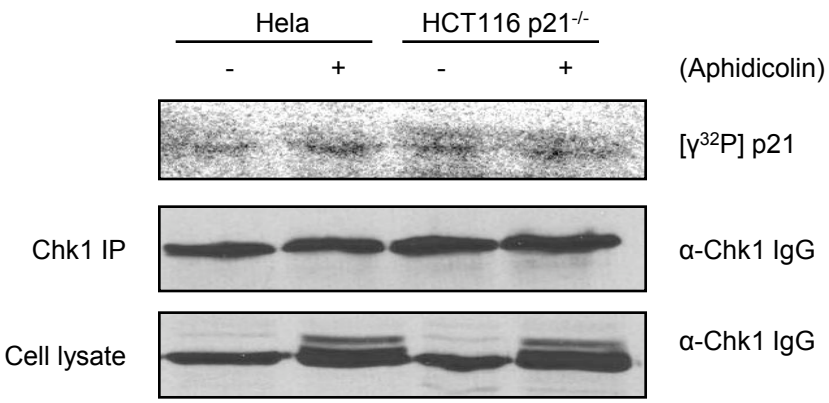

Figure 3.10 Cellular Chk1 is active towards recombinant human p21.

(A) Hela and HCT116 $p21^{-/-}$ cells were grown to >90% confluency and treated with 20 μM aphidicolin for 4 hours before harvested. 1 mg of the cellular lysate was subjected to Chk1 immunoprecipitation by sheep α-Chk1 IgG before assembled with 0.6 μg of recombinant p21 for [γ^{32}P]-ATP kinase assay. The kinase reactions were resolved by 12% SDS-PAGE and [γ^{32}P] incorporation into p21 was visualised by autoradiography (First panel). Chk1 immunoprecipitation was validated by immunoblotting with mouse α-Chk1 IgG (Second panel). The cell lysates were resolved by 12% SDS-PAGE and immunoblotted with mouse α-Chk1 IgG (Third panel).

A

```
|CHK1_HUMAN      MAVPFVEDWDLVQTLGEGAYGEVQLAVNRVTEEAVAVKIVDMKRAVDCPENIKKEICINK 60
|CHK1_CHICK      MAVPFVEDWDLVQTLGEGAYGEVQLAVNRRTEEAVAVKIVDMKRAADCPENIKKEICINK 60
                ***************************** ***************.************** 

|CHK1_HUMAN      MLNHENVVKFYGHRREGNIQYLFLEYCSGGELFDRIEPDIGMPEPDAQRFFHQLMAGVVY 120
|CHK1_CHICK      MLNHENVVKFYGHRREGATQYLFLEYCSGGELFDRIEPDIGMPEPEAQRFFQQLIAGVVY 120
                ****************  *************************:*****:**:***** 

|CHK1_HUMAN      LHGIGITHRDIKPENLLLDERDNLKISDFGLATVFRYNNRERLLNKMCGTLPYVAPELLK 180
|CHK1_CHICK      LHSMGITHRDLKPENLLLDERDNLKISDFGLATVFKHNGRERLLNKMCGTLPYVAPELLR 180
                **.:******:************************::*.******************** 

|CHK1_HUMAN      RREFHAEPVDVWSCGIVLTAMLAGELPWDQPSDSCQEYSDWKEKKTYLNPWKKIDSAPLA 240
|CHK1_CHICK      RPEFRAEPVDVWACGVVLTAMLAGELPWDQPSDSCQEYSDWKERKTYLAPWRKIDSAPLA 240
                * **:*******:**:*****************************:**** **:******** 

|CHK1_HUMAN      LLHKILVENPSARITIPDIKKDRWYNKPLKKGAKRPRVTSGGVSESPSGFSKHIQSNLDF 300
|CHK1_CHICK      LLHKILTENPTARITIPDIKKDRWYCRPLKKGTKRGRVSSGGVTESPGALPKHIRSDTDF 300
                ******.***:************** :*****:** **:****:***..:.***:*: ** 

|CHK1_HUMAN      SPVNSASSEENVKYSSSQPEPRTGLSLWDTSPSYIDKLVQGISFSQPTCPDHMLLNSQLL 360
|CHK1_CHICK      SPVKSALGEDKASYSTSQPEPGTGGALWDSSTGSIDRLVQGISFSQPACPEHMLLNSQLL 360
                ***:** .*::..**:***** ** :***:*.. **:**********:**:********* 

|CHK1_HUMAN      GTPGSSQNPWQRLVKRMTRFFTKLDADKSYQCLKETCEKLGYQWKKSCMNQVTISTTDRR 420
|CHK1_CHICK      GTPGSSQSPWQRLVRRMTRFFTKLDADGSYRSLRDVCEKMGYGWKQSCTNQVTISTTDRR 420
                *******.******:************ **:.*::.***:** **:** *********** 

|CHK1_HUMAN      NNKLIFKVNLLEMDDKILVDFRLSKGDGLEFKRHFLKIKGKLIDIVSSQKVWLPAT 476
|CHK1_CHICK      NNKLIFKVNLLEMESRILVDFRLSKGDGLEFKRHFLKIKGKLSDVVSTQKVWLPPP 476
                *************:.:************************** *:**:******..
```

Figure 3.11 Sequence alignment of full-length human and chick Chk1.

(A) ClustalW2 sequence alignment reveals 84% homology between human and chick Chk1.'*' means that residues in that column are identical; ':' means that residues in that column are conserved; '.' means that residues in that column are semi-conserved.

A

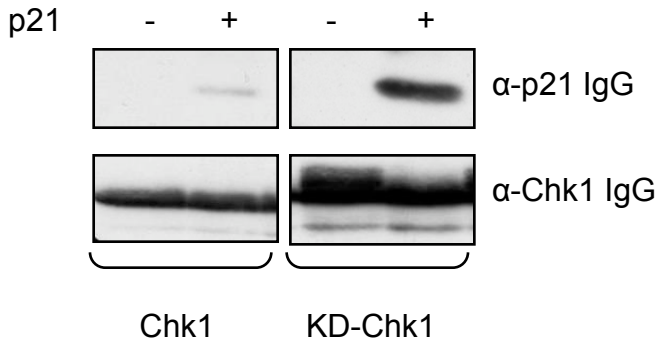

Figure 3.12 Co-immunoprecipitation of human p21 and chick Chk1.

(A) Chick full-length Chk1 or kinase-dead Chk1 (KD-Chk1) was transfected into Cos1 cells alone or together with human p21. Chick Chk1 was immunoprecipitated from Cos1 cells by α-C-terminal Chk1 IgG and resolved by 12% SDS-PAGE before transferred to nitrocellulose membrane. p21 was detected by immunoblotting with α-p21 IgG. Immunoprecipitated Chk1 was detected by immunoblotting with α-Chk1 IgG (In collaboration with Prof. David Gillespie's group) (Data provided by Mary Scott).

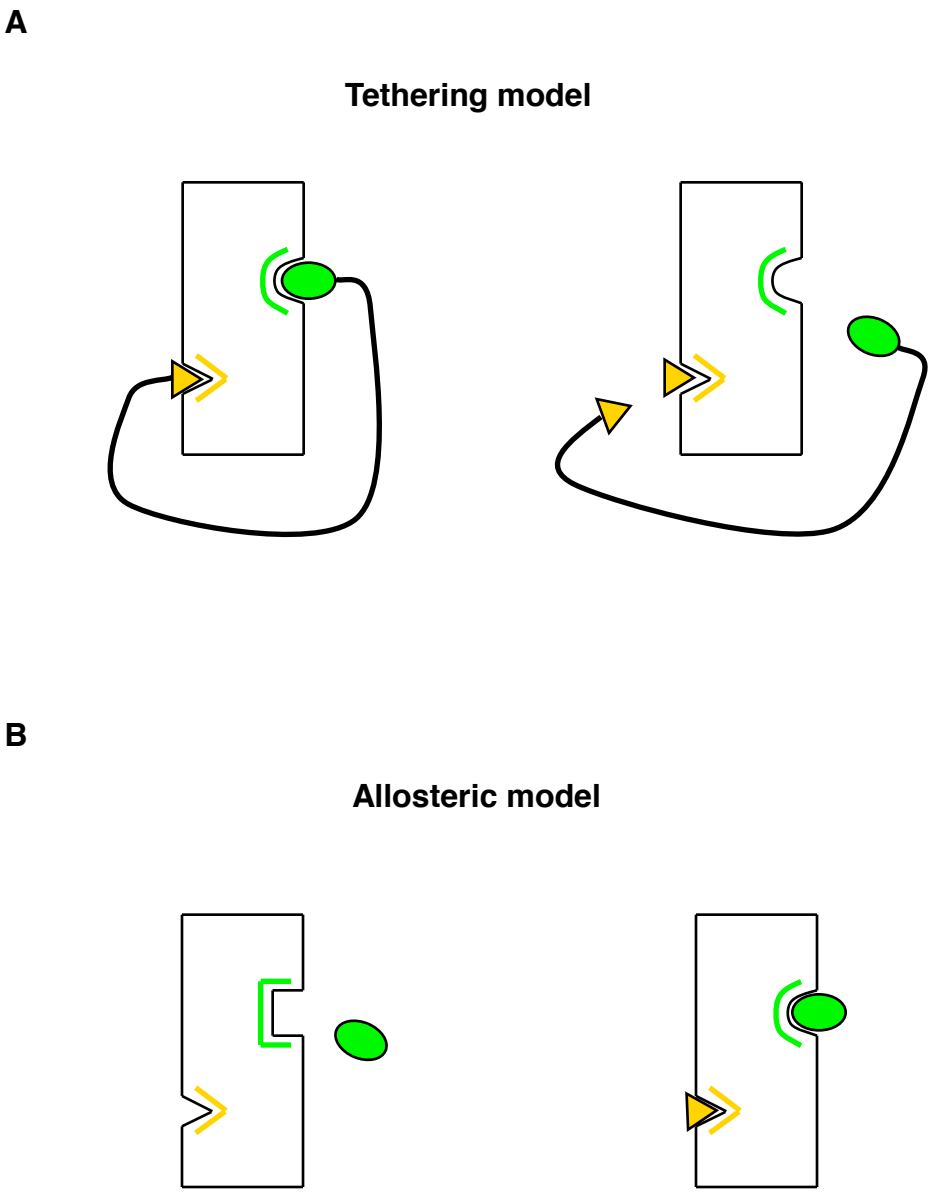

Figure 3.13 A schematic illustration of docking mechanisms in protein-substrate recognition.

(A) "Tethering model". In this model, the docking motif (orange triangle) serves to tether the substrate to the enzyme with no or little influence on the enzyme structural changes or kinase activity. Substrate tethering can be inhibited in the presence of competitive docking ligands, leading to poor catalytic activity towards the substrate. (B) "Allosteric model". In this model, docking ligand (orange triangle) binding to the docking groove (orange cleft) induces kinase conformational changes that allow better substrate accessibility to the active site (green pit). *Adapted from REMENYI, A., GOOD, M. C. & LIM, W. A. (2006) Docking interactions in protein kinase and phosphatase networks. Curr Opin Struct Biol, 16, 676-85.*

A

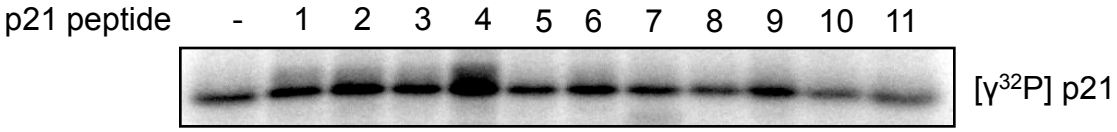

Figure 3.14 Recombinant human Chk1 activity towards recombinant human p21 can be stimulated by p21 docking peptide.

(A) Kinase reactions containing 100 ng of Chk1 and 0.6 μg of p21 with or without 5 μg of p21 peptide were assembled in the presence of [γ^{32}P]-ATP. The reaction products were resolved by 12% SDS-PAGE and [γ^{32}P] incorporation into p21 was visualised by autoradiography.

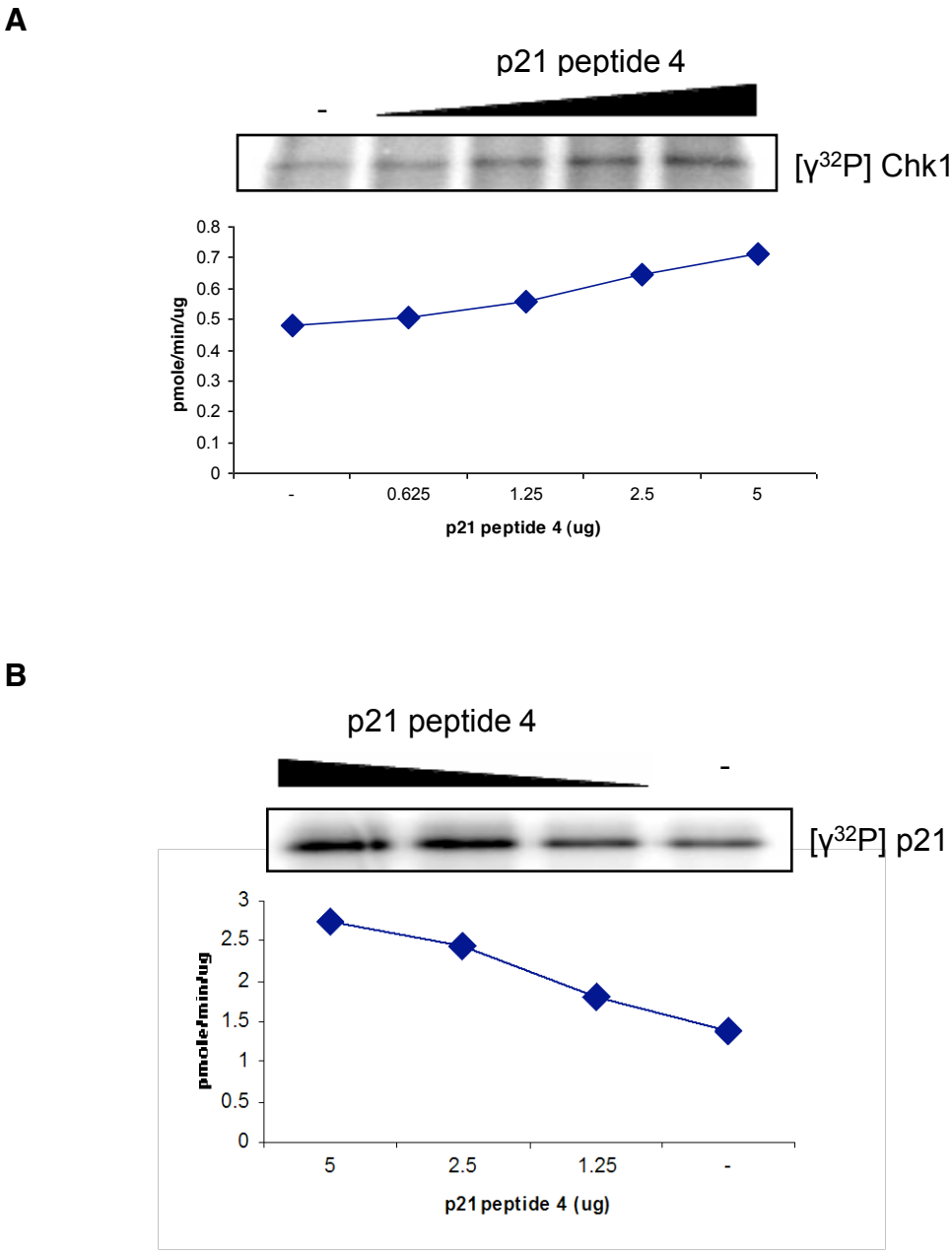

Figure 3.15 Recombinant human Chk1 activity towards recombinant human p21 is stimulated by p21 peptide 4.

(A) Kinase reactions containing 100 ng of Chk1 and titration of p21 peptide 4 (0.625 µg to 5 µg) were assembled in the presence of [γ^{32}P]ATP. The reaction products were resolved in 10% SDS-PAGE. [γ^{32}P] incorporation into Chk1 was visualised by autoradiography. (B) Kinase reactions containing 100ng of Chk1, 1 µg of p21 and titration of p21 peptide 4 (1.25 µg to 5 µg) were assembled in the presence of [γ^{32}P]ATP. The reaction products were resolved by 12% SDS-PAGE. [γ^{32}P] incorporation into p21 was visualised by autoradiography.

A

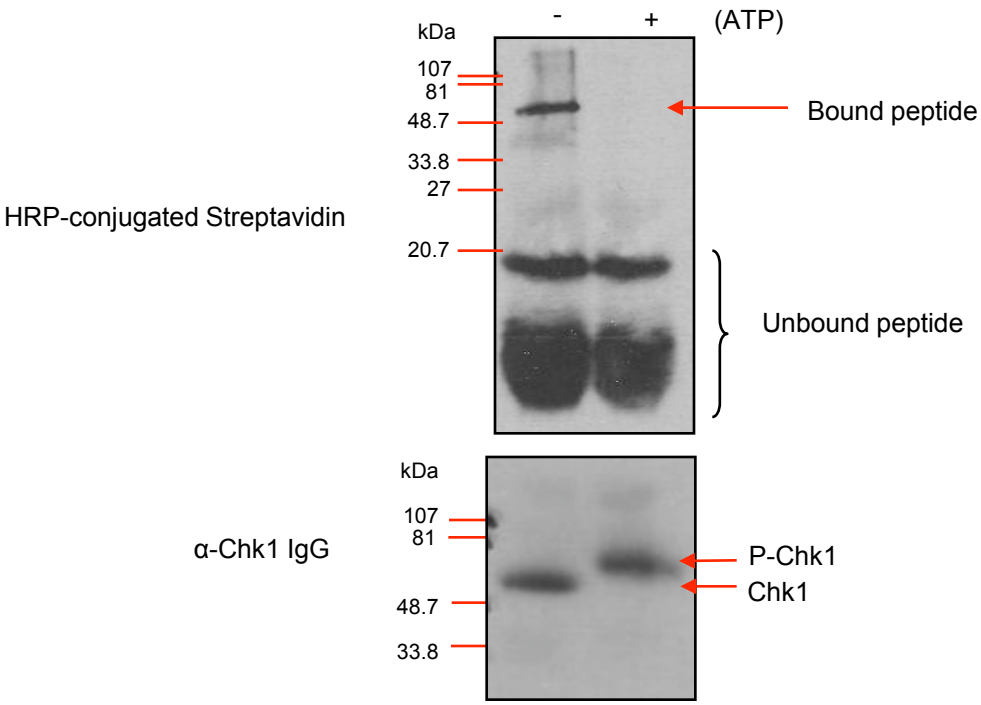

Figure 3.16 p21 peptide 4 binds to recombinant human Chk1 in an ATP-dependent manner.

(A) Kinase reactions containing 100 ng of Chk1 and 5 μg of p21 peptide 4 were assembled in the presence or absence of 1 mM unlabelled ATP. The reactions were stopped by addition of sample buffer (without SDS/DTT) before resolved by 10% or 15% non-denaturing PAGE (without SDS) and transferred to nitrocellulose membrane. Biotinylated p21 peptide 4 was detected with HRP-conjugated streptavidin whilst Chk1 protein was detected using α-Chk1 IgG.

A

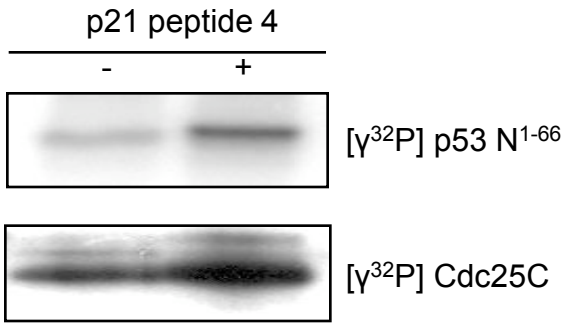

Figure 3.17 p21 peptide 4 can stimulate recombinant human Chk1 activity towards the N-terminal domain of recombinant human p53 (N^{1-66}) and recombinant human Cdc25C.

(A) Kinase reactions containing 100 ng of Chk1 and 100 ng of p53 N^{1-66} or Cdc25C with or without 5 μg of p21 peptide 4 were assembled in the presence of [γ^{32}P]ATP. The reaction products were resolved by 12% SDS-PAGE. [γ^{32}P] incorporation into p53 N^{1-66} and Cdc25C was visualised by autoradiography.

A

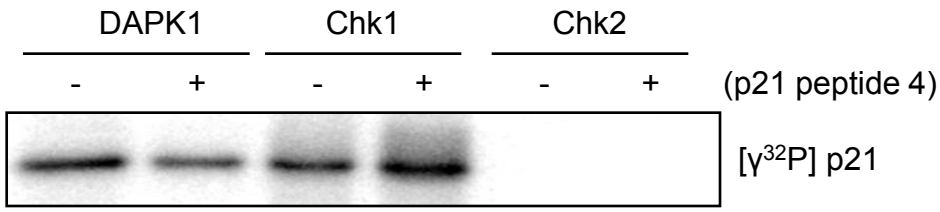

Figure 3.18 p21 peptide 4 can allosterically stimulate recombinant human Chk1 but not recombinant human DAPK1 and Chk2 activity.

(A) Kinase reactions containing 100 ng of DAPK1 core/Chk1/Chk2 and 0.6 μg of p21 with or without 5 μg of p21 peptide 4 were assembled in the presence of [γ^{32}P]ATP. The reaction products were resolved by 12% SDS-PAGE. [γ^{32}P] incorporation into p21 was visualised by autoradiography.

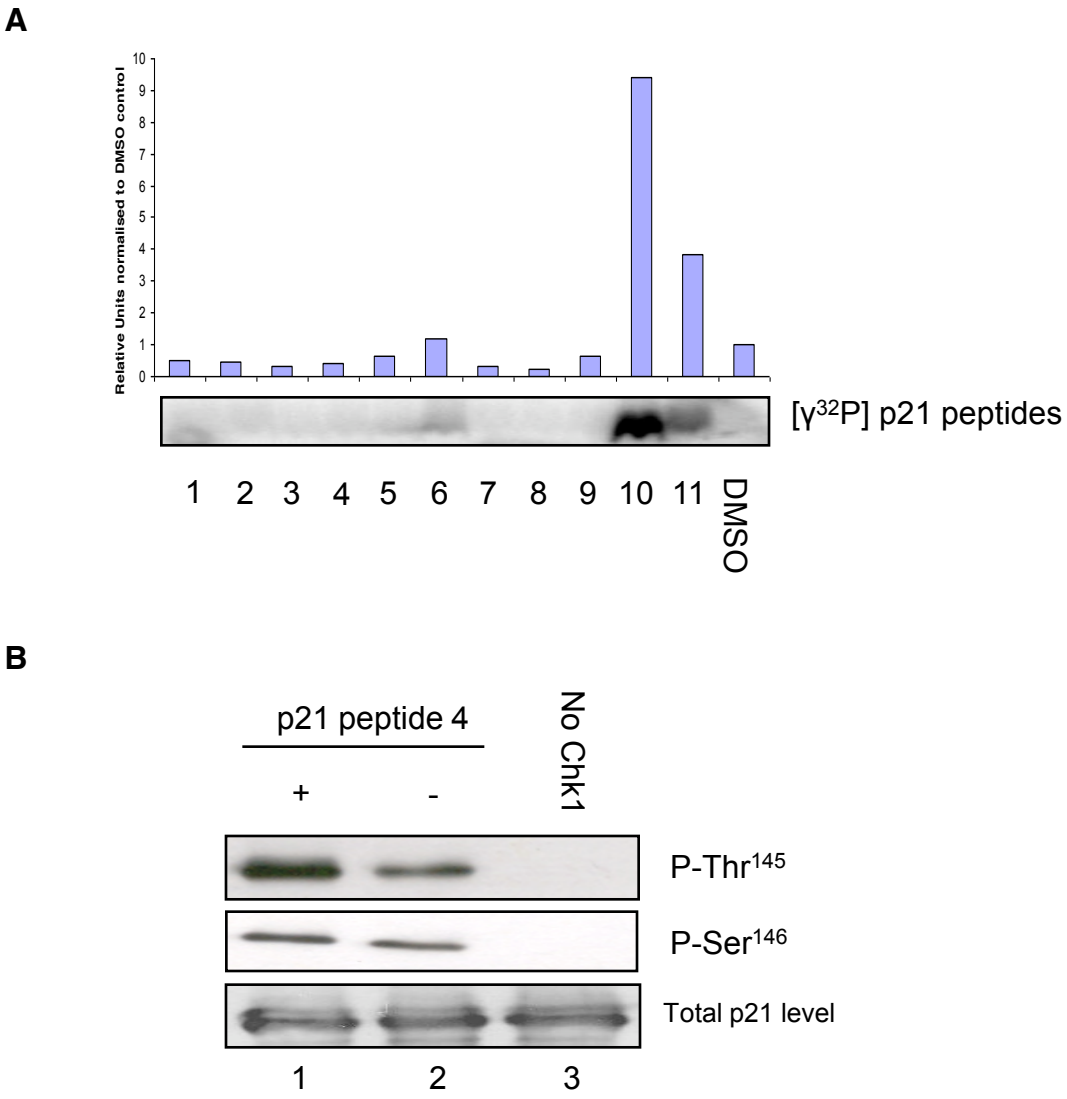

Figure 3.19 p21 phosphorylation profile is not affected by p21 peptide 4.

(A) Kinase reaction containing 60 ng of Chk1, 1 μg of indicated p21 peptide, 5 μg of p21 peptide 4 and [γ^{32}P]ATP were assembled. DMSO was used as negative control in the absence of p21 peptide 4. The reaction products were resolved by 15% SDS-PAGE and [γ^{32}P] incorporation into p21 peptides were visualised by autoradiography, quantified by phosphorimager and normalised to DMSO control. (B) Western blot analysis of p21 phosphorylation. Kinase reaction containing 60 ng of Chk1 and 1 μg of p21 with/without 5 μg of p21 peptide 4 in the presence of unlabelled ATP were assembled. The reaction products were resolved by 12% SDS-PAGE and transferred to nitrocellulose. Phosphorylation was detected using α-p21 phospho-Thr^{145} IgG and α-p21 phospho-Ser^{146} IgG. Total p21 level was detected with mouse α-p21 IgG.

A

Peptide 4 Alanine scan

R46A	**A**ERWNFDFVTETPLEGDFAW
E47A	R**A**RWNFDFVTETPLEGDFAW
R48A	RE**A**WNFDFVTETPLEGDFAW
W49A	RER**A**NFDFVTETPLEGDFAW
N50A	RERW**A**FDFVTETPLEGDFAW
F51A	RERWN**A**DFVTETPLEGDFAW
D52A	RERWNF**A**FVTETPLEGDFAW
F53A	RERWNFD**A**VTETPLEGDFAW
V54A	RERWNFDF**A**TETPLEGDFAW
T55A	RERWNFDFV**A**ETPLEGDFAW
E56A	RERWNFDFVT**A**TPLEGDFAW
T57A	RERWNFDFVTE**A**PLEGDFAW
P58A	RERWNFDFVTET**A**LEGDFAW
L59A	RERWNFDFVTETP**A**EGDFAW
E60A	RERWNFDFVTETPL**A**GDFAW
G61A	RERWNFDFVTETPLE**A**DFAW
D62A	RERWNFDFVTETPLEG**A**FAW
F63A	RERWNFDFVTETPLEGD**A**AW
W65A	RERWNFDFVTETPLEGDFA**A**

B

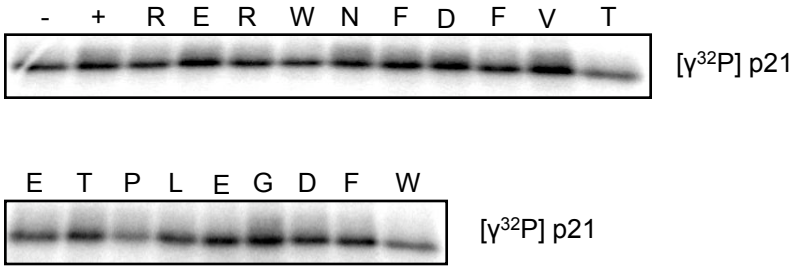

Figure 3.20 Identification of critical residues involved in p21 allosteric docking.

(A) Indication of the positioning of alanine mutation made within p21 peptide 4. (B) Kinase reactions containing 100 ng of Chk1, 0.6 µg of p21 and 5 µg of indicated peptide 4 were assembled in the presence of [γ^{32}P]-ATP. (-) indicates DMSO control, (+) indicates wild-type p21 peptide 4 and the amino acid letter represents the alanine mutation in place of that residue. The reaction products were resolved by 12% SDS-PAGE before visualised by autoradiography.

A

Full-length p21	K_m μM
Set 1	1.43
Set 2	1.82
Set 3	1.96
Average	1.74
S.D	0.27

B

p21 peptide 10	K_m μM
Set 1	2.77
Set 2	8.89
Set 3	2.39
Average	4.68
S.D	3.65

Figure 3.21 Kinetic constant for recombinant human Chk1 with respect to recombinant human p21.

(A and B) Kinase reactions containing 100 ng of Chk1 and (A) p21 in the range of 0.28 μM to 8.83 μM or (B) p21 peptide 10 in the range of 2.065 μM to 165 μM were assembled in the presence of [γ^{32}P]ATP. The reaction products containing p21 were resolved by 12% SDS-PAGE and reaction products containing p21 peptide 10 were spotted onto p81 chromatography paper. [γ^{32}P] incorporation were quantified using phosphorimager. The Michaelis-Menten parameters were fitted via the Hanes plot using hyperbolic regression software (Hyper.version 1.1s, J. Easterby, University of Liverpool) and kinetic constants were calculated as means ± standard deviation.

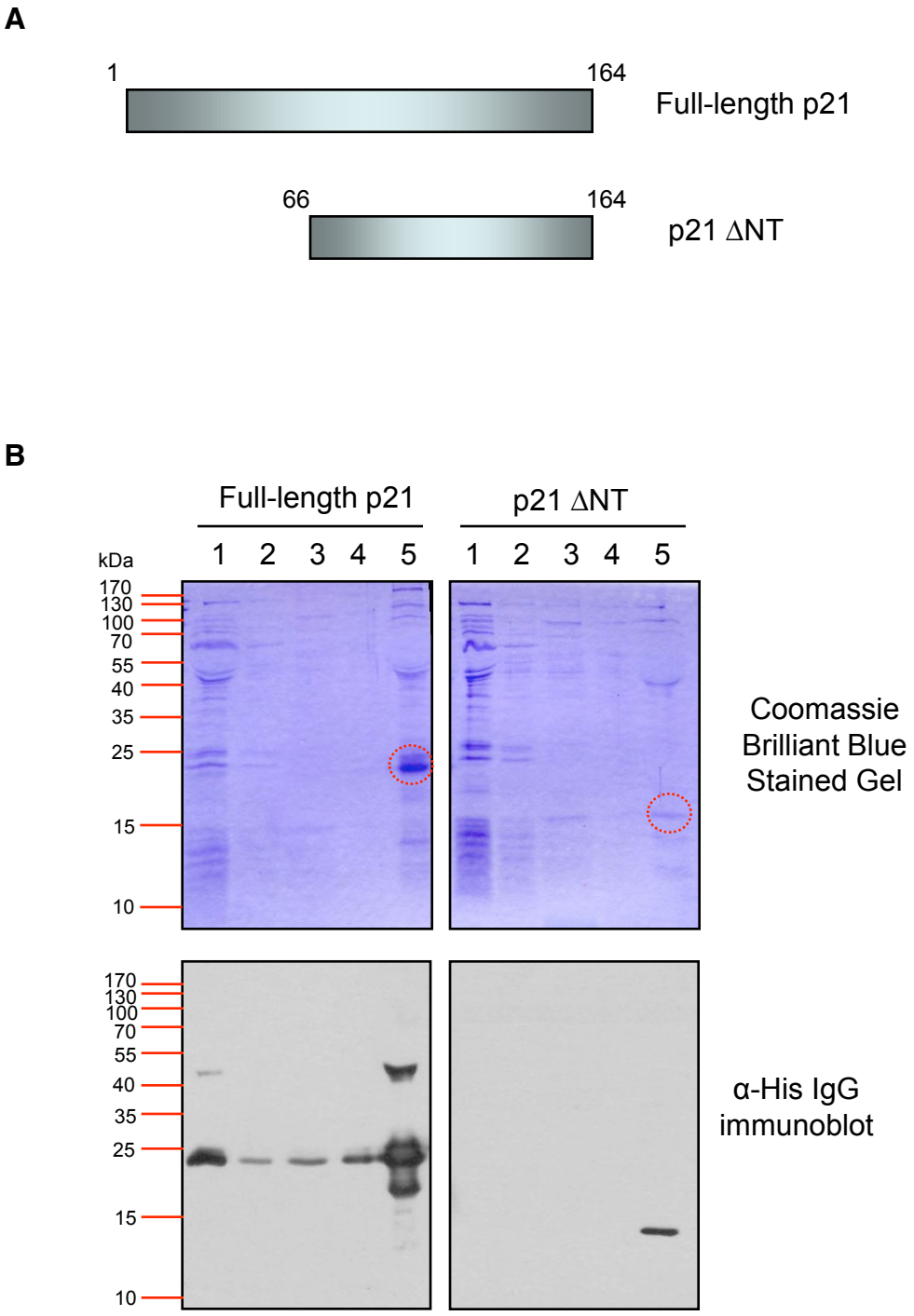

Figure 3.22 Purification of recombinant human His-tagged full length p21 and p21 ΔNT.

(A) Schematic diagram of full-length p21 and p21 ΔNT mutant where the first 65 amino acids from the N-terminal end is deleted. (B) Two-step purification of His-tagged full-length p21 and p21 ΔNT. p21 proteins were purified from inclusion bodies before passing through the Ni-NTA agarose column. Fractions obtained from the Ni-NTA agarose column were analysed on a 12% SDS-PAGE gel stained by coomassie brilliant blue or subjected to α-His IgG immunoblotting. Lanes: 1, Flow-through; 2, Wash I fraction; 3, Wash II fraction; 4, Wash III fraction; 5, Eluted fraction. Dotted circles indicate full-length p21 or p21 ΔNT.

A

µl	0	0.1	0.2	0.5	1
p21 FL (R.L.U)	0.00405	0.024	0.5888	1.3885	2.6615
p21 ΔNT (R.L.U)	0.0027	0.02405	0.12325	0.34085	0.77235

• 1 µl of full-length p21 = 100 ng

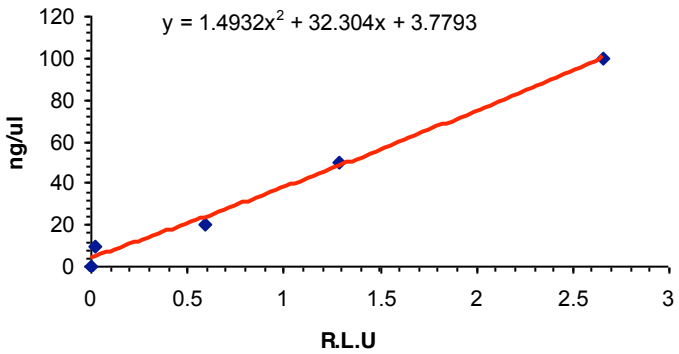

• Thus, using the equation,

0.77235 (R.L.U) of p21 ΔNT = 29.6 ng

Figure 3.23 Normalisation of recombinant human His-tagged full length p21 and p21 **ΔNT**.

(A) The concentration of His-tagged full length p21 and p21 ΔNT were normalised using the ELISA fomat as described in the *Materials and Methods* 2.7.1. The relative light units values obtained for full-length p21 were computed to construct a XY scatter plot. From the plot, an equation is derived and used to calculate the concentration for p21 ΔNT. Calculations were written above.

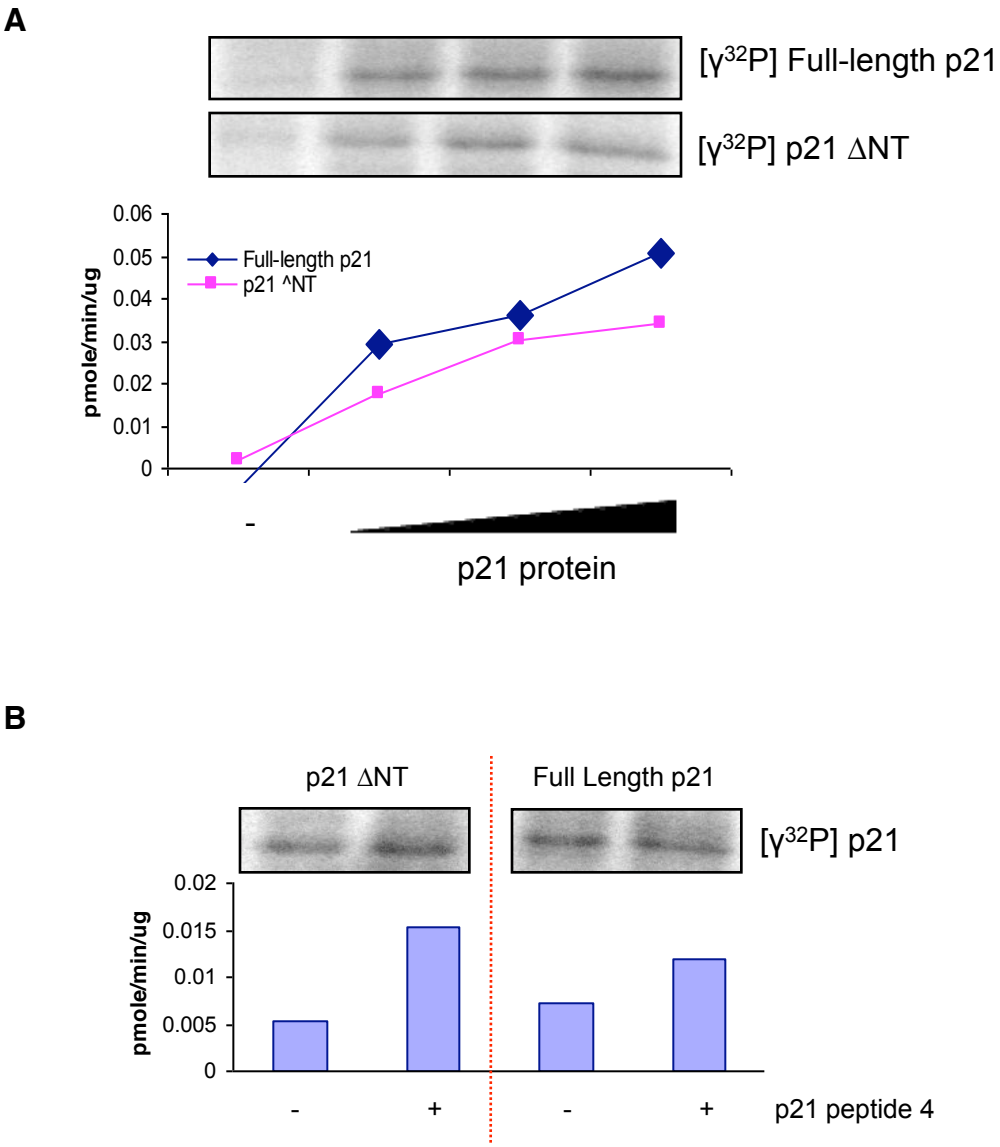

Figure 3.24 Recombinant human Chk1 is less active towards recombinant human p21 **ΔNT** mutant

(A) Kinase reactions containing 100 ng of Chk1 and full length p21 or p21 ΔNT in the range of 0 ng to 120 ng were assembled in the presence of [γ^{32}P]ATP. The reaction products were resolved in 12% SDS-PAGE and [γ^{32}P] incorporation into p21 were visualised by autoradiography and quantified using phosphorimager. (B) Kinase reactions containing 100ng Chk1 and 80 ng of either full length p21 or p21 ΔNT were assembled in the presence of [γ^{32}P]ATP with or without 5 μg of p21 peptide 4. The reaction products were resolved in 12% SDS-PAGE and [γ^{32}P] incorporation into p21 were visualised by autoradiography and quantified using phosphorimager.

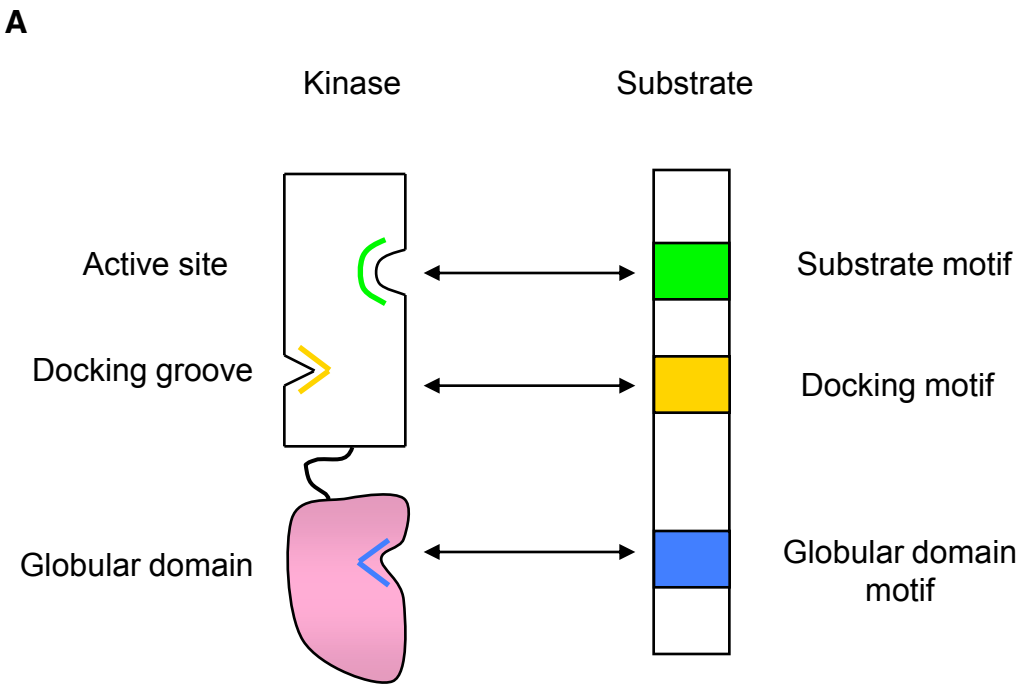

Figure 3.25 A schematic illustration of protein-substrate recognition mechanism.

(A) Protein kinases and substrates have acquired a number of motifs that can aid in protein-substrate recognition. The substrate phosphorylation site motif is targeted by the enzyme's active site while globular domain helps to tether the substrate to its canonical kinase. Substrate docking motif that fits into the kinase docking groove also helps to achieve a more stringent substrate selectivity and may function in the allosteric regulation of the enzyme. *Adapted from REMENYI, A., GOOD, M. C. & LIM, W. A. (2006) Docking interactions in protein kinase and phosphatase networks. Curr Opin Struct Biol, 16, 676-85.*

A

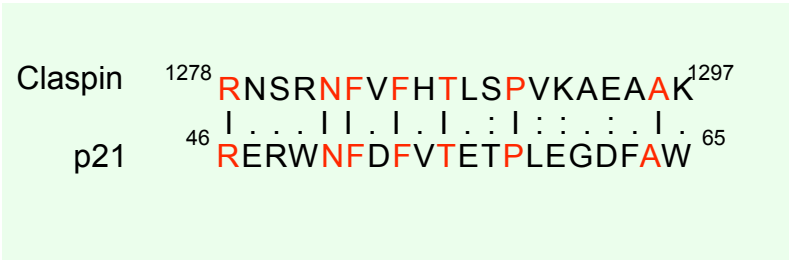

B

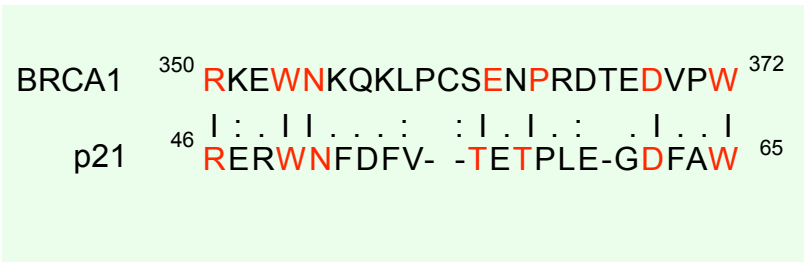

Figure 3.26 Sequence alignment of Claspin and BRCA1 with p21 peptide 4.

(A and B) Sequence alignment identified p21 peptide 4 homology to the C-terminal domain of Claspin (A) and N-terminal domain of BRCA1 (B). Conserved residues are coloured red.

A

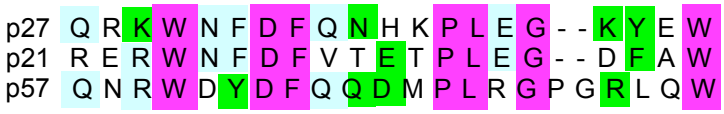

Figure 3.27 Sequence alignment of p21 peptide 4 region with p27 and p57.

(A) Identical residues in all three sequences are shaded magenta. Identical residues in two sequences are shaded blue while similar residues are shaded green.

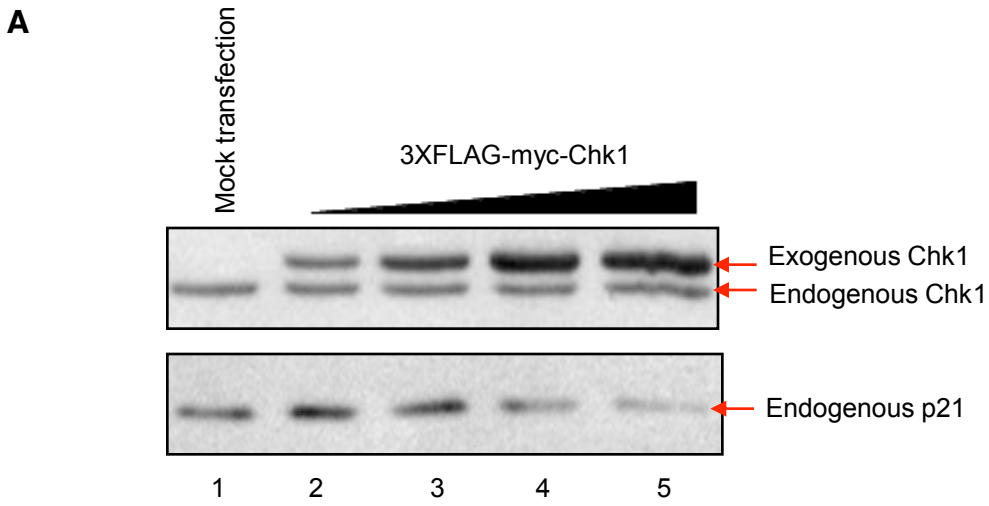

Figure 3.28 Overexpression of exogenous Chk1 leads to decreased endogenous p21 level
(A) Hela cells were grown to 90% confluency before mock transfected or transfected with vector encoding 3xFLAG-myc-Chk1 (0.5 μg to 3 μg) for 24 hours. Cells were harvested and lysed. 50 μg of lysates were resolved by 10% or 12% SDS-PAGE before transferred to nitrocellulose membrane. Chk1 was detected using mouse α-Chk1 IgG and p21 was detected using mouse α-p21 IgG. (Data from Vikram Narayan)

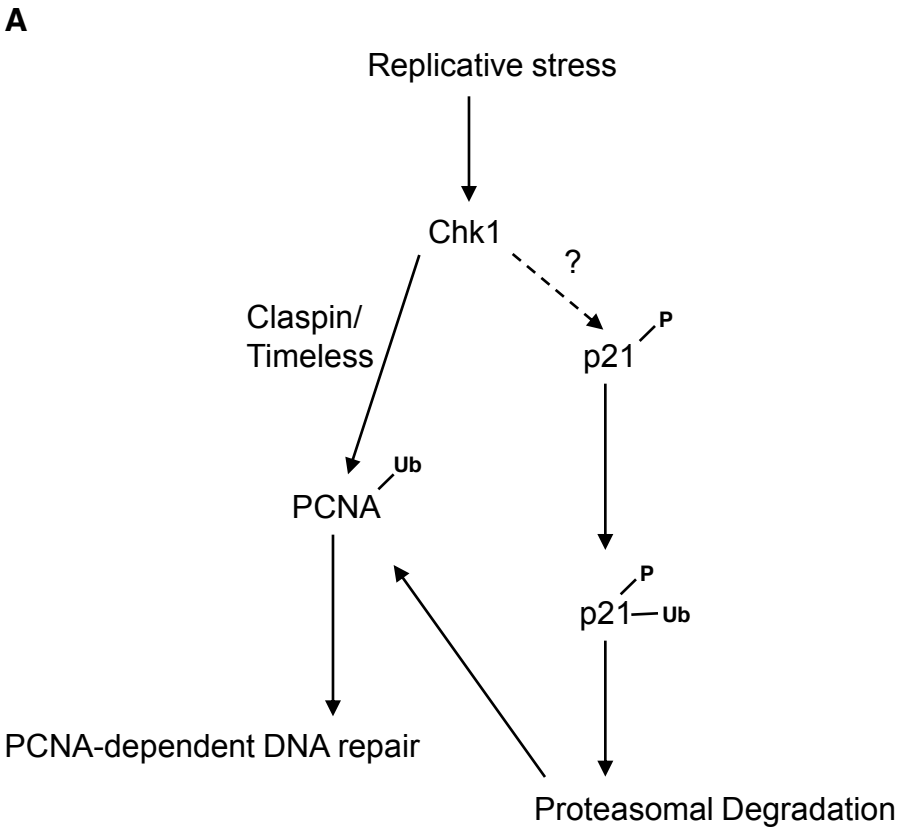

Figure 3.29 Schematic model of a Chk1-dependent pathway in PCNA-dependent DNA repair

(A) In response to replicative stress, a stable Chk1-Claspin complex together with Timeless protein is required for PCNA monoubiquitination, leading to efficient DNA repair. Chk1 could also signal to p21 Ser^{146} to mediate ubiquitin-dependent degradation of p21. Downregulation of p21 then facilitates PCNA monoubiquitination. The dotted line and question mark denote possible signalling pathway. Ub represents ubiquitination; P represents phosphorylation.

CHAPTER 4: CHARACTERISATION OF ALLOSTERIC REGULATION OF CHK1

4.1 Introduction

In the last chapter, a peptidomimetic ligand based on a p21 N-terminal region was able to function as a substrate docking site and allosterically modulate Chk1 catalytic activity. However the mechanistic basis of the allosteric action on Chk1 is not clear. This chapter identifies an N-terminal Chk1 region that has homology to the stimulatory p21 peptide 4 and also exhibits activating effect on Chk1 function. Furthermore, the allosteric mechanism of activating peptides on Chk1 catalytic activity is examined here. Therefore, I will give a brief introduction to the structural model of Chk1 and the functions of its domains.

4.1.1 Chk1 structural model

Chk1 is a nuclear protein made up of 476 amino acids (Sanchez et al., 1997). It mainly consists of a well-conserved N-terminal kinase domain (1-265 amino acids), a flexible linker region (~ 50 residues) and a less conserved C-terminal regulatory domain which includes an SQ/TQ region recognised by ATR (Chen et al., 2000, Katsuragi and Sagata, 2004) (Figure 1.3).

4.1.2 Chk1 N-terminal domain

The crystal structure of the Chk1 N-terminal domain has been elucidated and it has a canonical kinase two-fold lobe (N-terminal β-lobe and C-terminal α-lobe) with an ATP-binding site in-between. The kinase domain appears to adopt an active conformation with the activation loop stabilised by its secondary structure and side

chain interactions (Chen et al., 2000). This mechanism of Chk1 is unlike the activation of many other kinases where phosphorylation of the activation loop is required. In the case of Chk2, phosphorylation of Thr^{383} and Thr^{387} at the activation loop are required for activity (Lee and Chung, 2001, Ahn et al., 2002); however there is no equivalent threonine residue in the activation loop of the Chk1 kinase domain. The amino acid sequences of the activation loop also suggested that it is more flexible in yeast Chk1 proteins compared to human Chk1, which may explain the different substrate preferences (Chen et al., 2000). Kinetic analyses have shown that the conserved kinase domain in isolation is 20-fold more active than full-length Chk1, suggesting that the C-terminal domain negatively regulates Chk1 kinase activity. It is also suggested that the kinase domain may exhibit a structural basis for substrate selectivity based on the crystal structure study where the two conserved hydrophobic pockets and glutamic acid $(Glu)^{91}$ and lysine $(Lys)^{166}$ in the Chk1 kinase domain are important for substrate selectivity. In addition, the hydrophobic side chain at P-5 and P+1 positions, arginine at P+3 position and the steric restriction at P-2 position of the Cdc25C peptide substrate are also critical for Chk1 substrate specificity (Chen et al., 2000).

ATR phosphorylates Chk1 at Ser^{317} and Ser^{345} in response to genotoxic stress. It was shown that deletion of the Chk1 kinase domain resulted in a strong Ser^{345} phosphorylation on the C-terminal domain in the absence of genotoxic stress, leading to the suggestion that the Chk1 kinase domain may sterically inhibit ATR-dependent phosphorylation on Ser^{345} and therefore the interaction with other

proteins or phosphorylation at sites other than Ser^{345} may be the initial activation event of Chk1 (Ng et al., 2004).

Genetic analysis showed that *CHK1* frameshift mutations in genetically unstable colorectal and endometrial cancers resulted in truncated protein of 243 and 238 amino acids, affecting the N-terminal kinase domain. This could result in an inactive enzyme, thus leading to attenuation of cell cycle arrest and giving the tumours a growth advantage (Bertoni et al., 1999).

4.1.3 Chk1 C-terminal domain

It is noted that many protein kinases contain regulatory domains that may function to interact with other proteins or to activate/inhibit its kinase domain by an intramolecular mechanism (Ng et al., 2004). The Chk1 C-terminal region contains several motifs which are conserved across species but exhibits no sequence homology to other proteins. It has been suggested that the C-terminal domain can negatively regulate the access of substrate to the kinase domain by interacting with the substrate-binding site at the front of the N-terminal region (Chen et al., 2000). An example of such an auto-inhibitory function is observed with several kinases including titin (Mayans et al., 1998). However the direction of the C-terminal linker showed that the C-terminal domain is more likely to interact with the back of the kinase domain, limiting the kinase lobe movement; a negative regulatory mechanism which has been observed in the regulation of Src family kinase activity (Chen et al., 2000). In any case, the interaction between the kinase domain and the

regulatory domain is likely to be intra-molecular (Katsuragi and Sagata, 2004). This autoinhibition mechanism prevents spurious activation of Chk1 signalling pathway.

It was observed that truncation of the C-terminal domain resulted in strong Chk1 kinase activity compared to full-length Chk1 (Oe et al., 2001). However in another report, weak kinase activity is observed when the whole C-terminal domain is deleted, in stark contrast to the Chk1 crystal structure data where Chk1 kinase domain by itself is 20-fold more active than full-length Chk1 (Chen et al., 2000, Ng et al., 2004). This suggested that the Chk1 C-terminal domain could also have an activating function on the N-terminal kinase domain.

A bipartite nuclear localisation sequence (NLS) was identified within the C-terminal domain of *Xenopus* Chk1 (xChk1); it comprises of two basic regions (^{374}KR^{375} and ^{456}KIKKK^{460}) and an essential internal sequence in between which are fairly conserved among species. Interestingly, deletion or mutation of the NLS caused a significant activation of the kinase which is not due to cytoplasmic localisation of the mutants. This prompted suggestion that the auto-inhibitory region may overlap with the NLS (Katsuragi and Sagata, 2004).

Phosphorylation at the SQ/TQ motifs of xChk1 appears to play a role in relieving auto-inhibition as it prevented regulatory domain and kinase domain interactions. This suggests that phosphorylation of the SQ/TQ motifs might induce a

conformational change in the C-terminal regulatory domain, causing a release of its auto-inhibitory function on the kinase domain (Katsuragi and Sagata, 2004).

4.1.4 Objectives

In the last chapter, p21 was characterised as a potential novel Chk1 substrate *in vitro* with Ser^{146} as the major phospho-acceptor site and this could be physiologically relevant. However the significance of it is largely outwith the scope of this project. On the other hand, p21 was shown to contain an N-terminal allosteric docking site for Chk1 and this positively modulated Chk1 catalytic activity. The mechanism of how Chk1 autoinhibition is counteracted has been elusive. Elucidating the mechanism will help towards designing better non-ATP Chk1 inhibitors. Therefore in this chapter, I want to use p21 as a tool to delineate the allosteric activation of Chk1 mechanism.

4.2 Results

Chk1 is an autoinhibited protein. However the mechanism of how Chk1 autoinhibition is relieved or reinforced has not been elucidated. There are numerous mechanisms by which autoinhibition can be relieved. The most common regulation is the displacement of the inhibitory domain by an interacting protein. Other mechanisms include post-translational modifications, leading to the displacement of the inhibitory domain or proteolysis of the inhibitory domain or allosteric action of a binding protein partner (Pufall and Graves, 2002). Defining such an autoinhibitory mechanism will guide towards the discovery of better designed non-ATP Chk1 inhibitors. In the last chapter, p21 was shown to contain an allosteric signal for Chk1 catalytic activity. Therefore I am interested in using p21 as a model substrate in understanding the allosteric regulation of Chk1 function.

4.2.1 Identification of an allosteric activating peptide within the αF region of Chk1 N-terminal kinase domain

In the last chapter, I demonstrated that Chk1 utilised a docking interaction to enhance substrate recognition of p21 as a substrate. Studies with other kinases have shown that docking interactions not only function to tether the substrate to Chk1 but also appear to allosterically affect the enzyme leading to enhanced catalytic activity (Remenyi et al., 2006). The N-terminal domain and C-terminal domain of Chk1 have been shown to interact intramolecularly leading to autoinhibition of Chk1 catalytic activity (Katsuragi and Sagata, 2004). In turn, this

leads to the idea that p21 may disrupt binding of the C-terminal domain to a pseudo-docking site in the N-terminal kinase domain of Chk1. It is possible that p21 or p21 peptide 4 would act as a competitive inhibitor to disrupt intramolecular Chk1 interactions between the kinase and the regulatory domain (Figure 4.1). To test this I first carried out a sequence alignment between p21 peptide 4 and full-length Chk1, this highlighted a potential homology between p21 peptide 4 and the αF region (amino acids 189 to 208) of the Chk1 N-terminal catalytic domain (Figure 4.2A). Sequence alignment also revealed that the αF region of Chk1 is fairly conserved across the species (Figure 4.2B), suggesting that it may have an important role in the regulation of Chk1 activity. Thus it is possible that the N-terminal αF region of Chk1 forms the intramolecular binding interface with the C-terminal domain. Peptidomimetic ligands which share the critical amino residues required for this interface are then able to compete for binding to the C-terminal domain, leading to the disruption of intramolecular interaction. Using a more 'neutral' experimental approach to identify a potential pseudo-docking site, a library of overlapping biotinylated 20-mer peptides spanning across the whole length of Chk1 was synthesised (Figure 4.3A). In addition, a peptide equivalent to the full sequence of p21 peptide 4 was synthesised (Chk1 peptide 32). Each Chk1 peptide was analysed for its ability to allosterically stimulate Chk1 activity towards p21 in [γ^{32}P]-ATP kinase assays (Figure 4.3B). Interestingly, only Chk1 peptide 14 and peptide 32, both of which share homology with p21 peptide 4 and form part of the αF region, displayed a positive allosteric effect on Chk1 activity towards p21. Chk1 peptide 14, which encodes most of the p21 peptide 4 sequence, showed a higher stimulating effect than peptide 32 which covers the full homology

sequence. This suggested that peptides based on the αF-region of Chk1 which shared homology with p21 peptide 4 were able to allosterically activate Chk1, whereas peptides from other regions of Chk1 had no effect on activity or were inhibiting. As Chk1 peptide 14 showed greater stimulation of Chk1 activity towards p21, further studies were undertaken. Figure 4.4 shows that Chk1 peptide 14 stimulated Chk1 activity towards p21 (Figure 4.4A) and Chk1 autophosphorylation (Figure 4.4B) in a concentration-dependent manner, similar to that observed for p21 peptide 4 in chapter 3 (Figure 3.5B and C).

4.2.2 Cellular Chk1 activity can be modulated by docking peptides

I have shown that recombinant human Chk1 purified from insect cells can be stimulated allosterically by p21 peptide 4 and Chk1 peptide 14. However it is not clear if cellular Chk1 is amenable to the effects of peptidomimetic ligands. Furthermore, whether the p21 status of the cells used will affect the ability of the peptidomimetic ligands to activate Chk1 is not clear. In order to address those questions, I first characterised the stability and aphidicolin-dependent activation of Chk1 using isogenic HCT116 wild-type ($p21^{+/+}$) and HCT116 $p21^{-/-}$ cells. The possible effect of p21 status on the stability of Chk1 in HCT116 wild-type and HCT116 $p21^{-/-}$ cells was assessed in the presence of translation inhibitor cycloheximide. Cycloheximide was added to the cells and the decay of Chk1 due to protein degradation was determined by immunoblot. Figure 4.5 showed that levels of Chk1 protein were stable in both cell lines up to 4 hours, suggesting that p21 does not affect the stability of Chk1 protein or the steady state levels of the

protein. Immunoblotting with α-p21 IgG confirmed the absence of p21 protein in HCT116 $p21^{-/-}$ cells.

Next both HCT116 wild-type and $p21^{-/-}$ cells were either transfected with C-terminally V5-tagged Chk1 (V5-Chk1) or mock transfected with empty vector. In the previous chapter, I showed that aphidicolin treatment lead to the appearance of a slower-mobilised form of Chk1 protein; however immunoprecipitation of the endogenous Chk1 protein does not capture the slower-mobilised form. This form was thought to be the activated Chk1. Therefore to overcome the IP problem, a V5-tagged-Chk1 vector was made. After 24 hours, the transfected cells were treated with either 20 μM of aphidicolin or ethanol before harvested and lysed after 4 hr. Figure 4.6 showed the presence of V5-tagged Chk1 in transfected cells using α-V5 IgG (lower panel; lane 5 to 8). V5-tag adds a few kDa to the molecular weight of the Chk1, so the exogenous V5-Chk1 appeared as slower mobilised form of Chk1 on the immunoblot with α-Chk1 IgG (Figure 4.6; upper panel; compare lane 1 and 5). This should not be confused with activated form of Chk1 protein when cells were treated with DNA damaging agents (Figure 4.6; upper panel; compare lane 2 and 5). Immunoblots of the lysates showed that Chk1 protein was activated after aphidicolin treatment by the appearance of slow-mobilised form of Chk1 protein (Figure 4.6; upper panel; lane 2, 4, 6, 8). This form was not detected when the cells were treated with ethanol (Figure 4.6; upper panel lane 1, 3, 5, 7). Interestingly, the slow-mobilised, activated forms were not detected in aphidicolin-treated V5-Chk1 (Figure 4.6; lower panel; compare lane 5 to 6). This may suggest that either V5-Chk1 is not activated in response to

aphidicolin-treatment or it is already activated regardless of genotoxic stress. The data showed that p21 status of the cells does not affect the steady-state levels of Chk1, the aphidicolin activation of Chk1 and also the expression levels of exogenous V5-Chk1.

The lysates were subjected to Chk1 immunoprecipitation using either sheep α-Chk1 IgG for endogenous Chk1 or α-V5 IgG for exogenous Chk1 and immunoprecipitated Chk1 was immunoblotted (Figure 4.7). Interestingly, it showed that significantly more endogenous Chk1 protein was immunoprecipitated from HCT116 $p21^{-/-}$ cells than from HCT116 wild-type cells (Figure 4.7A; compare lane 1 and 2 to 3 and 4), although the total levels of Chk1 protein in whole cell lysate were the same (Figure 4.6; upper panel; lane 1 to 4). It should be noted that the band detected at around 50 kDa was of Chk1 and not the IgG heavy chain. Figure 4.7B showed that immunoprecipitated samples from HCT116 cells using either sheep α-Chk1 IgG for endogenous Chk1 or mouse α-V5 IgG for exogenous Chk1 were resolved in 10% SDS-PAGE before transferred to nitrocellulose membrane. The membrane was detected for the presence of Ig light and heavy chain by using either rabbit α-mouse secondary IgG or rabbit α-sheep secondary IgG. The result showed that only the IgG light chain was detected, but not the heavy chain, suggesting that the bands detected at around 50 kDa was that of Chk1 and not the IgG heavy chain (Figure 4.7A and B). Therefore the differential level of immunoprecipitated Chk1 may suggest differences in the conformation, modification status or Chk1 interacting proteins in HCT116 wild-type and HCT116 $p21^{-/-}$ cells, leading to a difference in the exposure of antigen

epitope. The immunoblot also showed that the activated forms of endogenous Chk1 were not immunoprecipitated (Figure 4.7A; compare lane 1 and 3 to lane 2 and 4).

In contrast, less exogenous V5-Chk1 was immunoprecipitated from HCT116 $p21^{-/-}$ cells than from HCT116 wild-type cells (Figure 4.7A; compare lane 5 and 6 to 7 and 8), even though the total levels of V5-Chk1 protein in whole cell lysate were the same (Figure 4.6; lower panel; lane 5 to 8). This again suggested differences in the conformation, modification status or Chk1 interacting proteins in HCT116 wild-type and HCT116 $p21^{-/-}$ cells, leading to a difference in the exposure of antigen epitope.

To test whether cellular Chk1 is amenable to the effects of docking peptides, immunoprecipitated Chk1 was subjected to [γ^{32}P]-ATP kinase assay with or without p21 peptide 4 (P) or Chk1 peptide 14 (C) using Chktide as a substrate (Figures 4.8 and 4.9). These experiments were repeated twice with consistent results. Chktide is a Cdc25C-derived peptide (KKKVSRSGLYRSPSMPENLNRPR) targeted by Chk1. The results showed that the activity of endogenous Chk1 in both HCT116 wild-type and HCT $p21^{-/-}$ cells can be stimulated by both peptidomimetic ligands. There was only a marginal increase of aphidicolin-treated Chk1 compared to ethanol-treated Chk1 (Figure 4.8; lane 1, 4, 7, 10). Chk1 peptide 14 stimulated endogenous HCT116 wild-type Chk1 activity with a 8-fold increase compared to control while p21 peptide 4 stimulated endogenous HCT116 wild-type Chk1 activity with a 3-fold increase compared to

control (Figures 4.8; lane 1 to 6). Endogenous HCT116 $p21^{-/-}$ Chk1 was also stimulated by Chk1 peptide 14 with a 14-fold increase compared to control while p21 peptide 4 stimulated endogenous HCT116 $p21^{-/-}$ Chk1 by 5-fold compared to control (Figure 4.8; lane 7 to 12). Overall, endogenous Chk1 immunoprecipitated from HCT116 $p21^{-/-}$ cells were stimulated better by activating peptides (Chk1 peptide 14 and p21 peptide 4) as compared to endogenous Chk1 immunoprecipitated from HCT116 wild-type cells

Interestingly, exogenous V5-Chk1 activity from HCT116 wild-type cells was not amenable to the stimulating effects of p21 peptide 4 and Chk1 peptide 14 (Figures 4.9; lane 1 to 6), with only marginal increase of activity in the presence of peptidomimetic ligands. In contrast, exogenous V5-Chk1 activity from HCT116 $p21^{-/-}$ cells could be modulated by the stimulating effects of peptidomimetic ligands. The discrepancy would be even more pronounced if normalised to immunoprecipitated protein. Chk1 peptide 14 stimulated HCT116 $p21^{-/-}$ V5-Chk1 activity with a 6-fold increase compared to control while p21 peptide 4 stimulated HCT116 $p21^{-/-}$ V5-Chk1 activity with a 2-fold increase compared to control (Figures 4.9; lane 7 to 12). Consistent with the endogenous Chk1 activity data, Chk1 peptide 14 stimulated V5-Chk1 activity better than p21 peptide 4. Overall the data suggested that immunoprecipitated Chk1 from HCT116 $p21^{-/-}$ cells are more amenable to the stimulating effects of the peptides and Chk1 peptide 14 stimulated cellular Chk1 better than p21 peptide 4.

One interest to note is that in the HCT116 wild-type cells, Chk1 immunoprecipitates contained a high molecular weight phospho-protein which migrated at about 50 kDa (Figure 4.8A and 4.9A; lane 1 to 6). This could be Chk1 autophosphorylation or an unknown co-immunoprecipitated substrate of Chk1. Interestingly this was not detected in the HCT116 $p21^{-/-}$ Chk1 immunoprecipitation sample (Figure 4.8A and 4.9A; lane 7 to 12). To test whether this phosphorylated protein could be autophosphorylated Chk1 protein, endogenous and exogenous V5-Chk1 was immunoprecipitated from aphidicolin-treated or ethanol-treated HCT116 wild-type cells and subjected to a kinase assay with or without unlabelled ATP. Chktide was used as a substrate. The reaction products were resolved in 10% SDS-PAGE before transferred to nitrocellulose membrane. Chk1 protein was detected using mouse α-Chk1 antibodies. The rationale is that if cellular Chk1 undergoes autophosphorylation in the IP-kinase assay, it will migrate more slowly in the presence of ATP due to incorporation of phosphates. If not, Chk1 protein in the presence of ATP will migrate at the same molecular weight as Chk1 protein in the absence of ATP. Immunoblotting for immunoprecipitated endogenous Chk1 and V5-Chk1 in the kinase assay showed that in the presence of ATP, Chk1 migrated at the same molecular weight (Figure 4.10; lane 1, 2, 5, 6) with Chk1 in the absence of ATP (Figure 4.10; lane 3, 4, 7, 8). This suggested that immunoprecipitated V5-Chk1 did not autophosphorylate itself in the IP-kinase assay and that the high molecular weight phosphorylated protein observed in the autoradiography (Figure 4.8A and 4.9A; lane 1 to 6) was not due to autophosphorylation of Chk1 protein but could be a co-immunoprecipitated substrate of Chk1 in HCT116 wild-type cells. This further suggested that p21 may

play a role in the regulation of Chk1 protein. The unknown phospho-protein will be subjected to mass spectrometry analysis but in the meantime I decided to focus on biochemical approach to delineate the mechanistic basis of allosteric regulation of Chk1.

4.2.3 Characterisation of Chk1 (Ser→Ala$^{317/345}$) and Chk1 ΔC70 mutants

We have hypothesised that stimulation of Chk1 catalytic activity by Chk1 peptide 14 and p21 peptide 4 is mediated by the disruption of intramolecular interaction between the Chk1 autoinhibitory C-terminal domain and its N-terminal kinase domain. To further analyse the effects of intrasteric regulation of Chk1 by activating peptides, two Chk1 mutants were generated (Figure 4.11).

1. **Chk1 (Ser→Ala$^{317/345}$)** where the ATR-phosphorylation sites were mutated to non-phosphorylatable alanine residues. Phosphorylation on Ser^{317} and Ser^{345} are thought to enhance Chk1 kinase activity, suggesting a coupling of ATR phosphorylation sites and the enzymatic mechanism (Zhao and Piwnica-Worms, 2001). Furthermore, Ser^{317} and Ser^{345} phosphorylation were thought to disrupt intramolecular interaction of the Chk1 C-terminal domain and N-terminal domain, therefore leading to enhanced catalytic activity (Katsuragi and Sagata, 2004).

2. **Chk1 ΔC70** where the last 70 amino acids of the C-terminal domain are deleted. Deletion of this autoinhibitory region has been shown to give an increase in kinase activity (Katsuragi and Sagata, 2004).

The desired mutations were made in the Bacmid vector and Chk1 baculovirus were then generated using methods outlined in Chapter 2 and titrated before studies were carried out to determine optimal expression conditions for parameters such as viral dilution (multiplicity of infection) and incubation time (data not shown). Using these optimal conditions, His-tagged Chk1 wild-type and mutant proteins were expressed in *Sf9* insect cells system by infecting with Chk1 baculovirus. The expressed proteins were purified using the Ni-NTA columns. A coomassie blue stained gel showed that the purified Chk1 fraction was approximately 90 % pure and an immunoblot confirmed the presence of Chk1 protein in the fraction (Figure 4.12A; Lane 7). Infection of *Sf9* insect cells must have activated the stress response as Chk1 wild-type was found to be phosphorylated at Ser^{317} and Ser^{345}. This was not observed when Chk1 ($Ser \rightarrow Ala^{317/345}$) mutant was analysed (Figure 4.12B). However it should be noted that it is not known how much of the Chk1 WT protein population was phosphorylated at Ser^{317} and Ser^{345}.

To ensure that equal amounts of Chk1 wild-type and mutant proteins were tested, the concentrations of the purified Chk1 wild-type and mutant proteins were normalised against the known concentration of Chk1 wild-type protein in an ELISA format (Figure 4.13). First, I analysed the activity of normalised Chk1

proteins in a [γ^{32}P]-ATP kinase assay using p21 as substrate (Figure 4.14). As expected, deletion of the autoinhibitory region in Chk1, ΔC70, displayed a two-fold increase in catalytic activity as compared to the Chk1 wild-type protein. Interestingly, mutation at the ATR phosphorylation sites, Chk1 (Ser→Ala$^{317/345}$), did not affect catalytic activity and activity was comparable to the Chk1 wild-type protein. This could indicate that phosphorylation at the ATR sites does not affect intrinsic Chk1 kinase activity but more likely to affect Chk1 function in cells by regulating its interaction with other proteins or Chk1 localisation. However it is also possible that only 1% of the Chk1 WT protein population was phosphorylated at the ATR sites, leading to no discernible differences between Chk1 WT and Chk1 (Ser→Ala$^{317/345}$) catalytic activity. [γ^{32}P] incorporation into p21 was confirmed to be mediated by Chk1 rather than any contaminating kinases, as addition of debromohymenialdisine (DBH), an inhibitor of Chk1 and Chk2 (Curman et al., 2001), attenuate [γ^{32}P]-ATP incorporation by more than 90%.

To analyse Chk1 wild-type and mutant protein catalytic activity further, the kinetic constants for Chk1 with respect to p21 were measured (Figure 4.15). Experiments were repeated in triplicate and the kinetics constants were calculated as the mean ± standard deviation. In agreement with the earlier kinase assay (Figure 4.14), Chk1 ΔC70 exhibited about three-fold increase in V_{max} as compared to wild-type, while Chk1 (Ser→Ala$^{317/345}$) displayed a slightly lower activity than the wild-type enzyme yet not significant. However the K_{cat}/K_m values indicated that although Chk1 ΔC70 had higher catalytic activity compared to Chk1 wild-type, it was about 2.5-fold less efficient than Chk1 wild-type in phosphorylating p21. Chk1

(Ser→Ala$^{317/345}$) was also less efficient with 1.5-fold inefficiency compared to Chk1 wild-type. This may suggest that phosphorylation at Ser^{317} and Ser^{345} may influence catalytic activity. The disparate difference in K_{cat}/K_m between Chk1 wild-type and Chk1 ΔC70 could be attributable to the high K_m value of Chk1 ΔC70 where it is almost 5-fold higher than that of Chk1 wild-type protein, implying that the last 70 amino acids of Chk1 C-terminal domain might be important for substrate recognition/docking or stabilisation of the kinase domain.

4.2.4 Recombinant Chk1 ΔC70 is refractory to the stimulatory effects of activating peptides

After the kinetic constants for Chk1 wild-type and mutants proteins were analysed, I wanted to further delineate the effects of p21 peptide 4 and Chk1 peptide 14 on the activity of the recombinant Chk1 mutant proteins. Kinase reactions containing p21 and activating peptide were assembled and [γ^{32}P] incorporation into p21 in the presence of increasing concentrations of Chk1 was determined. As expected, the peptides exhibited a stimulating effect on the Chk1 wild-type protein, with p21 peptide 4 having a greater positive effect than Chk1 peptide 14 (Figure 4.16). This is in contrast to the data obtained for cellular Chk1 where Chk1 peptide 14 stimulated Chk1 catalytic activity better than p21 peptide 4 (Figures 4.8 and 4.9). This suggested that cellular Chk1 could carry post-translational modifications or interacting proteins that lead to the observed differential stimulating effects. For the recombinant human Chk1 expressed from insect cells, the stimulating effect seemed to plateau off at the highest enzyme concentration though probably due to

over-saturating amount of enzyme. Similarly, Chk1 (Ser→Ala$^{317/345}$) mutant protein activity was enhanced in the presence of the peptides, though the stimulating effect was not as pronounced as that observed with Chk1 wild-type protein. p21 peptide 4 was shown to be a better stimulator for Chk1 (Ser→Ala$^{317/345}$) mutant compared to Chk1 peptide 14. Interestingly, Chk1 ΔC70 mutant activity was refractory to the effect of the peptides with little difference in p21 phosphorylation in the presence or absence of activating peptides. In fact, the addition of Chk1 peptide 14 seemed to inhibit Chk1 ΔC70 mutant activity. This suggested that the last 70 amino acids of Chk1 C-terminal domain are displaced by the activating peptides (p21 peptide 4 and Chk1 peptide 14) in Chk1 wild-type or Chk1 (Ser→Ala$^{317/345}$) mutant. It also further suggested that this region is either required or is sufficient for activating peptides binding.

4.2.5 p21 peptide 4 stimulation enhances Chk1 enzymatic efficiency

Both p21 peptide 4 and Chk1 peptide 14 were able to stimulate Chk1 activity in a concentration-dependent manner; however these observations did not provide an insight as to whether allosteric activation of Chk1 will affect Chk1 enzymatic efficiency with regard to substrate utilisation. To test whether allosteric activation makes Chk1 a more efficient enzyme, the kinetics of p21 substrate utilisation by Chk1 were analysed in the presence or absence of either Chk1 peptide 14 and p21 peptide 4 (Figure 4.17). Chk1 wild-type (WT) was found to have a K_m of 3.06. In the presence of p21 peptide 4, Chk1 catalytic activity was clearly stimulated as seen by a decrease in K_m from 3.06 to 1.06 compared to in the absence of peptide.

Data showed that the presence of p21 peptide 4 influenced catalytic efficiency of Chk1 with a 3-fold higher K_{cat}/K_m value than unstimulated Chk1. This showed that p21 peptide 4 stimulation of Chk1 led to a much more efficient utilization of p21 as a substrate, keeping in line with findings of Figure 4.16.

Strikingly, in the presence of Chk1 peptide 14, Chk1 displayed an increased K_m from 3.06 to 5.19 compared to unstimulated Chk1. In contrast to p21 peptide 4, Chk1 displayed lower K_{cat}/K_m value in the presence of Chk1 peptide 14 compared to unstimulated Chk1, suggesting that Chk1 is not as efficient with Chk1 peptide 14. This is surprising as Chk1 peptide 14 showed the greatest stimulation of Chk1 activity towards p21 in Figure 4.16. Therefore the data showed that p21 peptide 4 makes Chk1 a more efficient enzyme, however Chk1 is less efficient in the presence of Chk1 peptide 14.

4.2.6 Binding of p21 peptide 4 to recombinant Chk1 ΔC70 mutant protein

In chapter 3, I demonstrated that binding of p21 peptide 4 to Chk1 wild-type was ATP-dependent (Figure 3.16). To test whether Chk1 peptide 14 binds to Chk1 and if the interaction is also ATP-dependent, Chk1 wild-type protein kinase was assembled with Chk1 peptide 14 with or without ATP in unlabelled kinase assay. The reaction products were resolved by 15 % non-denaturing PAGE (without SDS) and transferred to nitrocellulose membrane. Biotinylated Chk1 peptide 14 was detected with HRP-conjugated streptavidin whilst recombinant Chk1 protein was

detected with α-Chk1 IgG (Figure 4.18A). A band with a molecular weight of 10 kDa was observed when samples were probed with HRP-conjugated streptavidin, this represents unbound peptides. An additional band with a molecular weight of 55 kDa was also observed. This was thought to represent Chk1 peptide 14 bound to Chk1. This band was present in samples treated with or without ATP. Sample was migrated slower in the presence of ATP which was thought to represent Chk1 peptide 14 bound to autophosphorylated Chk1. The retarded mobility of autophosphorylated Chk1 was confirmed by immunoblot analysis with α-Chk1 antibodies. Data showed that Chk1 peptide 14 does indeed bind to Chk1 yet in contrast to p21 peptide 4, this interaction is not dependent or influenced by the presence of ATP.

Figure 4.16 showed that recombinant Chk1 ΔC70 protein was refractory to the stimulating effects of p21 peptide 4 and Chk1 peptide 14, leading to the possibility that the last 70 amino acids of the C-terminal domain may contain a potential docking site for the activating peptides. To test this possibility, Chk1 ΔC70 was assembled with the p21 peptide 4 in unlabelled kinase assay with or without ATP and resolved by non-denaturing gel electrophoresis. Interestingly, the HRP-conjugated streptavidin blot showed that p21 peptide 4 bound to Chk1 ΔC70 in an ATP-dependent manner (Figure 4.18B), where a band corresponding to the molecular weight of Chk1 ΔC70 was observed in the absence of ATP but not in +ATP conditions. The data suggested that although Chk1 ΔC70 activity was refractory to the stimulating effects of activating peptides, p21 peptide 4 could indeed bind to Chk1 ΔC70 protein.

4.2.7 Disruption of intramolecular interaction between Chk1 N-terminal and C-terminal domains by the activating peptides

I have demonstrated that p21 peptide 4 and Chk1 peptide 14 could bind to Chk1 protein. To test the possibility that activating peptides could disrupt the intramolecular interaction between Chk1 N-terminal and C-terminal domains, the chick Chk1 system of Prof Gillespie group was employed. The Gillespie group has generated the following mutants (Figure 4.19):

1. **chick Chk1 ΔC76** – where the last 76 amino acids of C-terminal domain was deleted.
2. **chick Chk1 ΔC166** – where the last 166 amino acids of C-terminal domain was deleted.
3. **chick Chk1 C-terminal domain** – lacking the majority of the kinase domain.

Cos1 cells were co-transfected with either chick Chk1 ΔC76 and chick Chk1 C-terminal domain or chick Chk1 ΔC166 and chick C-terminal domain for 24 hours and then harvested and lysed. Exogenous Chk1 was then immunoprecipitated from lysate with α-chick Chk1 C-terminal IgG and then immunoprecipitated chick Chk1 complexes were incubated with either p21 peptide 4 or Chk1 peptide 14. Then the supernatant was removed before the immunoprecipitated products were resolved by 10 % SDS-PAGE and transferred to nitrocellulose membrane. Chick Chk1 ΔC76 and Chk1 ΔC166 were detected using α-Chk1 IgG that recognises Chk1 N-terminal domain epitope.

Immunoprecipitated chick Chk1 was not detected when pcDNA empty vector was co-transfected with the chick Chk1 C-terminal domain (Figure 4.20A; lane 1 to 3). This showed that the immunoblotting α-Chk1 IgG only recognises chick Chk1 N-terminal domain. The IP-kinase assay also showed that transfecting chick Chk1 C-terminal domain alone did not yield any activity (Figure 4.20B). Figure 4.20A also showed that the immunoprecipitation α-chick Chk1 C-terminal IgG only recognises chick Chk1 C-terminal domain as chick Chk1 was not detected when chick Chk1 ΔC76 or Chk1 ΔC166 were transfected into Cos1 cells alone (Figure 4.20A: lane 4 and 10). Furthermore little or no activity was detected when chick Chk1 ΔC166 alone was transfected into Cos1 cells (Figure 4.20B).

When chick Chk1 ΔC76 or Chk1 ΔC166 were co-transfected with chick Chk1 C-terminal domain, chick Chk1 ΔC76 or Chk1 ΔC166 mutant protein was co-immunoprecipitated in a chick Chk1 C-terminal domain IP-kinase assay (Figure 4.20A; lane 7 and 11). This suggested that chick Chk1 C-terminal domain interact with the kinase domain constructs. In addition, kinase activity was detected from IP-kinase of co-transfected cells and interestingly, slightly lower catalytic activity was observed with chick Chk1 ΔC76 + C-terminal domain compared to chick Chk1 ΔC166 + C-terminal domain (Figure 4.20B). However following the addition of p21 peptide 4 or Chk1 peptide 14 to the IP-kinase assay, lower amount of co-immunoprecipitated chick Chk1 ΔC76 and chick Chk1 ΔC166 were detected (Figure 4.20A; lane 8, 9, 12 and 13) and higher Chk1 catalytic activity was detected (Figure 4.20B). Interestingly, as observed in Figures 4.8 and 4.9, Chk1 peptide 14 stimulated cellular chick Chk1 catalytic activity better than p21 peptide

4, which is in stark contrast to the recombinant human Chk1 data (Figure 4.16), This again suggested that cellular Chk1 could carry post-translational modifications or interacting proteins that lead to the differential stimulating effects. Overall the data suggested that p21 peptide 4 and Chk1 peptide 14 could disrupt the intramolecular interaction between chick Chk1 C-terminal domain and chick Chk1 ΔC76 or Chk1 ΔC166, leading to enhanced catalytic activity.

4.2.8 Mutation of conserved Tryptophan residues in the Chk1 N-terminal αF region resulted in loss of allosteric stimulation of catalytic activity

Chk1 N-terminal kinase domain and C-terminal regulatory domain are involved in intra-molecular interaction (Katsuragi and Sagata, 2004). Addition of Chk1 peptide 14 from the αF region of Chk1 kinase domain was able to abrogate this intra-molecular interaction and stimulate Chk1 activity towards p21. This suggested that the αF region could be involved in the association of the Chk1 N-terminal and C-terminal domains. To determine whether the αF region is crucial for intra-molecular interaction of Chk1, two conserved tryptophan residues (Trp^{192} and Trp^{208}) within αF region were mutated to alanine (Figure 4.21B). The two tryptophan residues were chosen because they are conserved throughout the species of Chk1 (Figure 4.21A) and furthermore alanine mutation of Trp^{65} within the p21 peptide 4, which was shown to align to Chk1 Trp^{208}, attenuate Chk1 stimulation (Figures 3.20 and 4.2).

Baculovirus carrying Trp→Ala$^{192/208}$ mutation were produced and used to infect insect cells. N-terminally His-tagged Chk1 (Trp→Ala$^{192/208}$) mutant protein was expressed in *Sf9* insect cells and purified using the Ni-NTA column (Figure 4.22A). Surprisingly, immunoblotting analysis revealed that the recombinant Chk1 (Trp→Ala$^{192/208}$) mutant appeared to be cleaved, migrating at about 30 kDa (Figure 4.22A; right panel; lane 5) as compared to Chk1 wild-type which migrated at about 50 kDa (Figure 4.22A; left panel; lane 5). The Chk1 (Trp→Ala$^{192/208}$) mutant form that appeared on the immunoblot reflected a C-terminal truncation because the antibodies (mouse monoclonal α-Chk1 IgG, Santa Cruz) used in this assay recognised the N-terminal Chk1 peptide. To assess whether cleavage of Chk1 (Trp→Ala$^{192/208}$) mutant protein happened intracellularly or if it occurred during the infected *Sf9* insect cells lysis procedure, direct lysis of the infected cells in SDS-PAGE sample buffer was analysed (Figure 4.23A). The immunoblot showed that the Chk1 (Trp→Ala$^{192/208}$) mutant cleavage happened during protein expression, suggesting that mutation at Trp^{192} and Trp^{208} makes Chk1 protein susceptible to proteolytic cleavage. The Chk1 (Trp→Ala$^{192/208}$) mutant form detected on the immunoblot seemed to represent the kinase domain as it migrated at approximately 30 kDa which is similar to the predicted molecular weight of the Chk1 kinase domain.

Longer exposure of the immunoblot did reveal however the presence of a small population of full-length Chk1 (Trp→Ala$^{192/208}$) mutant protein (data not shown). As the sample was contaminated with cleaved Chk1 (Trp→Ala$^{192/208}$) mutant protein, I wanted to separate the full-length protein from the cleaved protein and

test whether the full length Chk1 (Trp→Ala$^{192/208}$) mutant protein catalytic activity is affected by the mutations and if the mutant is still stimulated by Chk1 peptide 14. If Trp^{192} and Trp^{208} are involved at the intramolecular binding interface, mutation at these residues would be expected to disrupt Chk1 C-terminal-mediated autoinhibition of the kinase domain, leading to enhanced catalytic activity. Therefore, the purified recombinant Chk1 (Trp→Ala$^{192/208}$) fraction was subjected to gel filtration using the Superdex 200 column to separate the higher molecular weight full-length Chk1 (Trp→Ala$^{192/208}$) mutant protein from the lower molecular weight cleaved Chk1 (Trp→Ala$^{192/208}$) mutant protein form (Figure 4.23B). However, the immunoblot analysis revealed that the full-length Chk1 (Trp→Ala$^{192/208}$) mutant protein which migrated at about 50 kDa co-eluted from the gel-filtration column with the cleaved form which migrated at about 30 kDa (Figure 4.23B; lane 4 to 7), suggesting that the full-length Chk1 formed complexes with the cleaved Chk1.

Having failed to purify the full-length Chk1 (Trp→Ala$^{192/208}$) mutant protein from the sample pool, it was decided to further analyse the effects of Trp^{192} and Trp^{208} residues on Chk1 catalytic activity by transfecting C-terminally tagged V5-Chk1 wild-type and Chk1 (Trp→Ala$^{192/208}$) mutants into HCT116 wild-type cells. Immunoblotting for V5-Chk1 protein showed that exogenous V5-Chk1 (Trp→Ala$^{192/208}$) mutant protein was not cleaved as in the insect cells and it also migrated slower than the exogenous V5-Chk1 wild-type protein (Figure 4.24; lower panel; compare lane 2, 4, 6, 8 to lane 1, 3, 5, 7). Interestingly, as noticed in Figure 4.6, activated forms of V5-Chk1 wild-type and V5-Chk1 (Trp→Ala$^{192/208}$)

were not detected on the immunoblot (Figure 4.24; lower panel). This again suggested that that either V5-Chk1 is not activated in response to aphidicolin-treatment or it is already activated regardless of genotoxic stress.

Exogenous V5-tagged Chk1 proteins were immunoprecipitated from the cellular lysates. The immunoprecipitated sample was assembled with Chktide as substrate in the presence or absence of activating peptides in the [γ^{32}P]-ATP kinase assay. The reaction products were resolved by 15 % SDS-PAGE and [γ^{32}P] incorporation into Chktide was visualised by autoradiography (Figure 4.25A) and quantified by phosphorimager (Figure 4.25B). The data showed that both V5-Chk1 wild-type and V5-Chk1 (Trp→Ala$^{190/208}$) were active (Figure 4.25A; lane 1 to 4). Interestingly, ethanol-treated V5-Chk1 wild-type displayed 3-fold increased activity than aphidicolin-treated V5-Chk1 wild-type (Figure 4.25A; lane 1 and 2). However, there was no difference in catalytic activity between aphidicolin-treated V5-Chk1 (Trp→Ala$^{192/208}$) and ethanol-treated V5-Chk1 (Trp→Ala$^{192/208}$) (Figure 4.25A; lane 3 and 4). As expected, immunoprecipitated V5-Chk1 wild-type catalytic activity could be greatly stimulated by Chk1 peptide 14 (Figure 4.25A; compare lane 1 and 2 to lane 9 and 10), however in contrast, immunoprecipitated V5-Chk1 (Trp→Ala$^{192/208}$) catalytic activity was only mildly stimulated by Chk1 peptide 14 (Figure 4.25A; compare lane 3 and 4 to lane 11 and 12). p21 peptide 4 was shown to have a stimulating effect on V5-Chk1 (Trp→Ala$^{192/208}$) catalytic activity though the it was not as pronounced as on V5-Chk1 wild-type (Figure 4.25A; compare lane 5 and 6 to lane 7 and 8). Therefore the data suggested that

alanine mutation at Trp^{192} and Trp^{208} residues of Chk1 resulted in loss of allosteric stimulation by the activating peptides.

Peptidomimetic ligand based on the Chk1 αF region was able to abrogate intramolecular interaction between Chk1 N-terminal domain and its C-terminal domain, leading to enhanced catalytic activity. It was thought that mutating the conserved Trp^{192} and Trp^{208} in the Chk1 αF region will displaced the C-terminal domain, leading to enhanced catalytic activity. However, Trp^{192} and Trp^{208} mutation led to cleavage susceptibility in insect cells-expressed Chk1 (Trp→$Ala^{192/208}$) protein, appearance of slow-mobilised form of Chk1 (Trp→$Ala^{192/208}$) in SDS-PAGE. This suggested that Trp^{192} and Trp^{208} mutation may have a destabilising effect on Chk1 conformation. The destabilising effect could not be rescued by the activating peptides as transfected Chk1 (Trp→$Ala^{192/208}$) from HCT116 wild-type cells was refractory to allosteric stimulation compared to transfected Chk1 wild-type protein.

4.2.9 Allosteric activation of Chk1 resulted in lower requirement for arginine residue at P-3 position

Studies on p38 protein kinase showed that allosteric docking by peptidomimetic ligand induced conformational changes in the active site, which suggested the possibility that allosteric regulation could change the specificity of substrate recognition (Chang et al., 2002). To examine whether recombinant Chk1 wild-type protein allosterically activated by Chk1 peptide 14 and loss of autoinhibitory

region (Chk1 ΔC70 mutant protein) could result in change of substrate recognition specificity, [γ^{33}P]-ATP kinase assay with Chk1 wild-type protein or Chk1 wild-type protein allosterically activated by Chk1 peptide 14 or Chk1 ΔC70 mutant protein were performed using PepChip microarray. This microarray slide contained duplicate sets of 192 different peptides with a median length of nine amino residues, based on known phosphorylation sites in the PhosphoBase database (Figure 4.26). [γ^{33}P]-ATP was used to reduce the background signal. Kinase buffer was also optimised for this assay by ensuring that Chk1 catalytic activity and allosteric stimulation by Chk1 peptide 14 are not affected by the addition of Brij-35 which was used to reduce background signal. After the conditions were optimised, kinase reactions containing either Chk1 wild-type, Chk1 wild-type + Chk1 peptide 14 or Chk1 ΔC70 were assembled in the presence of [γ^{33}P]. The PepChip microarrays were incubated with the kinase reactions for 3 hours at 30^{o}C in a humidity chamber. After incubation, the kinase reactions were washed off and [γ^{33}P] incorporation into the peptide substrates on the microarray slides were visualised by autoradiography. The spot signals were correlated with the peptide sequences using the grid and spreadsheet provided by the manufacturer. Positive hits were tabulated and organised in a table format (Appendix 1). The data showed that all three forms of Chk1 protein shared some substrate peptides (coloured in yellow in Appendix 1). Interestingly, the microarray data showed that 24 substrate peptides were phosphorylated only in the presence of the Chk1 protein stimulated by Chk1 peptide 14 (not coloured in Appendix 1) (Figure 4.27). Although there were no substrate peptide phosphorylated exclusively by Chk1 ΔC70, it shared 10 common substrate peptides with allosterically activated Chk1.

Therefore, the data suggested that loss of autoinhibitory region (Chk1 ΔC70) and allosteric activation of Chk1 (Chk1 stimulated by Chk1 peptide 14) can lead to change in substrate specificity, allowing Chk1 to target substrates that do not fit with Chk1 consensus substrate specificity. 10 common peptide substrates phosphorylated by Chk1 ΔC70 and allosterically activated Chk1 suggested that deletion of the last 70 amino acids of Chk1 C-terminal domain may constitute the same effects as allosterically activated Chk1.

To further confirm that allosteric activation would allow Chk1 to tolerate substrate specificity changes, I selected 13 peptide substrates for further analysis (Figure 4.28). As shown in the earlier microarray data, among these 13 peptide substrates, peptides 1 to 7 were phosphorylated exclusively by allosterically activated Chk1 whilst peptides 11 and 12 were targeted by all three forms of Chk1. As some of the peptide substrates were found in species other than human, I also want to test whether the human equivalent of the substrate peptides can be phosphorylated by Chk1 as this might be a way of identifying potential novel substrates. Peptides 8 to 10 were human forms of peptide 2, 5 and 7 respectively, while peptide 13 is the human equivalent of peptide 12. The substrate peptides were assembled with either Chk1 wild-type protein or Chk1 wild-type stimulated by Chk1 peptide 14 in a [γ^{32}P]-ATP kinase assay (Figure 4.29). The data showed that Chk1 wild-type protein as well as allosterically activated Chk1 phosphorylated peptides 11 and 12, which has arginine residue in the P-3 position. Peptides 1 to 10 showed no [γ^{32}P] incorporation when assembled with Chk1 wild-type protein alone, in agreement with the PepChip microarray. In comparison, peptides 1 to 13 displayed [γ^{32}P]

incorporation in the presence of allosterically activated Chk1. In the presence of stimulatory Chk1 peptide 14, Chk1 activity towards peptide 12 was about 4.5 fold higher than in the absence of stimulatory peptide while allosterically activated Chk1 activity towards peptide 11 was about 2.5 fold higher as compared to non-activated Chk1. The data confirmed that allosteric activation could modulate Chk1 activity towards non-consensus peptide substrates.

4.2.10 Recombinant Chk1 is active towards Interleukin-1α

Using the PepChip microarray, Chk1 was shown to be active towards several novel substrates such as mouse Interleukin-1α. Furthermore, some of these novel substrates such as human Signal transducer and activator of transcription 1 (STAT1) are only targeted by Chk1 stimulated by the activating peptide.

To further characterise Chk1 activity towards these novel substrates, Chk1 protein kinase was assembled with titrating amounts of human interleukin-1α protein (Sigma Aldrich) or STAT1 protein (Biomol) for [γ^{32}P]-ATP kinase assay. The assay showed [γ^{32}P] incorporation into human interleukin-1α (Figure 4.30A) but not human STAT1 (Figure 4.30B). This suggested that interleukin-1α could be a novel Chk1 substrate. Although, STAT1 was not phosphorylated in this kinase assay, the microarray data showed that STAT1 peptide could only be phosphorylated in the presence of Chk1 stimulated by activating peptide (Figure 4.27).

To test whether stimulation of Chk1 by peptide 4 could enhance catalytic activity towards interleukin-1α and also switch substrate specificity towards STAT1, Chk1 was assembled with interleukin-1α or STAT1 for [γ^{32}P]-ATP kinase assay in the presence or absence of Chk1 peptide 14. Figure 4.31A showed that Chk1 catalytic activity towards interleukin-1α was only slightly enhanced in the presence of activating peptide (compare lane 2 and 3). In contrast to the Pepchip microarray data, no detectable [γ^{32}P] incorporation into STAT1 was observed despite the stimulation of Chk1 by activating peptide (Figure 4.31B; lane 2 and 3). The data indicated that Chk1, whether allosterically activated or not, is not active towards human STAT1 protein. In contrast, human interleukin-1α could represent a potential novel substrate for Chk1.

4.3 Discussion

4.3.1 An allosteric activating motif is located within the αF region of Chk1 N-terminal kinase domain

It was hypothesised that p21 or p21 peptide 4 would act as a competitive inhibitor to disrupt intramolecular binding of Chk1 C-terminal regulatory domain to a pseudo-docking site in the Chk1 N-terminal kinase domain (Figure 4.1). To test this, sequence alignment showed that the αF region of the Chk1 N-terminal kinase domain shared sequence similarity to stimulatory p21 peptide 4. Furthermore, Chk1 αF region is conserved across species, suggesting that this region might be important for the regulation of Chk1 activity (Figure 4.2). Kinase assays with peptides spanning across the whole length of Chk1 showed that only peptidomimetic ligands based on the αF region (Chk1 peptide 14 and 32) were able to stimulate Chk1 activity towards p21, whereas most of the peptides demonstrated a negligible or an inhibitory effect on Chk1 catalytic activity (Figure 4.3B). Kinase assays on Chk1 immunoprecipitated from HCT116 wild-type and HCT116 $p21^{-/-}$ cells also showed that cellular Chk1 can be modulated by p21 peptide 4 and Chk1 peptide 14 (Figures 4.8 and 4.9). An interest to note is that immunoprecipitated Chk1 from HCT116 $p21^{-/-}$ cells were stimulated better by the activating peptides compared to immunoprecipitated Chk1 from HCT116 wild-type cells (Figures 4.8 and 4.9). Furthermore, the IP-kinase assay also detected the presence of an unknown phospho-protein from the HCT116 wild-type Chk1 immuno-complex but this was not detected from the HCT116 $p21^{-/-}$ immuno-complex (Figure 4.8 and 4.9). Therefore the data suggests that there may be a difference in the conformation, modification status or Chk1 interacting proteins in

HCT116 wild-type and HCT116 $p21^{-/-}$ cells. Tools such as mass spectrometry may be exploited to examine the differences of Chk1 modification status in +/- p21 background. In addition, it would be interesting to investigate the possibility that p21 might function as a regulatory molecule for Chk1 catalytic activity in vivo by transfecting p21 back into the HCT116 $p21^{-/-}$ cells.

Biochemical analysis has suggested that Chk1 autoinhibition is dependent on the association of the Chk1 C-terminal regulatory domain with its N-terminal kinase domain (Katsuragi and Sagata, 2004). In this study, I have demonstrated that this could occur through the αF region in the N-terminal kinase domain forming a crucial intramolecular binding interface with the C-terminal regulatory domain. Chk1 peptide 14 based on the Chk1 αF region is able to bind to Chk1 which is not dependent or influenced by ATP (Figure 4.18). This is in stark contrast to p21 peptide 4 binding to Chk1 which is ATP-dependent (Figure 3.16). Data has also showed that peptidomimetic ligands based on the Chk1 αF region are able to disrupt intramolecular interaction between the Chk1 C-terminal domain and its N-terminal domain (Figure 4.20). This most likely results in the displacement of the inhibitory C-terminal domain from the kinase domain, leading to increased Chk1 catalytic activity.

4.3.2 Differential activity of Chk1 mutant proteins

To further characterise the effects of Chk1 peptide 14, two Chk1 mutants were synthesised (Figure 4.11):

1. **Chk1 (Ser→Ala$^{317/345}$)** where the ATR phosphorylation sites were mutated to alanine residues.
2. **Chk1 ΔC70** where the last 70 amino acids of the C-terminal regulatory domain were deleted.

Kinase assays confirmed that Chk1 ΔC70 exhibited higher catalytic activity (approximately two-fold) than Chk1 wild-type protein (Figure 4.14) due to the loss or partial loss of autoinhibitory region, which is in line with reported observation (Katsuragi and Sagata, 2004). Autoinhibition often involves the presence of a pseudosubstrate domain located in the regulatory region. The above data suggested that a pseudosubstrate region might be located on the last 70 amino acids of Chk1. The pseudosubstrate region normally contains the substrate consensus sequence with a non-phosphorylatable residue in place of Ser/Thr residue. However sequence alignment of the p21 phosphorylation motif (alanine residue was in place of Ser^{146} residue) with full-length Chk1 has identified a potential pseudosubstrate region within the C-terminal domain (amino acids 371 to 381) but not within the last 70 amino acids (Figure 4.32). Interestingly, mutation of *Xenopus* Chk1 at Thr^{377} within the TRF motif led to enhanced catalytic activity (Wang and Dunphy, 2000) and this TRF motif is located within the potential pseudosubstrate region, suggesting that mutation of Thr^{377} might disrupt the intramolecular interaction between the potential pseudosubstrate region and the active site. Interestingly, the

TRF motif is conserved across the species of Chk1, implying that this motif may be important for Chk1 regulation. One possibility is that the last 70 amino acids are required to anchor the pseudosubstrate to the active site. The second possibility is that a pseudosubstrate region that does not conform to the Chk1 substrate consensus sequence resides within the last 70 amino acid. Therefore, more experiments are needed to confirm the presence of a pseudosubstrate region within Chk1 protein.

Although, Chk1 ΔC70 displayed a two-fold higher catalytic activity than Chk1 wild-type, kinetic analysis showed that Chk1 ΔC70 demonstrated about 2.5-fold lower K_{cat}/K_m than Chk1 wild-type. This illustrated that Chk1 ΔC70 was a less efficient enzyme than Chk1 wild-type in utilising p21 (Figure 4.15). This was due to an observed 5-fold higher K_m for Chk1 ΔC70 as compared to Chk1 wild-type. The high K_m value suggests that p21 could not docked properly to Chk1 ΔC70 and a crucial p21 docking groove was located along the last 70 amino acids. In the absence of a potential p21 docking groove, the substrate may diffuse away easily before they get phosphorylated by Chk1, thus leading to the higher K_m.

Chk1 activation induced by DNA damage has been reported to involve ATR-mediated phosphorylation at Ser^{317} and Ser^{345} and these phosphorylations are thought to enhance catalytic activity (Zhao and Piwnica-Worms, 2001). However, in our assays, the Chk1 (Ser→$Ala^{317/345}$) mutant demonstrated similar catalytic activity to Chk1 wild-type, suggesting that phosphorylation at the ATR sites does not confer higher catalytic activity (Figure 4.14). It is also possible that only 1% of

the Chk1 WT protein population was phosphorylated ATR sites, therefore leading to minimal differences in activity between Chk1 WT and Chk1 (Ser→Ala$^{317/345}$). Gel filtration analysis by Zhao and Piwnica-Worms, 2001, showed that overexpression of Chk1 phosphorylated at Ser^{317} and Ser^{345} in HeLa cells eluted at higher molecular weight and had a higher catalytic activity, with Chk1 (Ser→Ala$^{317/345}$) mutant which eluted at lower molecular weight exhibiting poor catalytic activity. This may suggest that phosphorylation at Chk1 Ser^{317} and Ser^{345} per se does not confer enhanced catalytic activity but may result in association with cellular activator molecule which leads to higher kinase activity.

4.3.3 Chk1 ΔC70 mutant protein was refractory to the stimulating effects of the activating peptides

The Chk1 kinase assays with activating peptides showed that Chk1 (Ser→Ala$^{317/345}$) catalytic activity can be stimulated by p21 peptide 4 and Chk1 peptide 14, albeit with a slightly lower activating effect as compared to Chk1 wild-type protein (Figure 4.16). Interestingly, Chk1 ΔC70 was refractory to the effect of the activating peptides. This data suggests that the last 70 amino acids can form a docking groove for the activating peptides which explains the loss of peptide-activating effect on Chk1 ΔC70. However, peptide-binding assay using non-denaturing gel electrophoresis showed that the p21 peptide 4 was capable of associating with Chk1 ΔC70 in an ATP-dependent manner (Figure 4.18B), suggesting that loss of the last 70 amino acids was not crucial to activating peptides docking but was crucial to the activating peptide-mediated allosteric

stimulation. Using the chick Chk1 system in collaboration with Prof Gillespie group, a domain comprising the last 70 amino acids was not able to initiate intramolecular interaction with Chk1 N-terminal kinase domain (MT Scott, personal communication); however, a full complement of the Chk1 C-terminal domain was able to intramolecularly interact with the Chk1 N-terminal domain (Figure 4.20A). Furthermore, addition of the activating peptides was able to disrupt the intramolecular interaction (Figure 4.20A), leading to enhanced Chk1 catalytic activity (Figure 4.20B). The above data suggested that the activating peptides could bind to a region outwith the last 70 amino acids of the Chk1 C-terminal domain (C70) and possibly allosterically displace C70 from the Chk1 kinase domain through conformational change and/or modifications. Preliminary data have showed that a Chk1 peptide corresponding to amino acids 406 to 420 within C70 was autophosphorylated by Chk1 itself (Figure 4.33A). Mass spectrometry has indicated that Chk1 Ser^{407} is the major phospho-acceptor site (Figure 4.33B). Therefore it is possible that post-translational modification of Chk1 Ser^{407} is required to stabilise Chk1 C70 displacement from the kinase domain.

Data has showed that p21 peptide 4 stimulated recombinant Chk1 catalytic activity better than Chk1 peptide 14 (Figure 4.16). This is in stark contrast to the data obtained for cellular Chk1 where Chk1 peptide 14 stimulated Chk1 catalytic activity better than p21 peptide 4 (Figures 4.8 and 4.9). One explanation for this discrepancy is that cellular Chk1 protein is in complex with additional co-factors or regulatory proteins that results in better activation by Chk1 peptide 14 than p21

peptide 4 or that the post-translational modification status of cellular Chk1 differs from the insect cell expressed protein. Kinetic analysis indicated that recombinant human Chk1 was a far more efficient enzyme in the presence of p21 peptide 4 due to a lower K_m value (Figure 4.17). Surprisingly, Chk1 was less efficient enzymatically when incubated with Chk1 peptide 14 due to a low K_m value (Figure 4.17). The reason for this is not clear. To elucidate the effects of activating ligands on Chk1 structural conformation and dynamics, biophysical experiments such as NMR spectroscopy would be needed.

4.3.4 Mutation at conserved tryptophan residues within the Chk1 N-terminal αF region destabilised Chk1 kinase domain structure

Ligands based on Chk1 N-terminal α-F region were able to stimulate Chk1 activity but were ineffective towards Chk1 ΔC70. One possible mechanism is that Chk1 αF region forms a binding interface with the C-terminal domain and sterically blocks substrate access to the active site through the action of the last 70 amino acids of the C-terminal domain. Ligands based on the α-F region were able to compete for the intramolecular binding interface, thus removing the steric block on the active site, leading to enhanced catalytic activity. To test that the αF region is involved in an intramolecular binding interface, two conserved tryptophan residues (Trp^{192} and Trp^{208}) were mutated to alanine residues. The two tryptophan residues were chosen because they are conserved throughout the species of Chk1 (Figure 4.21A) and furthermore alanine mutation of Trp^{65} within the p21 peptide 4, which was shown to align to Chk1 Trp^{208}, attenuate Chk1 stimulation (Figures

3.20 and 4.2). Recombinant Chk1 (Trp→Ala$^{192/208}$) mutant protein was shown to be susceptible to C-terminal cleavage in the *Sf9* insect cells system and a small population of the full length mutant was found to associate with the cleaved protein (Figure 4.22 and 4.23).

Immunoprecipitated exogenous V5-Chk1 (Trp→Ala$^{192/208}$) mutant from HCT116 wild-type cells revealed that the Chk1 (Trp→Ala$^{192/208}$) mutant protein could retain intrinsic catalytic activity but was refractory to the stimulating effect of the activating peptides (Figures 4.24 and 4.25). The crystal structure of Chk1 kinase domain revealed that the invariant PW residues (Pro^{207}/Trp^{208} and Pro^{230}/Trp^{231}) form van der Waals contact with the hydrophobic core of the kinase domain C-terminal lobe, which could stabilise the hydrophobic pocket important for substrate interaction (Chen et al., 2000). Perhaps by mutating Trp^{208}→Ala^{208}, the integrity of Chk1 kinase domain structure is greatly destabilised. This could be the reason why insect cell-expressed Chk1 (Trp→Ala$^{192/208}$) was susceptible to cleavage. Destabilisation of the Chk1 (Trp→Ala$^{192/208}$) mutant protein also means that the activating peptides have little effect on Chk1 (Trp→Ala$^{192/208}$) catalytic activity in our assays. Therefore it is difficult to assess whether the Chk1 αF region, particularly Trp^{192} and Trp^{208} is critical to intramolecular interaction between the Chk1 C-terminal domain and its N-terminal domain. Perhaps the best way forward is to make single alanine mutation across the conserved residues in the Chk1 αF region and biochemically assess its effect on catalytic activity.

4.3.5 Allosteric activation resulted in Chk1 substrate specificity change

The presence of a consensus phosphorylation site in a protein does not ensure that the protein is a substrate *in vivo*. Furthermore, authentic phosphorylation sites do not always fit with the consensus sequence, suggesting that allosteric regulation is often involved in substrate recognition (Ubersax et al., 2003). Indeed allosteric docking by peptidomimetic ligand has been shown to induce conformational changes in the p38 protein kinase active site (Chang et al., 2002). To assess whether Chk1 substrate recognition can be altered by allosteric activation and loss of the autoinhibitory region (Chk1 ΔC70), PepChip microarray analysis was performed with Chk1 wild-type protein +/- activating Chk1 peptide 14 or Chk1 ΔC70. The data showed that 18 peptide substrates were phosphorylated by all three forms of Chk1. Sequences of these common substrate peptides were fed into Weblogo program (University of California, Berkeley) to generate consensus logo which revealed that Chk1 had a strong preference for arginine residue in the P-3 position (Figure 4.34A), that is in line with the published data (O'Neill et al., 2002).

It was further shown that allosterically activated Chk1 was able to phosphorylate 34 peptide substrates not recognised by Chk1 wild-type protein in the absence of Chk1 peptide 14 (Appendix 1). The consensus sequence of these peptide substrates revealed that allosterically activated Chk1 had less preference for the arginine residue in P-3 position and it was able to phosphorylate tyrosine residue in addition to serine and threonine residues (Figure 4.34B). Determination of substrate motifs for Chk1 by oriented-peptide library approach showed that Chk1

preferentially phosphorylated tyrosine over serine and threonine residues (O'Neill et al., 2002). Furthermore, analysis of yeast protein kinases showed several examples of Ser/Thr kinases that can phosphorylated tyrosine residue to some extent (Zhu et al., 2000).

There were no peptide substrate phosphorylated exclusively by Chk1 ΔC70, however it shared 10 common peptide substrates with allosterically activated Chk1. The consensus sequence of these 10 common peptide substrates showed that Chk1 ΔC70 protein also had less preference for the arginine residue in P-3 position (Figure 4.34C). Therefore, the data suggested that loss of the autoinhibitory region (Chk1 ΔC70) and allosteric activation of Chk1 (Chk1 stimulated by Chk1 peptide 14) can lead to change in substrate specificity, allowing Chk1 to target substrates that do not fit with Chk1 consensus substrate specificity. This was confirmed in Figure 4.29 where allosterically activated Chk1 was active towards peptides 1 to 10 and 13 which lack the arginine residue at P-3 position, although the presence of arginine residue at P-3 position (peptide 11 and 12) mediated better peptide substrates utilisation by allosterically activated Chk1. Modelling study of Chk1 with peptide substrate revealed that Chk1 also preferred a hydrophobic amino residue at P+1 position (Chen et al., 2000). This might explained the 2-fold increase of [γ^{32}P] incorporation into peptide 12 which has a hydrophobic phenylalanine residue at P+1 position as compared to peptide 11.

Overall, the data showed that allosteric stimulation may change Chk1 substrate specificity towards non-consensus sequence. Although Chk1 ΔC70 and peptide-

stimulated Chk1 has similar effect, allosteric activation and deletion of the regulatory domain are not equivalent suggesting that Chk1 ΔC70 is not in an active conformation. Physiologically, this could suggest that although Chk1 has a strong preference for substrates with a –Rxx(S/T)- motif, allosteric stimulation may change Chk1 substrate specificity towards non-consensus sequence, thus widening the pool of physiological substrates. In addition, we could also potentially activate Chk1 activity towards a certain biochemical pathway by a specific allosteric peptide.

4.3.6 Additional determinant(s) needed for Chk1 substrate recognition

In the PepChip microarray, human STAT1 peptide (KGTGYIKTE) was found to be phosphorylated only by stimulated Chk1 in the presence of Chk1 peptide 14 (Appendix 1). To test for this, human STAT1 protein was assembled with Chk1 wild-type protein kinase for [γ^{32}P]-ATP kinase assay in the presence or absence of Chk1 peptide 14. However, the autoradiography only showed [γ^{32}P] incorporation into Chk1 and no detectable [γ^{32}P] incorporation into STAT1 (Figures 4.30B and 4.31B). This suggested that Chk1 protein kinase is not active towards human STAT1 protein, even under stimulating conditions. In contrast, mouse interleukin-1α peptide (KRRLSFSET) was determined to be phosphorylated by Chk1 protein kinase in PepChip microarray (Appendix 1). Further [γ^{32}P]-ATP kinase assays showed [γ^{32}P] incorporation into the human form of interleukin-1α protein (Figures 4.30A and 4.31B), suggesting that human interleukin-1α could form as a novel *in vitro* Chk1 substrate. Although the human interleukin-1α contains a

slightly different phosphorylation motif (KRRLSLSQS) from the mouse interleukin-1α peptide (KRRLSFSET), the Chk1 consensus substrate sequence (RxxS/T) is represented in both forms of interleukin-1α. In contrast, four Rxx(S/T) phosphorylation motifs are found in human STAT1, however, [γ^{32}P]-ATP kinase assays showed that human STAT1 protein was not phosphorylated by Chk1. This could suggest that either the human STAT1 Rxx(S/T) motifs are not exposed to Chk1 or that the Rxx(S/T) motif is not the sole requirement for Chk1 substrate recognition and other determinant such as a distinct docking/allosteric site is needed.

4.4 Conclusions

In this chapter, I have showed that Chk1 also contains an allosteric signal (Chk1 peptide 14) within the N-terminal αF region which shared sequence similarity with activating p21 peptide 4. These activating peptides (p21 peptide 4 and Chk1 peptide 14) could modulate the activity of recombinant human and chick Chk1 and cellular Chk1 by disrupting the intramolecular interaction between the Chk1 C-terminal domain and N-terminal domain. However recombinant human insect cell-expressed Chk1 ΔC70 mutant protein (deletion of the last 70 amino acids of Chk1 C-terminal domain) which retained binding to p21 peptide 4 proved to be refractory to the stimulating effects of the activating peptides. It was shown that additional determinant(s) other than a consensus substrate sequence is required for Chk1 substrate recognition and indeed allosteric activation of Chk1 could result in phosphorylation of non-consensus substrate specificity. Mutation of conserved

$Trp^{192/208}$ destabilises Chk1 conformation, leading to cleavage susceptibility. Furthermore, the activating peptides failed to stimulate Chk1 ($Trp \rightarrow Ala^{192/208}$) mutant protein activity.

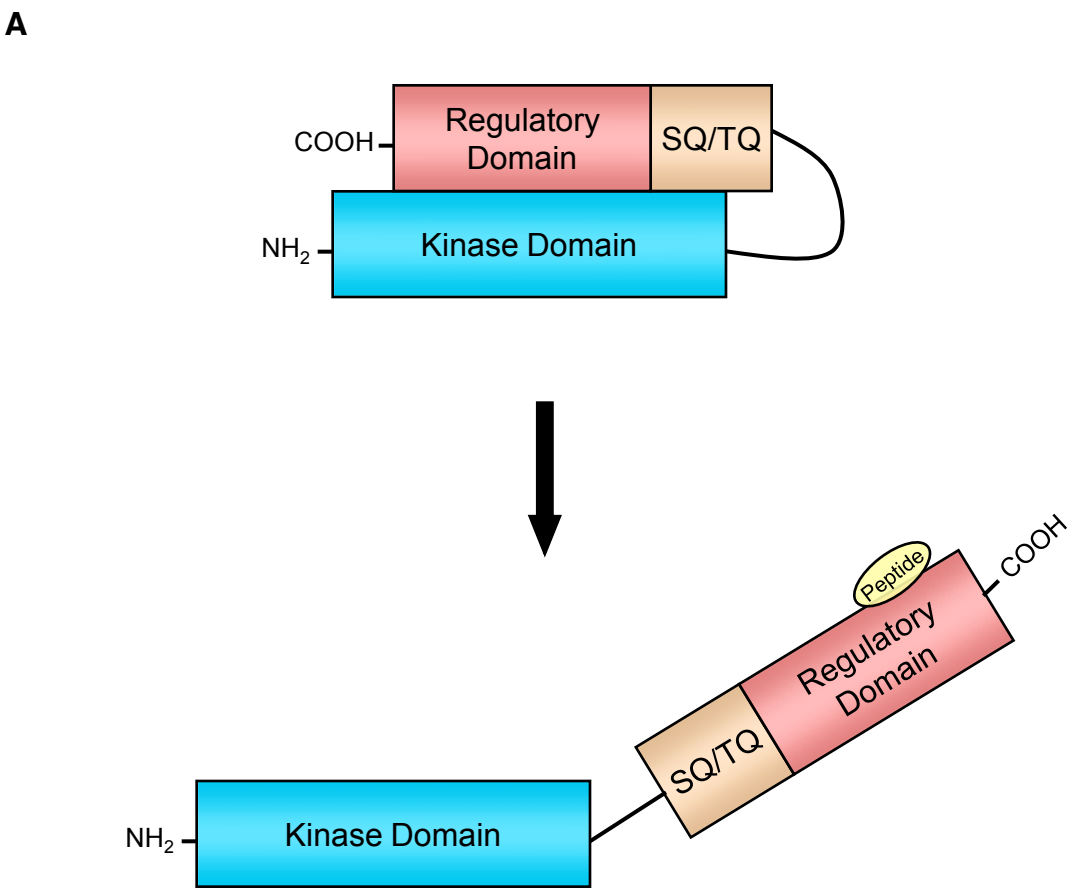

Figure 4.1 A simple illustration of p21 peptide 4-dependent allosteric stimulation of Chk1.

(A) This hypothetical model shows that Chk1 protein kinase adopts a 'closed' conformation for autoinhibition of catalytic activity. Allosteric activation by p21 peptide 4 prevents autoinhibition by stimulating Chk1 to adopt an 'open' conformation.

A

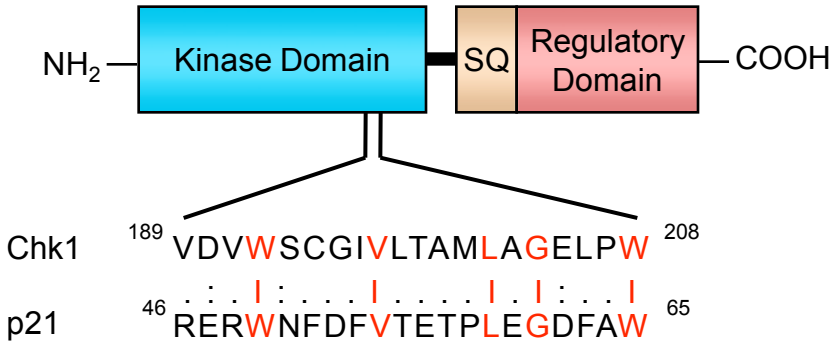

B

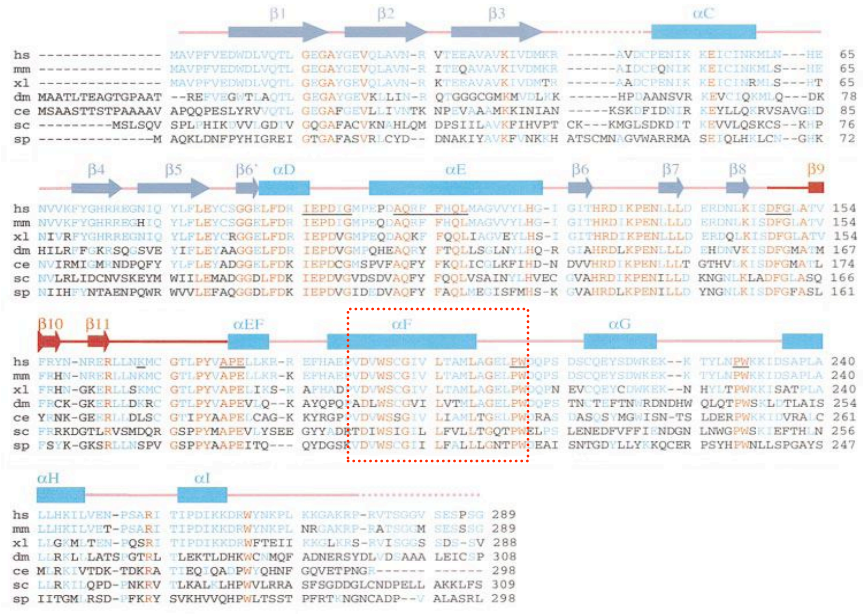

Figure 4.2 Shared homology of p21 docking peptide with Chk1 N-terminal region.
(A) A schematic diagram of Chk1 structure. p21 peptide 4 sequence was aligned to a sub-region spanning amino acids 189 to 208 within Chk1 N-terminal kinase domain using EMBOSS Pairwise Alignment Algorithms. SQ represents the ATR phosphorylation motif (SQ). (B) ClustalW sequence alignment of Chk1 kinase domains of human (hs), mouse (mm), *Xenopus* (xl), *Drosophila* (dm), *C. elegans* (ce), *S. cerevisiae* (sc) and *S. pombe* (sp). Secondary structural elements of human Chk1 are shown above the alignment. The numbers of amino acids are shown on the right. Invariant residues of Chk1 among these species are in red and human Chk1 residues that are also conserved in other species are in cyan. The shared homology region with p21 docking peptide is boxed within red dotted line. This diagram is adapted from *Chen et al., 2000*.

A

Chk1 peptide sequences

1	^{1}MAVPFVEDWDLVQTLGEGAY^{20}	17	^{241}LLHKILVENPSARITIPDIK^{260}
2	^{16}GEGAYGEVQLAVNRTEEAV^{35}	18	^{256}IPDIKKDRWYNKPLKKGAKR^{275}
3	^{31}TEEAVAVKIVDMKRAVDCPE^{50}	19	^{271}KGAKRPRVTSGGVSESPSGF^{290}
4	^{46}VDCPENIKKEICINKMLNHE^{65}	20	^{286}SPSGFSKHIQSNLDFSPVNS^{305}
5	^{61}MLNHENVVKFYGHRREGNIQ^{80}	21	^{301}SPVNSASSEENVKYSSSQPE^{320}
6	^{76}EGNIQYLFLEYCSGGELFDR^{95}	22	^{316}SSQPEPRTGLSLWDTSPSYI^{335}
7	^{91}ELFDRIEPDIGMPEPDAQRF^{110}	23	^{331}SPSYIDKLVQGISFSQPTCP^{350}
8	^{106}DAQRFFHQLMAGVVYLHGIG^{125}	24	^{346}QPTCPDHMLLNSQLLGTPGS^{365}
9	^{121}LHGIGITHRDIKPENLLLDE^{140}	25	^{361}GTPGSSQNPWQRLVKRMTRF^{380}
10	^{136}LLLDERDNLKISDFGLATVF^{155}	26	^{376}RMTRFFTKLDADKSYQCLKE^{395}
11	^{151}LATVFRYNNRERLLNKMCGT^{170}	27	^{391}QCLKETCEKLGYQWKKSCMN^{410}
12	^{166}KMCGTLPYVAPELLKRREFH^{185}	28	^{406}KSCMNQVTISTTDRRNNKLI^{425}
13	^{181}RREFHAEPVDVWSCGIVLTA^{200}	29	^{426}FKVNLLEMDDKILVDFRLSK^{445}
14	^{196}IVLTAMLAGELPWDQPSDSC^{215}	30	^{441}FRLSKGDGLEFKRHFLKIKG^{460}
15	^{211}PSDSCQEYSDWKEKKTYLNP^{230}	31	^{457}KIKGKLIDIVSSQKVWLPAT^{476}
16	^{226}TYLNPWKKIDSAPLALLHKI^{245}	32	^{191}VWSCGIVLTAMLAGELPWDQ^{210}

B

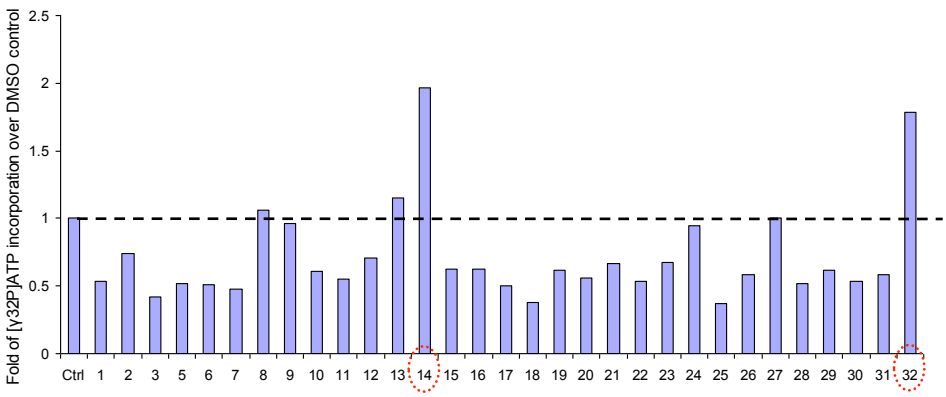

Figure 4.3 Recombinant human Chk1 activity towards recombinant human p21 can be stimulated by N-terminal Chk1 peptide.

(A) Biotinylated overlapping Chk1 20-mer peptides with SGSG spacing were resuspended in DMSO. (B) Kinase reactions containing 60 ng of Chk1, 1 µg of p21, 1 mM of indicated Chk1 peptides in the presence of [γ^{32}P]ATP were assembled. DMSO was used as a control in the absence of Chk1 peptides. The reaction products were resolved in 12% SDS-PAGE and [γ^{32}P] incorporation into p21 was quantified by phosphorimager and normalised to DMSO control.

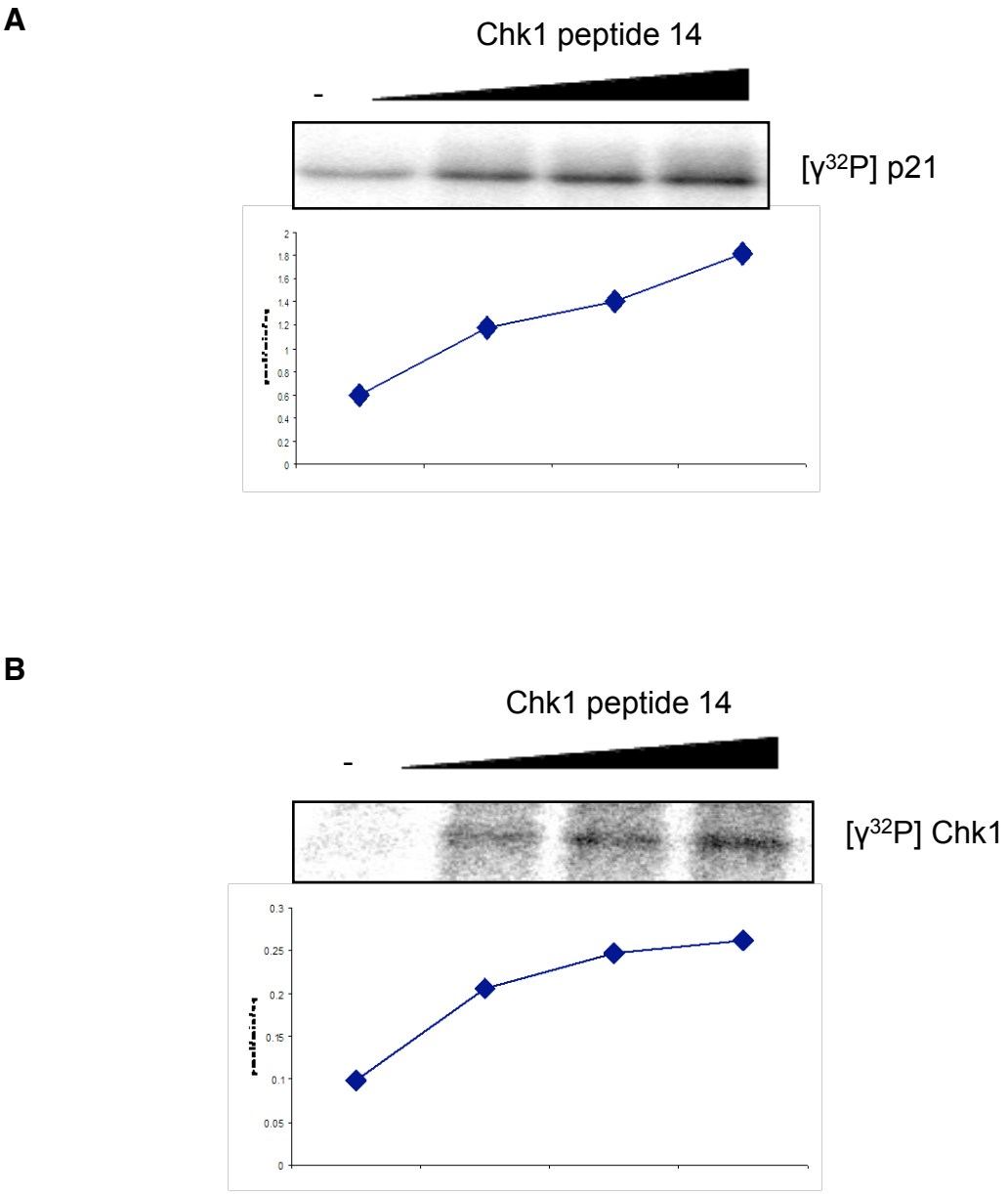

Figure 4.4 Recombinant human Chk1 activity towards recombinant human p21 is stimulated by Chk1 peptide 14.

(A) Kinase reactions containing 100 ng of Chk1, 1 µg of p21 and titration of Chk1 peptide 14 (0.625 µg to 2.5 µg) were assembled in the presence of [γ^{32}P]ATP. The reaction products were resolved in 12% SDS-PAGE. [γ^{32}P] incorporation into p21 was visualised by autoradiography and quantified by phosphorimager. (B) Kinase reactions containing 100ng of Chk1 and titration of Chk1 peptide 14 (0.625 µg to 2.5 µg) were assembled in the presence of [γ^{32}P]ATP. The reaction products were resolved by 10% SDS-PAGE. [γ^{32}P] incorporation into Chk1 was visualised by autoradiography and quantified by phosphorimager.

A

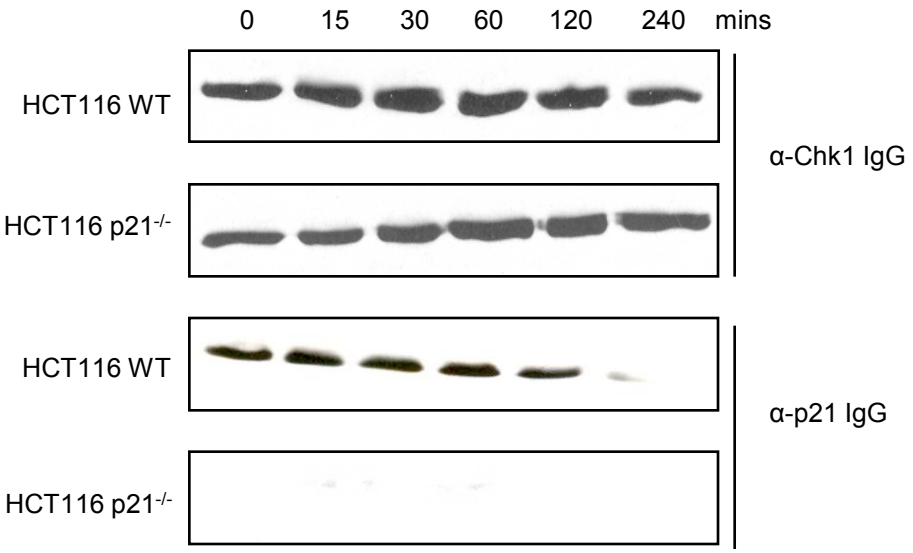

Figure 4.5 p21 status of HCT116 cell line does not affect the half-life of endogenous Chk1.

(A) HCT116 WT and HCT116 $p21^{-/-}$ cells were grown to >90% confluency before treated with 30 μg/ml of cycloheximide. The cells were harvested at the indicated time point and 0 min refers to untreated cells. 50 μg of whole cell lysates were resolved by 10% or 12% SDS-PAGE before transferred to nitrocellulose membranes. Chk1 protein was detected using mouse α-Chk1 IgG and p21 protein was detected with mouse α-p21 IgG.

A

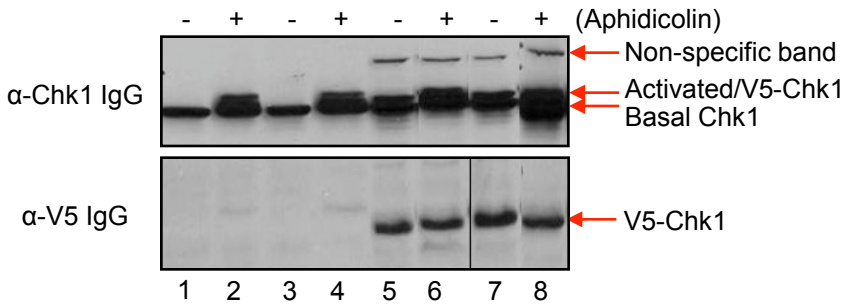

Lane	Cell line	Endogenous or V5-Chk1	Aphidicolin treatment
1	HCT116 wild type	Endogenous	-
2	HCT116 wild type	Endogenous	+
3	HCT116 $p21^{-/-}$	Endogenous	-
4	HCT116 $p21^{-/-}$	Endogenous	+
5	HCT116 wild type	V5-Chk1 WT	-
6	HCT116 wild type	V5-Chk1 WT	+
7	HCT116 $p21^{-/-}$	V5-Chk1 WT	-
8	HCT116 $p21^{-/-}$	V5-Chk1 WT	+

Figure 4.6 Immunoblot of endogenous or exogenous Chk1 protein from HCT116 wild-type or $p21^{-/-}$ cells (+/- aphidicolin treatment).

(A) HCT116 WT and HCT116 $p21^{-/-}$ cells were grown to >90% confluence before transfected with C-terminally V5-tagged Chk1 wild-type or mock-transfected with empty vector. After 24 hrs, the cells were either treated with 20 μM aphidicolin or ethanol as control for 4 hrs. The cells were harvested and 50 μg of whole cell lysates were resolved by 10% SDS-PAGE before transferred to nitrocellulose membranes. Chk1 protein was detected using mouse α-Chk1 IgG and exogenous V5-tagged Chk1 protein was detected using mouse α-V5 tag IgG.

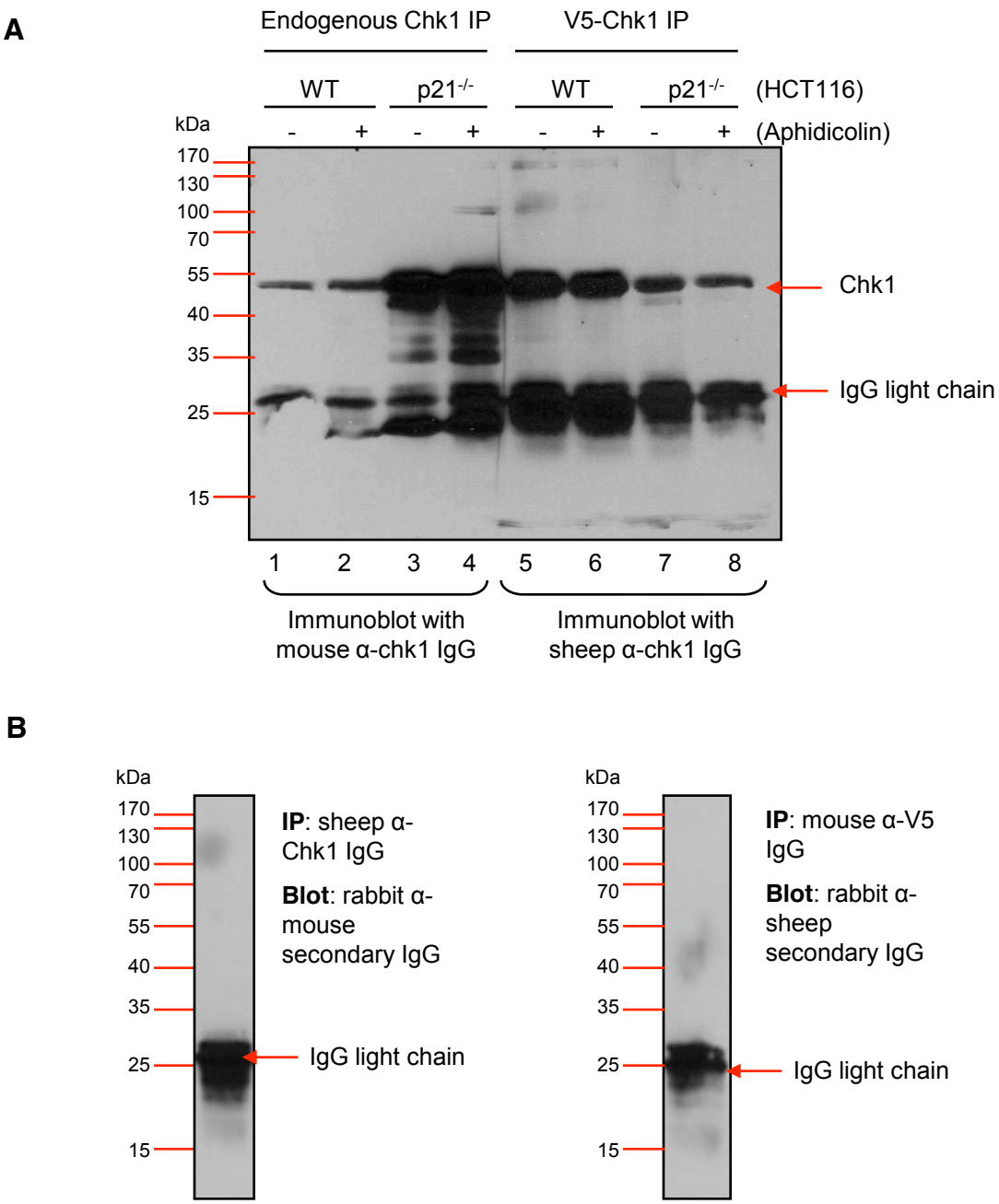

Figure 4.7 Immunoprecipitation of endogenous or exogenous Chk1 protein from HCT116 wild-type and HCT116 p21$^{-/-}$ cells.

(A) HCT116 WT and HCT116 p21$^{-/-}$ cells were grown to >90% confluency before transfected with C-terminally V5-tagged Chk1 wild-type or mock-transfected with empty vector. After 24 hrs, the cells were either treated with 20 μM aphidicolin or ethanol for 4 hours. 1 mg of lysate was used for Chk1 immunoprecipitation using either sheep α-Chk1 IgG or mouse α-V5 tag IgG and Protein G sepharose beads. Unbound proteins were washed off before bound proteins were eluted off the IgG-beads with SDS-sample buffer. The immunoprecipitated proteins were resolved by 10% SDS-PAGE before transferred to nitrocellulose membrane. Chk1 protein was detected using either mouse α-Chk1 IgG or sheep α-Chk1 IgG. (B) HCT116 WT cells were transfected with C-terminally V5-tagged Chk1 wild-type or mock-transfected with empty vector. 1 mg of lysate was then used for Chk1 immunoprecipitation using either sheep α-Chk1 IgG or mouse α-V5 tag IgG and Protein G sepharose beads. The immunoprecipitated proteins were resolved by 10% SDS-PAGE before transferred to nitrocellulose membrane. Ig light chains and heavy chains were detected using rabbit α-mouse secondary IgG (left panel) or rabbit α-sheep secondary IgG (right panel).

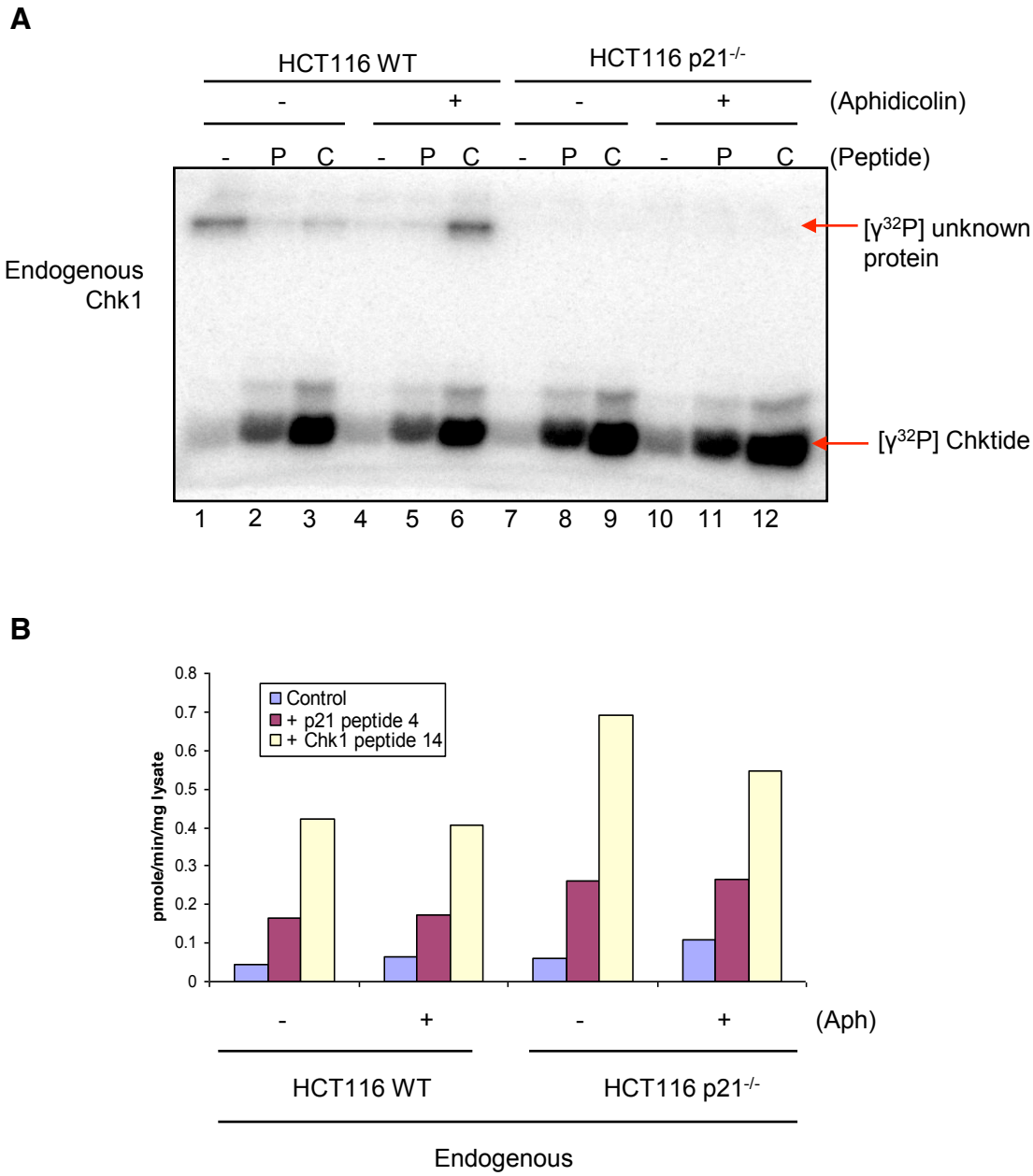

Figure 4.8 Immunoprecipitation-kinase assay of endogenous Chk1 proteins from HCT116 wild-type and HCT116 p21$^{-/-}$ cells.

(A and B) HCT116 WT and HCT116 p21$^{-/-}$ cells were grown to >90% confluency before mock-transfected with empty vector. After 24 hrs, the cells were either treated with 20 μM aphidicolin or ethanol for 4 hours. The cells were harvested and lysed. 1 mg of lysate was used for Chk1 immunoprecipitation-kinase using either sheep α-Chk1 IgG or mouse α-V5 tag IgG and Protein G sepharose beads. Unbound proteins were washed off. Kinase reactions containing 0.2 mM of Chktide with or without 5 μg of p21 peptide 4 (P) or Chk1 peptide 14 (C) in the presence of [γ^{32}P]-ATP were assembled with the immunoprecipitated sample. The reaction products were resolved by 15% SDS-PAGE. [γ^{32}P] incorporation into Chktide was visualised by autoradiography and quantified by phosphorimager.

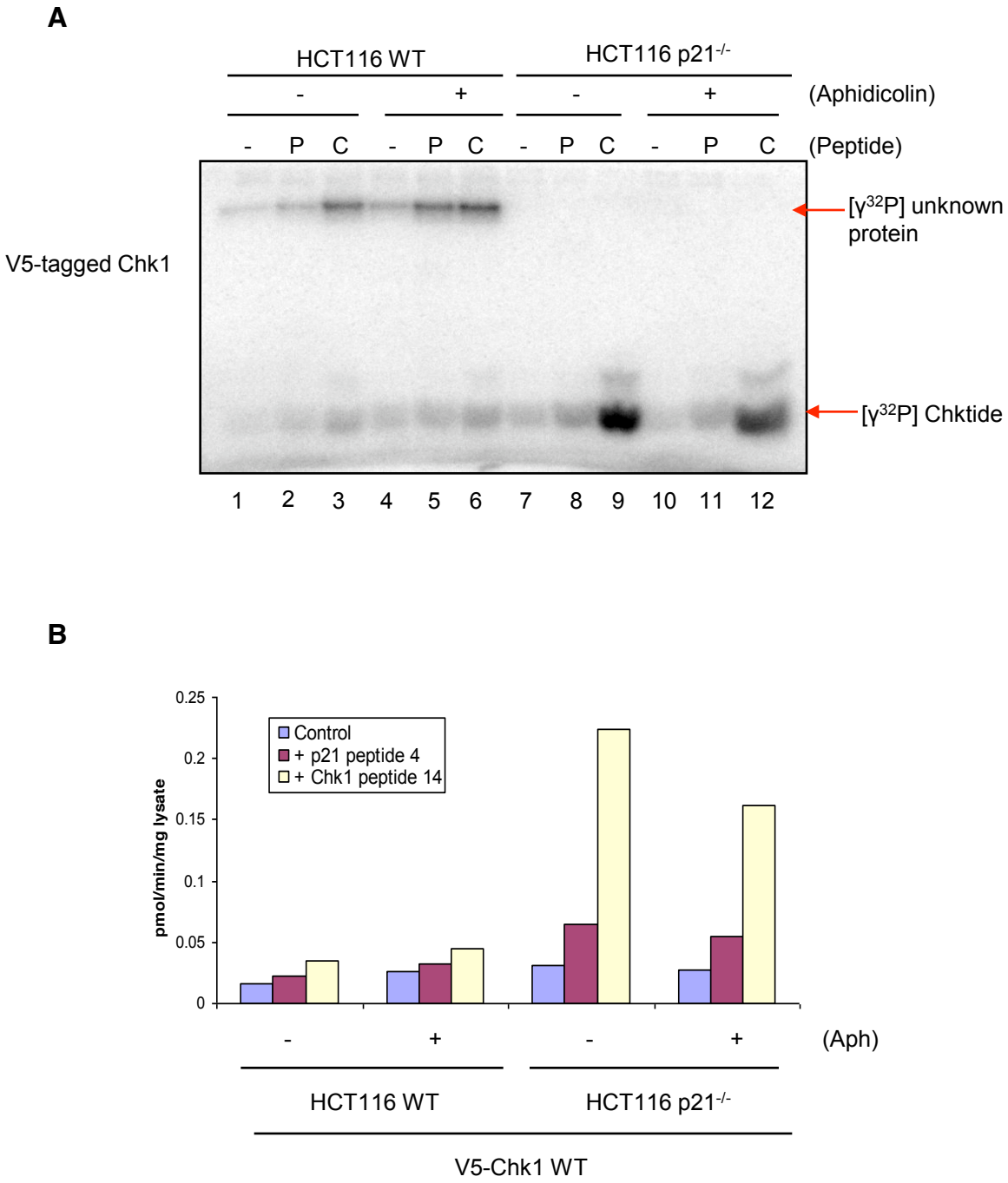

Figure 4.9 Immunoprecipitation-kinase assay of exogenous V5-Chk1 proteins from HCT116 wild-type and HCT116 p21$^{-/-}$ cells.

(A and B) HCT116 WT and HCT116 p21$^{-/-}$ cells were grown to >90% confluency before transfected with C-terminally V5-tagged Chk1 wild-type. After 24 hrs, the cells were either treated with 20 μM aphidicolin or ethanol for 4 hours. The cells were harvested and lysed. 1 mg of lysate was used for Chk1 immunoprecipitation-kinase using either sheep α-Chk1 IgG or mouse α-V5 tag IgG and Protein G sepharose beads. Unbound proteins were washed off. Kinase reactions containing 0.2 mM of Chktide with or without 5 μg of p21 peptide 4 (P) or Chk1 peptide 14 (C) in the presence of [γ^{32}P]-ATP were assembled with the immunoprecipitated sample. The reaction products were resolved by 15% SDS-PAGE. [γ^{32}P] incorporation into Chktide was visualised by autoradiography and quantified by phosphorimager.

A

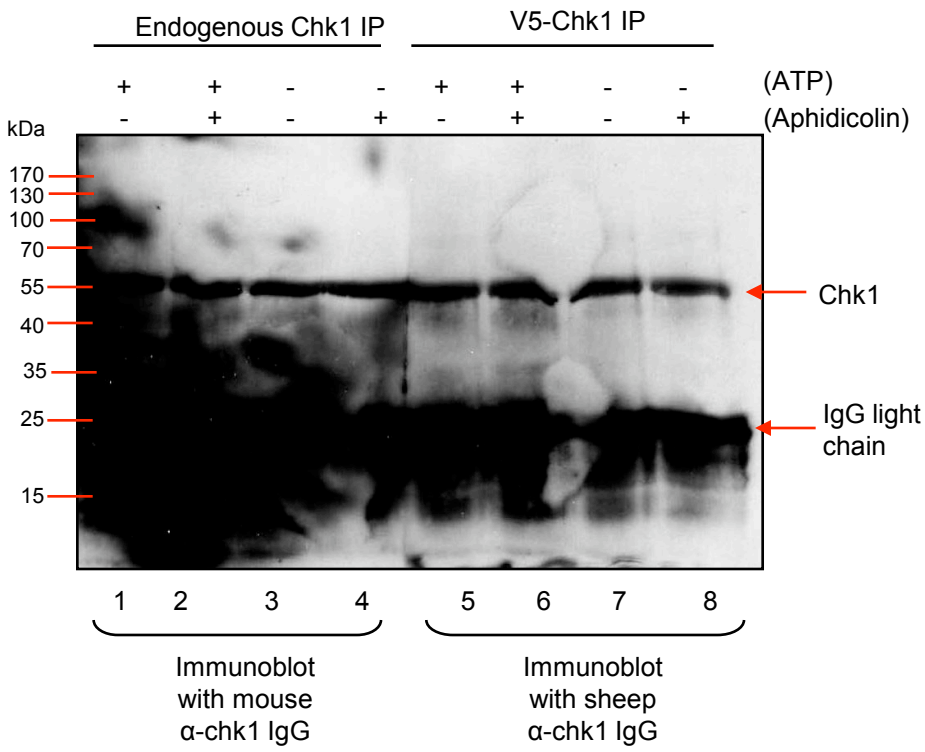

Figure 4.10 Chk1 autophosphorylation was not detected in HCT116 wild-type Chk1 IP-kinase assay.

(A) HCT116 WT cells were grown to >90% confluency before transfected with C-terminally V5-tagged Chk1 wild-type. After 24 hrs, the cells were either treated with 20 μM aphidicolin or ethanol for 4 hours. The cells were harvested and lysed. 1 mg of lysate was used for Chk1 immunoprecipitation using mouse α-V5 tag IgG and Protein G sepharose beads. Unbound proteins were washed off. Kinase reactions containing 0.2 mM of Chktide and unlabelled ATP were assembled with the immunoprecipitated sample. The reaction products were resolved by 10% SDS-PAGE before transferred to nitrocellulose membrane. Chk1 protein was detected using sheep α-Chk1 IgG.

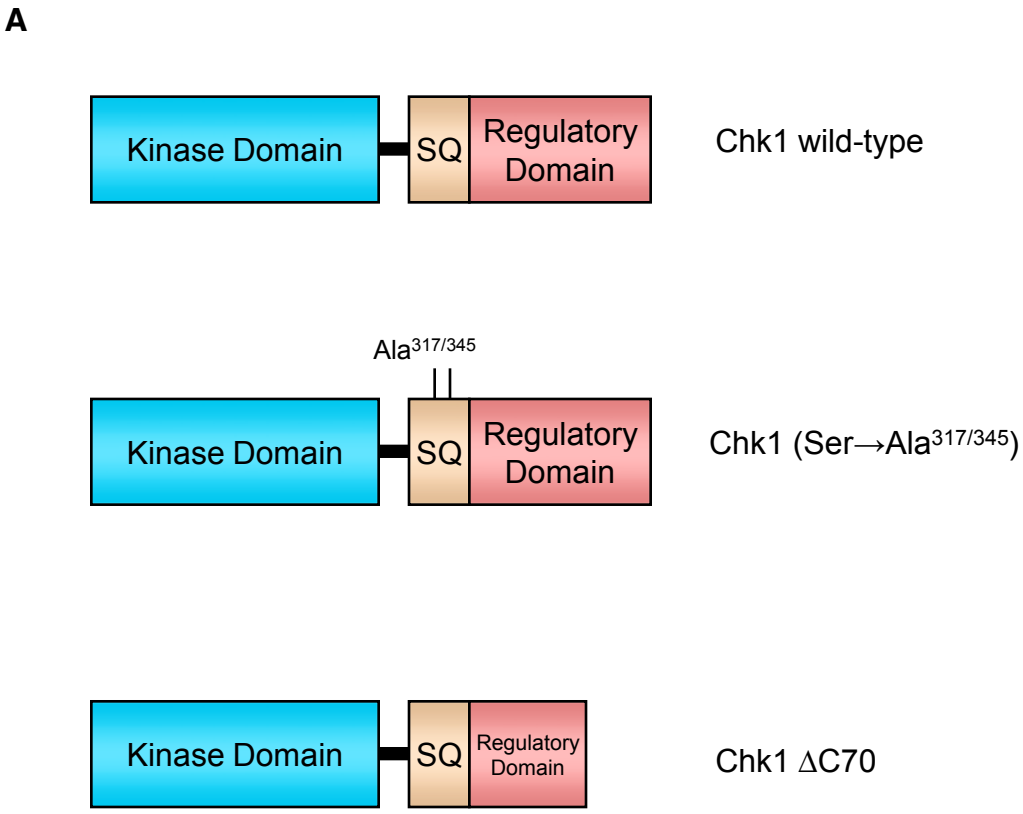

Figure 4.11 Schematic diagram of Chk1 wild-type and mutants.

(A) Schematic diagram of full-length Chk1 wild-type (WT), Chk1 (Ser→Ala$^{317/345}$) mutant and Chk1 ΔC70 mutant where the last 70 amino acids from the C-terminal end is deleted.

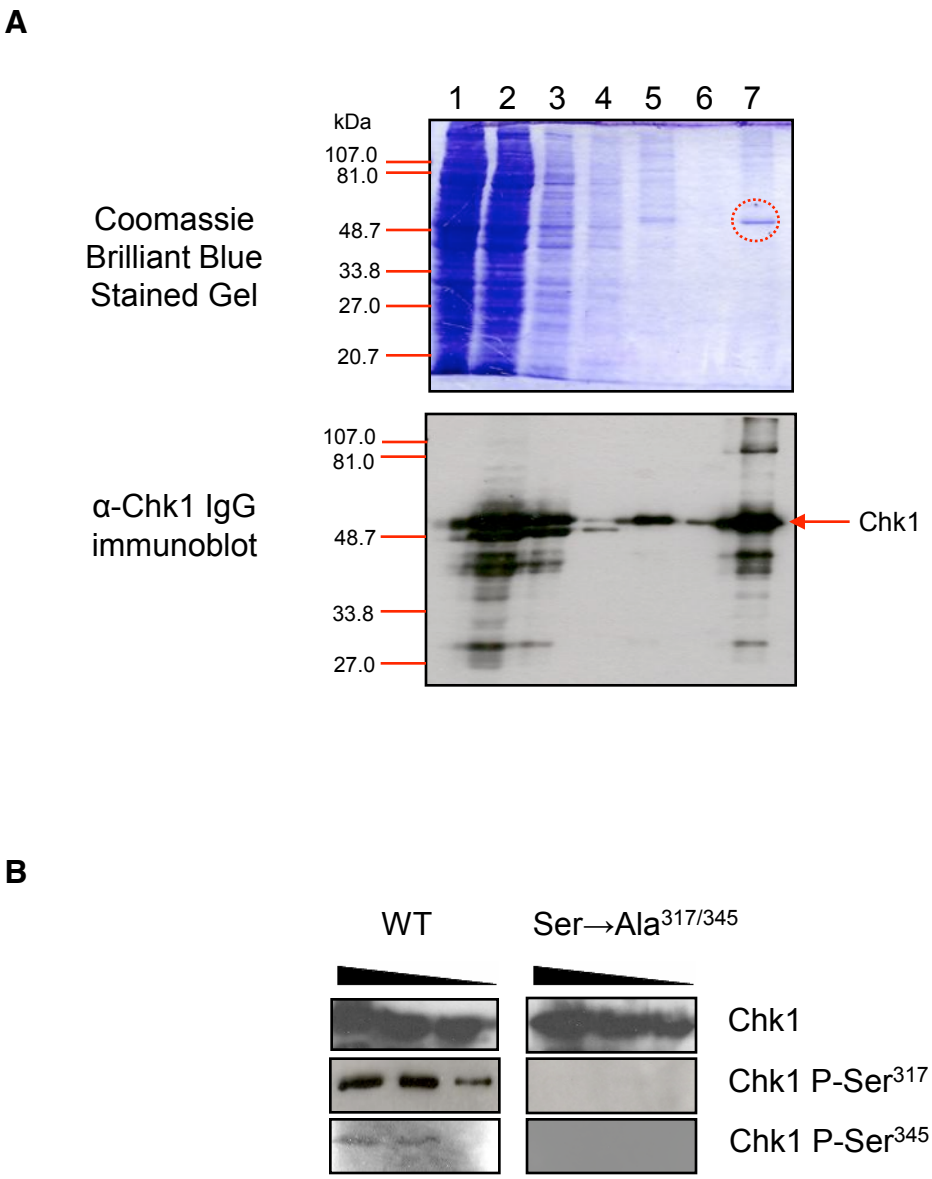

Figure 4.12 Purification of recombinant human insect-cell expressed Chk1 WT and mutants.

(A) His-tagged Chk1 wild-type (WT) and mutants were expressed in Sf9 insect cell system and purified from the Ni-NTA agarose column. Fractions from the Ni-NTA agarose column were analysed on a 10% SDS-PAGE gel stained by coomassie brilliant blue or subjected to α-Chk1 IgG immunoblot. Lanes: 1, uninfected cell lysate; 2, infected cell lysate; 3, Flow-through fraction; 4, Wash I fraction; 5, Wash II fraction; 6, Wash III fraction; 7, Eluted fraction. Dotted circle indicates Chk1 WT. (B) Immunoblot analysis of Sf9-expressed Chk1 WT and Chk1 (Ser→Ala$^{317/345}$) phosphorylation status. Titrating amounts of Chk1 were resolved in 10% SDS-PAGE and transferred to nitrocellulose. Phosphorylation was detected using α-Chk1 phospho-Ser^{317} IgG and α-Chk1 phospho-Ser^{345} IgG. Total Chk1 was detected using α-Chk1 IgG.

A

µl	0	0.2	0.5	1	2
Chk1 WT (R.L.U)	0.0905	30.725	57.93	71.48	101.3
Chk1 (Ser→Ala$^{317/345}$) (R.L.U)	0.0882	23.16	59.73	95.53	129.3
Chk1 ΔC70 (R.L.U)	0.0664	13.6	24.825	45.735	70.485

• 1 µl of Chk1 WT = 50 ng,

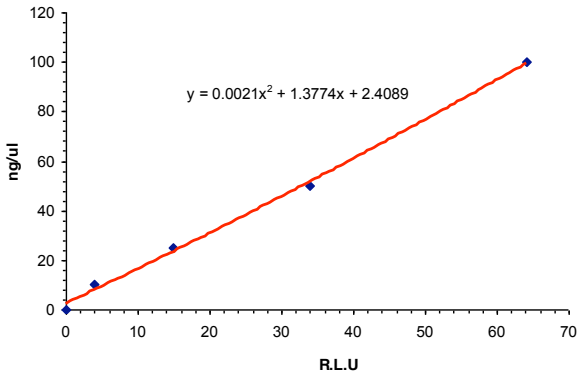

• Thus, using the equation,

95.53 (R.L.U) of Chk1 (Ser→Ala$^{317/345}$) = 153 ng

Figure 4.13 Normalisation of His-tagged full length Chk1 WT and Chk1 mutants.

(A) The concentration of His-tagged full length Chk1 WT and Chk1 mutants were normalised using the ELISA assay as described in the *Materials and Methods*. The relative light units values obtained for Kudos Chk1 WT were computed to construct a XY scatter plot. From the plot, an equation is derived and used to calculate the concentration for Chk1 WT and Chk1 mutants. Calculations were written above.

A

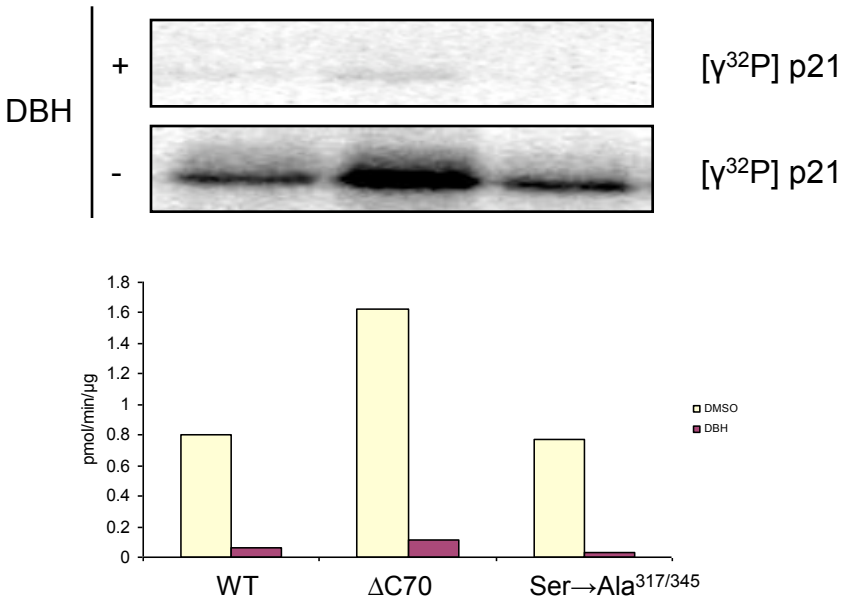

Figure 4.14 Recombinant human Chk1 kinase activity can be enhanced by a C-terminal 70 amino acid deletion but not affected by mutation at ATR phosphorylation sites.

(A) Kinase reactions containing 1 µg of p21 and [γ^{32}P]-ATP with or without 20 µM DBH were assembled in the presence of 100 ng of Chk1 WT or Chk1 (Ser→Ala$^{317/345}$) or Chk1 (ΔC70). DBH was dissolved in DMSO. The reaction products were resolved by 12% SDS-PAGE and [γ^{32}P] incorporation into p21 was visualised by autoradiography and quantified by phosphorimager.

A

Chk1 WT	K_m mM	V_{max} pCi/min/µg	K_{cat} min^{-1}	K_{cat}/K_m min^{-1}/mM^{-1}
Set 1	1.43	512.4	27884.30	19458.68
Set 2	1.82	457.6	24902.13	13659.97
Set 3	1.96	361.4	19667.03	10018.86
Average	1.74	443.80	24151.2	14379.2
Standard Deviation	0.27	76.44	4159.8	4760.8

Chk1 (Ser→$Ala^{317/345}$)	K_m mM	V_{max} pCi/min/µg	K_{cat} min^{-1}	K_{cat}/K_m min^{-1}/mM^{-1}
Set 1	1.88	450.1	24479.59	13048.82
Set 2	1.74	244.5	13297.62	7633.54
Set 3	1.45	228.0	12400.24	8557.79
Average	1.69	307.53	16725.8	9746.7
Standard Deviation	0.22	123.74	6729.9	2896.8

Chk1 ΔC70	K_m mM	V_{max} pCi/min/µg	K_{cat} min^{-1}	K_{cat}/K_m min^{-1}/mM^{-1}
Set 1	6.08	784.7	36355.15	5979.47
Set 2	10.10	823.6	38157.39	3777.96
Set 3	9.04	1713.0	79363.29	8775.24
Average	8.41	1107.10	51291.9	6177.6
Standard Deviation	2.08	525.09	24327.2	2504.5

Figure 4.15 Kinetic constants for recombinant human Chk1 wild-type and mutants with respect to recombinant human p21.

(A) Kinetics data of Chk1 WT and mutants. Kinase reaction containing Chk1 WT or mutants and full length p21 in the range of 0.28 µM to 8.83 µM were assembled in the presence of [γ^{32}P]ATP. The reaction products were resolved on 12% SDS-PAGE and [γ^{32}P] incorporation into p21 was quantified by phosphorimager. The Michaelis-Menten parameters were fitted via the Hanes plot using hyperbolic regression software (Hyper,version 1.1s, J. Easterby, University of Liverpool) and kinetic constants were calculated as the mean ± standard deviation.

A

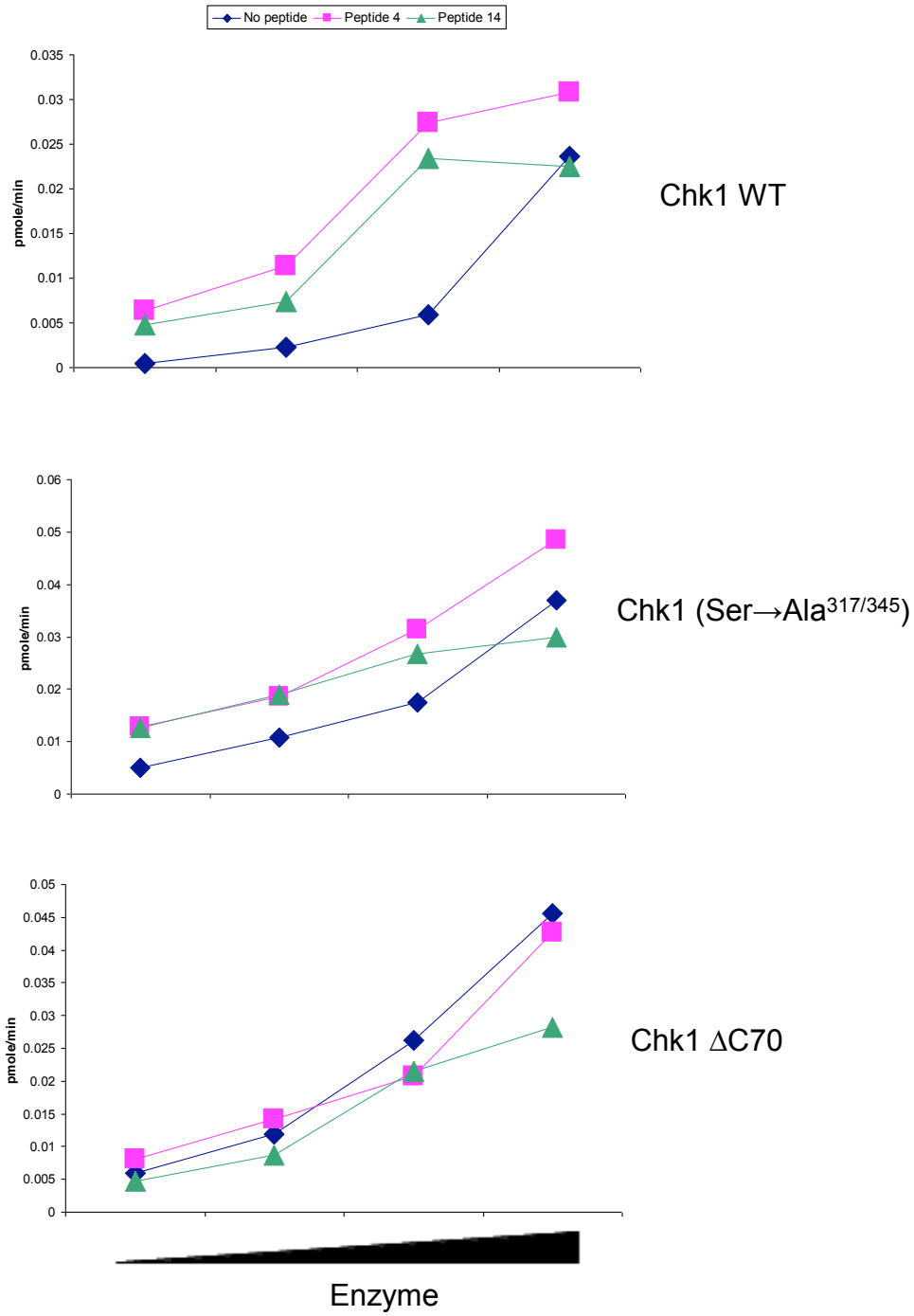

Figure 4.16 Recombinant human Chk1 ΔC70 is refractory to the effect of the activating peptides.

(A) Kinase reactions containing 1 µg of p21 and titration of Chk1 WT or mutants (Ser→Ala$^{317/345}$ or ΔC70) (12 to 120 ng) with or without 5 µg of p21 peptide 4 or Chk1 peptide 4 were assembled. The reaction products were resolved in 12% SDS-PAGE and [γ^{32}P] incorporation into p21 was quantified by phosphorimager.

A

Chk1	K_m mM	V_{max} pCi/min/µg	K_{cat} min^{-1}	K_{cat}/K_m min^{-1}/mM^{-1}
Set 1	3.13	338.50	18416.76	5876.44
Set 2	3.29	225.80	13917.30	4228.90
Set 3	3.12	328.10	17850.92	5723.28
Set 4	2.69	674.80	36713.82	13668.59
Average	3.06	399.30	21721.70	7374.30
Standard Deviation	0.26	187.31	10191.14	4261.50

Chk1 + Chk1 peptide 14	K_m mM	V_{max} pCi/min/µg	K_{cat} min^{-1}	K_{cat}/K_m min^{-1}/mM^{-1}
Set 1	5.00	212.70	11572.36	2315.86
Set 2	5.67	470.80	25614.80	4517.40
Set 3	4.92	917.30	49907.51	10154.12
Average	5.19	533.60	29031.56	5662.79
Standard Deviation	0.41	356.47	19394.63	4042.50

Chk1 + p21 peptide 4	K_m mM	V_{max} pCi/min/µg	K_{cat} min^{-1}	K_{cat}/K_m min^{-1}/mM^{-1}
Set 1	0.75	196.20	10674.65	14215.80
Set 2	1.54	215.60	11730.14	7621.92
Set 3	1.52	302.50	16458.11	10863.44
Set 4	0.44	538.00	29270.95	66193.91
Average	1.06	313.08	17033.46	24723.77
Standard Deviation	0.55	156.91	8537.11	27777.52

Figure 4.17 Kinetic constants for recombinant human Chk1 wild-type in the presence of peptides with respect to recombinant human p21.

(A) Kinetics data of Chk1 wild-type in the presence of p21 peptide 4 and Chk1 peptide 14. Kinase reaction containing 100 ng/µl of Chk1 and full length p21 in the range of 0.28 to 8.83 µM and 5 µg of peptide were assembled in the presence of [γ^{32}P]ATP. The reaction products were resolved on 12% SDS-PAGE and [γ^{32}P] incorporation into p21 was quantified by phosphorimager. The Michaelis-Menten parameters were fitted via the Hanes plot using hyperbolic regression software (Hyper,version 1.1s, J. Easterby, University of Liverpool) and kinetic constants were calculated as the mean ± standard deviation.

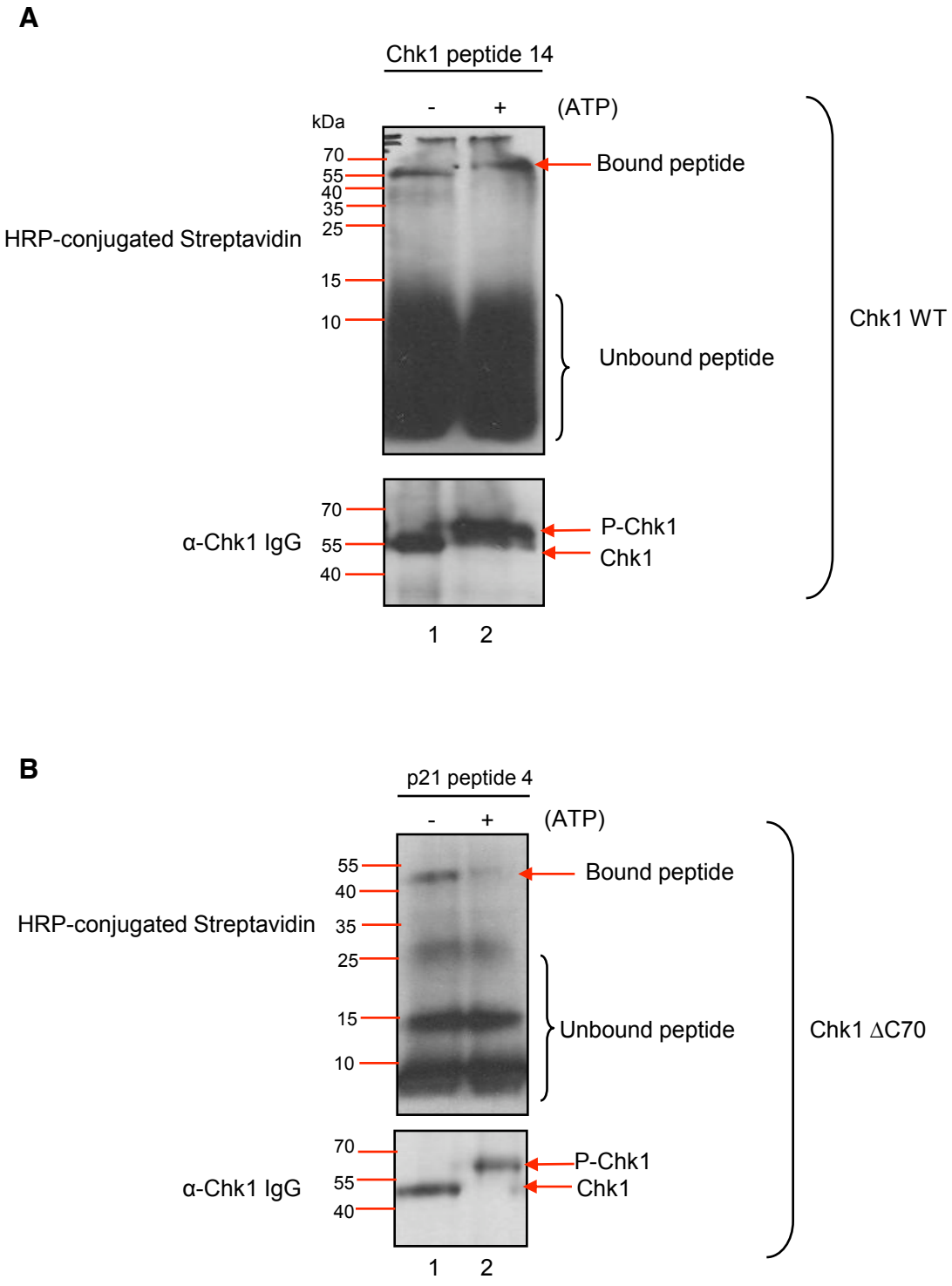

Figure 4.18 Non-denaturing gel electrophoresis of peptides and Chk1 binding assay.

(A) Kinase reactions containing 100 ng of Chk1 WT and 5 µg of Chk1 peptide 14 were assembled in the presence or absence of unlabelled ATP. The reactions were stopped by addition of sample buffer (without SDS/DTT) before resolved by 10% or 15% non-denaturing PAGE (without SDS) and transferred to nitrocellulose membrane. Biotinylated Chk1 peptide 14 was detected with HRP-conjugated streptavidin whilst Chk1 protein was detected using α-Chk1 IgG. (B) Kinase reactions containing 100 ng of Chk1 ΔC70 and 5 µg of p21 peptide 4 were assembled in the presence or absence of unlabelled ATP. The reactions were stopped by addition of sample buffer (without SDS/DTT) before resolved by 10% or 12% non-denaturing PAGE (without SDS) and transferred to nitrocellulose membrane. Biotinylated p21 peptide 4 was detected with HRP-conjugated streptavidin whilst Chk1 protein was detected using α-Chk1 IgG.

A

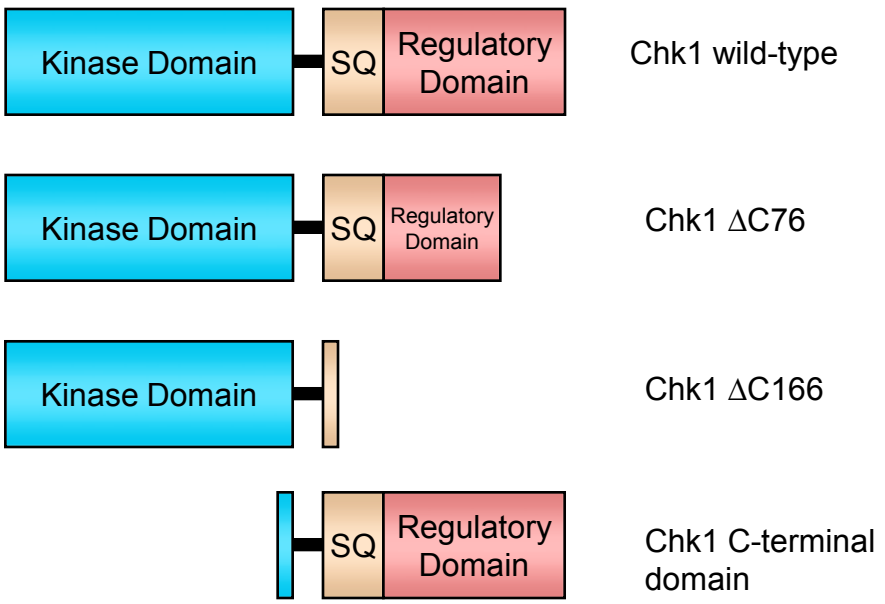

Figure 4.19 Schematic diagram of chick Chk1 mutants.

(A) Schematic diagram of chick Chk1 wild-type, Chk1 ΔC76 mutant, Chk1 ΔC166 mutant and Chk1 C-terminal domain proteins.

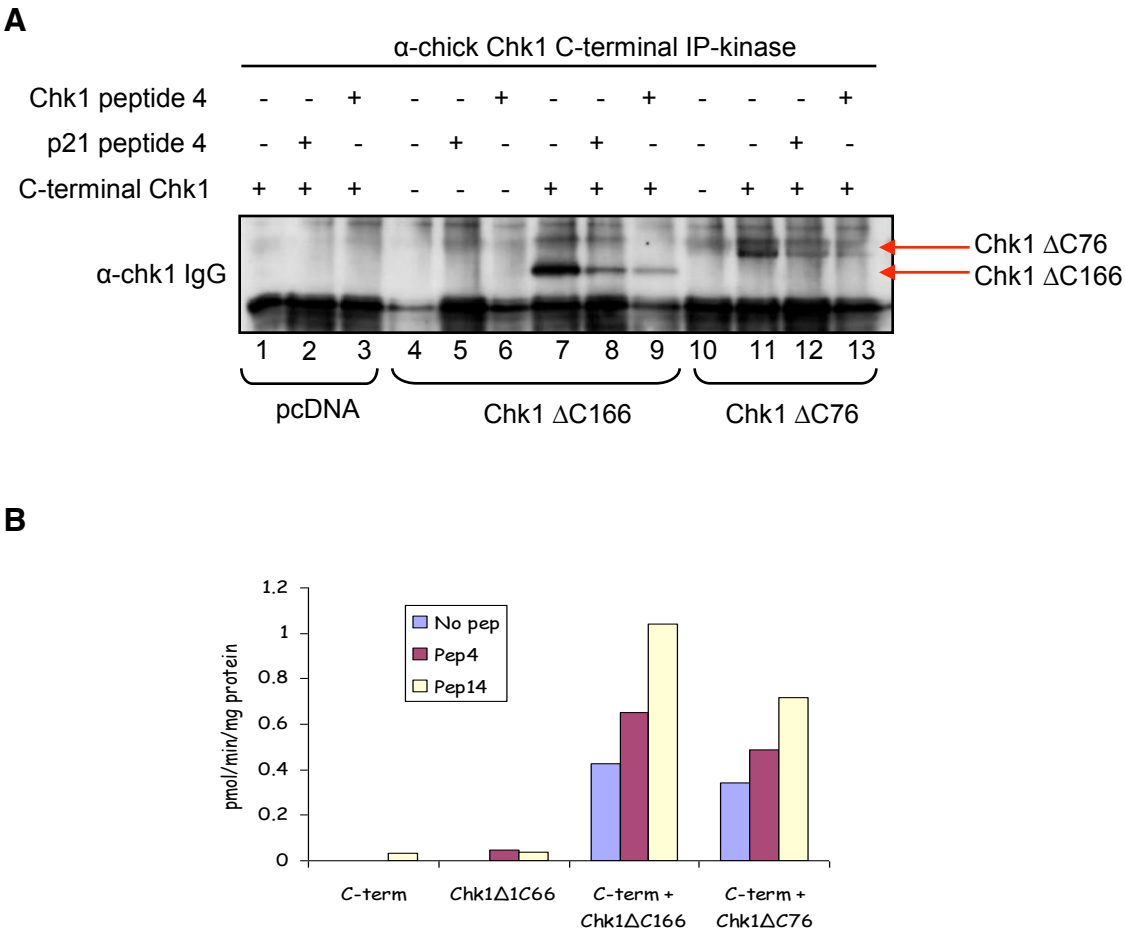

Figure 4.20 p21 peptide 4 and Chk1 peptide 14 dissociates the intra-molecular interaction between chick Chk1 N-terminal domain and C-terminal domain.

(A) Cos1 cells were co-transfected with chick Chk1 ΔC76 and chick Chk1 C-terminal domain or chick Chk1 ΔC166 and chick Chk1 C-terminal domain for 24 hrs. The cells were harvested and lysed. 1 mg of lysate was subjected to Chk1 immunoprecipitation with α-chick C-terminal Chk1 IgG. Kinase reactions containing 5 μg of either p21 peptide 4 or Chk1 peptide 14 were assembled with Chk1 immunoprecipitated sample in the presence of unlabelled ATP. The reaction products were resolved by 10% SDS-PAGE and transferred to nitrocellulose membrane. Chk1 protein was detected using α-N-terminal Chk1 IgG. (B) Cos1 cells were co-transfected with chick Chk1 ΔC76 and chick Chk1 C-terminal domain or chick Chk1 ΔC166 and chick Chk1 C-terminal domain. As control, Cos1 cells were transfected with chick Chk1 C-terminal domain or chick Chk1 ΔC166 alone. The cells were harvested and lysed. 1 mg of lysate was subjected to Chk1 immunoprecipitation with α-chick C-terminal Chk1 IgG. Kinase reactions containing 0.2 mM of Chktide and either p21 peptide 4 or Chk1 peptide 14 or DMSO were assembled with Chk1 immunoprecipitated sample in the presence of [γ^{32}P]-ATP. The reaction products were resolved by 15% SDS-PAGE and [γ^{32}P] incorporation into Chktide was quantified by phosphorimager.

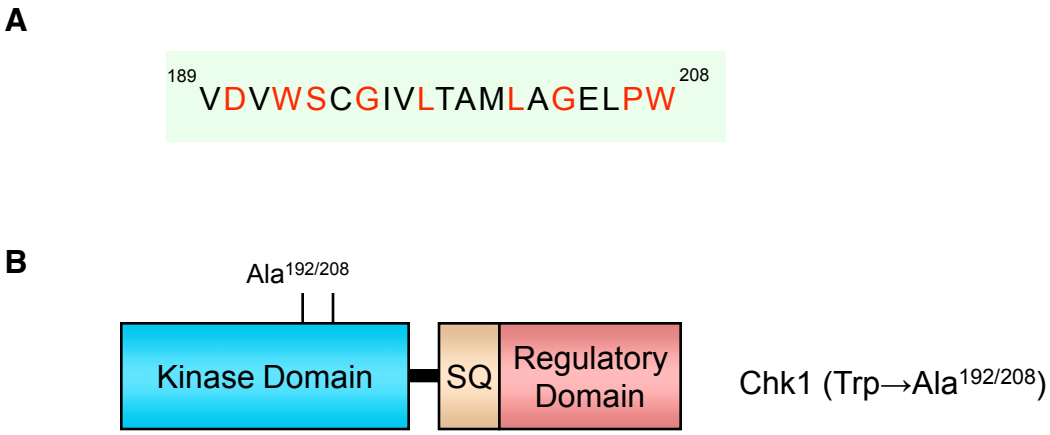

Figure 4.21 Schematic diagram of Chk1 mutant **(Trp→Ala**$^{192/208}$).

(A) Amino acids sequence of Chk1 αF region. Residues in red are conserved across the species of Chk1. (B) Schematic diagram of Chk1 mutant (Trp→Ala$^{192/208}$).

A

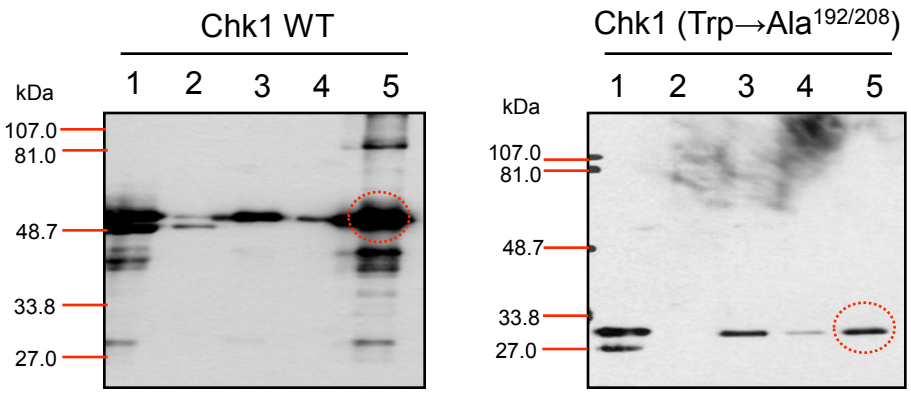

Figure 4.22 Purification of recombinant human insect-cell expressed Chk1 mutant **(Trp→Ala$^{192/208}$)**.

(A) His-tagged Chk1 mutant was expressed in Sf9 insect cell system and purified from Ni-NTA agarose column. Fractions from the Ni-NTA agarose column were resolved on a 10% SDS-PAGE gel before transferring to nitrocellulose membrane and immunoblotted with α-Chk1 IgG. The left panel shows immunoblot of Chk1 WT purification and the right panel shows immunoblot of Chk1 mutant (Trp→Ala$^{192/208}$) with the full-length Chk1 and truncated Chk1 circled respectively. Lane: 1, Flow-through fraction; 2, wash fraction I; 3, wash fraction II; 4, wash fraction III; 5, eluted fraction.

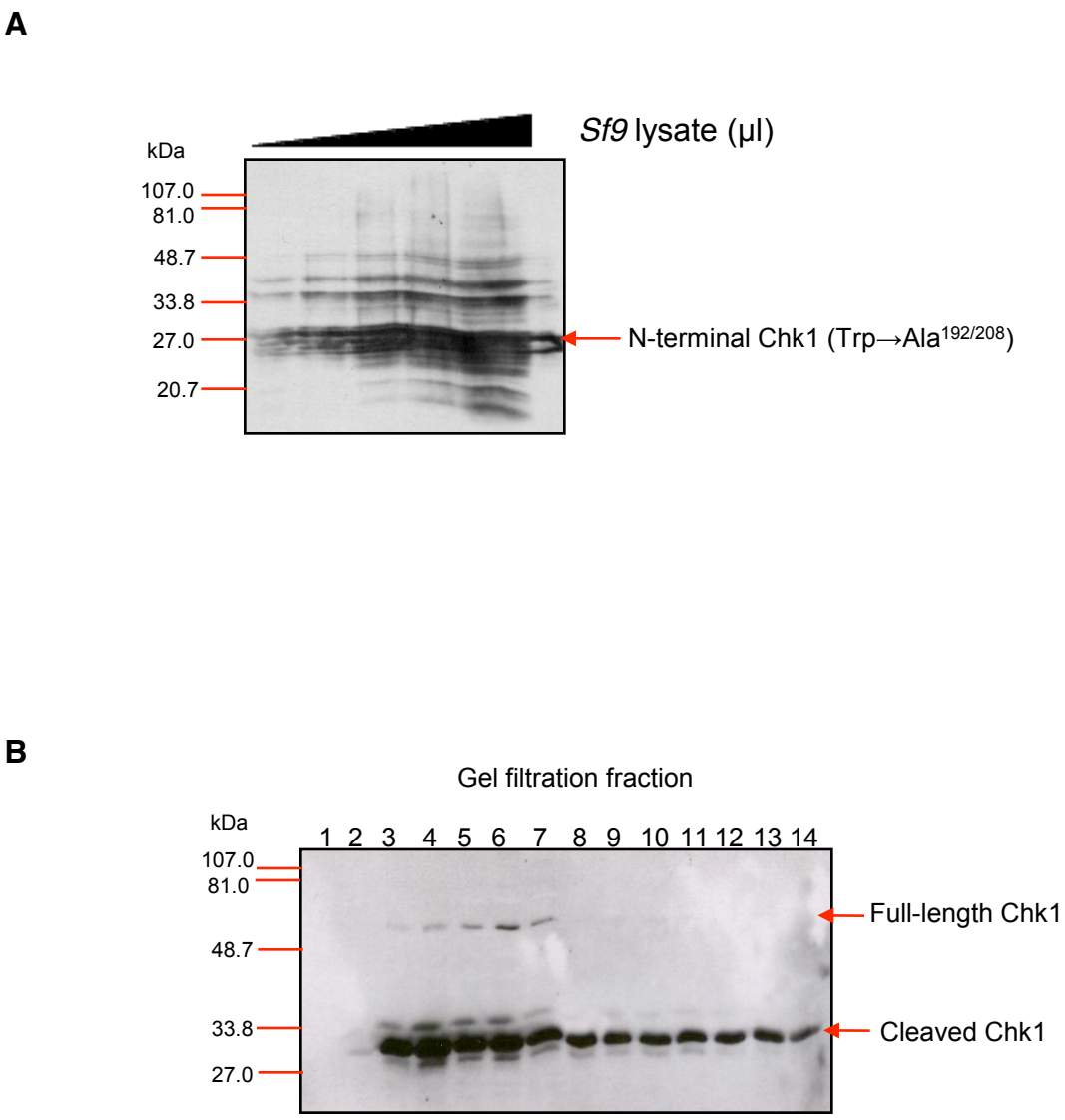

Figure 4.23 Mutation of Chk1 (**Trp→Ala**$^{192/208}$) render susceptibility to cleavage.

(A) Chk1 mutant (Trp→Ala$^{192/208}$)-infected Sf9 insect cells were lysed directly with SDS-sample buffer before a titrating amount of lysate (10 µl to 200 µl) were resolved in 10% SDS-PAGE gel and transferred to nitrocellulose membrane. Total Chk1 level was detected using α-Chk1 IgG. (B) Chk1 (Trp→Ala$^{192/208}$) is purified from Sf9 insect cells before loaded onto a gel filtration column Superdex 200 (Amersham Bioscience). 10 µl of the fractions were resolved in a 10% SDS-PAGE and transferred to nitrocellulose membrane. Total Chk1 level was detected using α-Chk1 IgG.

A

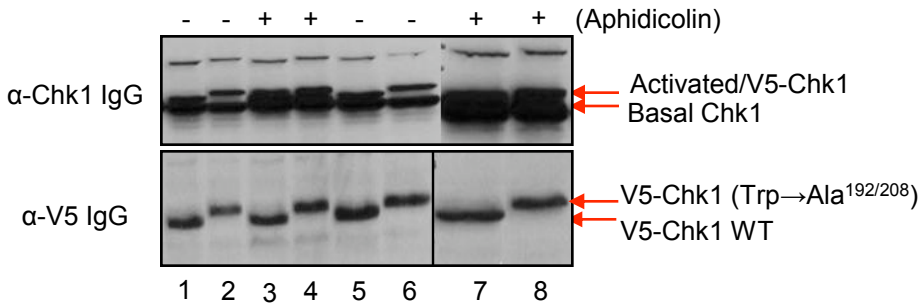

Lane	Cell line	V5-Chk1	Aphidicolin treatment
1	HCT116 wild type	V5-Chk1 WT	-
2	HCT116 wild type	V5-Chk1 (Trp→Ala$^{192/208}$)	-
3	HCT116 wild type	V5-Chk1 WT	+
4	HCT116 wild type	V5-Chk1 (Trp→Ala$^{192/208}$)	+
5	HCT116 p21$^{-/-}$	V5-Chk1 WT	-
6	HCT116 p21$^{-/-}$	V5-Chk1 (Trp→Ala$^{192/208}$)	-
7	HCT116 p21$^{-/-}$	V5-Chk1 WT	+
8	HCT116 p21$^{-/-}$	V5-Chk1 (Trp→Ala$^{192/208}$)	+

Figure 4.24 Immunoblot of exogenous Chk1 protein from HCT116 wild-type or p21$^{-/-}$ cells (+/- aphidicolin treatment).

(A) HCT116 WT and HCT116 p21$^{-/-}$ cells were grown to >90% confluence before transfected with C-terminally V5-tagged Chk1 wild-type or V5-tagged Chk1 (Trp→Ala$^{192/208}$). After 24 hrs, the cells were either treated with 20 μM aphidicolin or ethanol as control for 4 hrs. The cells were harvested and 50 μg of whole cell lysates were resolved by 10% SDS-PAGE before transferred to nitrocellulose membranes. Chk1 protein was detected using mouse α-Chk1 IgG and exogenous V5-tagged Chk1 protein was detected using mouse α-V5 tag IgG.

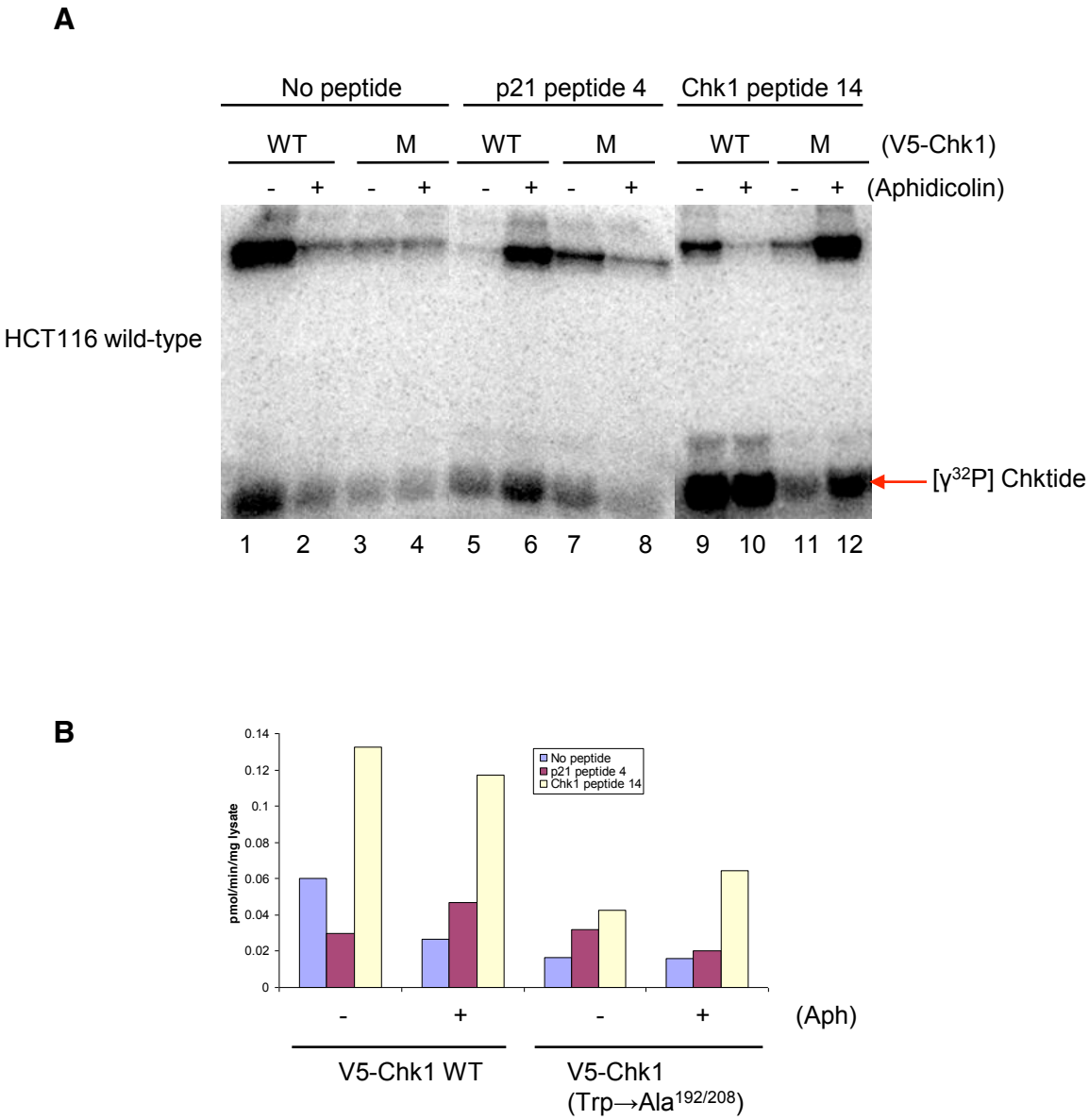

Figure 4.25 Immunoprecipitation-kinase assay of exogenous V5-Chk1 WT or V5-Chk1 (**Trp→Ala**$^{192/208}$) mutant proteins from HCT116 wild-type cells.

(A and B) HCT116 WT cells were grown to >90% confluency before transfected with C-terminally V5-tagged Chk1 wild-type (W) or Chk1 (Trp→Ala$^{192/208}$) (M). After 24 hrs, the cells were either treated with 20 μM aphidicolin or ethanol as control for 4 hours. The cells were harvested and lysed. 1 mg of lysate was used for Chk1 immunoprecipitation-kinase using mouse α-V5 tag IgG and Protein G sepharose beads. Unbound proteins were washed off. Kinase reactions containing 0.2 mM of Chktide with or without 5 μg of p21 peptide 4 or Chk1 peptide 14 in the presence of [γ^{32}P]-ATP were assembled with immunoprecipitated sample. The reaction products were resolved by 15% SDS-PAGE. [γ^{32}P] incorporation into Chktide was visualised by autoradiography and quantified by phosphorimager.

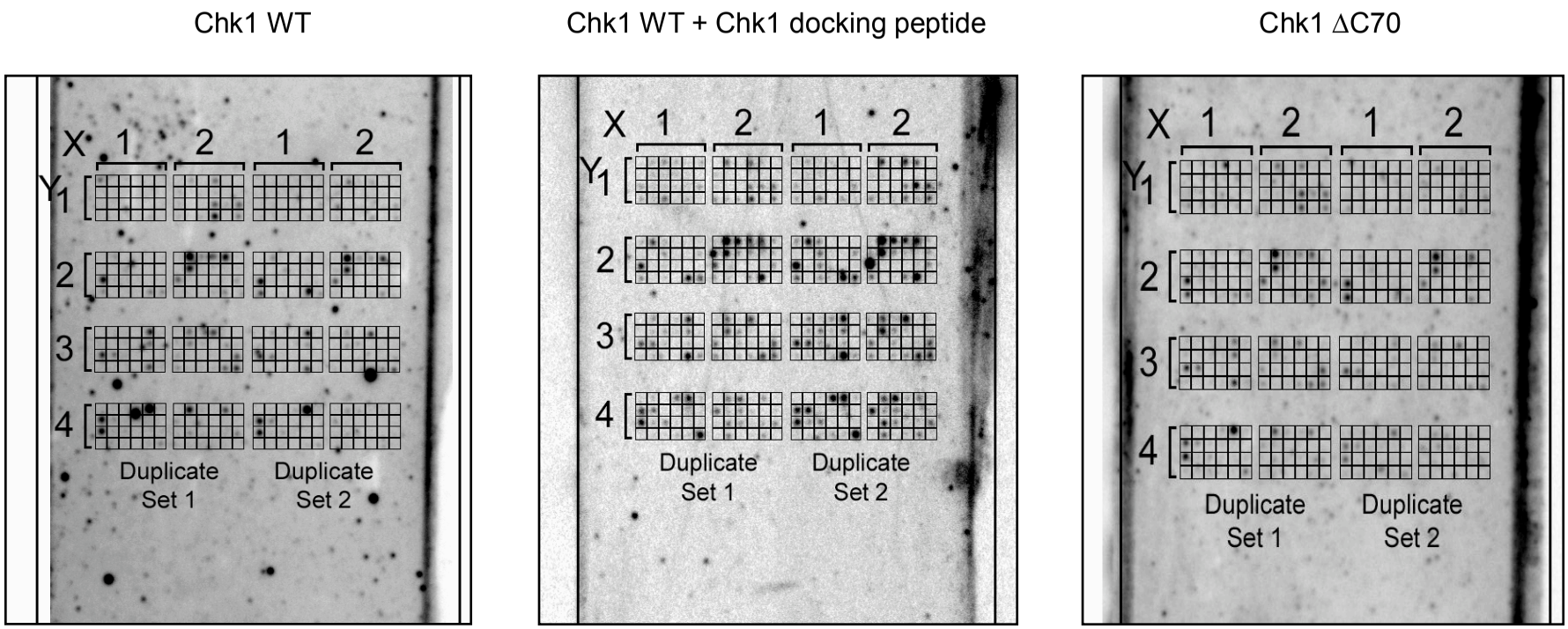

Figure 4.26 Pepchip Chk1 kinase assays.

(A) Peptide microarrays containing 2 x 192 peptides derived from known phosphorylation sites of kinases (PhosphoBase) were assayed with Chk1 WT or Chk1 WT with Chk1 docking peptide or Chk1 ΔC70. The figure shows the duplicate array of peptides on each slides. The array is composed of a series of 7 x 4 spots in subarrays with 2 subarrays on the *x* axis and 4 subarray on the *y* axis. The peptide array was subjected to γ-^{33}P kinase assay with the indicated Chk1.

A

S/N	Sequence	Target Protein
1	KGTGYIKTE	Signal transducer and activator of transcription 1-alpha/beta_Human
2	KNDKSKTWQ	Eukaryotic translation initiation factor 4E_Human
3	KPGFSPQPS	Protein phosphatase 1 regulatory subunit 3A_Rabbit
4	KRKQISVR	Glycogen phosphorylase, muscle form_Human
5	KRKQISVRG	Glycogen phosphorylase, muscle form_Human
6	KRKRSRKES	Histone H2B type 1-C/E/F/G/I_Human
7	KRNSSPPPS	Plasma membrane calcium-transporting ATPase 1_Human
8	KRRRSSKDT	Glutamate [NMDA] receptor subunit zeta-1 [Precursor]_Human
9	KSLNYIDLD	Insulin receptor substrate 1_Rat
10	KSRWSGSQQ	RAF proto-oncogene serine/threonine-protein kinase_Human
11	KTETSQVAP	Rhodopsin_Human
12	LDDQYTSSS	Tyrosine-protein kinase Tec_Mouse
13	LGGGTFDIS	Chaperone protein dnaK_E.coli
14	LMAPSEEDH	Insulin-like growth factor-binding protein 1 [Precursor]_Human
15	LQRYSSDPT	Epidermal growth factor receptor [Precursor]_Human
16	LRRASVAQL	Pyruvate kinase isozymes R/L_Rat
17	LRRLSTKYR	Tyrosine-protein phosphatase non-receptor type 12_Human
18	LSEHSSPEE	Protein phosphatase 1 regulatory subunit 1B_Bovin
19	LSGESDLEI	DNA topoisomerase 2_Yeast
20	PENDYEDVE	Hematopoietic lineage cell-specific protein_Human
21	PKRGSGKDG	Myelin basic protein_Bovine
22	PPSAYATVK	Annexin A2_Chick
23	PSPKTPPGS	Microtubule-associated protein tau_Rat
24	QGTLSKIFK	Myelin basic protein_Bovine

Figure 4.27 List of peptide sequences phosphorylated by stimulated Chk1 exclusively in the peptide microarray.

(A) Table listing the peptides (and its sequences) which are phosphorylated exclusively by Chk1 docking peptide-stimulated Chk1.

A

S/N	Sequence	Target Protein
1	LKLASPELE	Transcription factor AP-1_Human
2	PPSAYATVK	Annexin A2_Chick
3	LSELSRRRI	Eukaryotic translation initiation factor 2 subunit α_Yeast
4	KVPQTPLHT	MAP kinase-activated protein kinase 2_Rabbit
5	KSLNYIDLD	Insulin receptor substrate 1_Rat
6	LDDQYTSSS	Tyrosine-protein kinase Tec_Mouse
7	PSPKTPPGS	Microtubule-associated protein Tau_Rat
8	PPSAYGSVK	Annexin A2-Human
9	NGLNYIDLD	Insulin receptor substrate 1_Human
10	PAPKTPPSS	Microtubule-associated protein Tau_Human
11	KRFGSKAHM	Nitric Oxide synthase, brain_Rat
12	LRMFSFKAP	γ-aminobutyric acid receptor subunit γ-2 (Precursor)_Bovin
13	LYQFSFVGL	γ-aminobutyric acid receptor subunit γ-2 (Precursor)_Human

Figure 4.28 List of peptide sequences selected for further kinase assays.

(A) Biotinylated peptides were synthesised with a –GG- spacer. Peptide 1 to 7 were identified in the peptide microarray that were phosphorylated by Chk1 WT stimulated with Chk1 peptide 14 or Chk1 ΔC70. Peptide 8 to 10 are human forms of peptide 2, 5 and 7 respectively whereas peptide 11 and 12 are readily phosphorylated by all three forms of Chk1 used in the peptide microarray. Peptide 13 is the human form of peptide 12.

A

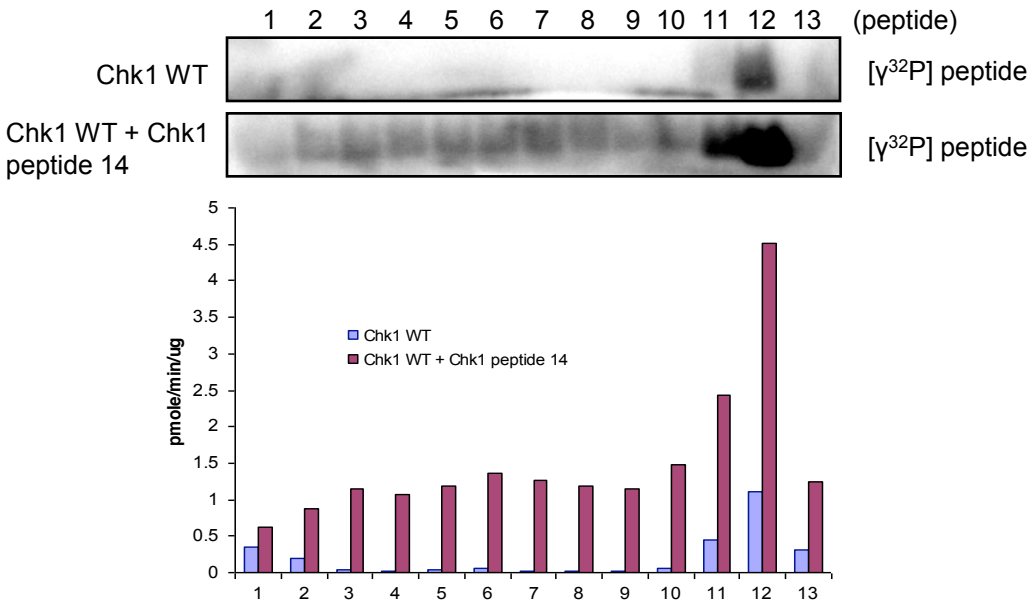

Figure 4.29 Recombinant human Chk1 activity towards peptide substrates can be modulated by stimulatory Chk1 peptide 14.

(A) Kinase reactions containing 100 ng of Chk1 and 0.5 μg of peptide as listed in Figure 4.17 were assembled in the presence of [γ^{32}P]-ATP with or without 5 μg of Chk1 peptide 14. The reaction products were resolved by 12% SDS-PAGE and [γ^{32}P] incorporation into the peptides were visualised by autoradiography and quantified by phosphorimager.

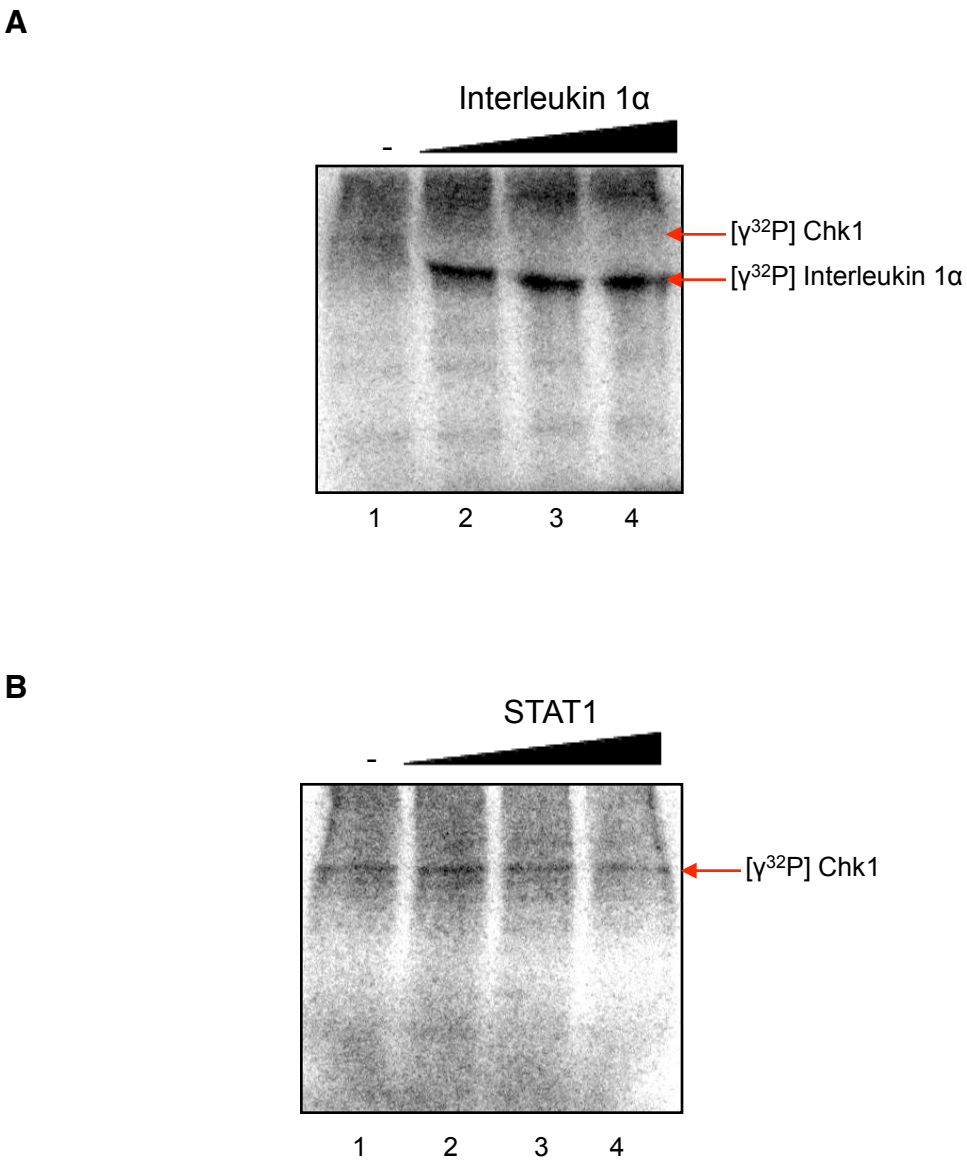

Figure 4.30 Recombinant human Chk1 is active towards recombinant human Interleukin 1α but not recombinant human STAT1.

(A) Kinase reactions containing 100 ng of Chk1 WT and titration of interleukin 1α (1 to 3 ng) were assembled in the presence of [γ^{32}P]ATP. The reaction products were resolved in 12% SDS-PAGE. [γ^{32}P] incorporation was visualised by autoradiography. (B) Kinase reactions containing 100 ng of Chk1 WT and titration of STAT1 (1 to 3 µg) were assembled in the presence of [γ^{32}P]ATP. The reaction products were resolved in 10% SDS-PAGE. [γ^{32}P] incorporation was visualised by autoradiography.

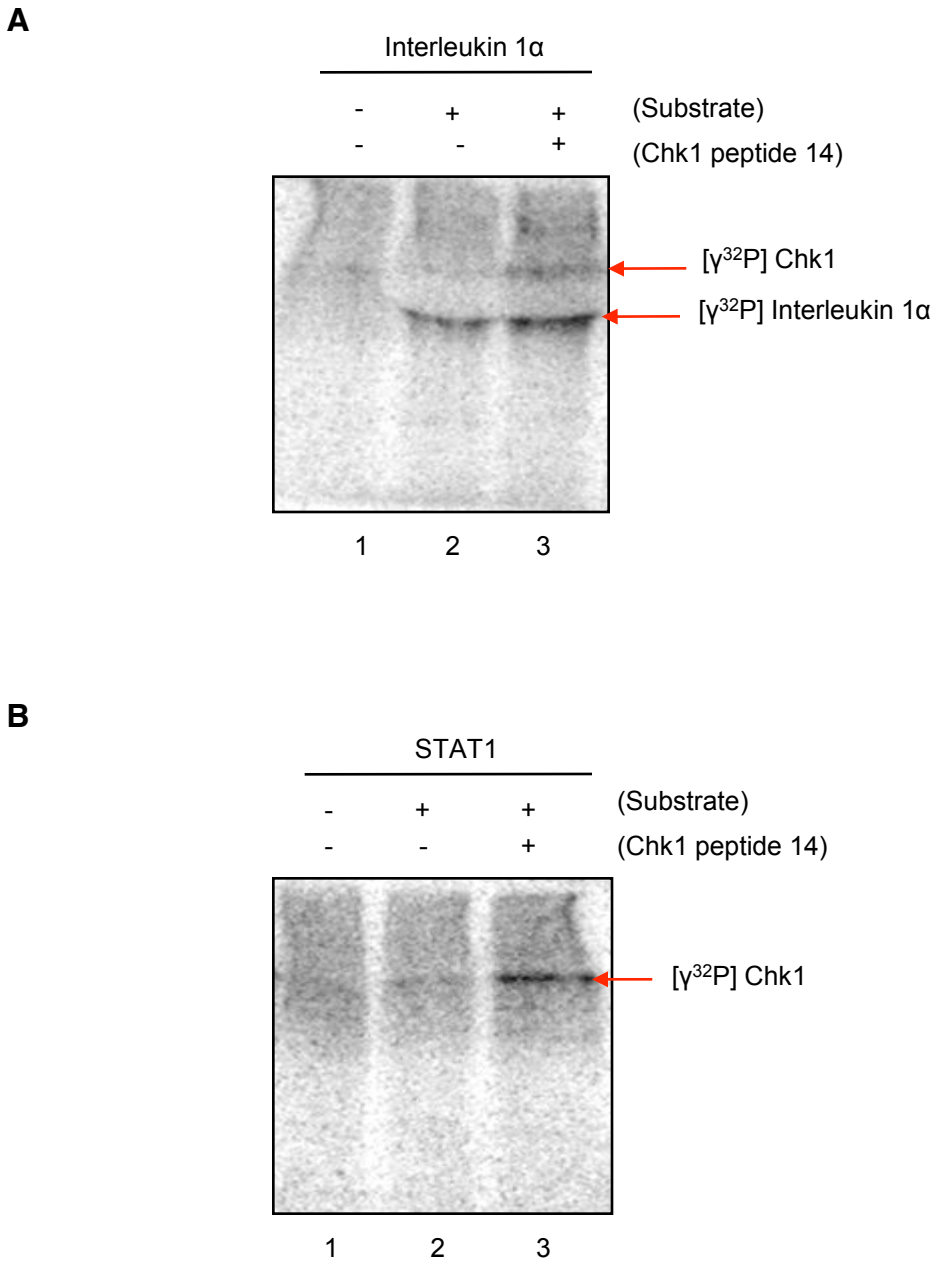

Figure 4.31 Stimulated Chk1 is not active towards recombinant human STAT1.

(A and B) Kinase reactions containing 2 ng of Interleukin 1α or 2 µg of STAT1 and 100 ng of Chk1 with or without Chk1 peptide 14 in the presence of [γ^{32}P]ATP. The reaction products were resolved in 10% SDS-PAGE. [γ^{32}P] incorporation was visualised by autoradiography.

A

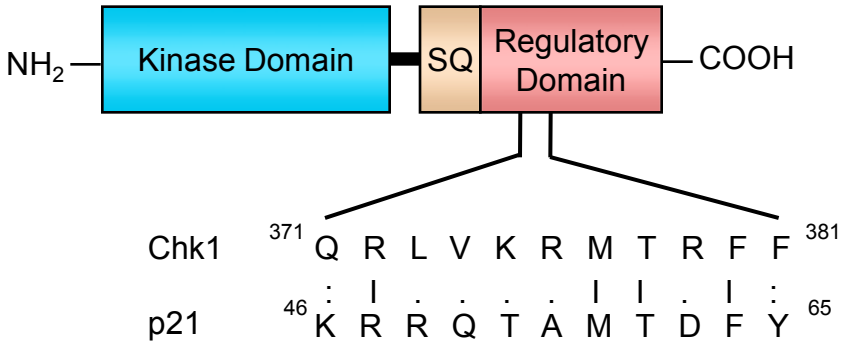

Figure 4.32 Sequence alignment identified a potential Chk1 pseudosubstrate region.

(A) Pseudosubstrate region often fits the substrate consensus sequence with a non-phosphorylatable residue in place of Ser/Thr/Tyr. Sequence alignment of p21 phosphorylation motif (Ser^{146} was replaced with Ala) with full-length Chk1 has identified a potential pseudosubstrate region within Chk1 C-terminal domain (amino acids 371 to 381).

A

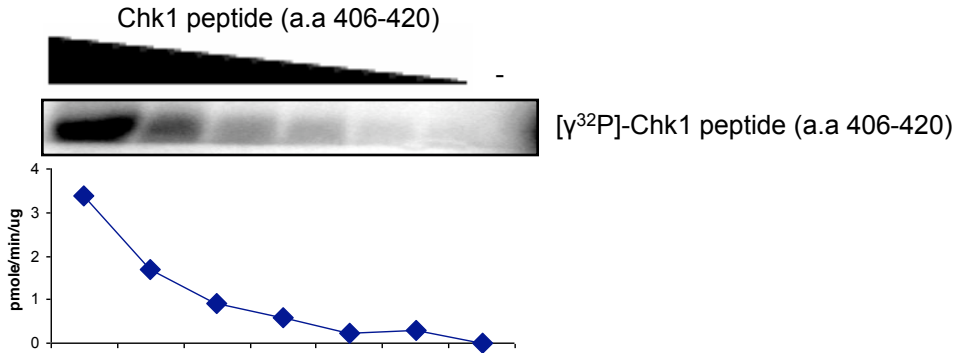

B

406 KSCMNQVTISTTDRR 420

Figure 4.33 Chk1 autophosphorylation in the C-terminus end

(A) Kinase reactions containing 100 ng of Chk1 and a titration of Chk1 peptide (a.a 406-420) (0.625 to 20 µg) were assembled for [γ^{32}P]-ATP kinase assay. The reaction products were resolved by 15% SDS-PAGE. [γ^{32}P] incorporation into Chk1 peptide (a.a 406-420) was visualised by autoradiograhpy and quantified by phosphorimager. (B) Sequence of Chk1 autophosphorylation peptide (amino acids 406-420). Mass spectrometry data have suggested that Ser406 is a potential autophosphorylation site.

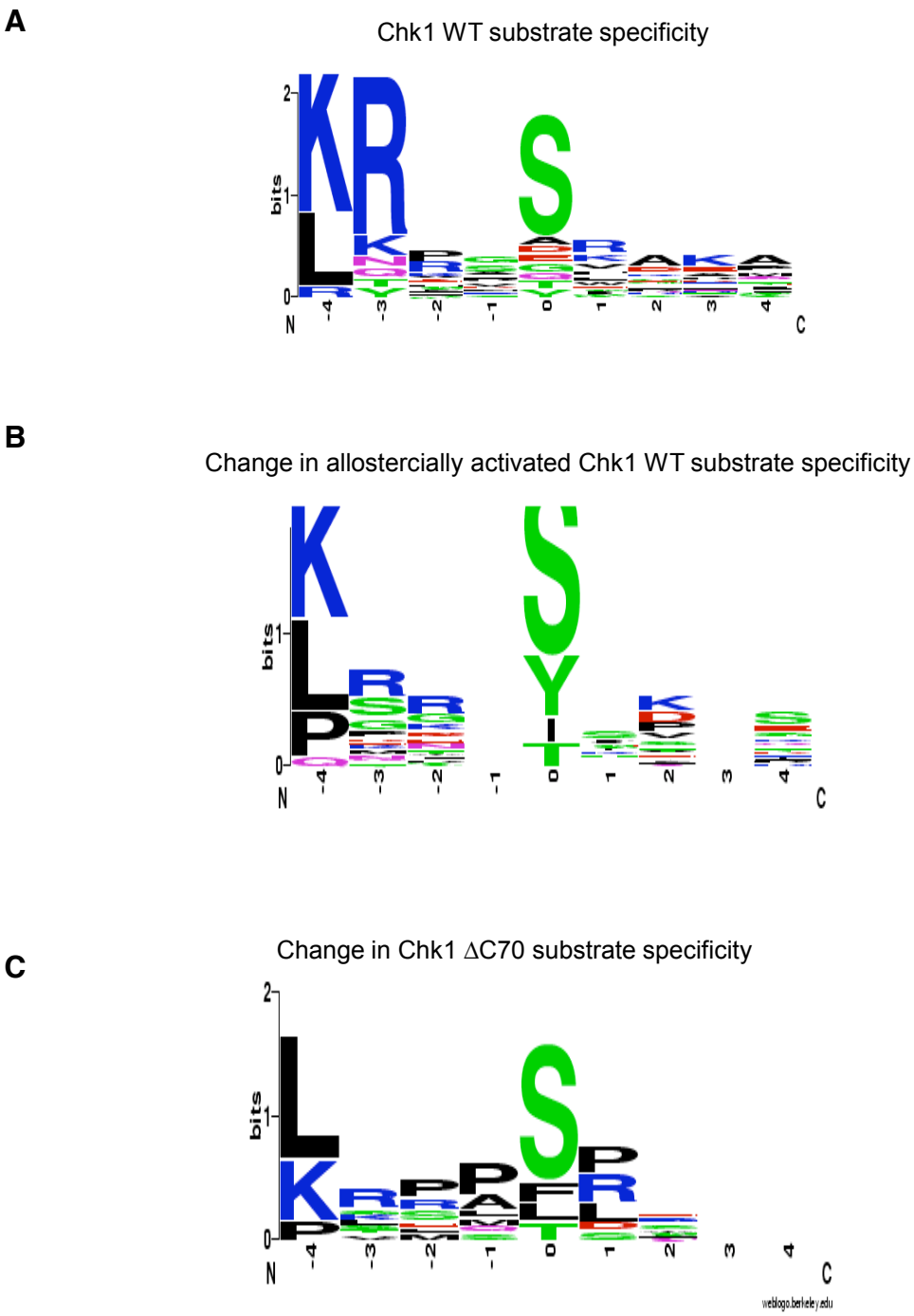

Figure 4.34 Loss of autoinhibitory region and allosteric activation result in Chk1 substrate specificity change.

Sequences of peptides phosphorylated by Chk1 were fed into WebLogo program (University of California, Berkeley) to generate consensus sequence logos. (A) Consensus sequence of substrate peptides phosphorylated by Chk1 wild-type protein. (B) Consensus sequence of substrate peptides phosphorylated only by Chk1 wild-type protein allosterically activated by Chk1 peptide 14. (C) Consensus sequence of substrate peptides phosphorylated only by Chk1 ΔC70.

CHAPTER 5: CONCLUSIONS AND FUTURE PERSPECTIVES

5.1 Regulation of Chk1 enzymatic mechanism

In this thesis, a p21 N-terminal region (p21 peptide 4) was identified to have an allosteric activating effect on Chk1 catalytic activity and also activated Chk1 to be a more efficient enzyme. Further studies showed that peptidomimetic ligands based on the Chk1 docking site from p21 was able to restore Chk1 catalytic activity towards a p21 mutant protein with an N-terminal domain deletion. This suggested that the peptide 4 region of p21 could function as an allosteric docking site for Chk1 substrate recognition. Indeed, protein kinases often recognise their substrates through interactions in regions distinct to the active site, in addition to a consensus substrate sequence (Remenyi et al., 2006, Goldsmith et al., 2007). These interactions involved linear docking motifs and are usually transient and weak (Neduva and Russell, 2005). Peptide binding assays revealed that p21 peptide 4 bound to Chk1 protein kinase and this interaction appeared to be ATP-dependent. Mutational analysis also identified critical residues in the p21 peptide 4 involved in allosteric activation as Thr^{55}, Pro^{58} and Trp^{65}. Interestingly, a αF region of the Chk1 N-terminal domain has been identified to share homology with p21 peptide 4. Similarly, peptidomimetic ligands based on this region (Chk1 peptide 14 and 32) were able to allosterically activate Chk1 catalytic activity. Mutation of conserved Trp^{192} and Trp^{208} residues is thought to destabilise the kinase domain, generating a Chk1 (Trp→$Ala^{192/208}$) mutant that is refractory to the stimulating effects of the activating peptides (p21 peptide 4 and Chk1 peptide 14).

Chk1 N-terminal kinase domain is constitutively active, exhibiting 20-fold more catalytic activity than full-length Chk1 *in vitro*, suggesting that the C-terminal

domain function to negatively regulate Chk1 activity in an autoinhibition model (Chen et al., 2000). Chk1 N-terminal domain and C-terminal domain has already been shown to interact intramolecularly (Katsuragi and Sagata, 2004). Intramolecular interactions between the catalytic domain and regulatory domain often mediate inhibition of catalytic activity by directly blocking substrate binding to the active site due to the presence of a pseudosubstrate or by allosterically inducing an inactive conformation (Huse and Kuriyan, 2002). In collaboration with Prof David Gillespie's group, we have shown that activating peptides were able to disrupt the intramolecular interaction between the chick Chk1 N-terminal domain and the C-terminal domain. Interestingly, a Chk1 ΔC70 mutant where the last 70 amino acids of the C-terminal domain were deleted proved to be refractory to the stimulating effects of the activating peptides. However the last 70 amino acids of the C-terminal domain (C70) by itself do not mediate intramolecular interaction with the Chk1 N-terminal domain (MT Scott, personal communication), implying that the intramolecular binding interface is outwith C70 and the activating peptides do not function to displace C70 directly. The fact that C70 is required for autoinhibition suggested that the activating peptides mediate its allosteric stimulation effects on the displacement of C70 through unknown mechanism; Several questions were left unanswered and several new questions were raised as result of this study;-

1. How do the last 70 amino acids of Chk1 C-terminal domain function in autoinhibition?
2. Do the last 70 amino acids of Chk1 contain a pseudosubstrate? Sequence alignment has identified a potential Chk1 pseudosubstrate outside the last

70 amino acids (Figure 4.32), though it is still possible that the last 70 amino acids harbour a potential pseudosubstrate.

3. Where is the activating peptide docking interface and how do the activating peptides allosterically induce a conformational change of the last 70 amino acids to activate Chk1 catalytic activity?
4. Chk1 undergoes autophosphorylation in the regulatory C-terminus end. Mass spectrometry data has suggested that one of the major phospho-acceptor sites resides at Ser^{407} (data not shown). However it is not clear what effect autophosphorylation has on Chk1 enzymatic regulation?
5. Is the C-terminal domain essential to the activity and/or function of Chk1? It has been shown recently that *S.pombe* Chk1 C-terminal domain contains both autoinhibitory and activating signal necessary for the function of Chk1 (Kosoy and O'Connell, 2008). Given the high degree of conservation in some regions of the C-terminal between *S.pombe* Chk1 and human Chk1, it is possible that human Chk1 could share similar mode of regulatory mechanism conferred by the C-terminal domain.

Based on the existing data, I proposed the following hypothetical model. Chk1 catalytic activity is autoinhibited through weak intramolecular interaction between the C-terminal regulatory domain and a pseudo-docking site (αF region) at the N-terminal kinase domain. This autoinhibition requires the presence of the last 70 amino acids of the C-terminal domain (C70) which is not involved in intramolecular interaction. In the response to DNA damage, Chk1 undergoes ATR-dependent phosphorylation at Ser^{317} and Ser^{345}. This phosphorylation event

positively regulates Chk1 localisation and activating ligands/substrates binding. Activation of Chk1 protein kinase is mediated by binding to an activating ligand/substrate that contains a high-affinity pseudo-docking site. This high-affinity intermolecular interaction disrupts the low-affinity intramolecular interaction and allosterically affects the displacement of C70 from the N-terminal kinase domain, resulting in an active conformation. Autophosphorylation of C70 at Ser^{407} and other possible sites stabilises this active conformation (Figure 5.1).

To gain valuable insight to the mechanistic basis of Chk1 allosteric activation and Chk1 C-terminal regulatory action, it is necessary to conduct biophysical studies such as NMR and more biochemical studies to ascertain the intramolecular interface and how allosteric regulation affects Chk1 conformational change and catalytic activity. Current Chk1 inhibitors studied are targeted towards the ATP-binding site (Tse et al., 2007). However these inhibitors must compete with the high intracellular ATP concentrations and also differentiate between the ATP-binding site of different protein kinases (Bogoyevitch et al., 2005). By elucidating the allosteric regulation mechanism, we can then design better non-ATP binding small-molecule inhibitors by stabilising the native autoinhibited conformation of Chk1 protein kinase.

5.2 Identifying more novel Chk1 substrates

Chk1 is a major player in checkpoint arrest and identifying novel Chk1 substrates will help to further delineate checkpoint signalling pathways. In chapter 3, Chk1 was shown to phosphorylate p21 at Ser^{146} *in vitro*. However more *in vivo* studies are required to confirm p21 is a novel substrate for Chk1. In chapter 4, I asked whether allosteric activation by the peptidomimetic ligand is able to change Chk1 substrate specificity or modulate its activity towards substrates that do not contain the Chk1 consensus phosphorylation motif, Rxx(S/T). Using the PepChip microarray, it was shown that allosteric activated Chk1 was able to target 24 peptide substrates not recognised by the non-allosteric activated Chk1 and Chk1 ΔC70 mutant protein. In contrast, further characterisation of allosteric activated Chk1 activity towards selected peptide substrates and STAT1 protein suggested that allosteric activation does not alter Chk1 substrate specificity. However it is still possible that allosteric regulation is required for Chk1 activity towards a substrate that does not contain the Chk1 consensus phosphorylation motif. Indeed it has been highlighted that Chk1 phosphorylates p53 Ser^{20} *in vitro* (Shieh et al., 2000) and sequences around Ser^{20} (ETF**S**D) do not fit the Rxx(S/T) motif.

Nevertheless the PepChip microarray does provide a useful proteomic screen for potential novel Chk1 substrates. Chk1 was shown in Chapter 4 to target human interleukin-1α protein. Interleukin-1α is a cytokine secreted by monocytes and macrophages and is involved in many immune responses such as inflammation (Dinarello, 1994). *In vitro* study has shown that the precursor form of interleukin-1α is phosphorylated at Ser^{90} by an unknown kinase (Beuscher et al., 1988).

Sequences around interleukin-1α Ser^{90} fit within the RxxS motif and thus Chk1 could be the protein kinase responsible for interkeukin-1α modification. Preliminary data from the Ball lab also indicated that Chk1 could target Interferon Regulatory Factor 1 (IRF1) as a substrate. Mass spectrometry and phospho-antibodies data showed that Chk1 phosphorylated IRF1 at Ser^{317} (Figure 5.2A). Interestingly, sequences around IRF Ser^{317} fit within the RxxS motif (Figure 5.2B). Thus, IRF1 could also form as a potential novel Chk1 substrate *in vivo*. To identify more novel Chk1 substrates which do not conform to the RxxS motif, we can transfect mammalian cells with activating peptide to allosterically activate Chk1 and look for changes in the phosphoproteome profile using mass spectrometry analysis.

Identification of a novel phosphorylation site from *in vitro*/*in vivo* studies is dependent on a specific protein kinase signalling pathway, but does not provide definitive proof that the protein kinase phosphorylates a substrate directly *in vivo* (Berwick and Tavare, 2004). A chemical genetics approach developed by the Shokat lab that relies on engineering a protein kinase to accept non-natural synthetic ATP analogue could overcome this problem (Liu et al., 1998). The ATP analogue is cell permeable and can be used to label substrates targeted by the engineered protein kinase. Moreover attachment of ATP analogue to substrates means that it cannot be removed by phosphatases. Modification and optimisation of this technique has helped to identify many novel substrates for Cdk1-cyclin B and ERK (Eblen et al., 2003, Blethrow et al., 2008). So it could be possible to adapt this approach to identify more novel Chk1 substrates.

A

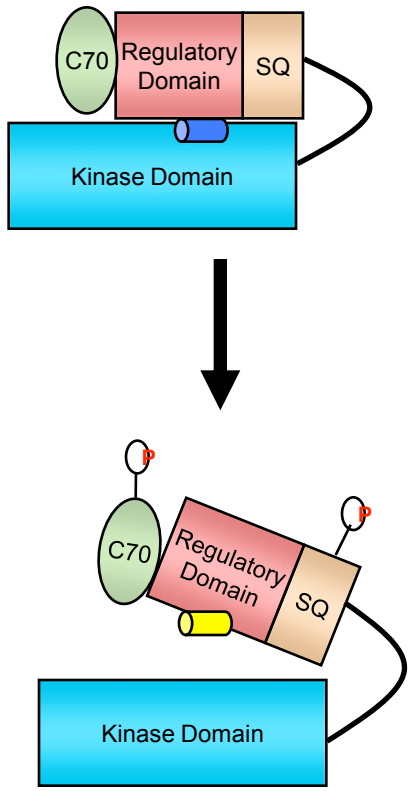

Figure 5.1 Schematic model of Chk1 autoinhibition and allosteric activation.
(A) (Upper) The C-terminal regulatory domain autoinhibited the N-terminal kinase domain through intramolecular interaction. The regulatory domain binds to a pseudo-docking site (blue cylinder tube) within the kinase domain and brings C70 to a close proximity with the kinase domain for autoinhibition. (Lower) Phosphorylation of Chk1 Ser^{317} and Ser^{345} regulates Chk1 localisation and activating ligand/substrate binding. The autoinhibitory intramolecular interaction is disrupted by high-affinity intermolecular interaction between the Chk1 regulatory domain and the docking site of activating ligand/substrate (yellow cylinder tube). This results in the displacement of C70 and Chk1 active conformation which is stabilised by C70 autophosphorylation.

A

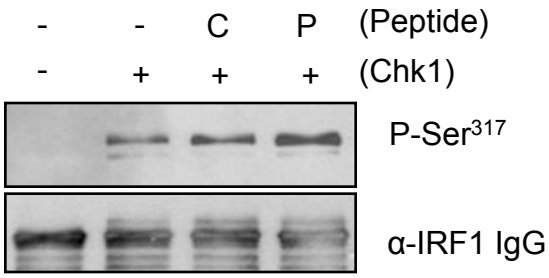

B

^{312}-PVRLPSIQA-^{320}

Figure 5.2 Chk1 phosphorylates IRF1 at Ser^{317} *in vitro*
(A) Kinase reactions containing 100 ng of Chk1 and 350 ng of GST-tagged IRF1 with/without p21 peptide 4 (P) or Chk1 peptide 4 (C) were assembled for 'cold' ATP kinase assay. The reaction products were resolved by 10% SDS-PAGE before transferred to nitrocellulose membrane. Phosphorylation was detected using sheep α-IRF phospho-Ser^{317} IgG and total IRF1 was detected using mouse α-IRF1 IgG. (B) Sequences around IRF1 Ser^{317}.

6. REFERENCES

ABRAHAM, R. T. (2001) Cell cycle checkpoint signaling through the ATM and ATR kinases. *Genes Dev,* 15**,** 2177-96.

ADHIKARY, S. & EILERS, M. (2005) Transcriptional regulation and transformation by Myc proteins. *Nat Rev Mol Cell Biol,* 6**,** 635-45.

AGARWAL, M. K., HASTAK, K., JACKSON, M. W., BREIT, S. N., STARK, G. R. & AGARWAL, M. L. (2006) Macrophage inhibitory cytokine 1 mediates a p53-dependent protective arrest in S phase in response to starvation for DNA precursors. *Proc Natl Acad Sci U S A,* 103**,** 16278-83.

AGARWAL, M. L., AGARWAL, A., TAYLOR, W. R., CHERNOVA, O., SHARMA, Y. & STARK, G. R. (1998) A p53-dependent S-phase checkpoint helps to protect cells from DNA damage in response to starvation for pyrimidine nucleotides. *Proc Natl Acad Sci U S A,* 95**,** 14775-80.

AHN, J., URIST, M. & PRIVES, C. (2004) The Chk2 protein kinase. *DNA Repair (Amst),* 3**,** 1039-47.

AHN, J. Y., LI, X., DAVIS, H. L. & CANMAN, C. E. (2002) Phosphorylation of threonine 68 promotes oligomerization and autophosphorylation of the Chk2 protein kinase via the forkhead-associated domain. *J Biol Chem,* 277**,** 19389-95.

AL-KHODAIRY, F., FOTOU, E., SHELDRICK, K. S., GRIFFITHS, D. J., LEHMANN, A. R. & CARR, A. M. (1994) Identification and characterization of new elements involved in checkpoint and feedback controls in fission yeast. *Mol Biol Cell,* 5**,** 147-60.

ALBERTS, B., JOHNSON, A., LEWIS, J., RAFF, M., KEITH, R. & WALTERS, P. (2002) *Molecular Biology of the Cell,* New York and London, Garland Science.

ANDO, K., OZAKI, T., YAMAMOTO, H., FURUYA, K., HOSODA, M., HAYASHI, S., FUKUZAWA, M. & NAKAGAWARA, A. (2004) Polo-like kinase 1 (Plk1) inhibits p53 function by physical interaction and phosphorylation. *J Biol Chem,* 279**,** 25549-61.

ARANGO, D., MARIADASON, J. M., WILSON, A. J., YANG, W., CORNER, G. A., NICHOLAS, C., ARANES, M. J. & AUGENLICHT, L. H. (2003) c-Myc overexpression sensitises colon cancer cells to camptothecin-induced apoptosis. *Br J Cancer,* 89**,** 1757-65.

ARLANDER, S. J., EAPEN, A. K., VROMAN, B. T., MCDONALD, R. J., TOFT, D. O. & KARNITZ, L. M. (2003) Hsp90 inhibition depletes Chk1 and sensitizes tumor cells to replication stress. *J Biol Chem,* 278**,** 52572-7.

ARLANDER, S. J., FELTS, S. J., WAGNER, J. M., STENSGARD, B., TOFT, D. O. & KARNITZ, L. M. (2006) Chaperoning checkpoint kinase 1 (Chk1), an Hsp90 client, with purified chaperones. *J Biol Chem,* 281**,** 2989-98.

ASADA, M., YAMADA, T., ICHIJO, H., DELIA, D., MIYAZONO, K., FUKUMURO, K. & MIZUTANI, S. (1999) Apoptosis inhibitory activity of cytoplasmic p21(Cip1/WAF1) in monocytic differentiation. *Embo J,* 18**,** 1223-34.

BABER-FURNARI, B. A., RHIND, N., BODDY, M. N., SHANAHAN, P., LOPEZ-GIRONA, A. & RUSSELL, P. (2000) Regulation of mitotic inhibitor Mik1 helps to enforce the DNA damage checkpoint. *Mol Biol Cell,* 11**,** 1-11.

BAKER, D. J., DAWLATY, M. M., GALARDY, P. & VAN DEURSEN, J. M. (2007) Mitotic regulation of the anaphase-promoting complex. *Cell Mol Life Sci,* 64**,** 589-600.

BAKKENIST, C. J. & KASTAN, M. B. (2003) DNA damage activates ATM through intermolecular autophosphorylation and dimer dissociation. *Nature,* 421**,** 499-506.

BALL, K. L., LAIN, S., FAHRAEUS, R., SMYTHE, C. & LANE, D. P. (1997) Cell-cycle arrest and inhibition of Cdk4 activity by small peptides based on the carboxy-terminal domain of p21WAF1. *Curr Biol,* 7**,** 71-80.

BARTEK, J., BARTKOVA, J. & LUKAS, J. (2007) DNA damage signalling guards against activated oncogenes and tumour progression. *Oncogene,* 26**,** 7773-9.

BARTEK, J. & LUKAS, J. (2003) Chk1 and Chk2 kinases in checkpoint control and cancer. *Cancer Cell,* 3**,** 421-9.

BARTEK, J. & LUKAS, J. (2007) DNA damage checkpoints: from initiation to recovery or adaptation. *Curr Opin Cell Biol,* 19**,** 238-45.

BEAN, L. J. & STARK, G. R. (2001) Phosphorylation of serines 15 and 37 is necessary for efficient accumulation of p53 following irradiation with UV. *Oncogene,* 20**,** 1076-84.

BEKKER-JENSEN, S., LUKAS, C., KITAGAWA, R., MELANDER, F., KASTAN, M. B., BARTEK, J. & LUKAS, J. (2006) Spatial organization of the mammalian genome surveillance machinery in response to DNA strand breaks. *J Cell Biol,* 173**,** 195-206.

BENDJENNAT, M., BOULAIRE, J., JASCUR, T., BRICKNER, H., BARBIER, V., SARASIN, A., FOTEDAR, A. & FOTEDAR, R. (2003) UV irradiation triggers ubiquitin-dependent degradation of p21(WAF1) to promote DNA repair. *Cell,* 114**,** 599-610.

BERTONI, F., CODEGONI, A. M., FURLAN, D., TIBILETTI, M. G., CAPELLA, C. & BROGGINI, M. (1999) CHK1 frameshift mutations in genetically unstable colorectal and endometrial cancers. *Genes Chromosomes Cancer,* 26**,** 176-80.

BERWICK, D. C. & TAVARE, J. M. (2004) Identifying protein kinase substrates: hunting for the organ-grinder's monkeys. *Trends Biochem Sci,* 29**,** 227-32.

BEUSCHER, H. U., NICKELLS, M. W. & COLTEN, H. R. (1988) The precursor of interleukin-1 alpha is phosphorylated at residue serine 90. *J Biol Chem,* 263**,** 4023-8.

BHATTACHARYYA, R. P., REMENYI, A., GOOD, M. C., BASHOR, C. J., FALICK, A. M. & LIM, W. A. (2006) The Ste5 scaffold allosterically modulates signaling output of the yeast mating pathway. *Science,* 311**,** 822-6.

BI, X., BARKLEY, L. R., SLATER, D. M., TATEISHI, S., YAMAIZUMI, M., OHMORI, H. & VAZIRI, C. (2006) Rad18 regulates DNA polymerase kappa and is required for recovery from S-phase checkpoint-mediated arrest. *Mol Cell Biol,* 26**,** 3527-40.

BIGGS, J. R., KUDLOW, J. E. & KRAFT, A. S. (1996) The role of the transcription factor Sp1 in regulating the expression of the WAF1/CIP1 gene in U937 leukemic cells. *J Biol Chem,* 271**,** 901-6.

BILLON, N., CARLISI, D., DATTO, M. B., VAN GRUNSVEN, L. A., WATT, A., WANG, X. F. & RUDKIN, B. B. (1999) Cooperation of Sp1 and p300 in the induction of the CDK inhibitor p21WAF1/CIP1 during NGF-mediated neuronal differentiation. *Oncogene,* 18**,** 2872-82.

BLAGOSKLONNY, M. V. (2002) Are p27 and p21 cytoplasmic oncoproteins? *Cell Cycle,* 1**,** 391-3.

BLASINA, A., DE WEYER, I. V., LAUS, M. C., LUYTEN, W. H., PARKER, A. E. & MCGOWAN, C. H. (1999) A human homologue of the checkpoint kinase Cds1 directly inhibits Cdc25 phosphatase. *Curr Biol,* 9**,** 1-10.

BLETHROW, J. D., GLAVY, J. S., MORGAN, D. O. & SHOKAT, K. M. (2008) Covalent capture of kinase-specific phosphopeptides reveals Cdk1-cyclin B substrates. *Proc Natl Acad Sci U S A,* 105**,** 1442-7.

BLOOM, J., AMADOR, V., BARTOLINI, F., DEMARTINO, G. & PAGANO, M. (2003) Proteasome-mediated degradation of p21 via N-terminal ubiquitinylation. *Cell,* 115**,** 71-82.

BLOOM, J. & PAGANO, M. (2004) To be or not to be ubiquitinated? *Cell Cycle,* 3**,** 138-40.

BOGOYEVITCH, M. A., BARR, R. K. & KETTERMAN, A. J. (2005) Peptide inhibitors of protein kinases-discovery, characterisation and use. *Biochim Biophys Acta,* 1754**,** 79-99.

BORGES, H. L., LINDEN, R. & WANG, J. Y. (2008) DNA damage-induced cell death: lessons from the central nervous system. *Cell Res,* 18**,** 17-26.

BRENNER, C., DEPLUS, R., DIDELOT, C., LORIOT, A., VIRE, E., DE SMET, C., GUTIERREZ, A., DANOVI, D., BERNARD, D., BOON, T., PELICCI, P. G., AMATI, B., KOUZARIDES, T., DE LAUNOIT, Y., DI CROCE, L. & FUKS, F. (2005) Myc represses transcription through recruitment of DNA methyltransferase corepressor. *Embo J,* 24**,** 336-46.

BRONDELLO, J. M., DUCOMMUN, B., FERNANDEZ, A. & LAMB, N. J. (2007) Linking PCNA-dependent replication and ATR by human Claspin. *Biochem Biophys Res Commun,* 354**,** 1028-33.

BROWN, E. J. & BALTIMORE, D. (2000) ATR disruption leads to chromosomal fragmentation and early embryonic lethality. *Genes Dev,* 14**,** 397-402.

BULAVIN, D. V., HIGASHIMOTO, Y., DEMIDENKO, Z. N., MEEK, S., GRAVES, P., PHILLIPS, C., ZHAO, H., MOODY, S. A., APPELLA, E., PIWNICA-WORMS, H. & FORNACE, A. J., JR. (2003) Dual phosphorylation controls Cdc25 phosphatases and mitotic entry. *Nat Cell Biol,* 5**,** 545-51.

BUNCH, R. T. & EASTMAN, A. (1996) Enhancement of cisplatin-induced cytotoxicity by 7-hydroxystaurosporine (UCN-01), a new G2-checkpoint inhibitor. *Clin Cancer Res,* 2**,** 791-7.

CAMPISI, J. & D'ADDA DI FAGAGNA, F. (2007) Cellular senescence: when bad things happen to good cells. *Nat Rev Mol Cell Biol,* 8**,** 729-40.

CANDE, C., CECCONI, F., DESSEN, P. & KROEMER, G. (2002) Apoptosis-inducing factor (AIF): key to the conserved caspase-independent pathways of cell death? *J Cell Sci,* 115**,** 4727-34.

CARTER, A. D. & SIBLE, J. C. (2003) Loss of XChk1 function triggers apoptosis after the midblastula transition in Xenopus laevis embryos. *Mech Dev,* 120**,** 315-23.

CASINI, T. & PELICCI, P. G. (1999) A function of p21 during promyelocytic leukemia cell differentiation independent of CDK inhibition and cell cycle arrest. *Oncogene,* 18**,** 3235-43.

CAYROL, C. & DUCOMMUN, B. (1998) Interaction with cyclin-dependent kinases and PCNA modulates proteasome-dependent degradation of p21. *Oncogene,* 17**,** 2437-44.

CHANG, C. I., XU, B. E., AKELLA, R., COBB, M. H. & GOLDSMITH, E. J. (2002) Crystal structures of MAP kinase p38 complexed to the docking sites on its nuclear substrate MEF2A and activator MKK3b. *Mol Cell,* 9**,** 1241-9.

CHEHAB, N. H., MALIKZAY, A., STAVRIDI, E. S. & HALAZONETIS, T. D. (1999) Phosphorylation of Ser-20 mediates stabilization of human p53 in response to DNA damage. *Proc Natl Acad Sci U S A,* 96**,** 13777-82.

CHEN, I. T., AKAMATSU, M., SMITH, M. L., LUNG, F. D., DUBA, D., ROLLER, P. P., FORNACE, A. J., JR. & O'CONNOR, P. M. (1996a) Characterization of p21Cip1/Waf1 peptide domains required for cyclin E/Cdk2 and PCNA interaction. *Oncogene,* 12**,** 595-607.

CHEN, J., JACKSON, P. K., KIRSCHNER, M. W. & DUTTA, A. (1995) Separate domains of p21 involved in the inhibition of Cdk kinase and PCNA. *Nature,* 374**,** 386-8.

CHEN, J., SAHA, P., KORNBLUTH, S., DYNLACHT, B. D. & DUTTA, A. (1996b) Cyclin-binding motifs are essential for the function of p21CIP1. *Mol Cell Biol,* 16**,** 4673-82.

CHEN, M. S., RYAN, C. E. & PIWNICA-WORMS, H. (2003a) Chk1 kinase negatively regulates mitotic function of Cdc25A phosphatase through 14-3-3 binding. *Mol Cell Biol,* 23**,** 7488-97.

CHEN, P., LUO, C., DENG, Y., RYAN, K., REGISTER, J., MARGOSIAK, S., TEMPCZYK-RUSSELL, A., NGUYEN, B., MYERS, P., LUNDGREN, K., KAN, C. C. & O'CONNOR, P. M. (2000) The 1.7 A crystal structure of human cell cycle checkpoint kinase Chk1: implications for Chk1 regulation. *Cell,* 100**,** 681-92.

CHEN, Y. & SANCHEZ, Y. (2004) Chk1 in the DNA damage response: conserved roles from yeasts to mammals. *DNA Repair (Amst),* 3**,** 1025-32.

CHEN, Z., XIAO, Z., CHEN, J., NG, S. C., SOWIN, T., SHAM, H., ROSENBERG, S., FESIK, S. & ZHANG, H. (2003b) Human Chk1 expression is dispensable for somatic cell death and critical for sustaining G2 DNA damage checkpoint. *Mol Cancer Ther,* 2**,** 543-8.

CHEN, Z., XIAO, Z., GU, W. Z., XUE, J., BUI, M. H., KOVAR, P., LI, G., WANG, G., TAO, Z. F., TONG, Y., LIN, N. H., SHAM, H. L., WANG, J. Y., SOWIN, T. J., ROSENBERG, S. H. & ZHANG, H. (2006) Selective Chk1 inhibitors differentially sensitize p53-deficient cancer cells to cancer therapeutics. *Int J Cancer,* 119**,** 2784-94.

CHILD, E. S. & MANN, D. J. (2006) The intricacies of p21 phosphorylation: protein/protein interactions, subcellular localization and stability. *Cell Cycle,* 5**,** 1313-9.

CHINI, C. C. & CHEN, J. (2003) Human claspin is required for replication checkpoint control. *J Biol Chem,* 278**,** 30057-62.
CHINI, C. C. & CHEN, J. (2006) Repeated phosphopeptide motifs in human Claspin are phosphorylated by Chk1 and mediate Claspin function. *J Biol Chem,* 281**,** 33276-82.
CHINI, C. C., WOOD, J. & CHEN, J. (2006) Chk1 is required to maintain Claspin stability. *Oncogene*.
CHO, S. H., TOOULI, C. D., FUJII, G. H., CRAIN, C. & PARRY, D. (2005) Chk1 is essential for tumor cell viability following activation of the replication checkpoint. *Cell Cycle,* 4**,** 131-9.
CHUANG, L. S., IAN, H. I., KOH, T. W., NG, H. H., XU, G. & LI, B. F. (1997) Human DNA-(cytosine-5) methyltransferase-PCNA complex as a target for p21WAF1. *Science,* 277**,** 1996-2000.
CLAASSEN, G. F. & HANN, S. R. (2000) A role for transcriptional repression of p21CIP1 by c-Myc in overcoming transforming growth factor beta - induced cell-cycle arrest. *Proc Natl Acad Sci U S A,* 97**,** 9498-503.
CLARKE, C. A., BENNETT, L. N. & CLARKE, P. R. (2005) Cleavage of claspin by caspase-7 during apoptosis inhibits the CHK1 pathway. *J Biol Chem*.
CLARKE, C. A. & CLARKE, P. R. (2005) DNA-dependent phosphorylation of Chk1 and Claspin in a human cell-free system. *Biochem J,* 388**,** 705-12.
COLLINS, I. & GARRETT, M. D. (2005) Targeting the cell division cycle in cancer: CDK and cell cycle checkpoint kinase inhibitors. *Curr Opin Pharmacol,* 5**,** 366-73.
COLMAN, M. S., AFSHARI, C. A. & BARRETT, J. C. (2000) Regulation of p53 stability and activity in response to genotoxic stress. *Mutat Res,* 462**,** 179-88.
COWLING, V. H. & COLE, M. D. (2006) Mechanism of transcriptional activation by the Myc oncoproteins. *Semin Cancer Biol,* 16**,** 242-52.
CRAIG, A., SCOTT, M., BURCH, L., SMITH, G., BALL, K. & HUPP, T. (2003) Allosteric effects mediate CHK2 phosphorylation of the p53 transactivation domain. *EMBO Rep,* 4**,** 787-92.
CURMAN, D., CINEL, B., WILLIAMS, D. E., RUNDLE, N., BLOCK, W. D., GOODARZI, A. A., HUTCHINS, J. R., CLARKE, P. R., ZHOU, B. B., LEES-MILLER, S. P., ANDERSEN, R. J. & ROBERGE, M. (2001) Inhibition of the G2 DNA damage checkpoint and of protein kinases Chk1 and Chk2 by the marine sponge alkaloid debromohymenialdisine. *J Biol Chem,* 276**,** 17914-9.
DALAL, S. N., SCHWEITZER, C. M., GAN, J. & DECAPRIO, J. A. (1999) Cytoplasmic localization of human cdc25C during interphase requires an intact 14-3-3 binding site. *Mol Cell Biol,* 19**,** 4465-79.
DANG, T., BAO, S. & WANG, X. F. (2005) Human Rad9 is required for the activation of S-phase checkpoint and the maintenance of chromosomal stability. *Genes Cells,* 10**,** 287-95.
DASH, B. C. & EL-DEIRY, W. S. (2005) Phosphorylation of p21 in G2/M promotes cyclin B-Cdc2 kinase activity. *Mol Cell Biol,* 25**,** 3364-87.
DE BOER, L., OAKES, V., BEAMISH, H., GILES, N., STEVENS, F., SOMODEVILLA-TORRES, M., DESOUZA, C. & GABRIELLI, B. (2008)

Cyclin A/cdk2 coordinates centrosomal and nuclear mitotic events. *Oncogene,* 27**,** 4261-8.
DELAVAINE, L. & LA THANGUE, N. B. (1999) Control of E2F activity by p21Waf1/Cip1. *Oncogene,* 18**,** 5381-92.
DI CUNTO, F., TOPLEY, G., CALAUTTI, E., HSIAO, J., ONG, L., SETH, P. K. & DOTTO, G. P. (1998) Inhibitory function of p21Cip1/WAF1 in differentiation of primary mouse keratinocytes independent of cell cycle control. *Science,* 280**,** 1069-72.
DI LEONARDO, A., LINKE, S. P., CLARKIN, K. & WAHL, G. M. (1994) DNA damage triggers a prolonged p53-dependent G1 arrest and long-term induction of Cip1 in normal human fibroblasts. *Genes Dev,* 8**,** 2540-51.
DINARELLO, C. A. (1994) The interleukin-1 family: 10 years of discovery. *Faseb J,* 8**,** 1314-25.
DODSON, G. E., SHI, Y. & TIBBETTS, R. S. (2004) DNA replication defects, spontaneous DNA damage, and ATM-dependent checkpoint activation in replication protein A-deficient cells. *J Biol Chem,* 279**,** 34010-4.
DONJERKOVIC, D. & SCOTT, D. W. (2000) Regulation of the G1 phase of the mammalian cell cycle. *Cell Res,* 10**,** 1-16.
DOTTO, G. P. (2000) p21(WAF1/Cip1): more than a break to the cell cycle? *Biochim Biophys Acta,* 1471**,** M43-56.
DOXSEY, S. J. (2001) Centrosomes as command centres for cellular control. *Nat Cell Biol,* 3**,** E105-8.
EBLEN, S. T., KUMAR, N. V., SHAH, K., HENDERSON, M. J., WATTS, C. K., SHOKAT, K. M. & WEBER, M. J. (2003) Identification of novel ERK2 substrates through use of an engineered kinase and ATP analogs. *J Biol Chem,* 278**,** 14926-35.
EJIMA, Y. & YANG, L. (1999) Determination of the genotype of a panel of human tumor cell lines for the human homologues of yeast cell cycle checkpoint control genes: identification of cell lines carrying homoallelic missense base substitutions. *Somat Cell Mol Genet,* 25**,** 41-8.
EKHOLM, S. V. & REED, S. I. (2000) Regulation of G(1) cyclin-dependent kinases in the mammalian cell cycle. *Curr Opin Cell Biol,* 12**,** 676-84.
EL-DEIRY, W. S., TOKINO, T., VELCULESCU, V. E., LEVY, D. B., PARSONS, R., TRENT, J. M., LIN, D., MERCER, W. E., KINZLER, K. W. & VOGELSTEIN, B. (1993) WAF1, a potential mediator of p53 tumor suppression. *Cell,* 75**,** 817-25.
EL-DEIRY, W. S., TOKINO, T., WALDMAN, T., OLINER, J. D., VELCULESCU, V. E., BURRELL, M., HILL, D. E., HEALY, E., REES, J. L., HAMILTON, S. R. & ET AL. (1995) Topological control of p21WAF1/CIP1 expression in normal and neoplastic tissues. *Cancer Res,* 55**,** 2910-9.
ESPANEL, X., WALCHLI, S., RUCKLE, T., HARRENGA, A., HUGUENIN-REGGIANI, M. & HOOFT VAN HUIJSDUIJNEN, R. (2003) Mapping of synergistic components of weakly interacting protein-protein motifs using arrays of paired peptides. *J Biol Chem,* 278**,** 15162-7.
FALCK, J., MAILAND, N., SYLJUASEN, R. G., BARTEK, J. & LUKAS, J. (2001) The ATM-Chk2-Cdc25A checkpoint pathway guards against radioresistant DNA synthesis. *Nature,* 410**,** 842-7.

FANG, G., YU, H. & KIRSCHNER, M. W. (1999) Control of mitotic transitions by the anaphase-promoting complex. *Philos Trans R Soc Lond B Biol Sci,* 354**,** 1583-90.

FEIJOO, C., HALL-JACKSON, C., WU, R., JENKINS, D., LEITCH, J., GILBERT, D. M. & SMYTHE, C. (2001) Activation of mammalian Chk1 during DNA replication arrest: a role for Chk1 in the intra-S phase checkpoint monitoring replication origin firing. *J Cell Biol,* 154**,** 913-23.

FERNANDEZ-CAPETILLO, O., LEE, A., NUSSENZWEIG, M. & NUSSENZWEIG, A. (2004) H2AX: the histone guardian of the genome. *DNA Repair (Amst),* 3**,** 959-67.

FOGARTY, P., CAMPBELL, S. D., ABU-SHUMAYS, R., PHALLE, B. S., YU, K. R., UY, G. L., GOLDBERG, M. L. & SULLIVAN, W. (1997) The Drosophila grapes gene is related to checkpoint gene chk1/rad27 and is required for late syncytial division fidelity. *Curr Biol,* 7**,** 418-26.

FORAY, N., MAROT, D., GABRIEL, A., RANDRIANARISON, V., CARR, A. M., PERRICAUDET, M., ASHWORTH, A. & JEGGO, P. (2003) A subset of ATM- and ATR-dependent phosphorylation events requires the BRCA1 protein. *Embo J,* 22**,** 2860-71.

FOTEDAR, R., BENDJENNAT, M. & FOTEDAR, A. (2004) Role of p21WAF1 in the cellular response to UV. *Cell Cycle,* 3**,** 134-7.

FOTEDAR, R., FITZGERALD, P., ROUSSELLE, T., CANNELLA, D., DOREE, M., MESSIER, H. & FOTEDAR, A. (1996) p21 contains independent binding sites for cyclin and cdk2: both sites are required to inhibit cdk2 kinase activity. *Oncogene,* 12**,** 2155-64.

FRASER, J. A. & HUPP, T. R. (2007) Chemical genetics approach to identify peptide ligands that selectively stimulate DAPK-1 kinase activity. *Biochemistry,* 46**,** 2655-73.

FROUIN, I., MAGA, G., DENEGRI, M., RIVA, F., SAVIO, M., SPADARI, S., PROSPERI, E. & SCOVASSI, A. I. (2003) Human proliferating cell nuclear antigen, poly(ADP-ribose) polymerase-1, and p21waf1/cip1. A dynamic exchange of partners. *J Biol Chem,* 278**,** 39265-8.

FUNK, J. O., WAGA, S., HARRY, J. B., ESPLING, E., STILLMAN, B. & GALLOWAY, D. A. (1997) Inhibition of CDK activity and PCNA-dependent DNA replication by p21 is blocked by interaction with the HPV-16 E7 oncoprotein. *Genes Dev,* 11**,** 2090-100.

GABAI, V. L., O'CALLAGHAN-SUNOL, C., MENG, L., SHERMAN, M. Y. & YAGLOM, J. (2008) Triggering senescence programs suppresses Chk1 kinase and sensitizes cells to genotoxic stresses. *Cancer Res,* 68**,** 1834-42.

GALEA, C. A., WANG, Y., SIVAKOLUNDU, S. G. & KRIWACKI, R. W. (2008) Regulation of cell division by intrinsically unstructured proteins: intrinsic flexibility, modularity, and signaling conduits. *Biochemistry,* 47**,** 7598-609.

GARCIA-WILSON, E. & PERKINS, N. D. (2005) p21WAF1/CIP1 regulates the p300 sumoylation motif CRD1 through a C-terminal domain independently of cyclin/CDK binding. *Cell Cycle,* 4**,** 1113-9.

GARTEL, A. L. & RADHAKRISHNAN, S. K. (2005) Lost in transcription: p21 repression, mechanisms, and consequences. *Cancer Res,* 65**,** 3980-5.

GARTEL, A. L. & TYNER, A. L. (1999) Transcriptional regulation of the p21((WAF1/CIP1)) gene. *Exp Cell Res,* 246**,** 280-9.

GATEI, M., SLOPER, K., SORENSEN, C., SYLJUASEN, R., FALCK, J., HOBSON, K., SAVAGE, K., LUKAS, J., ZHOU, B. B., BARTEK, J. & KHANNA, K. K. (2003) Ataxia-telangiectasia-mutated (ATM) and NBS1-dependent phosphorylation of Chk1 on Ser-317 in response to ionizing radiation. *J Biol Chem,* 278**,** 14806-11.

GERVAIS, J. L., SETH, P. & ZHANG, H. (1998) Cleavage of CDK inhibitor p21(Cip1/Waf1) by caspases is an early event during DNA damage-induced apoptosis. *J Biol Chem,* 273**,** 19207-12.

GOLDSMITH, E. J., AKELLA, R., MIN, X., ZHOU, T. & HUMPHREYS, J. M. (2007) Substrate and docking interactions in serine/threonine protein kinases. *Chem Rev,* 107**,** 5065-81.

GONG, D., POMERENING, J. R., MYERS, J. W., GUSTAVSSON, C., JONES, J. T., HAHN, A. T., MEYER, T. & FERRELL, J. E., JR. (2007) Cyclin A2 regulates nuclear-envelope breakdown and the nuclear accumulation of cyclin B1. *Curr Biol,* 17**,** 85-91.

GOTTIFREDI, V., KARNI-SCHMIDT, O., SHIEH, S. S. & PRIVES, C. (2001) p53 down-regulates CHK1 through p21 and the retinoblastoma protein. *Mol Cell Biol,* 21**,** 1066-76.

GROTH, A., LUKAS, J., NIGG, E. A., SILLJE, H. H., WERNSTEDT, C., BARTEK, J. & HANSEN, K. (2003) Human Tousled like kinases are targeted by an ATM- and Chk1-dependent DNA damage checkpoint. *Embo J,* 22**,** 1676-87.

GUI, C. Y., NGO, L., XU, W. S., RICHON, V. M. & MARKS, P. A. (2004) Histone deacetylase (HDAC) inhibitor activation of p21WAF1 involves changes in promoter-associated proteins, including HDAC1. *Proc Natl Acad Sci U S A,* 101**,** 1241-6.

GULBIS, J. M., KELMAN, Z., HURWITZ, J., O'DONNELL, M. & KURIYAN, J. (1996) Structure of the C-terminal region of p21(WAF1/CIP1) complexed with human PCNA. *Cell,* 87**,** 297-306.

HARPER, J. W. (1997) Cyclin dependent kinase inhibitors. *Cancer Surv,* 29**,** 91-107.

HARPER, J. W., ADAMI, G. R., WEI, N., KEYOMARSI, K. & ELLEDGE, S. J. (1993) The p21 Cdk-interacting protein Cip1 is a potent inhibitor of G1 cyclin-dependent kinases. *Cell,* 75**,** 805-16.

HARUKI, N., SAITO, H., TATEMATSU, Y., KONISHI, H., HARANO, T., MASUDA, A., OSADA, H., FUJII, Y. & TAKAHASHI, T. (2000) Histological type-selective, tumor-predominant expression of a novel CHK1 isoform and infrequent in vivo somatic CHK2 mutation in small cell lung cancer. *Cancer Res,* 60**,** 4689-92.

HASTAK, K., PAUL, R. K., AGARWAL, M. K., THAKUR, V. S., AMIN, A. R., AGRAWAL, S., SRAMKOSKI, R. M., JACOBBERGER, J. W., JACKSON, M. W., STARK, G. R. & AGARWAL, M. L. (2008) DNA synthesis from unbalanced nucleotide pools causes limited DNA damage that triggers ATR-CHK1-dependent p53 activation. *Proc Natl Acad Sci U S A,* 105**,** 6314-9.

HEFFERNAN, T. P., SIMPSON, D. A., FRANK, A. R., HEINLOTH, A. N., PAULES, R. S., CORDEIRO-STONE, M. & KAUFMANN, W. K. (2002)

An ATR- and Chk1-dependent S checkpoint inhibits replicon initiation following UVC-induced DNA damage. *Mol Cell Biol,* 22**,** 8552-61.

HEKMAT-NEJAD, M., YOU, Z., YEE, M. C., NEWPORT, J. W. & CIMPRICH, K. A. (2000) Xenopus ATR is a replication-dependent chromatin-binding protein required for the DNA replication checkpoint. *Curr Biol,* 10**,** 1565-73.

HENON, H., MESSAOUDI, S., ANIZON, F., ABOAB, B., KUCHARCZYK, N., LEONCE, S., GOLSTEYN, R. M., PFEIFFER, B. & PRUDHOMME, M. (2007) Bis-imide granulatimide analogues as potent Checkpoint 1 kinase inhibitors. *Eur J Pharmacol,* 554**,** 106-12.

HERBIG, U., JOBLING, W. A., CHEN, B. P., CHEN, D. J. & SEDIVY, J. M. (2004) Telomere shortening triggers senescence of human cells through a pathway involving ATM, p53, and p21(CIP1), but not p16(INK4a). *Mol Cell,* 14**,** 501-13.

HIRAO, A., KONG, Y. Y., MATSUOKA, S., WAKEHAM, A., RULAND, J., YOSHIDA, H., LIU, D., ELLEDGE, S. J. & MAK, T. W. (2000) DNA damage-induced activation of p53 by the checkpoint kinase Chk2. *Science,* 287**,** 1824-7.

HO, A. & DOWDY, S. F. (2002) Regulation of G(1) cell-cycle progression by oncogenes and tumor suppressor genes. *Curr Opin Genet Dev,* 12**,** 47-52.

HOUTGRAAF, J. H., VERSMISSEN, J. & VAN DER GIESSEN, W. J. (2006) A concise review of DNA damage checkpoints and repair in mammalian cells. *Cardiovasc Revasc Med,* 7**,** 165-72.

HU, B., ZHOU, X. Y., WANG, X., ZENG, Z. C., ILIAKIS, G. & WANG, Y. (2001) The radioresistance to killing of A1-5 cells derives from activation of the Chk1 pathway. *J Biol Chem,* 276**,** 17693-8.

HUSE, M. & KURIYAN, J. (2002) The conformational plasticity of protein kinases. *Cell,* 109**,** 275-82.

HUTCHINS, J. R., HUGHES, M. & CLARKE, P. R. (2000) Substrate specificity determinants of the checkpoint protein kinase Chk1. *FEBS Lett,* 466**,** 91-5.

HUTCHISON, C. & GLOVER, D. M. (1995) *Cell Cycle Control,* New York, IRL Press.

JACKMAN, M., LINDON, C., NIGG, E. A. & PINES, J. (2003) Active cyclin B1-Cdk1 first appears on centrosomes in prophase. *Nat Cell Biol,* 5**,** 143-8.

JACKSON, J. R., GILMARTIN, A., IMBURGIA, C., WINKLER, J. D., MARSHALL, L. A. & ROSHAK, A. (2000) An indolocarbazole inhibitor of human checkpoint kinase (Chk1) abrogates cell cycle arrest caused by DNA damage. *Cancer Res,* 60**,** 566-72.

JACOBS, J. J. & DE LANGE, T. (2005) p16INK4a as a second effector of the telomere damage pathway. *Cell Cycle,* 4**,** 1364-8.

JASCUR, T., BRICKNER, H., SALLES-PASSADOR, I., BARBIER, V., EL KHISSIIN, A., SMITH, B., FOTEDAR, R. & FOTEDAR, A. (2005) Regulation of p21(WAF1/CIP1) stability by WISp39, a Hsp90 binding TPR protein. *Mol Cell,* 17**,** 237-49.

JEONG, S. Y., KUMAGAI, A., LEE, J. & DUNPHY, W. G. (2003) Phosphorylated claspin interacts with a phosphate-binding site in the kinase domain of Chk1 during ATR-mediated activation. *J Biol Chem,* 278**,** 46782-8.

JIANG, K., PEREIRA, E., MAXFIELD, M., RUSSELL, B., GOUDELOCK, D. M. & SANCHEZ, Y. (2003) Regulation of Chk1 includes chromatin association and 14-3-3 binding following phosphorylation on Ser-345. *J Biol Chem,* 278**,** 25207-17.

JIANG, X., ZHAO, B., BRITTON, R., LIM, L. Y., LEONG, D., SANGHERA, J. S., ZHOU, B. B., PIERS, E., ANDERSEN, R. J. & ROBERGE, M. (2004) Inhibition of Chk1 by the G2 DNA damage checkpoint inhibitor isogranulatimide. *Mol Cancer Ther,* 3**,** 1221-7.

KANNOUCHE, P. L., WING, J. & LEHMANN, A. R. (2004) Interaction of human DNA polymerase eta with monoubiquitinated PCNA: a possible mechanism for the polymerase switch in response to DNA damage. *Mol Cell,* 14**,** 491-500.

KASTAN, M. B. & LIM, D. S. (2000) The many substrates and functions of ATM. *Nat Rev Mol Cell Biol,* 1**,** 179-86.

KATSURAGI, Y. & SAGATA, N. (2004) Regulation of Chk1 kinase by autoinhibition and ATR-mediated phosphorylation. *Mol Biol Cell,* 15**,** 1680-9.

KHANNA, K. K. & JACKSON, S. P. (2001) DNA double-strand breaks: signaling, repair and the cancer connection. *Nat Genet,* 27**,** 247-54.

KIM, G. Y., MERCER, S. E., EWTON, D. Z., YAN, Z., JIN, K. & FRIEDMAN, E. (2002) The stress-activated protein kinases p38 alpha and JNK1 stabilize p21(Cip1) by phosphorylation. *J Biol Chem,* 277**,** 29792-802.

KIM, R. (2005) Recent advances in understanding the cell death pathways activated by anticancer therapy. *Cancer,* 103**,** 1551-60.

KIM, S. T., LIM, D. S., CANMAN, C. E. & KASTAN, M. B. (1999) Substrate specificities and identification of putative substrates of ATM kinase family members. *J Biol Chem,* 274**,** 37538-43.

KING, F. W., SKEEN, J., HAY, N. & SHTIVELMAN, E. (2004) Inhibition of Chk1 by activated PKB/Akt. *Cell Cycle,* 3**,** 634-7.

KITAURA, H., SHINSHI, M., UCHIKOSHI, Y., ONO, T., IGUCHI-ARIGA, S. M. & ARIGA, H. (2000) Reciprocal regulation via protein-protein interaction between c-Myc and p21(cip1/waf1/sdi1) in DNA replication and transcription. *J Biol Chem,* 275**,** 10477-83.

KOPS, G. J., WEAVER, B. A. & CLEVELAND, D. W. (2005) On the road to cancer: aneuploidy and the mitotic checkpoint. *Nat Rev Cancer,* 5**,** 773-85.

KOSOY, A. & O'CONNELL, M. J. (2008) Regulation of Chk1 by Its C-terminal Domain. *Mol Biol Cell*.

KRAMER, A., LUKAS, J. & BARTEK, J. (2004a) Checking out the centrosome. *Cell Cycle,* 3**,** 1390-3.

KRAMER, A., MAILAND, N., LUKAS, C., SYLJUASEN, R. G., WILKINSON, C. J., NIGG, E. A., BARTEK, J. & LUKAS, J. (2004b) Centrosome-associated Chk1 prevents premature activation of cyclin-B-Cdk1 kinase. *Nat Cell Biol,* 6**,** 884-91.

KRIWACKI, R. W., HENGST, L., TENNANT, L., REED, S. I. & WRIGHT, P. E. (1996) Structural studies of p21Waf1/Cip1/Sdi1 in the free and Cdk2-bound state: conformational disorder mediates binding diversity. *Proc Natl Acad Sci U S A,* 93**,** 11504-9.

KUMAGAI, A. & DUNPHY, W. G. (2000) Claspin, a novel protein required for the activation of Chk1 during a DNA replication checkpoint response in Xenopus egg extracts. *Mol Cell,* 6**,** 839-49.

KUMAGAI, A. & DUNPHY, W. G. (2003) Repeated phosphopeptide motifs in Claspin mediate the regulated binding of Chk1. *Nat Cell Biol,* 5**,** 161-5.

KUMAGAI, A., KIM, S. M. & DUNPHY, W. G. (2004) Claspin and the activated form of ATR-ATRIP collaborate in the activation of Chk1. *J Biol Chem,* 279**,** 49599-608.

KUMAGAI, A., LEE, J., YOO, H. Y. & DUNPHY, W. G. (2006) TopBP1 activates the ATR-ATRIP complex. *Cell,* 124**,** 943-55.

KURZ, E. U., DOUGLAS, P. & LEES-MILLER, S. P. (2004) Doxorubicin activates ATM-dependent phosphorylation of multiple downstream targets in part through the generation of reactive oxygen species. *J Biol Chem,* 279**,** 53272-81.

KURZ, E. U. & LEES-MILLER, S. P. (2004) DNA damage-induced activation of ATM and ATM-dependent signaling pathways. *DNA Repair (Amst),* 3**,** 889-900.

LABAER, J., GARRETT, M. D., STEVENSON, L. F., SLINGERLAND, J. M., SANDHU, C., CHOU, H. S., FATTAEY, A. & HARLOW, E. (1997) New functional activities for the p21 family of CDK inhibitors. *Genes Dev,* 11**,** 847-62.

LACY, E. R., FILIPPOV, I., LEWIS, W. S., OTIENO, S., XIAO, L., WEISS, S., HENGST, L. & KRIWACKI, R. W. (2004) p27 binds cyclin-CDK complexes through a sequential mechanism involving binding-induced protein folding. *Nat Struct Mol Biol,* 11**,** 358-64.

LAGGER, G., DOETZLHOFER, A., SCHUETTENGRUBER, B., HAIDWEGER, E., SIMBOECK, E., TISCHLER, J., CHIOCCA, S., SUSKE, G., ROTHENEDER, H., WINTERSBERGER, E. & SEISER, C. (2003) The tumor suppressor p53 and histone deacetylase 1 are antagonistic regulators of the cyclin-dependent kinase inhibitor p21/WAF1/CIP1 gene. *Mol Cell Biol,* 23**,** 2669-79.

LAM, M. H., LIU, Q., ELLEDGE, S. J. & ROSEN, J. M. (2004) Chk1 is haploinsufficient for multiple functions critical to tumor suppression. *Cancer Cell,* 6**,** 45-59.

LEE, C. H. & CHUNG, J. H. (2001) The hCds1 (Chk2)-FHA domain is essential for a chain of phosphorylation events on hCds1 that is induced by ionizing radiation. *J Biol Chem,* 276**,** 30537-41.

LEE, J., GOLD, D. A., SHEVCHENKO, A., SHEVCHENKO, A. & DUNPHY, W. G. (2005) Roles of Replication Fork-interacting and Chk1-activating Domains from Claspin in a DNA Replication Checkpoint Response. *Mol Biol Cell*.

LEE, J., KUMAGAI, A. & DUNPHY, W. G. (2001) Positive regulation of Wee1 by Chk1 and 14-3-3 proteins. *Mol Biol Cell,* 12**,** 551-63.

LEE, J., KUMAGAI, A. & DUNPHY, W. G. (2003) Claspin, a Chk1-regulatory protein, monitors DNA replication on chromatin independently of RPA, ATR, and Rad17. *Mol Cell,* 11**,** 329-40.

LEE, J. H. & PAULL, T. T. (2005) ATM activation by DNA double-strand breaks through the Mre11-Rad50-Nbs1 complex. *Science,* 308**,** 551-4.

LEE, J. H. & PAULL, T. T. (2007) Activation and regulation of ATM kinase activity in response to DNA double-strand breaks. *Oncogene,* 26**,** 7741-8.
LEE, J. Y., YU, S. J., PARK, Y. G., KIM, J. & SOHN, J. (2007) Glycogen synthase kinase 3beta phosphorylates p21WAF1/CIP1 for proteasomal degradation after UV irradiation. *Mol Cell Biol,* 27**,** 3187-98.
LIANG, J. & SLINGERLAND, J. M. (2003) Multiple roles of the PI3K/PKB (Akt) pathway in cell cycle progression. *Cell Cycle,* 2**,** 339-45.
LIN, S. Y., LI, K., STEWART, G. S. & ELLEDGE, S. J. (2004) Human Claspin works with BRCA1 to both positively and negatively regulate cell proliferation. *Proc Natl Acad Sci U S A,* 101**,** 6484-9.
LING, Y. H., ZOU, Y. & PEREZ-SOLER, R. (2000) Induction of senescence-like phenotype and loss of paclitaxel sensitivity after wild-type p53 gene transfection of p53-null human non-small cell lung cancer H358 cells. *Anticancer Res,* 20**,** 693-702.
LINKE, S. P., CLARKIN, K. C., DI LEONARDO, A., TSOU, A. & WAHL, G. M. (1996) A reversible, p53-dependent G0/G1 cell cycle arrest induced by ribonucleotide depletion in the absence of detectable DNA damage. *Genes Dev,* 10**,** 934-47.
LIU, Q., GUNTUKU, S., CUI, X. S., MATSUOKA, S., CORTEZ, D., TAMAI, K., LUO, G., CARATTINI-RIVERA, S., DEMAYO, F., BRADLEY, A., DONEHOWER, L. A. & ELLEDGE, S. J. (2000) Chk1 is an essential kinase that is regulated by Atr and required for the G(2)/M DNA damage checkpoint. *Genes Dev,* 14**,** 1448-59.
LIU, S., BEKKER-JENSEN, S., MAILAND, N., LUKAS, C., BARTEK, J. & LUKAS, J. (2006) Claspin operates downstream of TopBP1 to direct ATR signaling towards Chk1 activation. *Mol Cell Biol,* 26**,** 6056-64.
LIU, Y., SHAH, K., YANG, F., WITUCKI, L. & SHOKAT, K. M. (1998) A molecular gate which controls unnatural ATP analogue recognition by the tyrosine kinase v-Src. *Bioorg Med Chem,* 6**,** 1219-26.
LOOG, M. & MORGAN, D. O. (2005) Cyclin specificity in the phosphorylation of cyclin-dependent kinase substrates. *Nature,* 434**,** 104-8.
LOPEZ-GIRONA, A., FURNARI, B., MONDESERT, O. & RUSSELL, P. (1999) Nuclear localization of Cdc25 is regulated by DNA damage and a 14-3-3 protein. *Nature,* 397**,** 172-5.
LOU, Z., MINTER-DYKHOUSE, K., WU, X. & CHEN, J. (2003) MDC1 is coupled to activated CHK2 in mammalian DNA damage response pathways. *Nature,* 421**,** 957-61.
LOWNDES, N. F. & MURGUIA, J. R. (2000) Sensing and responding to DNA damage. *Curr Opin Genet Dev,* 10**,** 17-25.
LU, X., NANNENGA, B. & DONEHOWER, L. A. (2005) PPM1D dephosphorylates Chk1 and p53 and abrogates cell cycle checkpoints. *Genes Dev,* 19**,** 1162-74.
LUKAS, C., BARTKOVA, J., LATELLA, L., FALCK, J., MAILAND, N., SCHROEDER, T., SEHESTED, M., LUKAS, J. & BARTEK, J. (2001) DNA damage-activated kinase Chk2 is independent of proliferation or differentiation yet correlates with tissue biology. *Cancer Res,* 61**,** 4990-3.

LUKAS, C., FALCK, J., BARTKOVA, J., BARTEK, J. & LUKAS, J. (2003) Distinct spatiotemporal dynamics of mammalian checkpoint regulators induced by DNA damage. *Nat Cell Biol,* 5**,** 255-60.

LUO, Y., HURWITZ, J. & MASSAGUE, J. (1995) Cell-cycle inhibition by independent CDK and PCNA binding domains in p21Cip1. *Nature,* 375**,** 159-61.

MAILAND, N., BEKKER-JENSEN, S., BARTEK, J. & LUKAS, J. (2006) Destruction of Claspin by SCFbetaTrCP restrains Chk1 activation and facilitates recovery from genotoxic stress. *Mol Cell,* 23**,** 307-18.

MAILAND, N., FALCK, J., LUKAS, C., SYLJUASEN, R. G., WELCKER, M., BARTEK, J. & LUKAS, J. (2000) Rapid destruction of human Cdc25A in response to DNA damage. *Science,* 288**,** 1425-9.

MAMELY, I., VAN VUGT, M. A., SMITS, V. A., SEMPLE, J. I., LEMMENS, B., PERRAKIS, A., MEDEMA, R. H. & FREIRE, R. (2006) Polo-like kinase-1 controls proteasome-dependent degradation of Claspin during checkpoint recovery. *Curr Biol,* 16**,** 1950-5.

MARTIN-CABALLERO, J., FLORES, J. M., GARCIA-PALENCIA, P. & SERRANO, M. (2001) Tumor susceptibility of p21(Waf1/Cip1)-deficient mice. *Cancer Res,* 61**,** 6234-8.

MATSUOKA, S., BALLIF, B. A., SMOGORZEWSKA, A., MCDONALD, E. R., 3RD, HUROV, K. E., LUO, J., BAKALARSKI, C. E., ZHAO, Z., SOLIMINI, N., LERENTHAL, Y., SHILOH, Y., GYGI, S. P. & ELLEDGE, S. J. (2007) ATM and ATR substrate analysis reveals extensive protein networks responsive to DNA damage. *Science,* 316**,** 1160-6.

MATSUOKA, S., HUANG, M. & ELLEDGE, S. J. (1998) Linkage of ATM to cell cycle regulation by the Chk2 protein kinase. *Science,* 282**,** 1893-7.

MATSUOKA, S., ROTMAN, G., OGAWA, A., SHILOH, Y., TAMAI, K. & ELLEDGE, S. J. (2000) Ataxia telangiectasia-mutated phosphorylates Chk2 in vivo and in vitro. *Proc Natl Acad Sci U S A,* 97**,** 10389-94.

MAYANS, O., VAN DER VEN, P. F., WILM, M., MUES, A., YOUNG, P., FURST, D. O., WILMANNS, M. & GAUTEL, M. (1998) Structural basis for activation of the titin kinase domain during myofibrillogenesis. *Nature,* 395**,** 863-9.

MCAINSH, A. D., MERALDI, P., DRAVIAM, V. M., TOSO, A. & SORGER, P. K. (2006) The human kinetochore proteins Nnf1R and Mcm21R are required for accurate chromosome segregation. *Embo J,* 25**,** 4033-49.

MCCONNELL, M. J., CHEVALLIER, N., BERKOFSKY-FESSLER, W., GILTNANE, J. M., MALANI, R. B., STAUDT, L. M. & LICHT, J. D. (2003) Growth suppression by acute promyelocytic leukemia-associated protein PLZF is mediated by repression of c-myc expression. *Mol Cell Biol,* 23**,** 9375-88.

MELINO, G., BERNASSOLA, F., RANALLI, M., YEE, K., ZONG, W. X., CORAZZARI, M., KNIGHT, R. A., GREEN, D. R., THOMPSON, C. & VOUSDEN, K. H. (2004) p73 Induces apoptosis via PUMA transactivation and Bax mitochondrial translocation. *J Biol Chem,* 279**,** 8076-83.

MERALDI, P., DRAVIAM, V. M. & SORGER, P. K. (2004) Timing and checkpoints in the regulation of mitotic progression. *Dev Cell,* 7**,** 45-60.
MIAO, H., SEILER, J. A. & BURHANS, W. C. (2003) Regulation of cellular and SV40 virus origins of replication by Chk1-dependent intrinsic and UVC radiation-induced checkpoints. *J Biol Chem,* 278**,** 4295-304.
MICHAEL, W. M., OTT, R., FANNING, E. & NEWPORT, J. (2000) Activation of the DNA replication checkpoint through RNA synthesis by primase. *Science,* 289**,** 2133-7.
MILLER, W. T. (2003) Determinants of substrate recognition in nonreceptor tyrosine kinases. *Acc Chem Res,* 36**,** 393-400.
MITRA, J. & ENDERS, G. H. (2004) Cyclin A/Cdk2 complexes regulate activation of Cdk1 and Cdc25 phosphatases in human cells. *Oncogene,* 23**,** 3361-7.
MOLDOVAN, G. L., PFANDER, B. & JENTSCH, S. (2007) PCNA, the maestro of the replication fork. *Cell,* 129**,** 665-79.
MORGAN, D. O. (1997) Cyclin-dependent kinases: engines, clocks, and microprocessors. *Annu Rev Cell Dev Biol,* 13**,** 261-91.
MORRIS, M. C., HEITZ, A., MERY, J., HEITZ, F. & DIVITA, G. (2000) An essential phosphorylation-site domain of human cdc25C interacts with both 14-3-3 and cyclins. *J Biol Chem,* 275**,** 28849-57.
MURRAY, A. & HUNT, T. (1993) *The cell cycle: an introduction,* New York and Oxford, Oxford University Press.
NAKAJO, N., OE, T., UTO, K. & SAGATA, N. (1999) Involvement of Chk1 kinase in prophase I arrest of Xenopus oocytes. *Dev Biol,* 207**,** 432-44.
NEDUVA, V. & RUSSELL, R. B. (2005) Linear motifs: evolutionary interaction switches. *FEBS Lett,* 579**,** 3342-5.
NG, C. P., LEE, H. C., HO, C. W., AROOZ, T., SIU, W. Y., LAU, A. & POON, R. Y. (2004) Differential mode of regulation of the checkpoint kinases CHK1 and CHK2 by their regulatory domains. *J Biol Chem,* 279**,** 8808-19.
NIGG, E. A. (2001) Mitotic kinases as regulators of cell division and its checkpoints. *Nat Rev Mol Cell Biol,* 2**,** 21-32.
NIIDA, H., KATSUNO, Y., BANERJEE, B., HANDE, M. P. & NAKANISHI, M. (2007) Specific role of Chk1 phosphorylations in cell survival and checkpoint activation. *Mol Cell Biol,* 27**,** 2572-81.
NOMURA, M., NOMURA, N. & YAMASHITA, J. (2005) Geldanamycin-induced degradation of Chk1 is mediated by proteasome. *Biochem Biophys Res Commun,* 335**,** 900-5.
NORBURY, C. J. & HICKSON, I. D. (2001) Cellular responses to DNA damage. *Annu Rev Pharmacol Toxicol,* 41**,** 367-401.
O'CONNELL, M. J., RALEIGH, J. M., VERKADE, H. M. & NURSE, P. (1997) Chk1 is a wee1 kinase in the G2 DNA damage checkpoint inhibiting cdc2 by Y15 phosphorylation. *Embo J,* 16**,** 545-54.
O'NEILL, T., GIARRATANI, L., CHEN, P., IYER, L., LEE, C. H., BOBIAK, M., KANAI, F., ZHOU, B. B., CHUNG, J. H. & RATHBUN, G. A. (2002) Determination of substrate motifs for human Chk1 and hCds1/Chk2 by the oriented peptide library approach. *J Biol Chem,* 277**,** 16102-15.

OE, T., NAKAJO, N., KATSURAGI, Y., OKAZAKI, K. & SAGATA, N. (2001) Cytoplasmic occurrence of the Chk1/Cdc25 pathway and regulation of Chk1 in Xenopus oocytes. *Dev Biol,* 229**,** 250-61.

PARDEE, A. B., LI, C. J. & REDDY, G. P. (2004) Regulation in S phase by E2F. *Cell Cycle,* 3**,** 1091-4.

PAULSEN, R. D. & CIMPRICH, K. A. (2007) The ATR pathway: fine-tuning the fork. *DNA Repair (Amst),* 6**,** 953-66.

PENG, C. Y., GRAVES, P. R., THOMA, R. S., WU, Z., SHAW, A. S. & PIWNICA-WORMS, H. (1997) Mitotic and G2 checkpoint control: regulation of 14-3-3 protein binding by phosphorylation of Cdc25C on serine-216. *Science,* 277**,** 1501-5.

PESCHIAROLI, A., DORRELLO, N. V., GUARDAVACCARO, D., VENERE, M., HALAZONETIS, T., SHERMAN, N. E. & PAGANO, M. (2006) SCFbetaTrCP-mediated degradation of Claspin regulates recovery from the DNA replication checkpoint response. *Mol Cell,* 23**,** 319-29.

PETERMANN, E., MAYA-MENDOZA, A., ZACHOS, G., GILLESPIE, D. A., JACKSON, D. A. & CALDECOTT, K. W. (2006) Chk1 requirement for high global rates of replication fork progression during normal vertebrate S phase. *Mol Cell Biol,* 26**,** 3319-26.

PETERS, J. M. (2006) The anaphase promoting complex/cyclosome: a machine designed to destroy. *Nat Rev Mol Cell Biol,* 7**,** 644-56.

PRINCE, S., CARREIRA, S., VANCE, K. W., ABRAHAMS, A. & GODING, C. R. (2004) Tbx2 directly represses the expression of the p21(WAF1) cyclin-dependent kinase inhibitor. *Cancer Res,* 64**,** 1669-74.

PUC, J., KENIRY, M., LI, H. S., PANDITA, T. K., CHOUDHURY, A. D., MEMEO, L., MANSUKHANI, M., MURTY, V. V., GACIONG, Z., MEEK, S. E., PIWNICA-WORMS, H., HIBSHOOSH, H. & PARSONS, R. (2005) Lack of PTEN sequesters CHK1 and initiates genetic instability. *Cancer Cell,* 7**,** 193-204.

PUC, J. & PARSONS, R. (2005) PTEN loss inhibits CHK1 to cause double stranded-DNA breaks in cells. *Cell Cycle,* 4**,** 927-9.

PUFALL, M. A. & GRAVES, B. J. (2002) Autoinhibitory domains: modular effectors of cellular regulation. *Annu Rev Cell Dev Biol,* 18**,** 421-62.

REMENYI, A., GOOD, M. C. & LIM, W. A. (2006) Docking interactions in protein kinase and phosphatase networks. *Curr Opin Struct Biol,* 16**,** 676-85.

ROBERSON, R. S., KUSSICK, S. J., VALLIERES, E., CHEN, S. Y. & WU, D. Y. (2005) Escape from therapy-induced accelerated cellular senescence in p53-null lung cancer cells and in human lung cancers. *Cancer Res,* 65**,** 2795-803.

RODRIGUEZ-VILARRUPLA, A., DIAZ, C., CANELA, N., RAHN, H. P., BACHS, O. & AGELL, N. (2002) Identification of the nuclear localization signal of p21(cip1) and consequences of its mutation on cell proliferation. *FEBS Lett,* 531**,** 319-23.

RODRIGUEZ-VILARRUPLA, A., JAUMOT, M., ABELLA, N., CANELA, N., BRUN, S., DIAZ, C., ESTANYOL, J. M., BACHS, O. & AGELL, N. (2005) Binding of calmodulin to the carboxy-terminal region of p21

induces nuclear accumulation via inhibition of protein kinase C-mediated phosphorylation of Ser153. *Mol Cell Biol,* 25**,** 7364-74.

ROOS, W. P. & KAINA, B. (2006) DNA damage-induced cell death by apoptosis. *Trends Mol Med,* 12**,** 440-50.

ROSHAL, M., KIM, B., ZHU, Y., NGHIEM, P. & PLANELLES, V. (2003) Activation of the ATR-mediated DNA damage response by the HIV-1 viral protein R. *J Biol Chem,* 278**,** 25879-86.

ROSSIG, L., BADORFF, C., HOLZMANN, Y., ZEIHER, A. M. & DIMMELER, S. (2002) Glycogen synthase kinase-3 couples AKT-dependent signaling to the regulation of p21Cip1 degradation. *J Biol Chem,* 277**,** 9684-9.

ROSSIG, L., JADIDI, A. S., URBICH, C., BADORFF, C., ZEIHER, A. M. & DIMMELER, S. (2001) Akt-dependent phosphorylation of p21(Cip1) regulates PCNA binding and proliferation of endothelial cells. *Mol Cell Biol,* 21**,** 5644-57.

ROTHBLUM-OVIATT, C. J., RYAN, C. E. & PIWNICA-WORMS, H. (2001) 14-3-3 binding regulates catalytic activity of human Wee1 kinase. *Cell Growth Differ,* 12**,** 581-9.

ROUSSEL, M. F. (1999) The INK4 family of cell cycle inhibitors in cancer. *Oncogene,* 18**,** 5311-7.

RUSSO, A. A., JEFFREY, P. D., PATTEN, A. K., MASSAGUE, J. & PAVLETICH, N. P. (1996) Crystal structure of the p27Kip1 cyclin-dependent-kinase inhibitor bound to the cyclin A-Cdk2 complex. *Nature,* 382**,** 325-31.

SANCAR, A., LINDSEY-BOLTZ, L. A., UNSAL-KACMAZ, K. & LINN, S. (2004) Molecular mechanisms of mammalian DNA repair and the DNA damage checkpoints. *Annu Rev Biochem,* 73**,** 39-85.

SANCHEZ, Y., BACHANT, J., WANG, H., HU, F., LIU, D., TETZLAFF, M. & ELLEDGE, S. J. (1999) Control of the DNA damage checkpoint by chk1 and rad53 protein kinases through distinct mechanisms. *Science,* 286**,** 1166-71.

SANCHEZ, Y., WONG, C., THOMA, R. S., RICHMAN, R., WU, Z., PIWNICA-WORMS, H. & ELLEDGE, S. J. (1997) Conservation of the Chk1 checkpoint pathway in mammals: linkage of DNA damage to Cdk regulation through Cdc25. *Science,* 277**,** 1497-501.

SAR, F., LINDSEY-BOLTZ, L. A., SUBRAMANIAN, D., CROTEAU, D. L., HUTSELL, S. Q., GRIFFITH, J. D. & SANCAR, A. (2004) Human claspin is a ring-shaped DNA-binding protein with high affinity to branched DNA structures. *J Biol Chem,* 279**,** 39289-95.

SAUSVILLE, E. A., ARBUCK, S. G., MESSMANN, R., HEADLEE, D., BAUER, K. S., LUSH, R. M., MURGO, A., FIGG, W. D., LAHUSEN, T., JAKEN, S., JING, X., ROBERGE, M., FUSE, E., KUWABARA, T. & SENDEROWICZ, A. M. (2001) Phase I trial of 72-hour continuous infusion UCN-01 in patients with refractory neoplasms. *J Clin Oncol,* 19**,** 2319-33.

SCORAH, J., DONG, M. Q., YATES, J. R., 3RD, SCOTT, M., GILLESPIE, D. & MCGOWAN, C. H. (2008) A Conserved Proliferating Cell Nuclear Antigen-interacting Protein Sequence in Chk1 Is Required for Checkpoint Function. *J Biol Chem,* 283**,** 17250-17259.

SCOTT, M. T., INGRAM, A. & BALL, K. L. (2002) PDK1-dependent activation of atypical PKC leads to degradation of the p21 tumour modifier protein. *Embo J,* 21**,** 6771-80.

SCOTT, M. T., MORRICE, N. & BALL, K. L. (2000) Reversible phosphorylation at the C-terminal regulatory domain of p21(Waf1/Cip1) modulates proliferating cell nuclear antigen binding. *J Biol Chem,* 275**,** 11529-37.

SEGRELLES, C., MORAL, M., LARA, M. F., RUIZ, S., SANTOS, M., LEIS, H., GARCIA-ESCUDERO, R., MARTINEZ-CRUZ, A. B., MARTINEZ-PALACIO, J., HERNANDEZ, P., BALLESTIN, C. & PARAMIO, J. M. (2006) Molecular determinants of Akt-induced keratinocyte transformation. *Oncogene,* 25**,** 1174-85.

SEOANE, J., LE, H. V. & MASSAGUE, J. (2002) Myc suppression of the p21(Cip1) Cdk inhibitor influences the outcome of the p53 response to DNA damage. *Nature,* 419**,** 729-34.

SHEAFF, R. J., SINGER, J. D., SWANGER, J., SMITHERMAN, M., ROBERTS, J. M. & CLURMAN, B. E. (2000) Proteasomal turnover of p21Cip1 does not require p21Cip1 ubiquitination. *Mol Cell,* 5**,** 403-10.

SHERIDAN, D. L., KONG, Y., PARKER, S. A., DALBY, K. N. & TURK, B. E. (2008) Substrate Discrimination among Mitogen-activated Protein Kinases through Distinct Docking Sequence Motifs. *J Biol Chem,* 283**,** 19511-20.

SHIEH, S. Y., AHN, J., TAMAI, K., TAYA, Y. & PRIVES, C. (2000) The human homologs of checkpoint kinases Chk1 and Cds1 (Chk2) phosphorylate p53 at multiple DNA damage-inducible sites. *Genes Dev,* 14**,** 289-300.

SHIM, J., LEE, H., PARK, J., KIM, H. & CHOI, E. J. (1996) A non-enzymatic p21 protein inhibitor of stress-activated protein kinases. *Nature,* 381**,** 804-6.

SHIMADA, M., NIIDA, H., ZINELDEEN, D. H., TAGAMI, H., TANAKA, M., SAITO, H. & NAKANISHI, M. (2008) Chk1 is a histone H3 threonine 11 kinase that regulates DNA damage-induced transcriptional repression. *Cell,* 132**,** 221-32.

SHIOHARA, M., KOIKE, K., KOMIYAMA, A. & KOEFFLER, H. P. (1997) p21WAF1 mutations and human malignancies. *Leuk Lymphoma,* 26**,** 35-41.

SHIOMI, Y., SHINOZAKI, A., NAKADA, D., SUGIMOTO, K., USUKURA, J., OBUSE, C. & TSURIMOTO, T. (2002) Clamp and clamp loader structures of the human checkpoint protein complexes, Rad9-1-1 and Rad17-RFC. *Genes Cells,* 7**,** 861-8.

SHIROMIZU, T., GOTO, H., TOMONO, Y., BARTEK, J., TOTSUKAWA, G., INOKO, A., NAKANISHI, M., MATSUMURA, F. & INAGAKI, M. (2006) Regulation of mitotic function of Chk1 through phosphorylation at novel sites by cyclin-dependent kinase 1 (Cdk1). *Genes Cells,* 11**,** 477-85.

SHTIVELMAN, E., SUSSMAN, J. & STOKOE, D. (2002) A role for PI 3-kinase and PKB activity in the G2/M phase of the cell cycle. *Curr Biol,* 12**,** 919-24.

SMITS, V. A., REAPER, P. M. & JACKSON, S. P. (2006) Rapid PIKK-dependent release of Chk1 from chromatin promotes the DNA-damage checkpoint response. *Curr Biol,* 16**,** 150-9.

SOMASUNDARAM, K., ZHANG, H., ZENG, Y. X., HOUVRAS, Y., PENG, Y., ZHANG, H., WU, G. S., LICHT, J. D., WEBER, B. L. & EL-DEIRY, W.

S. (1997) Arrest of the cell cycle by the tumour-suppressor BRCA1 requires the CDK-inhibitor p21WAF1/CiP1. *Nature,* 389**,** 187-90.

SORENSEN, C. S., SYLJUASEN, R. G., FALCK, J., SCHROEDER, T., RONNSTRAND, L., KHANNA, K. K., ZHOU, B. B., BARTEK, J. & LUKAS, J. (2003) Chk1 regulates the S phase checkpoint by coupling the physiological turnover and ionizing radiation-induced accelerated proteolysis of Cdc25A. *Cancer Cell,* 3**,** 247-58.

SORIA, G., PODHAJCER, O., PRIVES, C. & GOTTIFREDI, V. (2006) P21Cip1/WAF1 downregulation is required for efficient PCNA ubiquitination after UV irradiation. *Oncogene,* 25**,** 2829-38.

STEVAUX, O. & DYSON, N. J. (2002) A revised picture of the E2F transcriptional network and RB function. *Curr Opin Cell Biol,* 14**,** 684-91.

STEVENS, C., SMITH, L. & LA THANGUE, N. B. (2003) Chk2 activates E2F-1 in response to DNA damage. *Nat Cell Biol,* 5**,** 401-9.

STEWART, G. S., WANG, B., BIGNELL, C. R., TAYLOR, A. M. & ELLEDGE, S. J. (2003) MDC1 is a mediator of the mammalian DNA damage checkpoint. *Nature,* 421**,** 961-6.

STROM, L., LINDROOS, H. B., SHIRAHIGE, K. & SJOGREN, C. (2004) Postreplicative recruitment of cohesin to double-strand breaks is required for DNA repair. *Mol Cell,* 16**,** 1003-15.

SUGIMOTO, K., SASAKI, M., ISOBE, Y., TSUTSUI, M., SUTO, H., ANDO, J., TAMAYOSE, K., ANDO, M. & OSHIMI, K. (2008) Hsp90-inhibitor geldanamycin abrogates G2 arrest in p53-negative leukemia cell lines through the depletion of Chk1. *Oncogene,* 27**,** 3091-101.

SUNG, Y. H., SHIN, J., SHIN, J. & LEE, W. (2001) Solution structure of p21(Waf1/Cip1/Sdi1) C-terminal domain bound to Cdk4. *J Biomol Struct Dyn,* 19**,** 419-27.

SUZUKI, A., TSUTOMI, Y., AKAHANE, K., ARAKI, T. & MIURA, M. (1998) Resistance to Fas-mediated apoptosis: activation of caspase 3 is regulated by cell cycle regulator p21WAF1 and IAP gene family ILP. *Oncogene,* 17**,** 931-9.

SUZUKI, A., TSUTOMI, Y., MIURA, M. & AKAHANE, K. (1999) Caspase 3 inactivation to suppress Fas-mediated apoptosis: identification of binding domain with p21 and ILP and inactivation machinery by p21. *Oncogene,* 18**,** 1239-44.

SYLJUASEN, R. G. (2007) Checkpoint adaptation in human cells. *Oncogene,* 26**,** 5833-9.

SYLJUASEN, R. G., JENSEN, S., BARTEK, J. & LUKAS, J. (2006) Adaptation to the ionizing radiation-induced G2 checkpoint occurs in human cells and depends on checkpoint kinase 1 and Polo-like kinase 1 kinases. *Cancer Res,* 66**,** 10253-7.

SYLJUASEN, R. G., SORENSEN, C. S., HANSEN, L. T., FUGGER, K., LUNDIN, C., JOHANSSON, F., HELLEDAY, T., SEHESTED, M., LUKAS, J. & BARTEK, J. (2005) Inhibition of human Chk1 causes increased initiation of DNA replication, phosphorylation of ATR targets, and DNA breakage. *Mol Cell Biol,* 25**,** 3553-62.

TAKAI, H., TOMINAGA, K., MOTOYAMA, N., MINAMISHIMA, Y. A., NAGAHAMA, H., TSUKIYAMA, T., IKEDA, K., NAKAYAMA, K.,

NAKANISHI, M. & NAKAYAMA, K. (2000) Aberrant cell cycle checkpoint function and early embryonic death in Chk1(-/-) mice. *Genes Dev,* 14**,** 1439-47.

TANG, H. Y., ZHAO, K., PIZZOLATO, J. F., FONAREV, M., LANGER, J. C. & MANFREDI, J. J. (1998) Constitutive expression of the cyclin-dependent kinase inhibitor p21 is transcriptionally regulated by the tumor suppressor protein p53. *J Biol Chem,* 273**,** 29156-63.

TANG, J., ERIKSON, R. L. & LIU, X. (2006a) Checkpoint kinase 1 (Chk1) is required for mitotic progression through negative regulation of polo-like kinase 1 (Plk1). *Proc Natl Acad Sci U S A,* 103**,** 11964-9.

TANG, J., ERIKSON, R. L. & LIU, X. (2006b) Ectopic expression of Plk1 leads to activation of the spindle checkpoint. *Cell Cycle,* 5**,** 2484-8.

TANOUE, T., ADACHI, M., MORIGUCHI, T. & NISHIDA, E. (2000) A conserved docking motif in MAP kinases common to substrates, activators and regulators. *Nat Cell Biol,* 2**,** 110-6.

TIAN, H., FAJE, A. T., LEE, S. L. & JORGENSEN, T. J. (2002) Radiation-induced phosphorylation of Chk1 at S345 is associated with p53-dependent cell cycle arrest pathways. *Neoplasia,* 4**,** 171-80.

TIMARES, L., KATIYAR, S. K. & ELMETS, C. A. (2008) DNA damage, apoptosis and langerhans cells--Activators of UV-induced immune tolerance. *Photochem Photobiol,* 84**,** 422-36.

TOCZYSKI, D. P., GALGOCZY, D. J. & HARTWELL, L. H. (1997) CDC5 and CKII control adaptation to the yeast DNA damage checkpoint. *Cell,* 90**,** 1097-106.

TOUITOU, R., RICHARDSON, J., BOSE, S., NAKANISHI, M., RIVETT, J. & ALLDAY, M. J. (2001) A degradation signal located in the C-terminus of p21WAF1/CIP1 is a binding site for the C8 alpha-subunit of the 20S proteasome. *Embo J,* 20**,** 2367-75.

TOURNIER, S., LEROY, D., GOUBIN, F., DUCOMMUN, B. & HYAMS, J. S. (1996) Heterologous expression of the human cyclin-dependent kinase inhibitor p21Cip1 in the fission yeast, Schizosaccharomyces pombe reveals a role for PCNA in the chk1+ cell cycle checkpoint pathway. *Mol Biol Cell,* 7**,** 651-62.

TSE, A. N., CARVAJAL, R. & SCHWARTZ, G. K. (2007) Targeting checkpoint kinase 1 in cancer therapeutics. *Clin Cancer Res,* 13**,** 1955-60.

TSE, A. N. & SCHWARTZ, G. K. (2004) Potentiation of cytotoxicity of topoisomerase i poison by concurrent and sequential treatment with the checkpoint inhibitor UCN-01 involves disparate mechanisms resulting in either p53-independent clonogenic suppression or p53-dependent mitotic catastrophe. *Cancer Res,* 64**,** 6635-44.

TSURUTA, F., SUNAYAMA, J., MORI, Y., HATTORI, S., SHIMIZU, S., TSUJIMOTO, Y., YOSHIOKA, K., MASUYAMA, N. & GOTOH, Y. (2004) JNK promotes Bax translocation to mitochondria through phosphorylation of 14-3-3 proteins. *Embo J,* 23**,** 1889-99.

UBERSAX, J. A., WOODBURY, E. L., QUANG, P. N., PARAZ, M., BLETHROW, J. D., SHAH, K., SHOKAT, K. M. & MORGAN, D. O. (2003) Targets of the cyclin-dependent kinase Cdk1. *Nature,* 425**,** 859-64.

UNAL, E., ARBEL-EDEN, A., SATTLER, U., SHROFF, R., LICHTEN, M., HABER, J. E. & KOSHLAND, D. (2004) DNA damage response pathway uses histone modification to assemble a double-strand break-specific cohesin domain. *Mol Cell,* 16**,** 991-1002.

URIST, M., TANAKA, T., POYUROVSKY, M. V. & PRIVES, C. (2004) p73 induction after DNA damage is regulated by checkpoint kinases Chk1 and Chk2. *Genes Dev,* 18**,** 3041-54.

UZIEL, T., LERENTHAL, Y., MOYAL, L., ANDEGEKO, Y., MITTELMAN, L. & SHILOH, Y. (2003) Requirement of the MRN complex for ATM activation by DNA damage. *Embo J,* 22**,** 5612-21.

VAN VUGT, M. A., BRAS, A. & MEDEMA, R. H. (2004) Polo-like kinase-1 controls recovery from a G2 DNA damage-induced arrest in mammalian cells. *Mol Cell,* 15**,** 799-811.

VIDAL, A. & KOFF, A. (2000) Cell-cycle inhibitors: three families united by a common cause. *Gene,* 247**,** 1-15.

VITALE, I., GALLUZZI, L., VIVET, S., NANTY, L., DESSEN, P., SENOVILLA, L., OLAUSSEN, K. A., LAZAR, V., PRUDHOMME, M., GOLSTEYN, R. M., CASTEDO, M. & KROEMER, G. (2007) Inhibition of Chk1 Kills Tetraploid Tumor Cells through a p53-Dependent Pathway. *PLoS ONE,* 2**,** e1337.

WALLACE, M. & BALL, K. L. (2004) Docking-dependent regulation of the Rb tumor suppressor protein by Cdk4. *Mol Cell Biol,* 24**,** 5606-19.

WALTER, J. & NEWPORT, J. (2000) Initiation of eukaryotic DNA replication: origin unwinding and sequential chromatin association of Cdc45, RPA, and DNA polymerase alpha. *Mol Cell,* 5**,** 617-27.

WALWORTH, N., DAVEY, S. & BEACH, D. (1993) Fission yeast chk1 protein kinase links the rad checkpoint pathway to cdc2. *Nature,* 363**,** 368-71.

WALWORTH, N. C. & BERNARDS, R. (1996) rad-dependent response of the chk1-encoded protein kinase at the DNA damage checkpoint. *Science,* 271**,** 353-6.

WANG, H., LIU, D., WANG, Y., QIN, J. & ELLEDGE, S. J. (2001) Pds1 phosphorylation in response to DNA damage is essential for its DNA damage checkpoint function. *Genes Dev,* 15**,** 1361-72.

WANG, S. X. & DUNPHY, W. G. (2000) Activation of Xenopus Chk1 by mutagenesis of threonine-377. *FEBS Lett,* 487**,** 277-81.

WANG, X., ZOU, L., LU, T., BAO, S., HUROV, K. E., HITTELMAN, W. N., ELLEDGE, S. J. & LI, L. (2006) Rad17 phosphorylation is required for claspin recruitment and Chk1 activation in response to replication stress. *Mol Cell,* 23**,** 331-41.

WARBRICK, E., LANE, D. P., GLOVER, D. M. & COX, L. S. (1997) Homologous regions of Fen1 and p21Cip1 compete for binding to the same site on PCNA: a potential mechanism to co-ordinate DNA replication and repair. *Oncogene,* 14**,** 2313-21.

WARD, I. M., MINN, K. & CHEN, J. (2004) UV-induced ataxia-telangiectasia-mutated and Rad3-related (ATR) activation requires replication stress. *J Biol Chem,* 279**,** 9677-80.

WEBER, A., MARQUARDT, J., ELZI, D., FORSTER, N., STARKE, S., GLAUM, A., YAMADA, D., DEFOSSEZ, P. A., DELROW, J.,

EISENMAN, R. N., CHRISTIANSEN, H. & EILERS, M. (2008) Zbtb4 represses transcription of P21CIP1 and controls the cellular response to p53 activation. *Embo J,* 27**,** 1563-74.

WESTENDORF, J. J., ZAIDI, S. K., CASCINO, J. E., KAHLER, R., VAN WIJNEN, A. J., LIAN, J. B., YOSHIDA, M., STEIN, G. S. & LI, X. (2002) Runx2 (Cbfa1, AML-3) interacts with histone deacetylase 6 and represses the p21(CIP1/WAF1) promoter. *Mol Cell Biol,* 22**,** 7982-92.

WINTERS, Z. E., HUNT, N. C., BRADBURN, M. J., ROYDS, J. A., TURLEY, H., HARRIS, A. L. & NORBURY, C. J. (2001) Subcellular localisation of cyclin B, Cdc2 and p21(WAF1/CIP1) in breast cancer. association with prognosis. *Eur J Cancer,* 37**,** 2405-12.

WOO, R. A. & POON, R. Y. (2003) Cyclin-dependent kinases and S phase control in mammalian cells. *Cell Cycle,* 2**,** 316-24.

WYMAN, C. & KANAAR, R. (2006) DNA double-strand break repair: all's well that ends well. *Annu Rev Genet,* 40**,** 363-83.

XIAO, Z., CHEN, Z., GUNASEKERA, A. H., SOWIN, T. J., ROSENBERG, S. H., FESIK, S. & ZHANG, H. (2003) Chk1 mediates S and G2 arrests through Cdc25A degradation in response to DNA-damaging agents. *J Biol Chem,* 278**,** 21767-73.

XIAO, Z., XUE, J., SEMIZAROV, D., SOWIN, T. J., ROSENBERG, S. H. & ZHANG, H. (2005a) Novel indication for cancer therapy: Chk1 inhibition sensitizes tumor cells to antimitotics. *Int J Cancer,* 115**,** 528-38.

XIAO, Z., XUE, J., SOWIN, T. J., ROSENBERG, S. H. & ZHANG, H. (2005b) A novel mechanism of checkpoint abrogation conferred by Chk1 downregulation. *Oncogene,* 24**,** 1403-11.

XIAO, Z., XUE, J., SOWIN, T. J. & ZHANG, H. (2006) Differential roles of checkpoint kinase 1, checkpoint kinase 2, and mitogen-activated protein kinase-activated protein kinase 2 in mediating DNA damage-induced cell cycle arrest: implications for cancer therapy. *Mol Cancer Ther,* 5**,** 1935-43.

YAN, T., DESAI, A. B., JACOBBERGER, J. W., SRAMKOSKI, R. M., LOH, T. & KINSELLA, T. J. (2004) CHK1 and CHK2 are differentially involved in mismatch repair-mediated 6-thioguanine-induced cell cycle checkpoint responses. *Mol Cancer Ther,* 3**,** 1147-57.

YANG, X. H., SHIOTANI, B., CLASSON, M. & ZOU, L. (2008) Chk1 and Claspin potentiate PCNA ubiquitination. *Genes Dev,* 22**,** 1147-52.

YARDEN, R. I., PARDO-REOYO, S., SGAGIAS, M., COWAN, K. H. & BRODY, L. C. (2002) BRCA1 regulates the G2/M checkpoint by activating Chk1 kinase upon DNA damage. *Nat Genet,* 30**,** 285-9.

YOO, H. Y., JEONG, S. Y. & DUNPHY, W. G. (2006) Site-specific phosphorylation of a checkpoint mediator protein controls its responses to different DNA structures. *Genes Dev,* 20**,** 772-83.

YOO, H. Y., KUMAGAI, A., SHEVCHENKO, A., SHEVCHENKO, A. & DUNPHY, W. G. (2004) Adaptation of a DNA replication checkpoint response depends upon inactivation of Claspin by the Polo-like kinase. *Cell,* 117**,** 575-88.

YU, J. & ZHANG, L. (2003) No PUMA, no death: implications for p53-dependent apoptosis. *Cancer Cell,* 4**,** 248-9.

ZACHOS, G., BLACK, E. J., WALKER, M., SCOTT, M. T., VAGNARELLI, P., EARNSHAW, W. C. & GILLESPIE, D. A. (2007) Chk1 is required for spindle checkpoint function. *Dev Cell,* 12**,** 247-60.

ZACHOS, G., RAINEY, M. D. & GILLESPIE, D. A. (2003) Chk1-deficient tumour cells are viable but exhibit multiple checkpoint and survival defects. *Embo J,* 22**,** 713-23.

ZACHOS, G., RAINEY, M. D. & GILLESPIE, D. A. (2005) Chk1-dependent S-M checkpoint delay in vertebrate cells is linked to maintenance of viable replication structures. *Mol Cell Biol,* 25**,** 563-74.

ZHANG, J. M., WEI, Q., ZHAO, X. & PATERSON, B. M. (1999a) Coupling of the cell cycle and myogenesis through the cyclin D1-dependent interaction of MyoD with cdk4. *Embo J,* 18**,** 926-33.

ZHANG, Y., FUJITA, N. & TSURUO, T. (1999b) Caspase-mediated cleavage of p21Waf1/Cip1 converts cancer cells from growth arrest to undergoing apoptosis. *Oncogene,* 18**,** 1131-8.

ZHANG, Y. W., OTTERNESS, D. M., CHIANG, G. G., XIE, W., LIU, Y. C., MERCURIO, F. & ABRAHAM, R. T. (2005) Genotoxic stress targets human Chk1 for degradation by the ubiquitin-proteasome pathway. *Mol Cell,* 19**,** 607-18.

ZHANG, Z., HUANG, C., LI, J., LEONARD, S. S., LANCIOTTI, R., BUTTERWORTH, L. & SHI, X. (2001) Vanadate-induced cell growth regulation and the role of reactive oxygen species. *Arch Biochem Biophys,* 392**,** 311-20.

ZHAO, H. & PIWNICA-WORMS, H. (2001) ATR-mediated checkpoint pathways regulate phosphorylation and activation of human Chk1. *Mol Cell Biol,* 21**,** 4129-39.

ZHAO, H., WATKINS, J. L. & PIWNICA-WORMS, H. (2002) Disruption of the checkpoint kinase 1/cell division cycle 25A pathway abrogates ionizing radiation-induced S and G2 checkpoints. *Proc Natl Acad Sci U S A,* 99**,** 14795-800.

ZHENG, G. & YANG, Y. C. (2004) ZNF76, a novel transcriptional repressor targeting TATA-binding protein, is modulated by sumoylation. *J Biol Chem,* 279**,** 42410-21.

ZHOU, B. B. & ELLEDGE, S. J. (2000) The DNA damage response: putting checkpoints in perspective. *Nature,* 408**,** 433-9.

ZHOU, B. P., LIAO, Y., XIA, W., SPOHN, B., LEE, M. H. & HUNG, M. C. (2001) Cytoplasmic localization of p21Cip1/WAF1 by Akt-induced phosphorylation in HER-2/neu-overexpressing cells. *Nat Cell Biol,* 3**,** 245-52.

ZHU, H., KLEMIC, J. F., CHANG, S., BERTONE, P., CASAMAYOR, A., KLEMIC, K. G., SMITH, D., GERSTEIN, M., REED, M. A. & SNYDER, M. (2000) Analysis of yeast protein kinases using protein chips. *Nat Genet,* 26**,** 283-9.

ZHU, H., NIE, L. & MAKI, C. G. (2005) Cdk2-dependent Inhibition of p21 stability via a C-terminal cyclin-binding motif. *J Biol Chem,* 280**,** 29282-8.

ZOU, L., CORTEZ, D. & ELLEDGE, S. J. (2002) Regulation of ATR substrate selection by Rad17-dependent loading of Rad9 complexes onto chromatin. *Genes Dev,* 16**,** 198-208.

ZOU, L. & ELLEDGE, S. J. (2003) Sensing DNA damage through ATRIP recognition of RPA-ssDNA complexes. *Science,* 300**,** 1542-8.

ZOU, L., LIU, D. & ELLEDGE, S. J. (2003) Replication protein A-mediated recruitment and activation of Rad17 complexes. *Proc Natl Acad Sci U S A,* 100**,** 13827-32.

Appendix 1

List of peptides phosphorylated by Chk1 wild-type protein kinase

S/N	COL	ROW	SEQUENCE	TARGET PROTEIN
1	2	11	KKLGSKKPQ	SWISS;P04775;CIN2_RAT
2	11	5	KKRLSVERI	SWISS;P11388;TOPA_HUMAN
3	7	7	KNIVTPRTP	SWISS;P02687;MBP_BOVIN
4	5	9	KREASLDNQ	SWISS;P06593;PHY3_AVESA
5	5	13	KRFGSKAHM	SWISS;P29476;NOS1_RAT
6	1	7	KRPSARAKA	SWISS;P02687;MBP_BOVIN
7	1	11	KRPSDRAKA	SWISS;P02687;MBP_BOVIN
8	1	15	KRPSERAKA	SWISS;P02687;MBP_BOVIN
9	10	5	KRPSGRAKA	SWISS;P02687;MBP_BOVIN
10	10	9	KRPTQRAKY	SWISS;P02687;MBP_BOVIN
11	8	6	KRRGSVPIL	SWISS;P16452;42_HUMAN
12	8	10	KRRLSFSET	SWISS;P01582;IL1A_MOUSE
13	12	12	KRSGSVYEP	SWISS;P12798;KPBB_RABIT
14	9	5	KYRKSSLKS	SWISS;P22613;STP1_SHEEP
15	1	14	LQDDYEDMM	SWISS;P02730;B3AT_HUMAN
16	5	8	LRAPSWIDT	SWISS;P02510;CRAB_BOVIN
17	5	12	LRGPSWDPF	SWISS;P04792;HS27_HUMAN
18	8	1	LRKVSKQEE	SWISS;P50552;VASP_HUMAN
19	8	5	LRMFSFKAP	SWISS;P22300;GAC2_BOVIN
20	8	9	LRRASLGAA	BOS TAURUS (BOVINE) LIVER PYRUVATE KINASE (FRAGMENT)
21	1	8	RTKRSGSV	phosphorylase b kinase beta regulatory chain

	Peptide targeted by all three forms of Chk1
	Peptide targeted by Chk1 wild-type and Chk1 stimulated by Chk1 peptide 14
	Peptide targeted by Chk1 stimulated by Chk1 peptide 14 and Chk1 ΔC70

Appendix 1

List of peptides phosphorylated by Chk1 peptide 14-stimulated Chk1 protein kinase

S/N	COL	ROW	SEQUENCE	TARGET PROTEIN
1	8	15	KGTGYIKTE	SWISS;P42224;STA1_HUMAN
2	2	11	KKLGSKKPQ	SWISS;P04775;CIN2_RAT
3	11	5	KKRLSVERI	SWISS;P11388;TOPA_HUMAN
4	9	14	KNDKSKTWQ	SWISS;P06730;IF4E_HUMAN
5	7	7	KNIVTPRTP	SWISS;P02687;MBP_BOVIN
6	7	11	KPGFSPQPS	SWISS;Q00756;PPR3A_RABIT
7	5	9	KREASLDNQ	SWISS;P06593;PHY3_AVESA
8	5	13	KRFGSKAHM	SWISS;P29476;NOS1_RAT
9	7	12	KRKQISVR	SWISS;P11217;PHS2_HUMAN
10	3	6	KRKQISVRG	SWISS;P11217;PHS2_HUMAN
11	3	10	KRKRSRKES	SWISS;P02278;H2B_HUMAN
12	1	3	KRNSSPPPS	SWISS;P20020;ATCP_HUMAN
13	1	7	KRPSARAKA	SWISS;P02687;MBP_BOVIN
14	1	11	KRPSDRAKA	SWISS;P02687;MBP_BOVIN
15	1	15	KRPSERAKA	SWISS;P02687;MBP_BOVIN
16	10	1	KRPSFRAKA	SWISS;P02687;MBP_BOVIN
17	10	5	KRPSGRAKA	SWISS;P02687;MBP_BOVIN
18	10	9	KRPTQRAKY	SWISS;P02687;MBP_BOVIN
19	8	6	KRRGSVPIL	SWISS;P16452;42_HUMAN
20	8	10	KRRLSFSET	SWISS;P01582;IL1A_MOUSE
21	12	4	KRRRSSKDT	SWISS;Q05586;P35437;NMZ1_HUMAN
22	12	12	KRSGSVYEP	SWISS;P12798;KPBB_RABIT
23	4	13	KSLNYIDLD	SWISS;P35570;IRS1_RAT
24	2	10	KSRWSGSQQ	SWISS;P04049;KRAF_HUMAN
25	2	14	KTETSQVAP	SWISS;P02699;OPSD_BOVIN
26	6	8	KTSPSSSPA	SWISS;P19836;CTPT_RAT
27	6	16	KVPQTPLHT	SWISS;P49139;MKK2_RABIT
28	9	5	KYRKSSLKS	SWISS;P22613;STP1_SHEEP
29	9	13	LDDQYTSSS	SWISS;P24604;TEC_MOUSE
30	7	14	LGGGTFDIS	SWISS;P04475;DNAK_ECOLI
31	5	10	LGSPLRRR	SWISS;P20152;VIME_MOUSE
32	11	8	LKLASPELE	SWISS;P05412;AP1_HUMAN
33	11	12	LLPMSPEEF	SWISS;P42224;STA1_HUMAN
34	3	5	LMAPSEEDH	SWISS;P08833;IBP1_HUMAN
35	1	14	LQDDYEDMM	SWISS;P02730;B3AT_HUMAN
36	1	4	LQRYSSDPT	SWISS;P00533;P06268;EGFR_HUMAN
37	5	8	LRAPSWIDT	SWISS;P02510;CRAB_BOVIN
38	5	12	LRGPSWDPF	SWISS;P04792;HS27_HUMAN
39	8	1	LRKVSKQEE	SWISS;P50552;VASP_HUMAN
40	8	5	LRMFSFKAP	SWISS;P22300;GAC2_BOVIN
41	8	9	LRRASLGAA	BOS TAURUS (BOVINE) LIVER PYRUVATE KINASE (FRAGMENT)
42	8	13	LRRASLGAF	BOS TAURUS (BOVINE) LIVER PYRUVATE KINASE (FRAGMENT)
43	12	3	LRRASVAQL	SWISS;P12928;P04763;Q64618;KPYR_RAT
44	12	11	LRRLSTKYR	SWISS;Q05209;PTNC_HUMAN
45	10	4	LRRPSDQEV	SWISS;P16236;REL_CHICK
46	2	1	LSEHSSPEE	SWISS;P07516;PPR1B_BOVIN
47	2	5	LSELSRRRI	SWISS;P20459;IF2A_YEAST
48	2	9	LSGESDLEI	SWISS;P06786;TOP2_YEAST
49	11	3	PENDYEDVE	SWISS;P14317;HCLS1_HUMAN
50	1	5	PKRGSGKDG	SWISS;P02687;MBP_BOVIN
51	3	4	PPSAYATVK	SWISS;P17785;ANX2_CHICK
52	10	3	PRMPSLSVP	SWISS;P02719;CINA_ELEEL
53	8	16	PSPKTPPGS	SWISS;P19332;TAU_RAT
54	9	15	QGTLSKIFK	SWISS;P02687;MBP_BOVIN
55	1	8	RTKRSGSV	phosphorylase b kinase beta regulatory chain

	Peptide targeted by all three forms of Chk1
	Peptide targeted by Chk1 wild-type and Chk1 stimulated by Chk1 peptide 14
	Peptide targeted by Chk1 stimulated by Chk1 peptide 14 and Chk1 ΔC70

Appendix 1

List of peptides phosphorylated by Chk1 ΔC70 protein kinase

S/N	COL	ROW	SEQUENCE	TARGET PROTEIN
1	2	11	KKLGSKKPQ	SWISS;P04775;CIN2_RAT
2	11	5	KKRLSVERI	SWISS;P11388;TOPA_HUMAN
3	7	7	KNIVTPRTP	SWISS;P02687;MBP_BOVIN
4	5	9	KREASLDNQ	SWISS;P06593;PHY3_AVESA
5	5	13	KRFGSKAHM	SWISS;P29476;NOS1_RAT
6	1	7	KRPSARAKA	SWISS;P02687;MBP_BOVIN
7	1	11	KRPSDRAKA	SWISS;P02687;MBP_BOVIN
8	1	15	KRPSERAKA	SWISS;P02687;MBP_BOVIN
9	10	1	KRPSFRAKA	SWISS;P02687;MBP_BOVIN
10	10	9	KRPTQRAKY	SWISS;P02687;MBP_BOVIN
11	8	6	KRRGSVPIL	SWISS;P16452;42_HUMAN
12	8	10	KRRLSFSET	SWISS;P01582;IL1A_MOUSE
13	12	12	KRSGSVYEP	SWISS;P12798;KPBB_RABIT
14	6	8	KTSPSSSPA	SWISS;P19836;CTPT_RAT
15	6	16	KVPQTPLHT	SWISS;P49139;MKK2_RABIT
16	5	10	LGSPLRRR	SWISS;P20152;VIME_MOUSE
17	11	8	LKLASPELE	SWISS;P05412;AP1_HUMAN
18	11	12	LLPMSPEEF	SWISS;P42224;STA1_HUMAN
19	1	14	LQDDYEDMM	SWISS;P02730;B3AT_HUMAN
20	5	8	LRAPSWIDT	SWISS;P02510;CRAB_BOVIN
21	8	1	LRKVSKQEE	SWISS;P50552;VASP_HUMAN
22	8	5	LRMFSFKAP	SWISS;P22300;GAC2_BOVIN
23	8	9	LRRASLGAA	BOS TAURUS (BOVINE) LIVER PYRUVATE KINASE (FRAGMENT)
24	8	13	LRRASLGAF	BOS TAURUS (BOVINE) LIVER PYRUVATE KINASE (FRAGMENT)
25	10	4	LRRPSDQEV	SWISS;P16236;REL_CHICK
26	2	5	LSELSRRRI	SWISS;P20459;IF2A_YEAST
27	10	3	PRMPSLSVP	SWISS;P02719;CINA_ELEEL
28	1	8	RTKRSGSV	phosphorylase b kinase beta regulatory chain

	Peptide targeted by all three forms of Chk1
	Peptide targeted by Chk1 wild-type and Chk1 stimulated by Chk1 peptide 14
	Peptide targeted by Chk1 stimulated by Chk1 peptide 14 and Chk1 ΔC70